STUDIES ON MULTI-PURPOSE HEAT PUMP DRYER

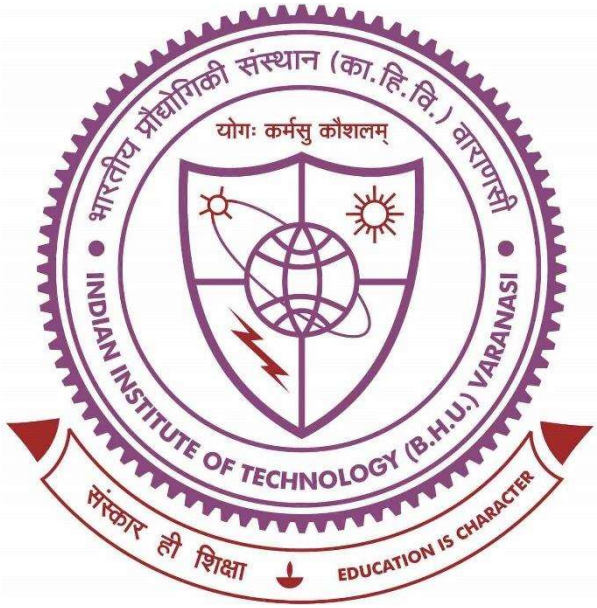

Thesis Submitted in Partial Fulfillment for the Award of Degree

DOCTOR OF PHILOSOPHY

by

AKHILESH SINGH

DEPARTMENT OF MECHANICAL ENGINEERING
INDIAN INSTITUTE OF TECHNOLOGY
(BANARAS HINDU UNIVERSITY)
VARANASI-221005

16131502 **2021**

CERTIFICATE

It is certified that the work contained in the thesis titled "**Studies on Multi-Purpose Heat Pump Dryer**" by **Akhilesh Singh** has been carried out under our supervision and that this work is not submitted elsewhere for any degree.

It is further certified that the student has satisfactorily fulfilled all the requirements of the Comprehensive examination, Candidacy, and SOTA for the award of the Ph.D. degree.

Dr. Jahar Sarkar
(Supervisor)
Department of Mechanical Engineering
IIT (BHU), Varanasi

Dr. Rashmi Rekha Sahoo
(Co-supervisor)
Department of Mechanical Engineering
IIT (BHU), Varanasi

DECLARATION BY THE CANDIDATE

I, **Akhilesh Singh,** certify that the work embodied in this thesis is my own bonafide work carried out by me under the supervision of **Dr. Jahar Sarkar** and co-supervision of **Dr. Rashmi Rekha Sahoo** for a period of 4 years and 10 months from December 2016 to October 2021 at IIT (BHU), Varanasi. The material contained in this thesis has not been submitted for the award of any other degree. I declare that I have faithfully acknowledged and given credits to the research workers wherever their works have been cited in my work in this thesis. I further declare that I have not willfully copied any others' work, paragraphs, text, data, results, etc. reported in journals, books, magazines, reports, dissertations, theses, etc. or available at websites and have not included them in this thesis and have not cited as my own work.

Date: 22/10/2021

Place: IIT (BHU), Varanasi **(Akhilesh Singh)**

CERTIFICATE BY THE SUPERVISORS

This is to certify that the above statement made by the candidate is correct to the best of my knowledge.

Dr. Jahar Sarkar **Dr. Rashmi Rekha Sahoo**

(Supervisor) **(Co-supervisor)**

Head of the Department

Mechanical Engineering Department, IIT (BHU), Varanasi

COPYRIGHT TRANSFER CERTIFICATE

Title of the Thesis: Studies on Multi-Purpose Heat Pump Dryer

Candidate's Name: Akhilesh Singh

COPYRIGHT TRANSFER

The undersigned hereby assigns to the Indian Institute of Technology (Banaras Hindu University) Varanasi all rights under copyright that may exist in and for the above thesis submitted for the award of the Ph.D. degree.

Date: 22/10/2021

Place: IIT (BHU), Varanasi (Akhilesh Singh)

Note: However, the author may reproduce or authorize others to reproduce material extracted verbatim from the thesis or derivative of the thesis for author's personal use provided that the source and University's copyright notice are indicated.

ACKNOWLEDGEMENTS

I take this opportunity to express my deep sense of gratitude to my supervisor **Dr. Jahar Sarkar** and co-supervisor **Dr. Rashmi Rekha Sahoo** for his continuous guidance and whole-hearted cooperation in carrying out this work. His meticulous and valuable review and constructive criticism of the manuscript have greatly improved the quality of work. Sir, for your faith in me and the desire to live up to your expectations, has constantly pushed me to work harder.

My grateful appreciation also goes to **Dr. Marshal** and **Dr. Amitesh Kumar** for serving on my research programme evaluation committee (RPEC). Thank you all for sparing your valuable time and assisting me throughout my research and completion of this thesis. I wish to extend my sincere thanks to **Prof. Santosh Kumar**, Head, Department of Mechanical Engineering for providing me the necessary resources to enable me to complete this research work. During my stay at IIT (BHU) Varanasi, I have met many people who have made this period of my life memorable and very pleasant. Among them, I would like to sincerely acknowledge the assistance and motivation provided by Prof. P. Ghosh, Dr. S. S. Mondal, Prof. S.K Shukla, Dr. Arnab Sarkar, Dr. Laltu Chandra and Dr. O. P. Singh. I want to thank my colleagues at IIT (BHU) Varanasi, especially to to Mr. Sumit Kumar Singh, Mr. Sujeet Yadav, Mr. Vivek Kumar, Mr. Ajit Pratap Singh, Mr. Sarvesh Kashyap, Mr. Mayaram Sahu, Mr. Ranjeet Kumar Rai, Mr. Chandrmani Yadav, Mr. Jay Prakash, Mr. Sarvesh Yadav, Mr. Dhruv Raj Karana, Mr. Vikash Kumar for encouraging me to finish this work.

The experimental part of this thesis has been carried out at the Department of Mechanical Engineering IIT (BHU) Varanasi. A number of persons have assisted and supported me in designing and development of the test rig. I would like to extend my sincere thanks to Mr. R. A. Ram, Mr. Kali Prasad, Mr. Surender Yadav, Mr. Moolchand, Mr. Shivlal Yadav for giving the valuable ideas while performing experiments and providing the measurement tools and instruments whenever needed for the research work without any hesitation.

I would like to acknowledge **my parents, family and other relatives** for not engaging me in any other affairs during my research duration and handling all the matters by themselves. I thank my parents for assisting me financially whenever needed and motivating me for my work. I would like to extend my hearty thanks to my brothers**,** who supported me a lot mentally as well as financially.

I would also like to thank **GOD** the Almighty for giving me the strength to remain on the path to success.

Date: 22-10-2021 **.....**

Place: IIT (BHU) Varanasi **(Akhilesh Singh)**

Table of Contents

List of Figures

List of Tables

List of Symbols

Nomenclatures

2A	Wavy height (m)
A_{fr}	Condenser frontal area (m^2)
A_i	Tube inside area (m^2)
A_o	Total outer surface area including fin and tube (m^2)
B_i	Biot number
c	Exergy cost per unit ($/kWh)
c_{pam}	Specific heat of moist air (kJ/kg-K)
c_{pa}	Specific heat of dry air (kJ/kg-K)
c_{pv}	Specific heat of water vapor air (kJ/kg-K)
C_L	Cost of labor ($)
C_L	Labor cost ($)
C_m	Maintenance cost ($)
C_{IC}	Initial investment cost ($)
C_p	Energy requirement cost ($)
$\dot{C}_{RU}$	Operating cost of drying system ($)
C_{RM}	Fresh product cost ($)
$\dot{C}_{Total}$	Total cost of drying system ($)
C_F	Total profit ($)
$\dot{C}_x$	Exergy cost rate ($/h)
D_{ha}	Hydraulic diameter of air side (m)
DR	Drying rate (1/s)
D_{eff}	Effective diffusivity (m^2/s)

e_x	Specific exergy (kJ/kg)
E_{xin}	Exergy input (kW)
E_{xout}	Exergy output (kW)
E_{dest}	Exergy destruction (kW)
f	Friction factor of air
f_{ex}	Exergoeconomic factor
F_p	Fin pitch (m)
F_h	Fin height (m)
G_a	Mass velocity of air (kg/m^2-s)
h	Specific enthalpy (kJ/kg)
h_{fg}	Latent heat of vaporization (kJ/kg)
h_a	Air heat transfer coefficient (W/m^2-K)
h_m	Air mass transfer coefficient (kg /m^2-s)
i	Interest rate
k	Thermal conductivity (W/m-K)
k_c	Drying constant (1/s)
L	Half thickness of chips
L_f	Length between two wavy fin (m)
L_d	Length of fin (m)
LMTD	Log mean temperature difference (K)
$\dot{m}_a$	Air mass flow rate (kg/s)
m_p	Weight of drying product (kg)
m_{pt}	Mass of drying material at any time (kg)
$\dot{m}_r$	Refrigerant mass flow rate (kg/s)
M_i	Initial wet weight of the product (kg)

M_d	Final dry weight of product (kg)
M_o	Initial moisture content of material (wet basis)
M_t	Moisture content of product at any time (wet basis)
M_{eq}	Equilibrium moisture content (wet basis)
MC	Moisture content (wet basis)
MR	Moisture ratio
m_w	Mass of water in product (kg)
$\dot{m}_{hw}$	Mass flow rate of hot water (kg/s)
n	Time period of payment
N	Speed of compressor (rpm)
Nu	Nusselt number
P_p	Payback period
P	Pressure (bar)
Pr	Prandtl number
p_t	Transverse pitch of fin (m)
Q	Heat transfer rate (kW)
R_{ex}	Ratio of exergy destruction to purchased equipment cost
R_c	Return of capital
Re	Reynolds number
S_f	Fin spacing (m)
t_d	Drying time (hour)
t_{op}	Annual operation time (hour)
s	Specific entropy (kJ/kg-K)
T_o	Dead state temperature (K)
T	Temperature (°C)

T_d	Dew point temperature (°C)
T_f	Fin thickness (m)
UA	Product of overall heat transfer coefficient and area (W/K)
V_a	Air velocity (m/s)
Vs	Swept volume of compressor (m^3)
W	Power input (kW)

Greek symbols

α	Intermittency ratio
η_{ex}	Exergy efficiency
η_{en}	Energy efficiency
η_{isen}	Isentropic efficiency of compressor
η_f	Fin efficiency
η_o	Overall efficiency of fin
η_{fn}	Fan efficiency
η_v	Volumetric efficiency of compressor
ω	Specific humidity of drying air (kg water/kg dry air)
ε	Emissivity factor
σ	Stephan–Boltzman constant ($W/m^2\text{-}K^4$)
φ	Maintenance factor
μ	Dynamic viscosity ($N/s\text{-}m^2$)
ρ	Density (kg/m^3)
υ	Specific volume (m^3/kg)

Abbreviations

COP_{hp}	Coefficient of performance of heat pump system
COP_{ws}	Coefficient of performance of the whole dryer system

CR	Cost ratio
CRF	System recovery factor
DC	Drying chamber
HP	Heat pump
HPD	Heat pump dryer
HE	Heat exchanger
IAHPD	Infrared assisted heat pump dryer
MER	Moisture extraction rate
MC	Moisture content
OHCOP	Overall-heating coefficient of performance
OCCOP	Overall cooling coefficient of performance
OSCOP	Overall system coefficient of performance
PEC	Cost of purchased equipment ($)
RH	Relative humidity
SAHPD	Solar-assisted heat pump dryer
SIAHPD	Solar-assisted-infrared-assisted heat pump dryer
SMER	Specific moisture extraction rate
SEC	Specific energy consumption
SWH	Solar water heater
WHR	Waste heat recovery
SWHE	Solar water heat exchanger

Subscripts

a	air
abs	absorbed
comp	compressor

cond	condenser
evap	evaporator
exp	expansion device
in	input
IR	infrared
M	drying material
out	output
r	refrigerant
w	water
hw	hot water
wb	wet basis
wi	hot water inlet
wo	hot water outlet

ABSTRACT

Heat pump drying of fruits, vegetables and biological materials is an interesting area of research. The main advantages of using a heat pump dryer (HPD) are the energy-saving potential with high energy efficiency and high moisture removal rate and the ability to control drying temperature and air humidity at the drying chamber inlet. The performance of the heat pump dryer can be enhanced by utilizing hybrid energy sources. The hybrid source heat pump dryer utilizes unconventional energy sources such as solar energy, ground source energy and waste heat recovery source with a heat pump system, which decreases the electric energy consumption with the improved thermal performance and drying time as compared to the simple heat pump dryer. The drying temperature range for the hybrid source heat pump dryer may be greater than the simple heat pump dryer, which improves the drying rate and energy efficiency. Various types of the simple HPD and the hybrid source HPD have been analyzed in this research, such as solar assisted HPD, HPD assisted with waste heat recovery from the engine exhaust, HPD with air conditioning and intermittent drying with solar assisted HPD. Furthermore, in view of phasing out the conventional refrigerant due to ozone layer depletion and global warming issues, the future refrigerant such as R1234yf, R1234ze (E), R152a and R600 are studied numerically for the heat pump drying applications. The R1234yf refrigerant is experimentally analyzed for the intermittent drying of food products with solar-assisted heat pump dryer.

An experimental facility of HPD has been developed to compare closed and open modes of drying on the basis of various energy, exergy and drying kinetic parameters. Total energy consumption is lowest for the closed system heat pump drying of banana and potato chips. The total energy consumptions for banana chips in the open and closed system are 3.3, 2.41 kWh and for potato chips are 3.564, 3.51 kWh, respectively. The closed system drying is found better on the basis of the performance parameters such as mass transfer coefficient, moisture extraction rate (MER), specific moisture extraction rate (SMER) and drying efficiency in the given humid and hot atmosphere for the fruits and the vegetable drying. The experimented heat pump dryer has been modeled numerically to compare various low-GWP refrigerants (R290, R600, R600a, R152a, R32, R1234yf and R1234ze(E)) as R134a substitutes. Within studied refrigerants, R152a and R32 yield better performance in terms of drying efficiency and specific moisture extraction rate; however, R152a may be more favorable for HPD due to lower GWP.

The solar and infrared assisted HPD has been developed and various thermal, economic and exergoeconomic performance parameters such as coefficient of performance (COP), overall heating coefficient of performance (OHCOP), energy requirement, drying time, energy efficiency, drying efficiency, MER, SMER, exergy destruction, investment cost, running cost, payback period, exergy destruction cost, exergoeconomic factor and the cost ratio have been evaluated for drying of different materials. The hybrid source heat pump dryer is found better in terms of SMER and energy efficiency as compared to the simple HPD. Solar-assisted HPD (SAHPD), infrared-assisted HPD and solar-infrared assisted HPD (SIAHPD) are compared and estimated that SAHPD system is better based on the basis of SMER, and SIAHPD is better than others based on MER in the given humid and hot atmosphere for drying of banana chips. The drying cost of the material per kg and the total energy consumption to

the system are minimum for the SAHPD and it is highest for the infrared assisted heat pump dryer. The drying cost per kg of material for the banana chips in simple HPD, IAHPD, SAHPD and SIAHPD are 0.488 $/kg, 0.497 $/kg, 0.469 $/kg and 0.484 $/kg, respectively.

Heat pump dryer assisted with the heat recovery from the diesel engine exhaust is developed and the experimental analyses is done by using energy-exergy and ecomonomic-exergoecomic methodology. Performance is compared with simple HPD for both open and closed loops. The radish chips are dried to remove moisture from 93.5% to 10.5% at an air velocity of 1.0 m/s in the drying chamber. Both energy and exergy efficiencies are found highest for waste heat recovery-assisted system. SMER (2.4 kg/kWh) and OHCOP (6.72) are higher for the waste heat recovery assisted system. The payback period for the HPD assisted with waste heat recovery over the simple HPD is 33 months. The lowest exergoeconomic factor is for expansion device in simple HPD and HPD assisted with waste heat recovery in a closed-loop system with determined values as 0.0918 and 0.1348. The total exergy destruction cost for the simple and hybrid systems is 0.10148 $/h and 0.1266 $/h, respectively.

The experiment is also performed for different intermittency ratios for radish drying with a solar-assisted heat pump dryer using future refrigerant R1234yf. The effects of total drying time (on-period + off-period) on various energetic, exergetic, and economic performances are investigated to extract moisture from 92.4% to 11.9%. Energy efficiency and drying efficiency are estimated higher for a lower intermittency ratio. The moisture extraction rate and specific moisture extraction rate are higher for intermittent drying as compared to continuous drying and increase with a decrease in intermittency ratio. The economic analysis concludes that the payback period is lower for a lower intermittency ratio. The payback period for intermittency ratio of 1, 0.66, 0.33

and 0.2 are estimated as 1.617 years, 1.459 years, 1.384 years, and 1.347 years, respectively. Present experimental thermo-economic analysis reveals that intermittent drying is much better (maximum enhancement of specific moisture extraction rate is 60.6%, that of energy efficiency is 56.4% and maximum reduction of drying cost is 37.9% with studied conditions) than continuous drying.

An integrated heat pump system for combined heat pump drying and air conditioning is experimentally studied as well. The main advantage of this combined system is that it gives the performance of both heat pump drying and air conditioning with a single energy input source. The experiment is performed for different atmospheric conditions to estimate the performance of the combined system using future refrigerant R1234yf in the heat pump system. The effects of the drying time, air inlet velocity and air inlet temperature to the evaporator and the condenser on the performance of the air conditioning and drying are investigated. The coefficient of performance for the combined operation is found to be much higher than that for the individual operation (heat pump drying or air conditioning), with an average value of 7.456 in the input temperature range of 26-45°C. The cooling air temperature and the humidity are 22.6-24.7°C and 40.4-50.2% (are in the comfort zone) with drying temperature of 62.1-63.9°C for the atmospheric temperature of 42-45°C. Hence, this system can be used for both drying and air conditioning purposes for the maximum atmospheric temperature of 45°C.

CHAPTER 1

INTRODUCTION

1.1. Motivation

With the increase in world population, the demand for the fruits, vegetables, and other agricultural products continuously going on increasing but the availability of these products depends on the seasonal and climatic conditions, so it is needed the storage and transportation of these products without any deterioration to fulfill the world demand. Dying is one of the oldest and best methods for preserving and maintaining the quality of agricultural products. Drying conserved the product by removing the amount of moisture content from the products, while freezing conserves the product by maintaining its temperature below the freezing point of water (Goh et al., 2011). The drying of the product permits less weight for transportation and less space for long time storage without deterioration. Drying methods include convention solar, oven, dehydrator, and heat pump system. The drying methods must be designed in compliance with the recent environmental and energy policies (Alves et al., 1998). People reported that drying is one of the most energy-intensive unit operations that easily account for up to 15% of all industrial energy utilizations. And it is well known that the conventional methods of drying the fruits, vegetables, medicine, drugs, and timbers are time-consuming processes with huge wastage of energy (Colak and Hepbasli, 2009). In many industrial drying processes, a very huge amount of energy is wasted, so it is needed to develop new technology in the area of drying which is more efficient and with low pollution emissions. Also, due to globalization and market expansion, a newly developed product quality must conform to a wide consumer's preferences and expectations. It was reported in a study that drying consumes up to 70% of the total energy in manufacturing wood products,

50% of the total energy consumption in the manufacturing of finished textile fabrics, and over 60% of the total energy needed for farm corn production (Mujumdar, 1995). Therefore, energy management is an essential part of the drying process and efficient energy conservation contributes significantly to the overall operating cost. By applying a better method of drying to the products it may be possible to reduce the energy requirement, drying cost, and environmental pollution with better product quality and color.

Different conventional methods of drying are available for food products and people used different methods of drying for industrial and domestic applications. The sun drying method is the oldest and most natural available source without any cost but it is a too time-consuming process and the intensity of the sun is also not constant, and the sun drying is mostly suitable for the fruits having high sugar and acid content. Vegetables and meats are not suitable for sun-drying due to the low content of sugar and acid in vegetables and meat (high protein). In sun drying the temperature (low) and the humidity is uncontrolled which may damage the food products which are outside the door (Ahmed et al., 2013). The power consumption in hot gas drying is very high and it is not ecofriendly due to pollution generation also it is not suitable for the low-temperature drying products with the high cost of drying. The vacuum drying is proposed to alleviate some disadvantages of hot air drying. The main purpose of vacuum-drying is to allow the removal of moisture under vacuum and hence at a lower temperature condition and oxygen content. Vacuum-drying is, therefore, suitable for heat- and oxygen-sensitive materials. During vacuum drying, the rate of evaporation increases (at a fixed temperature) since the boiling point of water is reduced. In addition, the effective hydraulic conductivity of a material increases under vacuum, so the resistance to mass transfer at the product surface reduces. Vacuum-drying consequently requires less drying

time than conventional hot air drying and in most cases results in a higher quality dried product. the main disadvantage of the vacuum dying is that it is suitable for the low temperature drying only and the power consumption is very high with the difficulty of maintaining the vacuum in the drying cabin (Amellal and Benamara, 2008). By combining the factors of heat, low humidity, and air flow, an oven can be used as a dehydrator. An oven is ideal for occasional drying of fruit leathers; banana chips or for preserving excess produce like celery or mushrooms. Because the oven is needed for everyday cooking, it may not be satisfactory for preserving agricultural food products. Oven drying is slower than dehydrators because it does not have a built-in fan for air movement. (However, some convection ovens do have a fan). It takes about two times longer to dry food in an oven than it does in a dehydrator. Thus, the oven is not as efficient as a dehydrator and uses more energy. Microwave drying is only suitable for the low quantity drying of the herbs and the vegetable leaves. The drying cost of microwave drying is high because energy consumption is high for the microwave heater and it is not successful for most other agricultural food products. Freeze-drying is typically used to preserve a perishable material or make the material more convenient for transport. Freeze-drying works by freezing the material and then reducing the surrounding pressure to allow the frozen water in the material to sublimate directly from the solid phase to the gas phase. It is the costly method of drying compared to the other method (Ahmed et al., 2013). The above discussed conventional methods of drying have some advantages and as well as disadvantages. So it is needed to develop a new method of drying that can minimize the disadvantages of the conventional method of drying.

Recently people are taking interest in utilizing the heat pump dryer (HPD) for drying fruits, vegetables, and biological materials. The heat pump is a very energy-efficient heating and cooling system, so it can be also used as a convective dryer

efficiently by removing the moisture from the products with a low cost of drying and high moisture removal rate. The main advantages of using heat pump dryer technology are the energy-saving potential with high energy efficiency and the ability to control drying temperature and air humidity at the drying chamber inlet which provides a wide range of drying conditions for the different materials dried at different temperatures (Claussen et al., 2007). So with the heat pump dryer, the temperature and the moisture-sensitive materials can be dried without deterioration of the product quality and color. Utilization of the heat pump as convective hot air dryers has been recognized as a new area of the application of the heat pump instead of heating and cooling only because the energy efficiencies of conventional dryers are generally very low, and the maximum value of the energy efficiency was for the simple conventional dryer as a value of 35% (Schmidt et al., 1998). Also, it was found that the heat pump dryer consumes 60–80% less energy as compared the conventional dryers operating in the same temperature range. Thus the heat pump dryer may be a feasible option for users who are not satisfied with the comparatively high energy consumption of conventional hot air dryers.

But the simple heat pump dryer having also some limitations the using the costly electric energy (responsible for greenhouse gases and flying ash production in thermal plants) and longer drying time due to low-temperature drying. The leakage of the conventional refrigerants directly into the atmosphere from the heat pump system also contributes to the ozone layer depletion and the global warming effect, so it is needed to study the performance of new refrigerants with low global warming potential (GWP) and ozone layer depletion potential (ODP) for the heat pump drying application. During the last decades, environmental issues have evolved from pollution and depletion of natural resources, such as climate change, and fossil fuel consumption contributes to these damages. From the viewpoint of environmental problems, developing sustainable and

renewable energy sources and improving the efficiency of systems using thermal energy has become important because renewable energy sources produce negligible pollution, and the cost of energy is also low. So it is needed to design and develop a new system that can remove the limitations of the simple heat pump dryer for the agricultural products drying and utilizes the renewable and other energy sources with the heat pump system. The hybrid source heat pump dryer utilizes unconventional energy sources such as solar energy, ground source energy, and waste heat recovery source with a heat pump system which decreases the electric energy consumption with the improved thermal performance and drying time as compared to the simple heat pump dryer. The drying temperature range for the hybrid source heat pump dryer may be greater than the simple heat pump dryer which improves the drying rate and energy efficiency. It is supposed that the heat pump dryer and the hybrid source heat pump dryer have better overall drying and thermal performance characteristics with a low cost of drying over the conventional drying methods. Recently hybrid source heat pump dryers as getting importance due to their enhanced thermal performance and lower environmental issues and drying cost, which has motivated to apply the solar energy source with heat pumps for food products drying. The drying performance of hybrid source HPD should be high due to higher drying temperature but the product temperature may be increased continuously by continuous drying, and the drying material (both product surface and quality) can be deteriorated due to continuous high-temperature heat input and hence the drying should be carried out at optimum temperature. To avoid the deterioration of the food products, intermittent drying may be applied because in intermittent, the energy supply is in different steps and the drying temperature may be maintained at an optimum level.

1.2. Heat pump dryer

The first heat pump dryer patent applications were started in 1973 and the first study on the heat pump dryer available in the open literature on the timber drying with the heat pump dryer evaluated the energy consumption and the performance parameters of the timber drying (Geeraert, 1976). The heat pump drying system is the combination of mainly two subsystems; a heat pump system and a drying chamber system. Heat pumps are a cooling and heating system (refrigerators) that delivers the heat energy (high temperature) in the condenser gained by cooling in an evaporator from a low-temperature energy medium (drying air) with the addition of further external energy (compressor energy input) to a higher temperature level. The term heat pump refers to the fact that it can be used as simultaneously in both the heating and cooling system (Mujumdar, 2006). In the heat pump, the cooling and heating system is used both for the moisture removal and the heating of the drying medium. Heat pumps are the device that can transfer heat from the natural heat sources available in the surrounding atmosphere, such as the air, ground, water, industrial or domestic waste, chemical reaction, or dryer exhaust air. The second most important part of the heat pump dryer is the drying chamber. The drying chamber may be of different types such as a tray, fluidized bed, rotary, or band conveyor type. Depending on the different types of energy utilization, the heat pump dryer can be classified as a simple heat pump dryer and the hybrid source heat pump dryer. Fig. 1.1 shows the classification of the heat pump dryer.

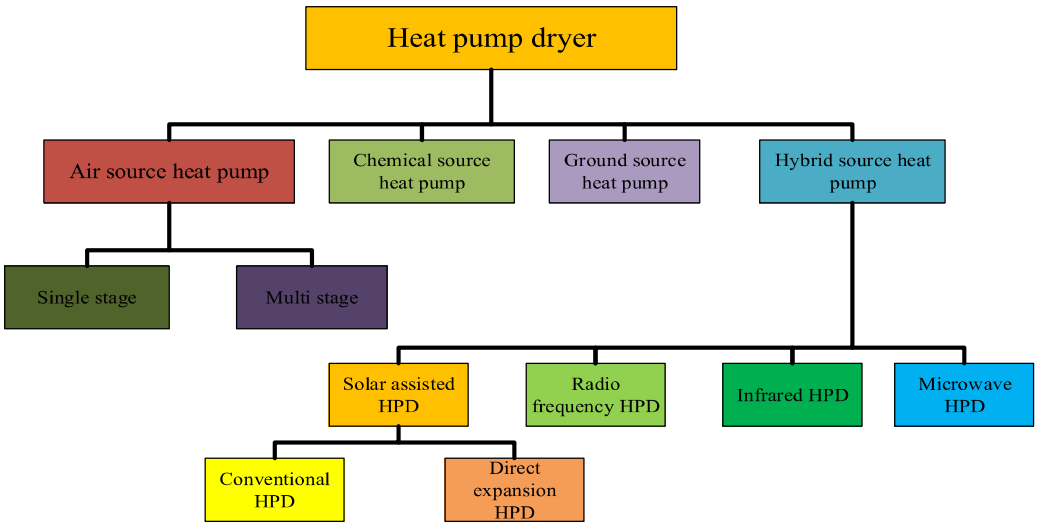

Fig. 1.1: Classification of heat pump dryer

1.2.1. Air source heat pump dryer

The main components of the air source heat pump drying systems are an evaporator, a condenser, a compressor, and an expansion device. As shown in Fig. 1.2, in a heat pump drying system, the working fluid (refrigerant) at low pressure and temperature is vaporized in the evaporator by heat removed from the dryer exhaust air (recirculated to evaporator). The compressor increases the pressure and the temperature of the refrigerant of the heat pump by consuming the high-grade energy (electric or mechanical) and discharges the refrigerant in a superheated state of vapor at high pressure to the condenser. The heat pump delivers the removed heat from the working fluid (refrigerant) to the working drying medium (drying air) in the condenser. In the drying system, the heated air coming out from the condenser is directly allowed to pass (recirculation) through the drying chamber where the drying medium removes the moisture from the product to be dried by exchanging energy. The refrigerant in the heat pump from the condenser is then throttled (isenthalpic expansion) to the low pressure by using an expansion device and then this low pressure and temperature refrigerant enter into the evaporator to complete the refrigeration cycle in the heat pup dryer. In the dying chamber, the hot and the dry air removes the moisture from the product and then passes

through the evaporator where the moisture of the air removes by the condensation process as the air temperature goes below the dew point temperature. In the simple heat pump dryer (air source), the input energy is only to the compressor (electric or mechanical) which is used to circulate the refrigerant in the cycle through the different components of the heat pump cycle.

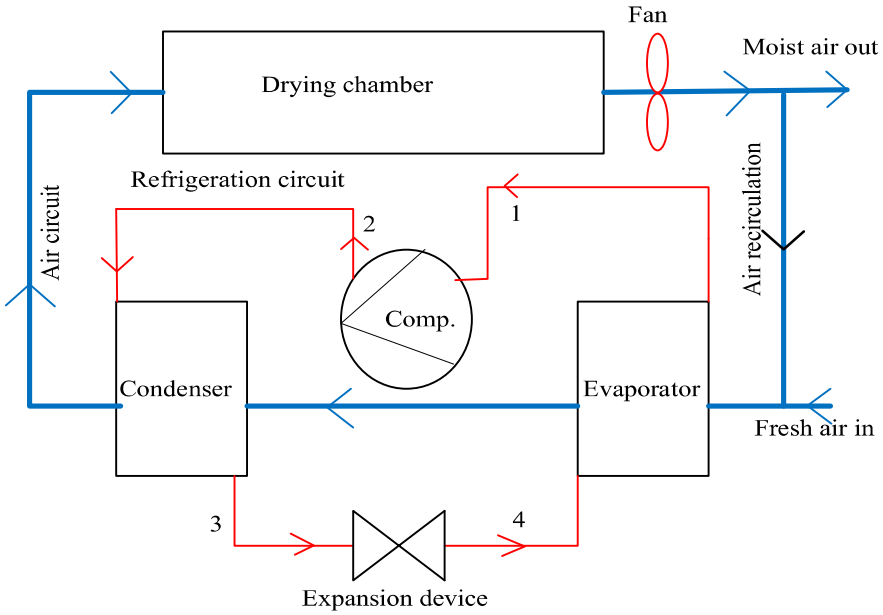

Fig. 1.2: Schematic diagram of heat pump dryer

1.2.2. Ground source heat pump dryer

In the ground source hybrid heat pump dryers, a renewable source of geothermal energy is utilized with the heat pump cycle for the drying of the products. In the ground source heat pump dryer, the refrigerant in the evaporator is converted into vapor by gaining the heat directly from the ground source instead of the recirculating drying air. Figure 1.3 represents the schematic of the ground source-assisted heat pump dryer. The ground is a thermally more stable heat exchange medium than air, essentially unlimited and always available. The ground source heat pump dryer exchange heat with the ground, and maintain a high level of performance even in colder climates. The main advantage of the ground source heat pump dryer is that it utilizes the renewable form of ground

source energy which reduces the electricity consumption of the compressor with improves the performance of the system.

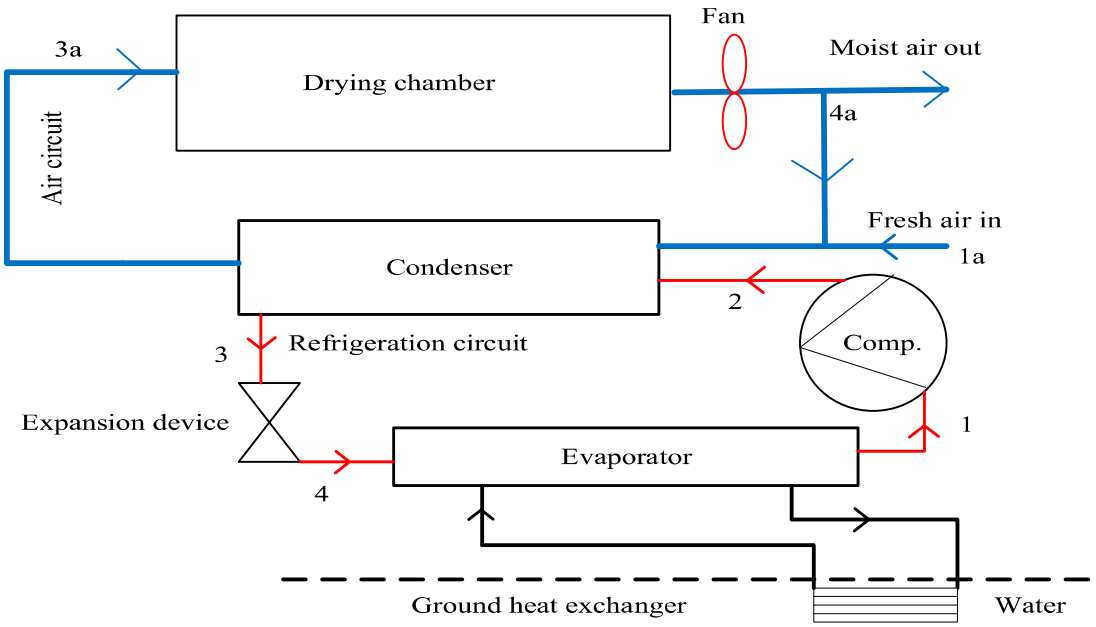

Fig. 1.3: Schematic diagram of ground source assisted heat pump dryer

1.2.3. Chemical source heat pump dryer

A chemical heat pump drying system that uses the chemical source of energy for the drying purpose may be an effective utilization of thermal energy in drying with energy-saving and less environmental impact. A heat pump dryer can store thermal energy in the form of chemical energy by an endothermic reaction and release it at various temperature levels for heat demands by exothermic reactions. Figure 1.4 represents the schematic of the chemical source heat pump dryer. A chemical heat pump dryer has potential for the heat recovery and dehumidification in the drying process by heat storage and high/low-temperature heat release. The chemical heat pump dryer can store thermal energy from the various source such as the waste heat from dryer exhaust, solar energy, geothermal energy, etc. in the form of chemical energy via an endothermic reaction in a suitably designed reactor and release the energy at various temperature levels during the heat-demand period by exothermic reactions.

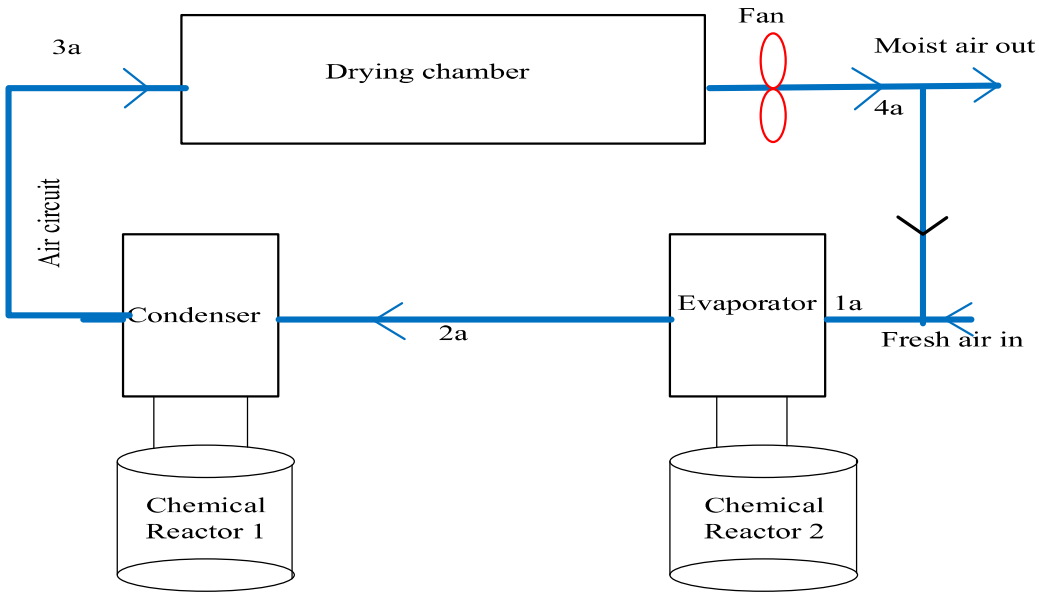

Fig. 1.4: Schematic diagram of chemical source heat pump dryer

1.3. Hybrid source heat pump dryer

Integration of the air source heat pump dryer with the other form of energy sources such as solar energy, ground source energy, etc. is called a hybrid source heat pump dryer. In the hybrid source heat pump dryer, the drying temperature can be higher than the simple air source. The main advantage of the hybrid source heat pump dryer is that it can utilize the renewable source of energy (Ex. Solar, ground source) with a heat pump for the drying purpose with better and improved performance than the air source heat pump dryer. A hybrid source of the heat pump dryer can provide effective control of the air humidity and the temperature in an energy-efficient manner. The hybrid source heat pump dryer can be classified based on the external source energy input. Fig. 1.1 shows the classification of the heat pump dryer.

1.3.1. Solar assisted heat pump dryer

A solar-assisted heat pump drying system is the combination of the vapor compression heat pump cycle and a solar collector and this combined system may be able to provide better thermal and drying performance than the simple heat pump dryer. Solar-assisted heat pump drying systems can be classified as conventional solar-assisted heat

pump drying systems and direct-expansion solar-assisted heat pump drying systems. In a direct expansion system, the solar collector system consists of a solar collector, a heat exchanger as the condenser, an expansion device, and a compressor. The solar collector is used as the evaporator of the heat pump system dryer and the refrigerant is directly vaporized in the solar collector–evaporator due to the solar energy input. But in a conventional solar-assisted heat pump dryer a separate solar collector and the heat exchanger are used with the heat pump cycle and the drying air is pre or post-heated in the solar heat exchanger while passing through the condenser. Figure 1.5 shows the schematic diagram of the conventional solar-assisted heat pump dryer. The main advantage of the soar-assisted heat pump dryer is that it can utilize the renewable source of solar energy (free of cost) with higher drying temperature and reduces the primary energy (electric) requirement which finally reduces the chances of pollution. Heat pumps driven by electricity produced from hydropower or renewable energy, reduce emissions more significantly than if the electricity is generated by coal, oil, or gas-fired power plants (Dincer, 2003).

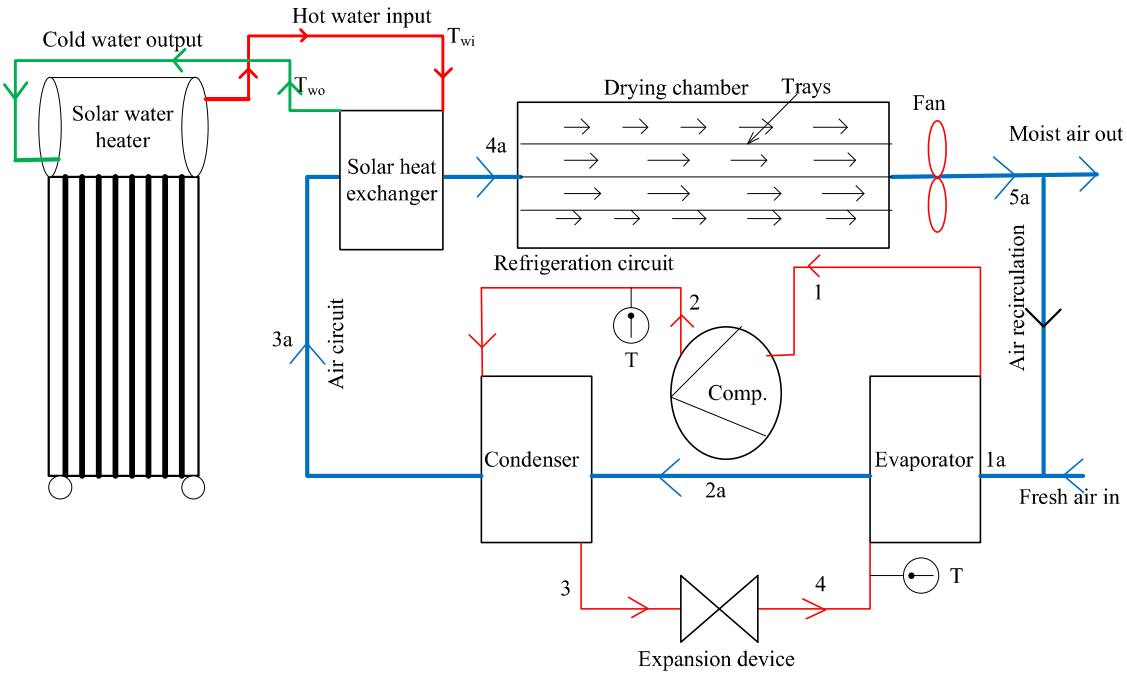

Fig. 1.5: Schematic diagram of Solar assisted heat pump dryer

1.3.2. Microwave-assisted heat pump dryer

Microwave-assisted heat pump dryer utilizes the energy of the microwave radiation with the heat pump cycle to remove the moisture from the product at a faster rate. This type of hybrid source heat pump dryer uses microwave radiation which penetrated the drying material which creates a vapor pressure gradient and removes the moisture from the product at a faster rate. However, the application of microwave drying in industrial processes has been relatively slow since this technique requires a high capital investment and suffers a low energy efficiency of drying when compared with conventional drying technologies. To make the economics of microwave drying more attractive for industrial applications, it is necessary to incorporate additional energy-conserving features, such as heat pumps (Shane et al., 1993). Figure 1.6 represents the microwave-assisted heat pump dryer.

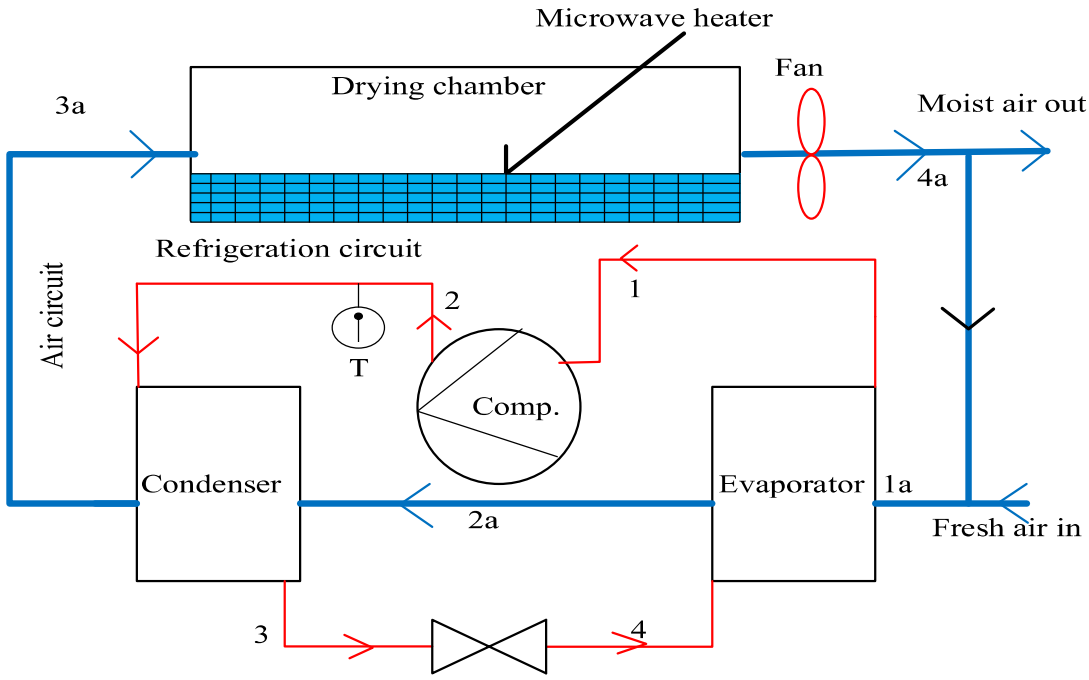

Fig. 1.6: Schematic diagram of microwave-assisted heat pump dryer

1.3.3. Infrared assisted heat pump dryer

Infrared-assisted heat pump dryer uses the infrared energy source with the heat pump cycle to remove the moisture from the drying product. In this type of hybrid source

heat pump dryer, the infrared radiation (heater or lamp) is installed inside the drying chamber, and the infrared radiation is penetrated inside the material and develops a vapor pressure gradient. Due to this developed vapor pressure gradient, the moisture extracted at the surface of the material and carried away by the hot drying air coming from the condenser of the heat pump. The infrared-assisted heat pump dryer is used where a faster rate of drying is required. This method is not too economical and eco-friendly due to the high energy consumption by the infrared radiation source. Figure 1.7 shows the schematic diagram of the infrared-assisted heat pump dryer.

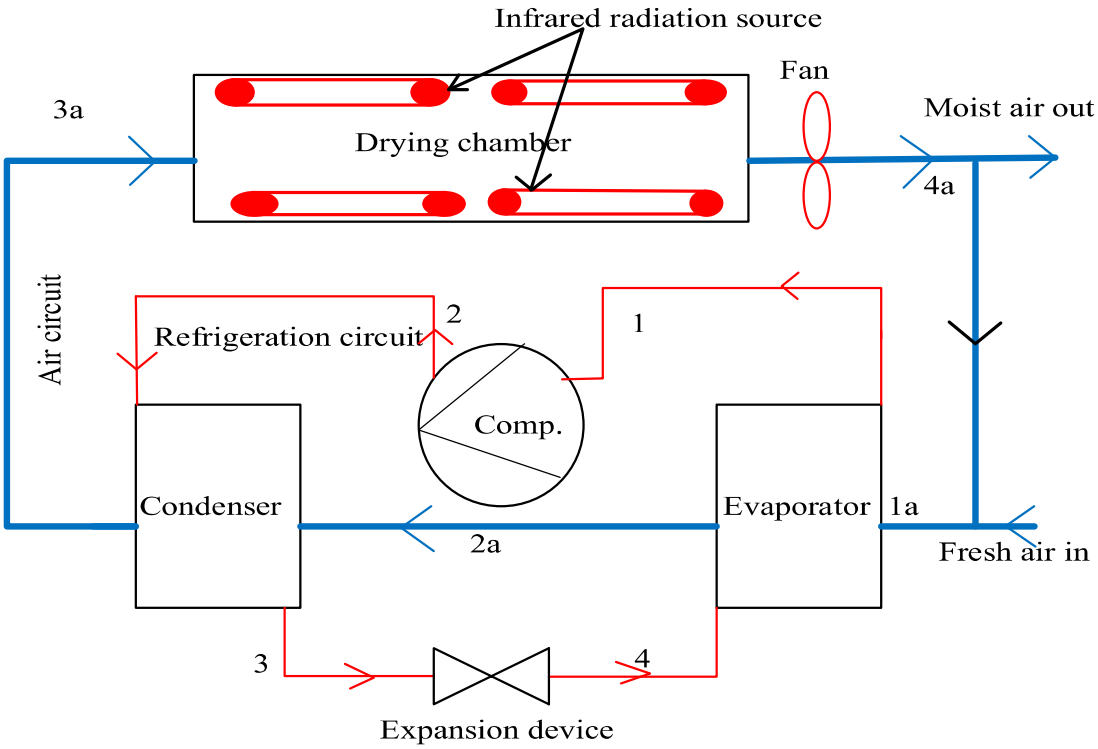

Fig. 1.7: Schematic diagram of infrared assisted heat pump dryer

1.3.4. Radio frequency assisted heat pump dryer

Radio frequency assisted heat pump dryer is the combination of the heat pump cycle and the radio frequency generating system capable of imparting radio frequency energy to the drying material at various stages of the drying process. This radio frequency energy helps to break the dipole bonds between the water molecules inside the products and removes the moisture at a faster rate as compared to the simple heat pump drying

system. Figure 1.8 represents the schematic diagram of the radio frequency assisted heat pump dryer.

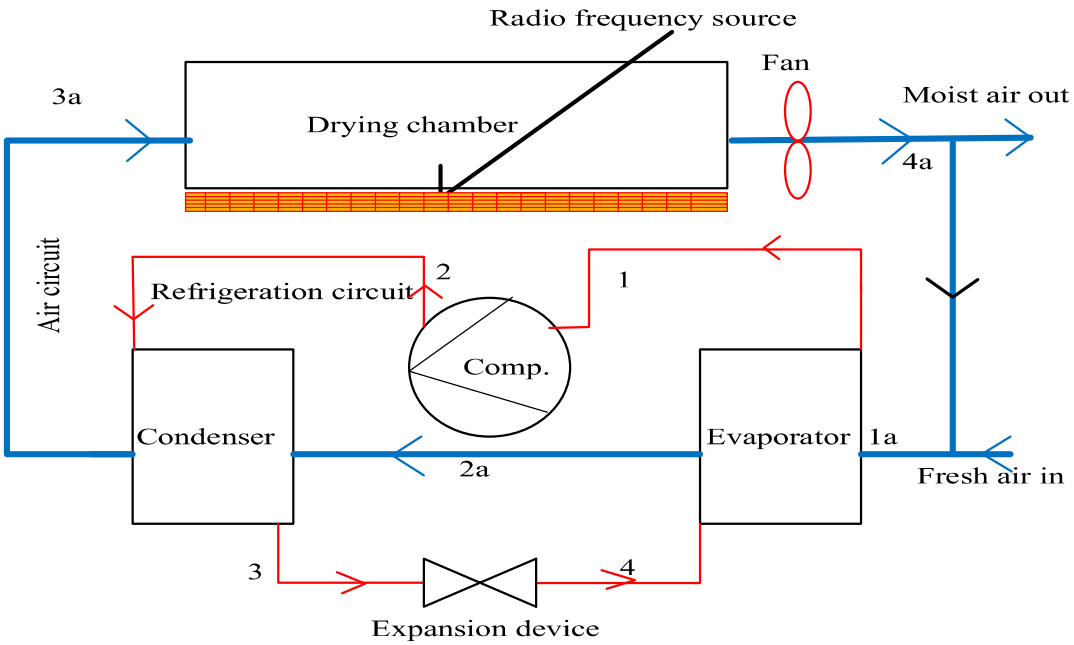

Fig. 1.8: Schematic diagram of radio frequency assisted heat pump dryer

1.4. Contribution of the study

The main contribution of this study is to design, develop, and performance analysis of the simple heat pump dryer and the hybrid source heat pump dryer for the drying of the different types of drying material. In this study, the experiment is performed for the drying of banana chips and potato with a simple air source heat pump dryer in an open and closed-loop system. The energetic and the exergetic performance comparison of the different low global warming potential (GWP) refrigerants have been carried out numerically for the heat pump drying application. The economic, exergoeconomic and the performance investigation is carried out for the hybrid source heat pump dryer which is the combination of the solar energy, infrared energy source, and the heat pump system for the radish chips drying. This study also studied the hybrid source heat pump dryer assisted with waste heat recovery from the IC engine exhaust (diesel engine). A solar-assisted heat pump dryer is developed and experimented with using the solar water heater

as a solar energy source and the economic, exergoeconomic, and thermal performance is investigated. The novelty of the present study is that the combination of the three types of energy solar, infrared, and the heat pump is studied for the food chips drying. The thermal performance, economic, and the exergorconomic study of the solar-assisted heat pump dryer is carried out in this study for the first time using the solar water heater as an energy source for the drying system. For the very first time, the waste heat from the exhaust of a diesel engine is utilized as the energy source with a heat pump dryer. The intermittent drying with a solar-assisted heat pump dryer is carried out for the first time in this research analysis using energy, exergy, and economic methods. A heat pump dryer with air conditioning (combine HPD + air conditioning) is studied to evaluate the performance of the combined system with a single energy input source. The variation of the different parameters such as moisture extraction rate (MER), specific moisture extraction rate (SMER), drying rate, drying efficiency, energy efficiency, second law efficiency, and the exergy destruction is studied according to with drying time.

1.5. Thesis structure

This study is distributed in nine chapters. In the **first chapter**, the basic background, including the simple heat pump dryer and hybrid source heat pump dryer and thesis contribution are provided. In the **second chapter,** a literature survey on the theoretical and experimental study on simple heat pump dryers and the theoretical and experimental study on hybrid source heat pump dryers including the drying temperature and the type of refrigerant, and the energy sources used. In the **third chapter**, a numerical study of the heat pump dryer for the design and the performance of a simple heat pump dryer for the different types of future refrigerants is studied and the performance of the drying system is evaluated. **The fourth chapter** included the design, development, and experimental analysis of the simple heat pump dryer for the dying potato and the banana

chips in an open and closed system. In the **fifth chapter**, design development and the performance analysis of the solar-infrared assisted heat pump dryer are included in the closed system for the drying of banana chips. In this chapter, the energy, exergy, economic, and the exergoeconomic analysis are performed. **The sixth chapter** contains the details about the performance analysis of the heat pump dryer with waste heat recovery from the IC engine exhaust using the energy-exergy and economic-exergoeconomic methodology. In the **seventh chapter**, the experimental study of the intermittent drying of the solar-assisted heat pump dryer is included with a closed system for the drying of the agricultural products. In this chapter, the performance, economic and exergoeconomic analysis of the solar-assisted heat pump intermittent drying of food chips is presented. The analysis of the heat pump dyer integrated with the air conditioning in a hot atmosphere is included in the **eighth chapter**. In this chapter, the performance of the heat pump dyer with air conditioning is carried out in a single heating and cooling system. Finally concluding remarks from the all numerical and experimental study of the heat pump dryer and the hybrid source heat pump dryer and the future scope of the present study are presented in the **ninth chapter**.

CHAPTER 2

LITERATURE REVIEW

In this chapter, literature on the heat pump dryer related to the simple heat pump dryer and hybrid source heat pump dryer is considered (theoretical and experimental work). The available open literature is divided into the four subsections for an easy understanding of the research gap, the first part contains the theoretical work done on a simple heat pump dryer, the second part contains the experimental work done on a simple heat pump dryer, the third part contains the theoretical work done on hybrid source heat pump dryer and fourth part contains the experimental work done on hybrid source heat pump dryer. Finally, the research gap and the objective of the current study are presented in this chapter.

2.1. Theoretical studies on simple heat pump dryer

Theoretical analysis of any system is done by applying the different mathematical models and solving the models by using different techniques and software. Theoretical analysis can be easily done as compared to the experimental analysis, which needs the design, development, and performance analysis of the experimental setup. The main advantage of applying the theoretical analysis is the reduction in the cost of the analysis. Many open works of literature are available on theoretical analysis of the simple heat pump dryer.

Schmidt et al. (1998) numerically compared the performance of the heat pump dryer using the CO_2 as a natural refrigerant with the R134a refrigerant. The authors concluded the better performance with the CO_2 heat pump dryer compared to the R-134a. Ogura and Mujumdar (2000) proposed the concept of a new eco-friendly chemical heat pump dryer that uses chemical energy in the heat pump. Achariyaviriya et al. (2000)

developed a mathematical model and perform the simulation using the moisture content of the papaya glace and also the simulation results were validated with the experiment. The simulation was done at a drying air temperature of 45°C, 10.3 kg/h of flow rate, and 70% of ambient relative humidity. The author concluded that the SMER decreases with an increase in the ambient humidity and temperature. Adapa et al. (2002) developed a simulation model of the heat pump dryer and validated the model with the experimental data for the drying of the chopped alfalfa in the temperature range of 30-45°C. Braun et al. (2002) numerically compared the performance of the air heat pump dryer (which works on the reverse Brayton cycle) with the conventional electric heater dryer for the clothes drying using the EES software and considered the air temperature at the inlet and outlet of drum dryer as 118°C and 38°C. The authors concluded that the improvement in energy efficiency was 40% over the conventional electric heater at an airflow rate of 110kg/h with an ambient relative humidity of 60%. Teeboonma et al. (2003) developed a mathematical model to study the optimum range of the different parameters such as recirculation ratio, by-pass ratio, and the drying air temperature for the fruit drying with the heat pump dryer and suggested a mathematical model for the mango and papaya slice drying. The author estimated the optimum drying condition for the papaya as 69% by-pass ratio, 100% recirculation ratio, 55°C air temperature, and 20.72kg/h air flow rate and for mango, it was like 71% by-pass ratio, 100% recirculation ratio, 55°C air temperature, and 30.88 kg/h air flow rate. Saensabai and Prasertsan (2003) studied the optimum operating mode of a heat pump dryer in different five modes within the ambient temperature range of 20-40°C. The authors observed that the drying rate and the ambient conditions mostly affect the operating mode of the heat pump dryer. Sarkar et al., 2006, numerically studied the heat pump dryer using the natural CO_2 gas as a refrigerant to investigate the performance of the system in different bypass air ratios and the air

recirculation ratio with different drying ambient temperatures (20-40°C), relative humidity (30-70%), efficiency and the mass flow rate of air. The author concluded that both SMER and the COP decrease with an increase in both bypass ratio and the air recirculation ratio. Soylemez et al. (2006) developed a mathematical model for the study of the heat pump drying system with heat recovery using thermodynamic economic methods to obtain the optimum operating condition of the system.

Pal and Khan (2008) presented the various design steps for the heat pump dryer (batch type) and calculated the different performance parameters for different drying air temperatures (30°C, 35°C, 40°C) and relative humidity (30%, 20%, 15%). The calculated values of SMER and COP of the system were 1.84kg/kWh and 4.1 respectively at a drying temperature of 40°C and relative humidity of 15%. Le et al. (2008) carried out the thermal and economic analysis of the absorption heat pump dryer for the wood chips drying. The considered drying temperature was 100°C. Ceylan and Aktaş (2008) used the artificial neural network to estimate the errors in the experimental results in the heat pump dryer for the hazelnuts at different velocities, moisture content, and drying air temperature. Li et al. (2009) numerically investigated the CO_2 heat pump dryer and compared the result of the two-stage heat pump dryer with the single stage. The author concluded that the MER was much higher for the two-stage as compared to the single stage. Lee and Kim (2009) performed the simulation of the heat pump dryer to obtain the various design parameters of a box-type dryer and validated the simulation result with the experimental for the radish dying. The simulation analysis of the system was carried out by considering the ambient temperature, relative humidity, and air flow rate of 20°C, 100%, and 30m^3/min respectively. The SMER and the COP were calculated as 3.64kg/kWh and 3.75 respectively at a drying chamber inlet temperature of 44.7°C. Minea (2010) developed a mathematical model to predict the error in the design of the

heat pump dryer which is responsible for the variation in the condenser and evaporator saturation pressure with damage to the compressor also. The author suggested the various correlation and methods for proper operation of the system. Lee et al. (2010) carried out the performance simulation of the tow stage heat pump dryer using the two different refrigerants (R-124, R-134a) in two different refrigeration cycles to get the high temperature (greater than 80°C) drying air. Also evaluated the various performance parameters of the heat pump dryer such as COP of high and low-temperature refrigeration cycle as 3.33 and 4.53 with SMER greater than 3.5kg/kWh and MER as 45.51kg/h. Rezk and Forsberg (2011) developed a numerical model and analyzed it by using CFD software comsol to reduce the energy consumption in the heat pump drying system. Cotton et al. (2011) studied the heat pump dryer by developing a mathematical model to evaluate the system performance in isothermal and adiabatic modes using energy, exergy, and economic methods. SMER and MER were calculated as 21.2kg/h and 4.2kg/kWh and for isothermal as 55.4kg/h and 13.7kg/kWh. Hii et al. (2013) investigated the kinetics of the cocoa beans drying with a heat pump dryer using the computer simulation at a constant drying temperature of 56°C. The author analyzed the effect of the shrinkage on the kinetics analysis but found a negligible effect. Hossain et al. (2013) developed a mathematical model to evaluate the performance of the heat pump dryer for aromatic plant drying. The average drying air relative humidity and the temperatures were 20% and 36.84°C respectively and the drying time was 89 hours to reduce the moisture content from 89 to 9% (w.b.) for valerian roots. The authors calculated the values of COP, SMER, and MER as 5.45, 0.038kg/kWh, and 140.03kg/h respectively.

Bengtsson et al. (2014) developed a simulation model of a heat pump tumble dryer to investigate the effect of the compressor cylinder volume and the heat exchange in the condenser on the drying time and the energy consumption in the system and the

simulation model was validated with the experimental results. The author concluded the reduction in drying time by 14% and an increase in energy consumption by 14% with an increase in cylinder volume by 50%. Erdem and Heperkan (2014) theoretically investigated the heat pump tumble drying with natural CO_2 refrigerant using MATLAB computer software, and the dependency of the various parameters on the energy consumption and the drying time was estimated. The author concluded that the optimum values of operating parameters (CO_2 inlet-outlet pressure and temperature to the condenser and evaporator) help to reduce the drying time and the energy consumption. Bockholt et al. (2016) studied the tool chain structure of the heat pump tumble dryer. TeGrotenhuis et al. (2017) developed a mathematical model for a new hybrid heat pump clothes dryer to increase the electric energy savings by 50% and concluded the COP of 2.5 at a drying temperature of 50°C in the dryer drum exhaust. Wang et al. (2018) carried out the analysis of the heat pump dryer with heat recovery using air to the air heat exchanger and heated the ambient air to 200°C and studied the different refrigerants to analyze the heat recovery with lower energy consumption. The author concluded that the R134a was the most promising refrigerant as compared to others in terms of energy efficiency. Holtkotter et al. (2018) studied the rapid controlling of the heat pump dryer for clothes drying. Sian and Wang (2019) numerically studied the CO_2 and R-134a heat pump dryer for clothes drying at ambient temperature and relative humidity of 25°C and 80%. The authors concluded that the CO_2 is having higher drying temperature as compared to the R-134a and also has higher SMER and COP. Brandt et al. (2019) carried out the simulation and experimental validation of the heat pump tumble dryer using the R-744 refrigerant and compare the result with other different refrigerants. Lee et al. (2019) developed a simulation model to study the performance of the heat pump tumble clothes dryer using the different design parameters of the components. Jokeil et al. (2020)

developed a numerical model and validated it with an experiment to study the heat pump dryer for the drying of the organic products using the CO_2 as a working refrigerant at a darting temperature of 50-70°C. It was concluded from the model that the closed-loop heat pump dryer is having 84 % more energy saving compared to the open-loop system and SMER was 4 times higher in a closed-loop system. Dai et al. (2020) developed a simulation model to study the thermodynamic and environmental potential of the heat pump dryer using the R-32and CO_2 mixture as working refrigerants.

Table: 2.1. Literature review on numerical analysis of simple heat pump dryer

Author	Drying product	Refrigerant	Drying temperature	Findings
Schmidt et al. (1998)	……	CO_2, R-134a	60°C	Better performance with CO_2 heat pump dryer compared to the R-134a.
Ogura and Mujumdar (2000)	……..	……..	50°C	The energy and exergy efficiency mostly depends on the chemical reaction.
Achariyaviriya et al. (2000)	Papaya glace	……	50°C	SMER decreases with an increase in the ambient humidity and temperature.
Adapa et al. (2002)	Alfalfa	R-134a	30-45°C	SMER was between 0.5 and 1.02kg/kW-h.
Braun et al. (2002)	Clothes	Air	118°C	The improvement in energy efficiency was 40% compared to the conventional electric heater.
Teeboonma et al. (2003)	Mango, papaya	R-22	55°C	The optimum drying condition was not the

				same for both products at same.
Saensabai, and Prasertsan (2003)	…….	R-22	20-40°C	HPD is suitable for a continuous dryer at constant dryer efficiency.
Sarkar et al. (2006)	…….	CO_2	55-73°C	Drying efficiency, RAR, ambient temperature, and airflow rate have more effect on the system compared to humidity and BAR.
Soylemez (2006)	……	……	25-65°C	Heat pump systems used for drying must be designed close to the optimum point.
Pal et al. (2008)	……..	R-134a	30-40°C	The values of SMER and COP of the system were 1.84 kg/kWh and 4.1 at a drying temperature of 40°C.
Le et al. (2008)	Wood	……	50-100°C	A heat recovery system is the most efficient and economic option.
Ceylan, and Aktaş (2008)	Hazelnut	……	40-50°C	The average error was found as 0.00653 for drying time with ANN.
Li et al. (2009)	…….	CO_2	50-60°C	MER was much higher for the two-stage as compared to the single-stage
Lee and Kim (2009)	Radish	R-134a	44.7°C	SMER and the COP were calculated as 3.64kg/kWh and 3.75 respectively.

Minea (2010)	Wood	.....	70-95°C	Intermittent methods improve the final quality of the product and reduce the total drying time.
Lee et al. (2010)	.....	R-124, R-134a	80°C	COP of high and low-temperature refrigeration cycles were 3.33 and 4.53 with SMER and MER greater than 3.5kg/kWh and 45.5 kg/h.
Rezk and Forsberg (2011)	.....	……..	……..	Design modification shows the improvement in pressure drop in the drying duct.
Cotton et al. (2011)	…….	R-134a	55-70°C	SMER and MER were calculated for adiabatic as 21.2kg/h and 4.2kg/kWh and for isothermal as 55.4 kg/h and 13.7kg/kWh.
Hii et al. (2013)	Cocoa beans	R-22	56°C	Found the negligible effect of the shrinkage on the kinetics analysis.
Hossain et al. (2013)	Aromatic plants	.....	36.84°C	The COP, SMER, and MER as 5.45, 0.038 kg/kWh, and 140.03kg/h respectively.
Bengtsson et al. (2014)	Textiles	R-134a	45-65°C	Reduction in drying time by 14% and increase in energy consumption by 14% with an increase in cylinder volume by 50%.

Erdem and Heperkan (2014)	Clothes	CO_2	.....	Inlet CO2 pressure and temperature to the condenser and evaporator have an acceptable effect on energy consumption and drying time.
Bockholt et al. (2016)	Clothes	.....	.....	Toolchain-based modeling reduces the modeling efforts.
TeGrotenhuis et al. (2017)	Clothes	R-134a	50°C	Concluded the electric energy savings of 50% and the COP of 2.5.
Wang et al. (2018)	.....	R32, R134a, R22, R290	113°C	Concluded the R134a as the most promising refrigerant as compared to others in terms of energy efficiency.
Holtkotter et al. (2018)	Clothes	.....	.....	Concluded the rapid controlling with optimum values.
Sian and Wang (2019)	Clothes	CO_2, R-134a	25-45°C	CO_2 HPD has a higher drying temperature, SMER and COP, compare to the R-134a heat pump system.
Brandt et al. (2019)	Clothes	R-290, R-744	.....	The highest exergy destruction takes place in the compressor.
Lee et al. (2019)	Clothes	R-134a	30-40°C	Increasing the airflow rate yields a higher COP value and a shorter drying time.

Jokeil et al. (2020)	Organic product	CO_2	50-70°C	Closed-loop HPD has 84% more energy-saving and 4 times SMER compared to the open-loop.
Dai et al. (2020)	…….	R-32, CO_2	……..	The SMER rate was improved.

2.2. Experimental studies on simple heat pump dryer

Experimental study of any system needs more time and investment as compared to the numerical analysis but provides the results of the actual condition and is more acceptable. Numbers of open literature are available containing experimental result data on the simple heat pump dryer. Klocker et al. (2001) experimented to evaluate the performance of the heat pump dryer using carbon dioxide. The authors experimented with the two types of the compressor and presented the result of MER, SMER, and SEC as 5kg/h, 2.05kg/kWh, and 0.49kWh/kg at the temperature of 50°C for the semi-hermetic compressor with the energy-saving potential of 65%. Ogura et al. (2002) experimented to investigate the chemical heat pump dryer (chemical reaction heat source). Oktay (2003) experimented to investigate the performance analysis of the heat pump drying system at the different airflow rates, recirculation ratio, and the bypass air ratio for the drying of the wet wool at a maximum air operating temperature of 50°C with R-22 as a working refrigerant. The COP of the whole system was in the range from 2 to 3.5 and SMER was in the range from 1.5 to 2.8 kg/kWh. Oktay, (2003) investigated the performance of the heat pump-assisted mechanical opener dryer for the wool drying in different modes of the recirculation air ratio and bypass air ratio with air velocity from 0.65 to 1.25m/s. The maximum drying temperature was set as 60°C and the refrigerant was R-22 used in this analysis in the ambient temperature and humidity of 15-20°C and

60% respectively. The SMER was in the range from 0.65 to 1.75kg/kWh and the heating coefficient of performance was from 2.47 to 3.95. Ameen and Bari (2004) investigated the performance of the drying chamber using the waste heat of the air conditioning condenser for clothes drying and the results were compared with the commercial dryer and outdoor natural drying. The authors concluded the drying air temperature was about 40°C and air velocity between 0.4-0.6m/s. in the humid atmospheric condition (temperature =28-29°C, humidity = 82-84%). The drying time (2 h) and the drying rate (0.424 kg/h) were much better as compared to the commercial dryer and outdoor natural drying with negligible energy consumption. Queiroz et al. (2004) investigated the drying kinetics of the tomato slices in a heat pump dryer using R-22 refrigerant and compared the result with electric heater drying. The experiment was done at drying temperatures of 40°C, 45°C, and 50°C, and air velocities of 1.5 and 2.0 m/s. The authors concluded the heat pump's effective COP was between 2.56 to 2.68 and then about 40% energy economy as compared to the electric resistance heater drying. Adapa and Schoenau (2005) designed, developed, and experimentally tested the recirculation heat pump dryer for the drying of the specialty crops and herbs in the temperature range of 30-35°C and concluded the SMER in between 0.06-0.61kg/kWh. Chua and Chou (2005) designed, fabricated, and analyzed the two-stage heat pump dryer for better heat recovery in two evaporators and condensers using the R-22 as the refrigerant. The author concluded that the more heat, up to 35% more can be recovered in a two-stage evaporator as compared to the single stage. Fatouh et al. (2006) designed and developed a heat pump dryer for herb drying using R-134a refrigerant and investigated the drying characteristics and the system performance. Experimental results showed that the system performance was better at a drying temperature of 55°C and air velocity of 2.7m/s. The author concluded that the lower size herb requires lower specific energy consumption and dying time.

Hawlader et al. (2006) studied the heat pump drying of the apple, guava, and potato in two inert environments (nitrogen and carbon dioxide) and compare the result with freeze and vacuum drying. The author observed the effect on surface porosity and color at drying temperature and relative humidity of 45°C and 10%. It was concluded that the modified heat pump dryer is having better food quality and the economy as compared to the freeze and vacuum drying. Hawlader et al. (2006) investigated the kinetics of the Indian ginger drying in a heat pump dryer using normal air, nitrogen, and carbon dioxide as drying medium. The experiment was performed at a drying temperature of 40°C, relative humidity of 10%, and air velocity of 0.7m/s and concluded that better product quality and lower drying time with nitrogen and carbon dioxide as compared to the normal air medium.

Ceylan et al. (2007) carried out the energy and exergy analyses of the heat pump dryer (using R-404A refrigerant) for the poplar and pine timber drying at drying air temperature and velocity of 40°C and 0.8 m/s. The author concluded the values of the drying time, COP, and SMER for the poplar and pine at 60% air recirculation ratio as 70h, 1.86 and 0.243kg/kWh and 50 h, 1.87 and 0.188kg/kWh respectively. Alves et al. (2008) designed and developed a two-stage heat pump dryer for the drying of the protein in a fluidized bed dryer. Shi et al. (2008) conducted an experimental investigation of the heat pump dryer (using R-134a refrigerant) for the drying of the horse mackerel and analyzed the effect of the different parameters on the performance and drying kinetics. The drying air temperature and the air velocity ranged from 20-30°C and 2.0-3.0m/s and the SMER was maximum for the bypass air ratio between 0.6-0.8. Pal et al. (2008) studied the drying of the green sweet pepper in a heat pump dryer at 30°C, 35°C, and 40°C temperature and in a hot air dryer at 45°C with a relative humidity range of 19-55%. It was concluded that the heat pump drying at 40°C required less drying time with

a better drying rate and SMER as compared to the hot air drying at 45°C. Phoungchandang et al. (2008) investigated the drying of the Kaffir lime leaf with a tray dryer and heat pump dryer and fitted the different drying models with experimental data for kinetics analysis at drying temperatures of 40°C, 50°C, and 60°C. Phoungchandang et al. (2009) experimentally investigated the performance of the heat pump dryer and compared the result with the tray drying and with the mixed-mode solar drying for the ginger in the temperature range of 40°C, 50°C, and 60°C. Erbay and Icier (2009) experimented to investigate the product quality of the energy potential for the olive leaf drying with a heat pump dryer (using R-407C refrigerant) and optimization of the drying conditions was done using the surface response methodology. The optimum drying air temperature and velocity were 53.43°C and 0.64m/s respectively. Artnaseaw et al. (2010) designed and developed a vacuum heat pump dryer (using R-22 refrigerant) for the chili drying to investigate the effect of the parameters such as temperature (50°C, 55°C, 60°C, 65°C) and pressure (10kPa, 20kPa, 30kPa, 40kPa) on the product quality and drying time. It was concluded that the drying time decreases with a decrease in pressure and increase in temperature of the drying medium and the Midilli model agrees the best for the red chili.

Jinjiang and Yaosen (2010) experimented to study the performance of the heat pump dryer with heat recovery for paddy drying. Chin and Law (2010) compared the intermittent heat pump drying (40.6°C) of Ganoderma tsugae with the freeze-drying (-18°C), convective hot air (50°C) drying, and vacuum drying (50°C). it was found that intermittent drying is having a higher energy efficiency as compared to the other drying methods. Hepbasli et al. (2010) designed and developed a heat pump dryer (using R-407C refrigerant) to investigate the exergoeconomic parameters for the drying of plum slices at drying air temperature between 45-55°C. The ratio of the exergy destruction

rates to capital cost varied between 1.668 and 2.063W/$ and its values were found higher for the compressor, evaporator, and heat recovery unit and need to be improved. Wang et al. (2011) studied the performance and economics of the heat pump drying (using R-22 refrigerant) of hawthorn cake and compared the result with the hot air drying. The drying temperature was in the range of 45-56°C for the heat pump and was between 40-70°C for hot air drying. The author found that at the same drying temperature, the drying rate of hawthorn cake was higher for heat pump drying. Phoungchandang and Saentaweesuk (2011) reported that the modified page model is best fitted for the drying of the sliced ginger with the heat pump dryer at drying temperatures of 40 and 60°C. Castell-Palou and Simal (2011) investigated the drying kinetics of the heat pump dryer for the drying of the pressed cheese and fitted it to the models to estimate the correlations. Mancini et al. (2011) compared the experimental and the theoretical results of the CO_2 heat pump dryer with the R-134a HPD for clothes drying. It was found that the CO_2 heat pump dryer performs better with energy-saving as compared to the R-134a. Gungor et al. (2012) experimentally determined the exergoeconomic analysis of the gas engine-driven heat pump dryer for the drying of the medicinal and aromatic plants and studied the effect of the various dead state temperature on the exergoeconomic parameters. Senadeera et al. (2012) carried out the experimental investigation of the two-stage heat pump drying of the bovine intestine in a fluidized bed dryer and it was concluded that the drying kinetics was mostly affected by temperature. Ong et al. (2012) studied the intermittent drying of the salak fruits with the heat pump dryer at different intermittent ratios and concluded that intermittent drying reduces the drying time by 36%. Hii et al. (2012) experimented to investigate the performance of a heat pump dryer for cocoa beans drying at drying temperatures of 28.2°C, 40.4°C, and 56°C. Minea (2012) experimentally analyzed the heat pump drying of the hardwood using the R-134a as a working refrigerant

in temperature ranges from 39-54°C. the author found the values of COP as 3 and SMER from 2.1 to 2.5kg/kWh. Shi et al. (2013) experimented to investigate the drying kinetics and characteristics of the heat pump drying of the yacon slices at different drying temperature ranges from 5-45°C. Yang et al. (2013) investigated and proposed a method to control the temperature in the closed-loop drying of the heat pump that can be used as a heating and refrigeration cycle.

Erbay and Hepbasli (2013) carried out the advanced exergy analysis of the heat pump dryer using the R-407C refrigerant for the plum drying at drying temperatures of 45°C, 50°C, 55°C, and air velocity of 1.5m/s to investigate the exergy destruction and the inefficiencies in the subcomponents. The author observed that the advanced exergy value increases from 65.94 to 91.95% with the increase in drying air temperature from 45 to 55°C and the inefficiencies in the compressor and condenser are due to internal operating conditions. Ganjehsarabi et al. (2014) experimentally carried out the exergoeconomic analysis of the heat pump tumbler dryer (using R-134a refrigerant) at a drying temperature of the 68°C. The COP values and the SMER were estimated as 2.28 and 1.08kg/kWh respectively. The author concluded that the condenser is having the highest exergy inefficiency (79%) and exergy destruction cost rate. Bellomare and Minetto (2015) studied the hydrocarbons refrigerant in the heat pump dryer such as R-290 and R-441A instead of R-407C and the author concluded the increase in energy consumption with the new refrigerants. Aktas et al. (2015) experimentally investigated the performance of the heat pump dryer (using R-134a refrigerant) for the bay leaves drying and optimized the parameters using the artificial neural network method at drying temperatures of 40°C, 45°C, and 50°C. The COP of the whole system and the energy utilization ratio varies from 2.4-3.2 and 0.22-0.75. Gao et al. (2016) studied the effect of the various drying parameters on the volatile compound in silver carp drying. The

experiment was performed for 5-35°C and concluded that the volatile compound content increases with an increase in velocity and by-pass air ratio. Bansal et al. (2016) studied the air leakage in heat pump clothes dryers to minimize the energy consumption using the new methods suggested by ASTM. Zhu et al. (2016) experimentally investigated the intermittent heat pump drying (using R-22 refrigerant) of the green soybean and analyzed the product kinetics at a drying temperature of 33°C. It was concluded that the intermittent drying and the intermittency give the best result as compared to continuous drying. Chapchaimoh et al. (2016) experimented to investigate the performance analysis of the heat pump dryer (using R-22 refrigerant) for the ginger drying at 50°C drying temperature using nitrogen as a working drying medium. For ginger, the SMER was 0.06 kg/MJ for air medium and 0.07kg/MJ for nitrogen and SEC was 16.67MJ/kg for air and 14.29MJ/kg for nitrogen. Jayaprakash et al. (2016) studied the effect of heat pump drying on the flavor of the tomato and compared the flavor of dried tomato with the fresh and freeze tomato. Yang et al. (2016) proposed a strategy to control the superheat and the drying air temperature simultaneously using a PID controller. Liu et al. (2017) designed and developed a heat pump drying room for the Lentinula edodes and concluded the remarkable energy saving with a better quality of the product as compared to the hot air drying method. Li et al. (2017) studied the effect of ultrasound-assisted osmotic dehydration as pre-treatment for the heat pump drying of the tilapia fillets. Gan et al. (2017) experimentally studied the heat pump dryer (using R-22 refrigerant) for the intermittent drying of the Malaysian edible bird's nest at a drying temperature of 28.6-40.6°C. It was estimated that intermittent drying at 28.6°C of temperature, 26.7% relative humidity, and 0.2 intermittency reduces the drying time by 84.2% with good color quality and energy efficiency. Aktas et al. (2017) experimentally investigated the drying kinetics and the performance analysis of the heat pump dryer (using R-410A refrigerant) for mint

leaves drying in a new cylindrical drying chamber at a drying temperature of 30°C and air velocity of 2, 2.5 and 3.0m/s. The COP of the heat pump and the heat gain in the heat recovery unit were 3.94 and 4.56kWh respectively. Coskun et al. (2017) investigated the drying kinetics of the tomato slices in the closed-loop heat pump dryer at a different drying temperature of 30-45°C. The author concluded the COP and the SMER of HPD as 2.71 and 0.324kg/kWh respectively. Shen et al. (2018) developed and investigated the dual-mode heat pump dryer which can be operated as a single-stage and cascade stage heat pump dryer system depending on the requirement of drying temperature. The maximum temperature that can be obtained was 70°C in cascade mode. Taseri et al. (2018) experimented to study the drying kinetics and the product quality of the grape pomace drying with a heat pump dryer (using R-410A refrigerant) at 45°C of drying temperature. Patel et al. (2018) have studied the performance of the thermoelectric heat pump dryer for clothes drying. Atalay (2019) carried out the comparative analysis of the solar dryer and the heat pump dryer for the drying of the tomato using the exergy and exergoeconomic methodology. Dikmen et al. (2019) experimented to investigate the performance of the vacuum heat pump dryer for the drying of the medical plants such as sweet basil, parsley, and dill leaves at the vacuum pressure of 0.6 bar and the drying temperatures of 36 and 46°C. Gataric et al. (2019) studied the heat pump tumble dryer for textile drying and analyzed the effect of the various parameters such as fan speed, drum speed, and weight and initial moisture content of the material. Mohammadi et al. (2019) studied the performance and kinetics of the heat pump dryer (using R-134a refrigerant) for kiwi fruits drying at drying temperatures of 45°C, 55°C, and 65°C. The authors calculated the convective mass transfer coefficient, SMER, SEC, and drying efficiency at 65°C and 100% air recirculation as 4.12-8.55 E^{-7} m/s, 0.11-0.15kg/kWh, 1.08-1.49 kWh/kg and 9.84-12.15 % respectively. Tajudin et al. (2019) experimented to

investigate the kinetics analysis of the Roselle calyx with a heat pump dryer and compared the result with a solar dryer at a temperature of 40°C, 50°C, and 60°C. Duan et al. (2019) developed a cascade heat pump dryer for the drying of the hawthorn cake to investigate the performance of the system in the temperature range between 66-68°C and compared the result with the hot air dryer. Kumar et al. (2020) experimented to study the performance of the heat pump dryer for the drying of the Moringa leaves under the vacuum pressure inside the drying chamber at the velocity of 1.1 and 1.4m/s. Onyocha et al. (2020) designed and developed a heat pump dryer using R-134 refrigerant for the fabrics drying at a temperature of 49°C. Tunckal and Doymaz (2020) studied the drying of the banana chips in the closed-loop heat pump drying system at different drying air temperatures and investigated the performance of the system and kinetics of the product.

Table: 2.2. Literature review on experimental analysis of simple heat pump dryer

Author	Drying product	Refrigerant	Drying temperature	Findings
Klocker et al. (2001)	Clothes	CO_2	50°C	MER = 5kg/h, SMER = 2.05kg/kWh, SEC = 0.49kWh/kg with 65% energy saving.
Ogura et al. (2002)	……..	……	130°C	Drying air temperature improved with enlarging the heat exchanger.
Oktay (2003)	Wet wool	R-22	50°C	The COP_{WS} = 2 - 3.5, SMER = 1.5 - 2.8kg/ kWh which depends on the recirculation air ratio.

Oktay and Hepbasli (2003)	Wet wool	R-22	60°C	SMER= from 0.65 - 1.75 kg/kWh and the heating coefficient of performance ranged from 2.47 to 3.95.
Ameen and Bari (2004)	Clothes	……..	40°C	The drying time (2h) and the drying rate (0.424 kg/h) were much better.
Queiroz et al. (2004)	Tomato	R-22	40°C, 45°C, 50°C	Heat pump effective COP between 2.56 to 2.68.
Adapa and Schoenau (2005)	Crops, herbs	R-134a	30-35°C	The re-circulating air in HPD made it 22% more energy efficient with 65% reduced drying time.
Chua and Chou (2005)	…….	R-22	……	Recovered 35 % more heat with the two-stage evaporator, with sub-cooler SMER and COP improved.
Fatouh et al. (2006)	Herbs	R-134a	55°C	Lower size herb requires lower specific energy consumption and dying time.
Hawlader et al. (2006)	Apple, guava, potato	……..	45°C	Modified atmosphere HPD having better food quality.
Hawlader et al. (2006)	Ginger	…….	40°C	Better product quality and lower drying time

				with nitrogen and CO_2 medium.
Ceylan et al. (2007)	Poplar, pine timber	R-404A	40°C	The drying time, COP, and SMER for the poplar and pine were 70h, 1.86, 0.243 kg/kWh, and 50h, 1.87, 0.188kg/kWh respectively
Alves et al. (2008)	Protein	…….	……	The two-stage drying is the more efficient and environmentally friendly method.
Shi et al. (2008)	Horse mackerel	R-134a	20-30°C	SMER was maximum for the bypass air ratio of 0.6-0.8.
Pal et al. (2008)	Green sweet pepper	…….	30°C, 35°C, 40°C, 45°C	HPD at 40°C requires less drying time with a better drying rate and SMER as compared to the hot air drying at 45°C.
Phoungchandang et al. (2008)	Kaffir lime leaf	…….	40°C, 50°C, 60°C	Heat pump drying reduced drying time.
Phoungchandang et al. (2009)	Ginger	……	40-60°C	Heat pump drying at 40°C showed the best color and quality of the ginger.
Erbay and Icie (2009)	Olive leaves	R-407C	45-55°C	The optimum drying air temperature and velocity were 53.43°C and 0.64m/s.

Artnaseaw et al. (2010)	Red chili	R-22	50-65°C	Midilli agrees with the best model for the red chili thin layer model.
Jinjiang and Yaosen (2010)	Paddy	……..	42-46°C	The reduction in total drying time, cost and energy consumption were 88%, 64%, and 58%.
Chin and Law (2010)	Ganoderma tsugae	……	40.6°C	Heat pump drying has better product quality.
Hepbasli et al. (2010)	Plum slice	R-407C	45-55°C	The exergy destruction rates to capital cost ratio varied between 1.668 and 2.063W/$.
Wang et al. (2011)	Hawthorn cake	R-22	40-70°C	The drying rate was higher for HPD at the same drying air temperature.
Phoungchandang and Saentaweesuk (2011)	Ginger	…….	40-60°C	The HPD with two-stage drying could reduce the drying time at 40 ◦C by 59.32%.
Castell-Palou and Simal (2011)	Cheese	…….	0°C, 4°C, 8°C, 12°C	The mean relative error (MRE = 2.9%).
Mancini et al. (2011)	Clothes	CO_2,R-134a	30-50°C	A CO_2 heat pump dryer can be recommended for a household dryer.
Gungor et al. (2012)	Medical plants	……	45°C	The performance of the drying process

				increases at low ambient temperature.
Senadeera et al. (2012)	Bovine intestine	R-134a	-5-25°C	The investigation showed that the drying kinetics were mostly affected by temperature.
Ong et al. (2012)	Salak fruit	……	26-90°C	The heat pump intermittent drying reduced the drying time by 36%.
Hii et al. (2012)	Cocoa beans	……	28-56°C	Percent retention of cocoa polyphenols ranged from 44% to 73% as compared to the freeze-dried sample.
Minea (2012)	Wood	R-134a	39-54°C	The COP as 3 and SMER from 2.1 to 2.5kg/kWh.
Shi et al. (2013)	Yacon	……	5-45°C	The effective diffusivity coefficients increased with increasing drying temperature.
Yang et al. (2013)	……	…….	30, 35, 38°C	The temperature fluctuations were reduced when using parallel conversion control.
Erbay and Hepbasli (2013)	Plums	R-407C	45-55°C	Inefficiencies in the compressor and condenser are due to

				internal operating conditions.
Ganjehsarabi et al. (2014)	Clothes	R-134a	68°C	The COP values and the SMER were estimated as 2.28 and 1.08kg/kWh.
Bellomare and Minetto (2015)	Clothes	R-290, R-441A, R-407C	……	Experimental data showed that R441A had very low compression efficiency.
Aktas et al. (2015)	Bay leaves	R-134a	40°C, 45°C, 50°C	The COP of the whole system and the energy utilization ratio varies from 2.4-3.2 and 0.22-0.75.
Gao et al. (2016)	Silver carp	……	5°C, 20°C, 35°C	optimum temperature, velocity, and bypass ratio for drying were 20°C, 1.65m/s, and 0.6 respectively.
Bansal et al. (2016)	Clothes	……..	…….	Conclude the ASTM as an effective method to determine the air leakage in drying system.
Zhu et al. (2016)	Green soybean	R-22	33°C	Intermittent drying gives the best result.
Chapchaimoh et al. (2016)	Ginger	R-22	50°C	The SMER was 0.06kg/MJ for air medium and 0.07 kg/MJ for nitrogen.

Jayaprakash et al. (2016)	Tomato	……..	40°C	The volatile and sensory profiles of heat pump dried tomato were better than freeze-dried tomato, with good content of fresh aroma.
Yang et al. (2016)	……	……..	28-31.2°C	The overshoot of drying temperature was less than 0.3°C and the superheat is controlled at 5±0.5°C during drying.
Liu et al. (2017)	Lentinula edodes	……..	33°C	The hump pump drying room is reasonable and reliable; the energy-saving and emission reduction effect is remarkable.
Li et al. (2017)	Tilapia fillets	……..	45°C	The ultrasound-assisted osmosis pre-treatment can improve the quality of the product.
Gan et al. (2017)	Bird's nest	R-22	28.6-40.6°C	Intermittent drying reduces the drying time by 84.2% with good color quality and energy efficiency.

Aktas et al. (2017)	Mint leaves	R-410A	30°C	COP of the heat pump and the heat gain in the heat recovery unit were 3.94 and 4.56 kWh respectively.
Coskun et al. (2017)	Tomato slices	…….	35°C, 40°C, 45°C	The SMER and COP of HPD were obtained as 0.324kg/kWh and 2.71.
Shen et al. (2018)	…….	R-22, R-134a	70°C	The COP of single-stage was higher.
Taseri et al. (2018)	Grape pomace	R-410A	45°C	The heat pump dryer has 51% less energy consumption compared to the convective dryer.
Patel et al. (2018)	Clothes	…….	35-40°C	A faster drying time of 96 min was observed as compared to the 159min in an electric heater.
Atalay (2019)	Tomato	R-404A	50-60°C	The exergoeconomic factor values were determined as 0.514 for solar dryer, and 0.045 for HPD.
Dikmen et al. (2019)	Sweet basil, parsley, dill leaves	……	36°C, 46°C	Chi-square values were found to be varying from $6.98E^{-07}$ to $1.2E^{-06}$ for sweet basil samples.

Gataric et al. (2019)	Textiles	……	……	This resulted in higher energy efficiency with high load, high drum speed, and low fan speed.
Mohammadi et al. (2019)	Kiwi fruits	R-134a	45°C, 55°C, 65°C	The SMER was found as 0.11-0.15kg/kWh.
Tajudin et al. (2019)	Roselle calyx	……..	40, 50, 60°C	Better product quality for the heat pump as compared to solar drying.
Duan et al. (2019)	Hawthorn cake	R-134a	66-68°C	The SMER was found to be 0.93kg/kWh.
Kumar et al. (2020)	Moringa leaves	R-134a	50°C	MER increases with a decrease in pressure and increase in temperature and velocity of drying air.
Onyocha et al. (2020)	Fabrics	R-134a	49°C	The COP of the system was estimated as 10.09.
Tunckal and Doymaz (2020)	Banana	……	37°C, 40°C, 43°C	The SMER and COP were obtained as 0.212kg/kWh and 3.059.

2.3. Theoretical studies on hybrid source heat pump dryer

The hybrid source heat pump dryer uses an extra source of energy assisted with the heat pump cycle to increase the performance of the drying system. Most of the researchers are working on the nonconventional source of energy to assist the heat pump dryer because of the availability at very low cost or free of cost. Many researchers have

worked theoretically on the solar-assisted, ground source-assisted, and infrared-assisted heat pump dryer using the mathematical modeling of the system.

Hawlader and Jahangeer (2006) developed a simulation program for the solar-assisted heat pump drying system and obtained the COP of 7.5 at 1800 rpm of compressor and SMER of 0.65 at 1200rpm for the 20kg drying of the green beans. Slim et al. (2008) developed a mathematical model to study the performance of the solar heat pump (using R-407C refrigerant) sludge drying system. For the mild climatic period, the COP of the heat pump was 5.2 and for the winter season, it was found to be 4.9. Kuan et al. (2019) proposed a numerical model to study the thermal performance of the solar-assisted heat pump dryer (using R-134a refrigerant) and compared the result with heat pump and solar dryer in different climatic conditions for the banana drying. The drying temperature ranges from 20-50°C for all types of systems. The author estimated the drying time for the heat pump dryer and solar dryer as 21h and 35h and solar-assisted heat pump dryer, the COP and SMER were 2.72 and 0.6kg/kWh. Ismaeel and Yumrutas (2020) developed a simulation model for the performance analysis of the solar-assisted heat pump dryer with energy storage and heat recovery using a flat plate solar collector. At a drying temperature of 60°C for wheat drying, the values of COP and SMER were 5.55 and 9.25kg/kWh with an airflow rate of 100kg/h.

Table: 2.3. Literature review on theoretical analysis of hybrid source HPD

Author	Drying product	Source of energy	Drying temperature	Findings
Hawlader and Jahangeer (2006)	Green beans	Solar energy	50°C	The COP of the system is 7.5 at 1800 rpm of compressor and SMER as 0.65 at 1200 rpm for the 20 kg.

Slim et al. (2008)	…….	Solar energy	50°C	For the mild climatic period, the COP of the heat pump was 5.2 and for the winter season, it was found to be 4.9.
Kuan et al. (2019)	Banana	Solar energy	20-50°C	The COP and SMER were 2.72 and 0.6kg/kWh.
Ismaeel and Yumrutas (2020)	Wheat	Solar energy	60°C	The values of COP and SMER were 5.55 and 9.25kg/kWh with an airflow rate of 100kg/h.

2.4. Experimental studies on hybrid source heat pump dryer

Many open experimental works of literature are available on the hybrid source heat pump dryer using solar energy, ground source energy, infrared energy, and other sources for the drying of the different products.

Best et al. (1996) experimented to investigate the performance analysis of the solar-assisted heat pump dryer for rice drying at an average drying temperature of 30.8°C. The estimated values of COP and SMER were 5.3 and 3.5kg/kWh respectively. Hawlader et al. (2003) designed and developed the solar-assisted heat pump dryer with water heating for the drying of the food grains at the drying. The experimental and simulation value of COP were found as 5.0 and 7.0 respectively with solar fraction values of 0.65 and 0.61 for simulation and experimental. Hawlader and Jahangeer (2006) investigated the performance of the solar-assisted heat pump dryer using the experimental analysis with the simulation model for the drying of the green beans at a drying temperature of 45-55°C. The COP, SMER, and the solar fractions were 7.0, 0.65kg/kWh, and 0.81 respectively. The authors concluded that both COP and SMER decrease with an increase in compressor speed. Xie et al. (2006) studied the solar-assisted heat pump dryer with energy storage for the drying of the agricultural products at

different temperatures of 40°C, 50°C, and 60°C respectively. COP of the solar-assisted heat pump drying system was 5.369, while it was 3.411 without solar assisted. Kuzgunkaya and hepbasli (2007) carried out the exergy analysis of the ground source-assisted heat pump dryer for laurel leaves drying and investigated the effect of the drying temperature on exergy loss and exergy efficiency. Colak et al. (2008) experimentally investigated the ground source-assisted heat pump dryer for the drying of the mint leaves in the temperature range of 40-50°C. Aktas et al. (2009) carried out the performance and the kinetic analysis of the solar dryer and the heat pump dryer for the apple slice drying at a temperature of 40°C for the heat pump and 16-30°C for the solar dryer. The effective moisture diffusivity for heat pump and solar dryer were $2.36E^{-8}$ and $1.03E^{-8}$ respectively with a drying time of 3.5h for heat pump drying. Fadhel et al. (2010) experimentally investigated the performance of the solar-assisted chemical heat pump dryer and also a simulation model was developed and compared the predicted results with the experimental data for the drying of the lemongrass at 55°C temperature and 30% of relative humidity. The solar fraction and the COP of the system were found as 0.713 and 2. Deng et al. (2011) studied the far-infrared assisted heat pump dryer and investigated the drying kinetics and properties of squid fillets at different combinations of the heat pump and infrared radiation. Gungor et al. (2011) analyzed the exergy performance of the gas engine-driven heat pump (using R-407C refrigerant) dryer with the utilization of the exhaust heat for heating the drying air for the drying of the medicinal and aromatic plants at a drying temperature of 45°C and air velocity of 1.0 m/s. It was concluded that 60% of exergy accounts for the gas engine, expansion valve, and drying ducts, and the overall exergy efficiency ranges from 48.24 to 51.28 %. Li et al. (2011) conducted the numerical and the experimental analysis of the solar-assisted heat pump dryer for the drying of the corn grain in house storage at drying temperature between 20-40°C. The

dying rate was increased with the increase of drying air by 8.9°C with solar-assisted heat pump drying. Mortezapour et al. (2012) carried out the experimental analysis of the hybrid solar-assisted photovoltaic heat pump dryer (using R-134a refrigerant) for the saffron drying at drying temperatures of 40°C, 50°C, and 60°C. It was concluded that the energy consumption decreases by 33% with solar-assisted HPD and the maximum values of drying efficiency and SMER were 72% and 1.16kg/kWh at 60°C of drying air.

Rahman et al. (2013) experimentally and numerically carried out the economic analysis of the solar-assisted heat pump dryer (using R-134a refrigerant) at a drying temperature of 50°C for the drying of food grains. Based on economic analysis, the payback period was found to be more than 4 years. Sevik et al. (2013) investigated the performance analysis of the solar-assisted heat pump dryer which can be used as only solar dryer and heat pump dryer as well as both together. The author dried the mushroom at drying temperatures of 45 and 55°C and found the SMER varies from 0.26 to 0.92kg/kWh. Zielinska et al. (2013) studied the microwave-assisted fluidized bed heat pump drying of the green peas and compared the result with the fluidized bed heat pump freeze-drying and fluidized bed heat pump convective hot air drying. Erbay and Hepbasli (2014) experimented and determined the advanced exergy analysis of the ground source heat pump dryer (using R-22 refrigerant) for food drying at a drying temperature of 45°C and relative humidity of 16-19%. The conventional and advanced exergy efficiency values were found as 77.05% and 93.5%. Sevik (2014) experimented to analyze the solar-assisted heat pump system for the drying of the tomato, strawberry, mint, and parsley at a drying temperature of 50°C. The specific moisture extraction rate was between 0.03 to 0.46kg/kWh. Mohanraj (2014) investigated the performance of the solar hybrid heat pump (using R-22 refrigerant) dryer for the copra drying in a hot and humid environment at a drying air temperature of 41-48°C. The average value of COP and SMER were found

as 2.54 and 0.79kg/kWh with higher quality as compared to the other drying methods. Wang et al. (2016) studied the infrared assisted heat pump dryer to investigate the moisture distribution and the kinetics of the squid fillets with infrared radiation at 100, 500, and 800 W. All the experiments were conducted at the drying temperature and air velocity of 40°C and 2m/s. The author concluded the significant effect of infrared radiation on the moisture distribution and rate of water sorption. Yahya et al. (2016) investigated the thermal performance of the solar dryer and the solar-assisted heat pump dryer for the drying of the cassava roots. The drying temperature was 40°C for the solar dryer and 45°C for the solar-assisted heat pump dryer at an air mass flow rate of 0.124kg/s and takes the drying time 13 h and 9 for SD and SAHPD. The average COP of the heat pump system was 3.38 with SMER of 0.38kg/kWh for solar dryer and 0.47kg/kWh for solar assisted HPD. Aktas et al. (2016) developed a heat pump dryer (using R-134a refrigerant) and the infrared and investigated the performance of both dryers for the drying of the stale bread at drying temperatures of 40°C, 45°C, and 50°C. The COP of the whole system was calculated as 3.7 and drying efficiency was 39% and 25% for the infrared dryer and heat pump dryer. Qiu et al. (2016) developed a solar-assisted heat pump drying system with heat recovery and thermal storage of the solar energy which can be operated as either a solar dryer, heat pump dryer, or solar-assisted heat pump dryer for the radish, pepper, and mushroom drying. The drying temperature ranged from 30°C to 50°C and calculate the COP varies from 3.21 to 3.49. The author calculated the payback period for the radish, pepper, and mushroom as 6 years, 4 years, and 2 years respectively. Ceylan and Gurel (2016) studied the thermal performance of the fluidized bed solar assisted heat pump drying system for the mint leaves drying using energy and exergy methodology at drying temperature of 45°C for the solar system and 50°C for the HPD system. The author calculated the energy and exergy efficiency of the

SAHPD system as 50% and 26% respectively with the COP of the HP system as 5.0. Tham et al. (2017) studied the performance of the solar greenhouse-assisted heat pump dryer for the drying of the Java tea and the Sabah snake grass.

Erbay and Hepbasli (2017) carried out the exergoeconomic investigation of the ground source heat pump (using R-22 refrigerant) dryer at a drying temperature of 40°C and relative humidity of 16-19%. From the exergoeconomic analysis, the author concluded the compressor is the most important component of the system with a total cost rate of 1.347$/h and exergoeconomic factor of 0.029. Aktas et al. (2017) conducted the experimental performance analysis of the hybrid source of drying system that combines the advantages of the infrared radiation and the heat pump system (using R-134a refrigerant) at a drying temperature of 45-50°C and air velocity of 0.5m/s for the grated carrot drying. The energy efficiency, COP, and exergy efficiency varied from 5.3-50%, 2.11-2.96, and 31.6-66.8% respectively.

Table: 2.4. Literature review on experimental analysis of hybrid source HPD

Author	Drying product	Source of energy	Drying temperature	Findings
Best et al. (1996)	Rice	Solar energy	30.8°C	The estimated values of COP and SMER were 5.3 and 3.5kg/kWh respectively.
Hawlader et al. (2003)	Foodgrains	Solar energy	.....	The experimental and simulation value of COP and solar fraction were found as 5.0 and 7.0 and 0.65 and 0.61.
Hawlader et al. (2006)	Green beans	Solar energy	45-55°C	The COP, SMER, and the solar fractions were 7.0,

				0.65kg/kWh, and 0.81 respectively.
Xie et al. (2006)	Agriculture product	Solar energy	40, 50, 60°C	The COP of the SAHP drying system is 5.369, while it is 3.411 without solar energy inputs.
Kuzgunkaya and Hepbasli (2007)	Laurel leaves	Ground source energy	40-50°C	The exergy efficiencies of the dryer increase with rising the drying air temperature.
Colak et al. (2008)	Mint leaves	Solar energy	40-50°C	The exergy efficiency was maximum at the temperature of 50°C and a drying air mass flow rate of 0.05kg/s.
Aktas et al. (2009)	Apple	Solar energy	40°C, 16-30°C	The effective moisture diffusivity for the heat pump and solar dryer were $2.36E^{-8}$ and $1.03E^{-8}$.
Fadhel et al. (2010)	Lemongrass	Solar energy	55°C	The solar fraction and the COP of the system were found as 0.713 and 2.
Deng et al. (2011)	Squid fillets	Infrared energy	50°C	HP dried squids had higher equilibrium moisture contents followed by HP + 5FIR and HP + 20FIR.
Gungor et al. (2011)	Medicinal, aromatic plants	Gas engine	45°C	The overall exergy efficiency ranges from 48.24 to 51.28%.
Li et al. (2011)	Corn grain	Solar energy	20-40°C	The dying rate was increased with the increase of drying air by 8.9°C with

				solar-assisted heat pump drying.
Mortezapour et al. (2012)	Saffron	Solar energy	40°C, 50°C, 60°C	The maximum values of drying efficiency and SMER were 72% and 1.16 kg/kWh at 60°C of drying air.
Rahman et al. (2013)	Foodgrains	Solar energy	50°C	The payback period was found to be more than 4 years.
Sevik et al. (2013)	Mushroom	Solar energy	45-55°C	Moisture extraction rate (SMER) values were found to vary between 0.26 and 0.92kg/kW h.
Zielinska et al. (2013)	Green peas	Microwave energy	…….	The hardness of the product increases with the microwave vacuum assisted.
Erbay and Hepbasli (2014)	Foodgrain	Solar energy	45°C	The conventional and advanced exergy efficiency values were found as 77.05% and 93.5%.
Sevik (2014)	tomato, strawberry, mint, parsley	Solar energy	50°C	The specific moisture extraction rate was between 0.03 to 0.46kg/kWh.
Mohanraj (2014)	Copra	Ground source energy	41-48°C	The average value of COP and SMER were found as 2.54 and 0.79kg/kWh.
Wang et al. (2016)	Squid fillets	Infrared energy	40°C	There was a significant effect of infrared radiation on the moisture

				distribution and rate of water sorption.
Yahya et al. (2016)	Cassava	Solar energy	40°C, 45°C	The SMER of 0.38kg/kWh for solar dryer and 0.47kg/kWh for solar assisted HPD.
Aktas et al. (2016)	Stale bread	Infrared energy	40°C, 45°C, 50°C	The COP of the whole system was calculated as 3.7.
Qiu et al. (2016)	Radish, pepper mushroom	Solar energy	30°C, 50°C	The payback period for the radish, pepper, and mushroom were 6 years, 4 years, and 2 years respectively.
Ceylan and Gurel (2016)	Mint leaves	Solar energy	40°C- 50°C	The energy and exergy efficiency of the SAHPD system as 50% and 26%.
Tham et al. (2017)	Java tea, Sabah snake grass	Solar energy	45°C	Applying the heat pump with a solar greenhouse improves the drying rate.
Erbay and Hepbasli (2017)	……..	Ground source energy	40°C	The compressor has a total cost rate of 1.347$/h and exergoeconomic factor of 0.029.
Aktas et al. (2017)	Carrot	Infrared energy	45°C, 50°C	The energy efficiency, COP, and exergy efficiency varied from 5.3-50%, 2.11-2.96, and 31.6-66.8% respectively.
Yahya et al. (2017)	Rice	Solar energy	80.6°C	The average SMER was 0.24kg/kWh with a payback period of 1.6 years.

EI khadraoui et al. (2017)	…….	Solar dryer	68°C	The energy efficiency of the solar energy accumulator reached 33.9%.
Rabha et al. (2017)	Ghost chili paper and ginger	Solar dryer	42-61°C	The SEC of the ghost chili and the ginger were 18.72kWh/kg and 8.82kWh/kg.
Lakshmi et al. (2019)	Stevia leaves	Solar dryer	50-59.5°C	The overall dryer efficiency and average exergy efficiency of the MFSCD were found as 33.5% and 59.1%, respectively.
Ekka et al. (2020)	Black ginger	Solar dryer	45-62°C	The estimated SECs for Case – 1 and Case – 2 were 1.0 kWh/kg and 0.56kWh/kg, respectively.
Ekka et al. (2020)	Red chili	Solar dryer	33-49.8°C	The FCMS dryer with PCM reduces the drying time by nearly 50%.
Khanlari et al. (2020)	Apricot	Solar air heater	45.9-50.8°C	The average efficiency of T-SAH was obtained as 45.56%, 53.29%, and 56.77% at 0.010, 0.013, and 0.015kg/s air flow rates, respectively.
Kumar et al. (2021)	…….	Solar dryer	……..	The value of energy and exergy efficiency of the SAH was obtained as 62.8% and 5.848%.

2.5. Research gap

After going through the literature survey, many literature gaps were found which are summarized below,

- No work is done on heat pump dryer using the low GWP refrigerants like R1234yf, R1234ze, and R152a (future refrigerants).
- No work is done on the solar-infrared-assisted heat pump dryer (SIAHPD)
- Little work is done on the economic and exergoeconomic analysis of the solar-assisted heat pump dryer
- No work is done on the heat pump dryer assisted with waste heat recovery from the exhaust of the IC engine
- No work is done on the intermittent drying of the solar-assisted heat pump dryer
- Little work is done on the heat pump dryer with air conditioning in a hot and humid environment

2.6. Objective of the present study

The research objectives of the present study are given below,

- Numerical analysis of heat pump dryer using low GWP refrigerants to compare their performances
- Design, development, and performance analyses of the dual-mode heat pump dryer
- Experimental study on solar-infrared assisted heat pump dryer and energy, exergy and economic analyses
- Experimental study on waste heat recovery assisted hybrid heat pump dryer and energy, exergy and economic analyses

- Experimental study on intermittent drying with solar-assisted heat pump dryer and energy, exergy, and economic analyses
- Experimental study on air conditioning integrated heat pump dryer and energy, exergy and economic analyses

CHAPTER 3

EXPERIMENTATION ON SIMPLE HEAT PUMP DRYER

This chapter deals with the fabrication of the simple vapor compression heat pump dryer (HPD), instrument details, and experimental procedure. The experiment was performed to compare the open and closed systems for the drying of the banana and the potato chips. The closed and open system analyses are important to study due to the recovery of waste heat at the dryer outlet as compared to the open system. The experimental setup consists of the drying cabin, compressor, condenser, evaporator, fan, expansion device, and trays inside the cabin. The result obtained from the experiment for the drying of the banana and the potato chips in an open and closed system is also discussed in this chapter. The uncertainty of the experiment is given in this chapter for the different performance parameters.

3.1. Experimental setup and procedure

The design, development, and fabrication of a batch-type convective heat pump dryer are done, and the experiment was performed for the drying of the different agricultural products in an open and closed-loop system. Fig. 3.1 represents the schematic diagram of the open and closed-loop heat pump drying system. The location of the different components of the system and the measuring instruments are shown in Fig. 3.1. The system is designed in such a manner that it can be operated in two modes (open loop and closed loop) based on the recirculation of the dryer exhaust air through the drying system. For the open mode system, the exhaust air from the drying chamber outlet was directly allowed to go into the atmosphere. Whereas, for the closed mode system, the drying air is forced to recirculate in the system by opening the sliding door between the evaporator inlet and drying chamber outlet. The basic components of the

heat pump system are compressor, condenser, evaporator, and expansion device. The R134a refrigerant is used in the heat pump system for the cooling and heating in the evaporator and condenser respectively.

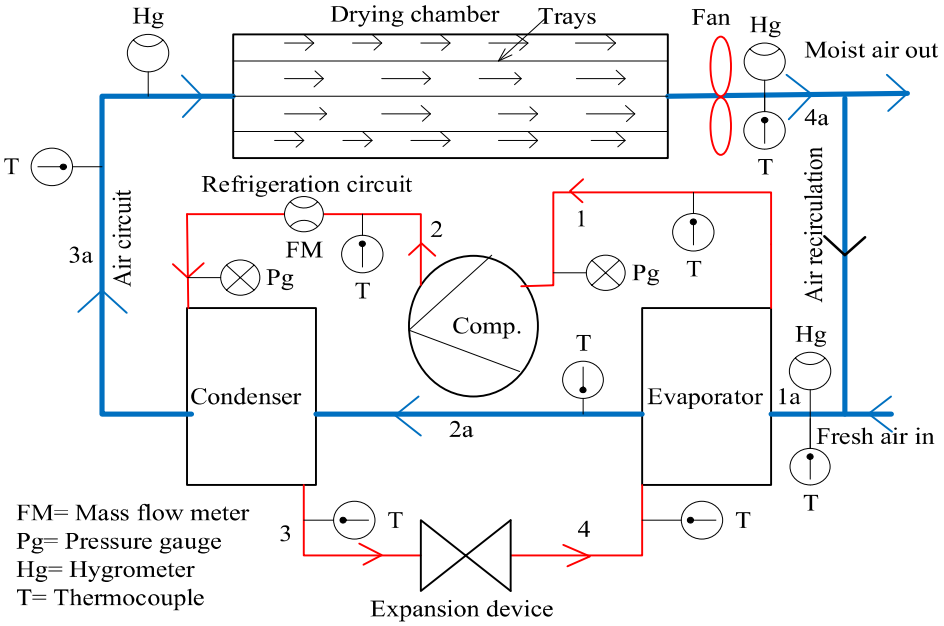

Fig. 3.1: Schematic diagram of the heat pump drying system

The evaporator, compressor, and condenser are fabricated in a line such that the evaporator (cooling and dehumidification) is located at the inlet of the drying system and the condenser is located just before the drying chamber inlet. The batch-type drying cabin consists of several trays inside it. The trays are made using aluminum strips, which have been designed to get uniform drying air-flow coverage by maintaining the optimum gap between the trays, and the stainless steel net to get the constant rate of moisture removal on both sides of the food chips by drying air. The gap between the two trays is 5cm and the area of each tray is 0.18m^2. The drying cabin wall is made of plywood, and thermocol sheet is used as insulating material inside the wall to minimize the heat transfer from drying air to the surrounding. The drying air is circulated in the HPD system by using a fan (located at the drying cabin outlet). The fan is fabricated at the drying cabin outlet to get stable and uniform distribution of the air inside the cabin through the trays. The

developed experimental setup is shown in Fig. 3.2 and the detailed specifications of the different components are listed in Table 3.1 and the properties of measuring instruments are given in Table 3.2.

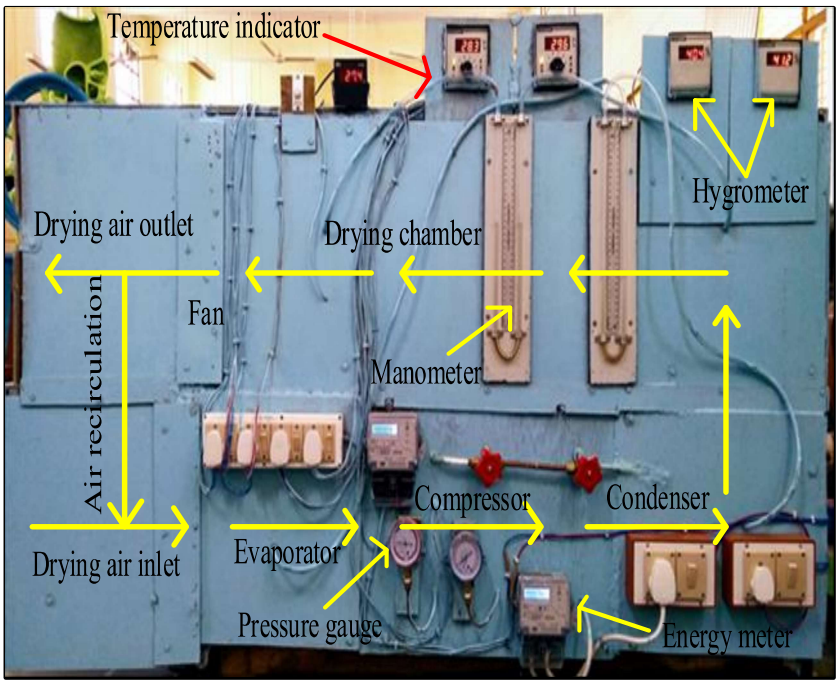

Fig. 3.2: Photograph of the developed experimental setup

Table: 3.1. Specification of the different components of the HPD system

Component	Specification
Compressor	Rated power requirement = 505 W, swept volume = 15.33 cm^3, rated voltage = 230 Volts, 50Hz refrigerant used = R134a
Condenser	Wavy fin and tube 4-row cross flow heat exchanger type, length of tube = 31.7 m, dimension = 30.48 cm × 33.02 cm, diameter of tube (inside) = 9.7mm
Evaporator	Wavy fin and tube 4-row cross flow heat exchanger type, length of tube = 23.6 m, dimension = 30.48 cm × 33.02 cm, diameter of tube (inside) = 9.7mm
Capillary tube	Inside tube diameter = 1.27 mm, total length of tube = 60 cm

Fan	Rated power =70 W, speed = 1350 rpm, total sweep = 300 mm
Drying chamber	Convective batch type, length of drying chamber = 0.7m, width = 0.35m, height = 0.4m, no of trays inside chamber = 8, gap between trays = 2.5 cm, capacity of drying chamber = 5 kg

Table: 3.2. Technical specification and uncertainty of measuring instrument

Instrument	Specification	Accuracy
Resistant thermometer (PT100)	Range -50 to 250°C,	± 0.5°C
Vane type anemometer	Velocity 0-20 m/s	± 2%
Hygrometer	0-100% relative humidity	± 2.5%
Energy meter	Supply 220V, 50 Hz	± 1%
Coriolis mass flow meter	Range: 0–0.5 kg/s, maximum pressure = 25 bar, maximum temperature = 200ºC	±0.5%
U-Tube manometer	Manometric fluid = water	± 1mm
Digital weighing machine	Measuring capacity of 10 kg	± 2%
Pressure gauge	Measuring pressure of 30 bar	± 3%

The pressure gauges (accuracy = ± 3%) and thermocouples (accuracy = ± 0.5°C) are installed at different locations to measure the condenser and evaporator pressures, and refrigerant temperatures in the heat pump system at the compressor inlet, outlet, condenser outlet, and the evaporator inlet. Hygrometers are installed to measure the relative humidity of air at locations of the evaporator inlet, drying chamber inlet, and drying chamber outlet. The U-tube manometers are used to calculate the total pressure

drop inside the drying chamber and the whole system. Energy meters are used to obtain the electrical energy consumption of the compressor and fan. The fan speed or air mass flow rate was controlled by an electric regulator, and the flow velocity of the drying air in the system is measured by using the vane type anemometer (accuracy $\pm$ of 2%). Velocity has been measured at different positions of a cross-section and then taken as the average. Weighing balance is used to measure the weight of the drying material before and after the experiment. The mass flow rate of refrigerant has been measured by Coriolis mass flowmeter installed at the compressor outlet.

The HPD system has been operated for the drying of the banana and potato chips in the laboratory. Both the fresh pilled potato and banana bought from the retailer were washed with clean water and sliced into 2mm size chips. 0.5kg of material was used per tray for the drying. The initial and final moisture contents of the products were determined by the oven method (Zambrano et al., 2019). The microwave oven was used to determine the initial moisture content and the sample was put inside the oven for 15-20min. A sample of 4kg of banana and potato chips (separately) was dried using the open system and closed system heat pump drying. The banana and potato chips were spread out on the tray in the drying chamber, and for the homogeneous drying, the banana and potato chips were mixed from time to time. The temperature inlet to the drying chamber depends on the amount of heat transfer in the condenser from the refrigerant to the air, the velocity of the circulating air and the permitted drying temperature of the products. Air recirculation ratio and drying temperature have been controlled by adjusting vanes and fan speed controller.

The experiment was performed to estimate the performance of the system and drying kinetics of the banana and potato chips in HPD. The drying air velocity and the temperature were adjusted to the required values. After that, the HPD system was started

to get the desired drying temperature. The mass flow rate of air (0.073kg/s) was kept constant for the drying of banana and potato in open and closed systems. Then the banana and potato chips are weighted in digital balance and spread over the trays and loaded inside the HPD drying chamber, and the fan was switched on to get the desired air mass flow rate (0.073kg/s). Then the initial readings of the energy meter were noted, and during the experiment, the temperature and the relative humidity of drying air at the inlet to the evaporator, the inlet to the dryer, and the outlet to the dryer were recorded periodically after every 10 minutes until the experiment ended. The weight loss from the drying material should be equal to the change in the humidity of the drying air from dryer inlet to outlet. Three replicates were performed for each experiment.

3.2. Data analysis

The performance of the HPD system depends on the different parameters such as the inlet condition of the air to the evaporator, air recirculation ratio, and air velocity flowing through the system. The heat delivered by the refrigerant to the drying air in the condenser is given by,

$$Q_{cond} = \dot{m}_a c_{pam} (T_{3a} - T_{2a}) \tag{3.1}$$

Where $\dot{m}_a$ $(= A_{fr} \rho_a V_a)$ is the mass flow rate of air and c_{pam} is the isobaric specific heat of humid air it is given as, $c_{pam} = c_{pa} + \omega_a c_{pv}$

The coefficient of the performance (COP) of the heat pump is defined as the ratio of the heat delivered in the condenser to the energy input to the compressor and is given by,

$$\mathrm{COP}_{hp} = \frac{Q_{cond}}{W_{comp}} \tag{3.2}$$

Similarly, COP for the whole system has been calculated by,

$$\mathrm{COP}_{ws} = \frac{Q_{cond}}{W_{comp} + W_{fan}} \tag{3.3}$$

The heat delivered rate in the condenser by refrigerants is also given by the following,

$$Q_{cond} = \dot{m}_r (h_2 - h_3) \tag{3.4}$$

Volumetric heating capacity is an important parameter of the heat pump (represents the rate of heat delivered per unit refrigerant volume flow rate in the compressor), which is given by,

$$\text{Volumetric heating capacity} = (h_2 - h_3)\rho_1 \tag{3.5}$$

The moisture removed from the product (m_w) at any time is the difference between the initial weight to the weight of the product at any time and is also equal to the moisture carried out by the drying air from the drying chamber. It is given by,

$$m_w = (m_{pi} - m_{pt}) = \dot{m}_a (\omega_{4a} - \omega_{3a}) t_d \tag{3.6}$$

The energy efficiency (the ratio of the energy used for removal of moisture from the product to the total energy required), which indicates how efficiently the energy consumed in the system removes the moisture from the product, is given by (Vieira et al., 2007),

$$\eta_{en} = \frac{h_{fg} m_w}{\mathrm{t}_d (W_{comp} + W_{fan})} \tag{3.7}$$

The SMER is defined as the amount of moisture removal per unit of energy consumed and is given as,

$$\text{SMER} = \frac{m_w}{\mathrm{t}_d (W_{comp} + W_{fan})} \tag{3.8}$$

Percentage of water loss from the product is calculated by the following,

$$\text{Water loss} = \frac{m_{pi} - m_{pt}}{m_{pi}} \tag{3.9}$$

The MER is defined as the moisture removed from the drying product per unit time and is given as,

$$\mathrm{MER} = \frac{m_w}{t_d} \tag{3.10}$$

Specific energy consumption (SEC) of the HPD system is the amount of energy required to evaporate the unit mass of the moisture from the product and is given by,

$$\mathrm{SEC} = \frac{\mathrm{t}_d (W_{comp} + W_{fan})}{\mathrm{m}_w} \tag{3.11}$$

The moisture content of the product on a dry basis and the moisture ratio (MR) can be given using the following,

$$\left(\mathrm{M}_t\right)_{\mathrm{db}} = \frac{m_{pt} - m_d}{m_d} \tag{3.12}$$

$$\mathrm{MR} = \frac{(M_t - M_{eq})}{(M_0 - M_{eq})} \tag{3.13}$$

As the equilibrium moisture content is very small as compared to moisture content at any time and initial moisture content, the moisture ratio has been simplified as,

$$\mathrm{MR} = \frac{M_t}{M_o} \tag{3.14}$$

The drying rate of the product during the drying has been calculated by,

$$\mathrm{DR} = \frac{M_{t+dt} - M_t}{dt} \tag{3.15}$$

The effective diffusivity coefficient of the sliced potato and banana chips during drying was estimated by using the simplified mathematical Fick's second model. According to Fick's second law, the drying behavior of sliced potato chips can be described by (Aktas et al., 2017),

$$\mathrm{MR} = \frac{8}{\pi^2}\sum_{n=1}^{\infty}\frac{1}{(2n-1)}exp\left(-\frac{(2n-1)^2\pi^2 D_{eff}t_d}{4L^2}\right) \tag{3.16}$$

Where D_{eff} is the effective diffusivity coefficient, L is the half-thickness of the potato and banana slice (m), and n is the positive integer. For long drying periods, the above Eq. can be simplified as (Aktas et al., 2017),

$$\mathrm{MR} = \frac{8}{\pi^2}exp\left(-\frac{\pi^2 D_{eff}t_d}{4L^2}\right) \tag{3.17}$$

$$\ln(\mathrm{MR}) = -\left(\frac{\pi^2 D_{eff}}{4L^2}\right)t_d + \ln\left(\frac{8}{\pi^2}\right) \tag{3.18}$$

The effective diffusivity (D_{eff}) of material is obtained by plotting from the experimental *MR* data in terms of *ln MR* with time (s) followed by the estimation of slope (Slope = $\frac{\pi^2 D_{eff}}{4L^2}$) using Eq. (3.18) (Ekka et al., 2020),

The convective mass transfer coefficient has been calculated by (Cengel and Ghajar, 2011),

$$h_m = \frac{B_i D_{eff}}{L} \tag{3.19}$$

Where, the Biot number can be calculated by (Dincer and Hussain, 2002),

$$B_i = 24.85\left(\frac{V_a}{k_c L}\right)^{-0.375} \tag{3.20}$$

Where, k_c is the drying constant of the product that can be calculated by the following relation (Aboltins, 2013),

$$k_c = -\mathrm{DR}/(M_t - M_{eq}) \tag{3.21}$$

Exergies of refrigerant and humid air at any state have been calculated by, respectively,

$$E_x = \dot{m}_r\left\{(h-h_o)-T_o(s-s_o)\right\} \tag{3.22}$$

$$E_{xa} = \dot{m}_a c_{pam} \left[(T_a - T_o) - T_o \ln\left(\frac{T_a}{T_o}\right) \right] \tag{3.23}$$

Hence, the exergy loss and exergy efficiency of compressor, condenser, expansion device, evaporator and dryer are given by, respectively (Ganjehsarabi et al., 2014),

$$Ex_{\text{dest},comp} = W_{comp} + Ex_1 - Ex_2, \quad \eta_{ex,comp} = \frac{Ex_2 - Ex_1}{W_{in}} \tag{3.24}$$

$$Ex_{\text{dest},cond} = Ex_2 - Ex_3 + Ex_{2a} - Ex_{3a}, \quad \eta_{ex,cond} = \frac{Ex_{3a} - Ex_{2a}}{Ex_2 - Ex_3} \tag{3.25}$$

$$Ex_{\text{dest,exp}} = Ex_3 - Ex_4, \quad \eta_{ex,\text{exp}} = \frac{Ex_4}{Ex_3} \tag{3.26}$$

$$Ex_{\text{dest},evap} = Ex_4 - Ex_1 + Ex_{1a} - Ex_{2a}, \quad \eta_{ex,evap} = \frac{Ex_{2a} - Ex_{1a}}{Ex_4 - Ex_1} \tag{3.27}$$

$$Ex_{\text{dest},dryer} = Ex_{3a} - Ex_{4a} + W_{fan}, \quad \eta_{ex,dryer} = \frac{Ex_{3a} - Ex_{4a}}{W_{fan}} \tag{3.28}$$

3.2.1. Experimental uncertainty

To support the experimental results, the uncertainty analysis has been carried out by using the method explained (Holman, 2001). Let the predicted parameter, R is a given function of the independently measured variables y_1, y_2, y_3, ……, y_n. Thus,

$$R = R\left(y_1^{u_1}, y_2^{u_2}, y_3^{u_3}, \ldots\ldots, y_n^{u_n}\right) \tag{3.29}$$

Let U_R be the uncertainty in the result and u_1, u_2, u_3, ……, u_n be the uncertainties in the independent variables then the uncertainty in the result having variation is given by the following

$$U_R = \left[\left(\frac{\partial R}{\partial y_1} u_1\right)^2 + \left(\frac{\partial R}{\partial y_2} u_2\right)^2 + \ldots\ldots\ldots\ldots + \left(\frac{\partial R}{\partial y_n} u_n\right)^2 \right]^{1/2} \tag{3.30}$$

The technical specifications of the measuring instruments and the uncertainties are provided in Table 3.2. Based on the measured parameters by various instruments, the

total experimental absolute uncertainties found for estimated values of Drying efficiency (DE), energy efficiency (η_{en}), total exergy destruction, moisture extraction rate (MER), total energy consumption, volumetric heating capacity, $(COP)_h$ and SMER are $\pm 9.47\%$, $\pm 13.43\ \%$, $\pm 1.81\%$, $\pm 2.236\%$, $\pm 1.49\%$, $\pm 3.96\%$, $\pm 4.12\%$, and $\pm 3.88\%$ respectively.

3.3. Results and discussion

Banana and potato chips have been dried in the HPD with and without recirculation of the drying air, and the performance of the HPD system has been investigated. The air velocity was fixed at about 0.6m/s for the open as well as the closed system for drying both banana and potato chips. For the open system, the drying air temperature for banana and potato chips was between 39.5°C to 43.8°C and 38.3°C to 42°C, respectively for the closed system drying of the banana and potato, the drying temperature was between 47.6°C to 51.8°C and 46°C to 53.7°C, respectively. The drying process has been carried out until the difference between the humidity at the drying chamber inlet and outlet becomes negligible, so the final MC of the product reaches to the desired value (11.6%). The experimental results obtained for the HPD system are listed in Table 3.3.

Table: 3.3. Performance comparison of experimental results

Performance parameter	Closed system		Open system	
	Banana	Potato	Banana	Potato
Average drying temperature (°C)	50.5	50.4	41.4	40.8
Drying time (min)	220	320	300	370
Initial- final moisture content (% w.b.)	84-11.6	83.5-11.5	84-11.6	83.5-11.5
Total energy consumption (kWh)	2.41	3.51	3.3	3.564

Volumetric heating capacity (MJ/m^3)	12.1	10.03	12.05	9.7
Average COP_{hp}	3.09	2.85	3.89	3.93
Average COP_{ws}	2.82	2.58	3.55	3.63
Average MER (kg/h)	0.8127	0.6745	0.62	0.6
Average SMER (kg/kWh)	1.248	1.0498	0.924	0.981
Average SEC (kWh/kg)	0.80128	0.95256	1.0822	1.01936
Average drying efficiency (%)	55.9	58.09	45.8	52.01
Average diffusivity (m^2/s)	$2.37E^{-10}$	$1.31E^{-10}$	$1.02E^{-10}$	$0.92E^{-10}$
Average mass transfer coefficient (m/s)	$9.89E^{-7}$	$7.78E^{-7}$	$2.15E^{-7}$	$2.23E^{-8}$

It can be observed that the closed system drying is best in terms of energy consumption, MER, SMER, and drying efficiency because specific energy consumption is the lowest in this system. However, the COP was good in the open system HPD drying for banana and potato chips as compared to the closed system because in the open system the values of humidity and temperature at the inlet to the evaporator are low (the COP of the heat pump increases with decrease in temperature and humidity at evaporator inlet). Average COP values of heat pump for an open and closed system for banana and potato chips are 3.89, 3.93, and 3.09 and 2.85 respectively, and the values of COP for heat pump obtained in the present study are in the acceptable range given in the literature from 2.8 to 3.7 (Aktas et al., 2015). The volumetric heating capacity indicates the heating capacity for a given compressor size and the average values for banana and potato chips in open and closed systems are 12.05, 12.1 and 9.7, 10.03MJ/m^3, respectively. From the experimental results, it can be estimated that the drying time is low and the moisture

extraction rate was maximum for the closed system drying for banana and potato chips as compared to the open system. Total drying times for banana and potato chips in open and closed system drying are 300, 370, and 220, 310minutes respectively. The moisture removed from the products mainly depends on the moisture diffusivity, and it increases with an increase in the drying air temperature and air velocity. Hence, the drying air inlet temperature and velocity are having a meaningful effect on the product moisture diffusivity as well as the mass transfer coefficient. The moisture from the interior of the product is forced to diffuse to the surface of the product and carried away by the drying air. The moisture diffusivity of banana and potato chips was estimated for open and closed mode drying using Eq. (3.18). The moisture diffusivity was calculated by plotting a graph between ln (MR) versus time. The average value of the moisture diffusivity of banana and potato chips varies from $1.02E^{-10}$ to $2.37E^{-10}m^2/s$ and $0.92E^{-10}$ to $1.31E^{-10}m^2/s$ for open and closed system drying. The average value of the mass transfer coefficient of potato and banana chips varies from $2.23E^{-8}$ to $2.15E^{-7}m/s$ and $7.78E^{-7}$ to $9.89\ E^{-7}m/s$ for open and closed system drying, and these values are close to the experimental result of mass transfer coefficient ($2.064E^{-7}m/s$) obtained in convective drying of the banana chips by Silva et al. (2012). The mass transfer coefficient and moisture diffusivity are quite higher for the closed system due to higher drying temperature as compared to an open system. Total energy consumption is lower for the closed system as compared to the open system due to the utilization of the energy of exhaust air from the drying chamber (leading to lower drying time and hence lower energy consumption). Exhaust energy is directly wasted in the atmosphere in an open system. The average drying efficiency is better for the closed system due to the getting of higher drying temperature for the same mass flow rate of inlet air. The average values of the specific energy consumption for banana and potato chips in open and closed system drying are 1.0822, 0.80128, and

1.01936, 0.95256kWh/kg respectively and the SEC is nearly 25.96% more in an open system as compared to the closed system for banana chips.

The total energy consumption in the HPD system mainly depends on the energy consumed by the compressor and the fan. The total energy consumption is lowest for the closed system as compared to the open HPD drying due to higher air temperature and less drying time at the same mass flow rate of the air. The energy consumption for banana and potato chips in the open and closed systems were 3.3, 2.41, and 3.564, 3.51kWh, respectively as shown in Fig. 3.3.

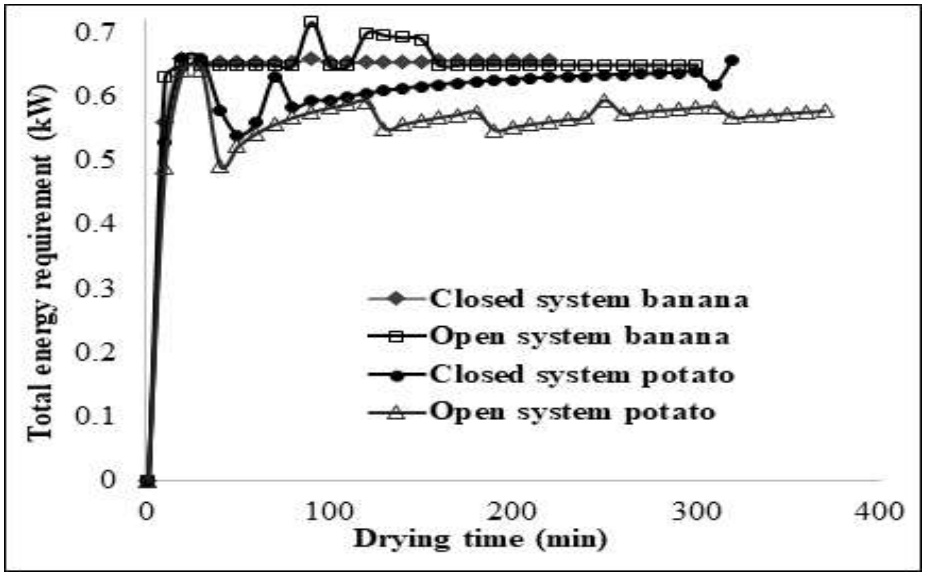

Fig. 3.3: Variation in energy requirement with drying time

Fig. 3.4 shows the drying air temperature at the dryer inlet. The average dryer inlet temperature is higher for the closed system drying as compared to the open system due to the recirculation of the dryer exit air directly to the evaporator, which utilizes the exit energy of the drying air, and the drying temperature is minimum for the open system for both banana and potato chips drying. The dryer inlet temperature depends on the condenser saturation temperature and the amount of heat delivered by the refrigerant to the air and the mass flow rate of the drying air. The condenser outlet temperature is fluctuating due to the change in the humidity and the temperature of the air inlet to the

evaporator. The average drying temperature for the open system is 41°C and the same for the closed system is 50.4°C.

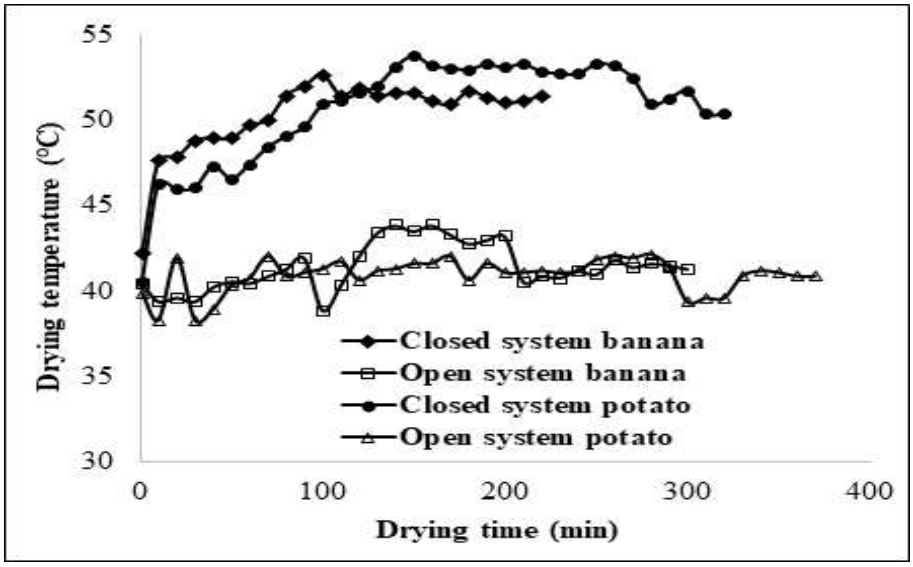

Fig. 3.4: Variation in drying temperature with drying time

Fig. 3.5 shows the variation of relative humidity at the dryer inlet with drying time. The relative humidity at the dyer inlet is higher for the closed system due to the recirculation of the air having higher moisture content. The moisture ratio is an important parameter in drying because it helps in the calculation of the moisture diffusivity and the mass transfer coefficient. It is defined as the ratio of the moisture content of the product at any time to the initial moisture content of the product, as shown in Fig. 3.6, the moisture ratio of the product decreases with the drying time due to the decrease in the moisture content of the product. The moisture ratio decreases at a faster rate for the closed system HPD due to the higher air temperature, which removes the moisture from the product at a greater rate. For the studied condition, initially, the moisture ratio decreases at a faster rate, but after some time as the moisture content decreases, it changes at a slower rate. The change in the moisture ratio is faster for the closed system banana chips drying because, for banana chips, the effective diffusivity was higher as compared to the potato chips.

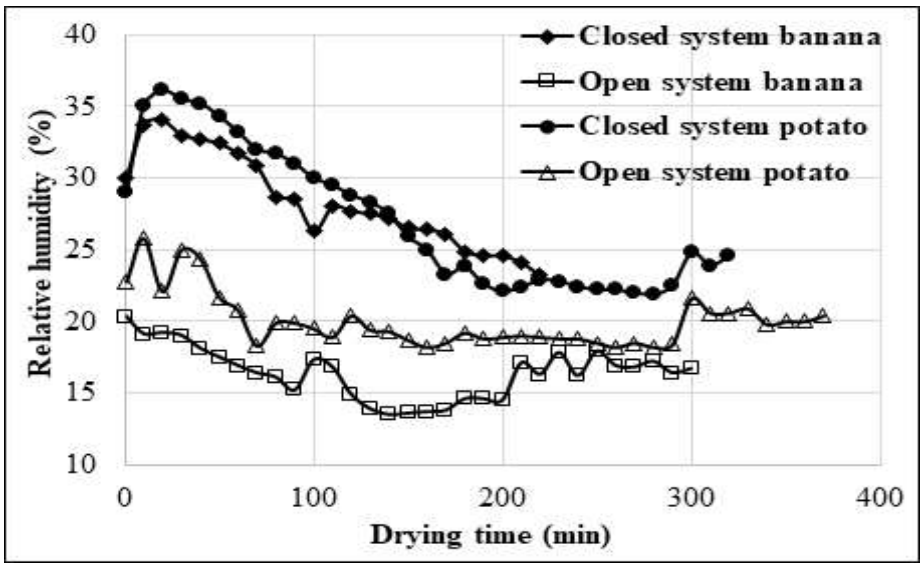

Fig. 3.5: Variation of relative humidity at dryer inlet with drying time

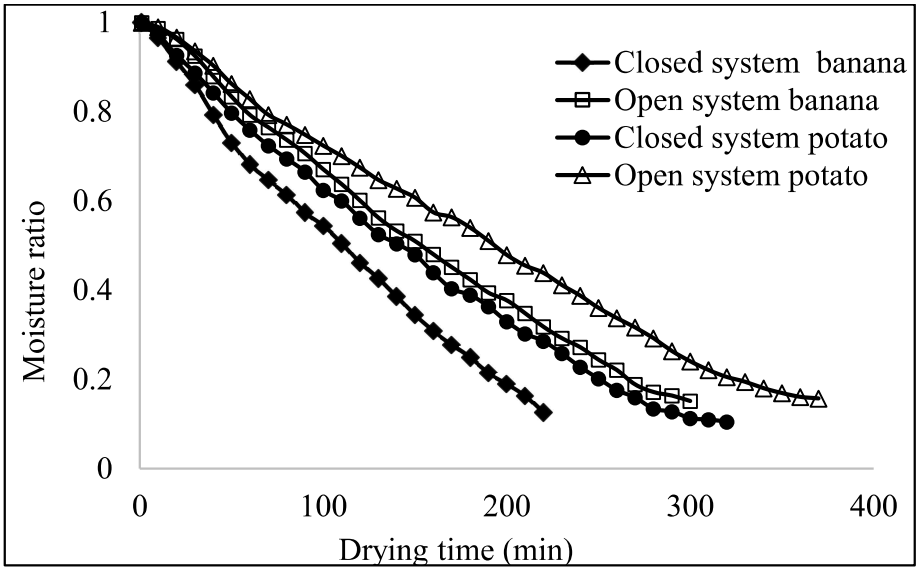

Fig. 3.6: Change in moisture ratio with drying time

Fig. 3.7 shows the variation in the percentage of water loss from the product with the drying time. As shown in the figure, the water loss increases with time because as time increases, the moisture from the product removes, and the weight of the product decreases. For studied design and operating conditions, water loss is maximum for the closed system drying of the banana chips due to the higher value of mass transfer coefficient and moisture diffusivity.

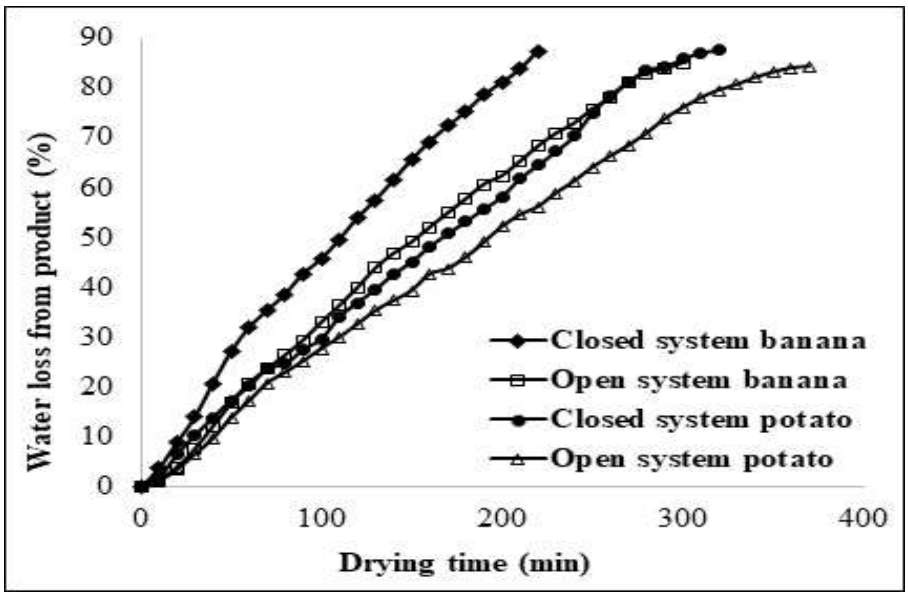

Fig. 3.7: Variation in water loss from the product with drying time

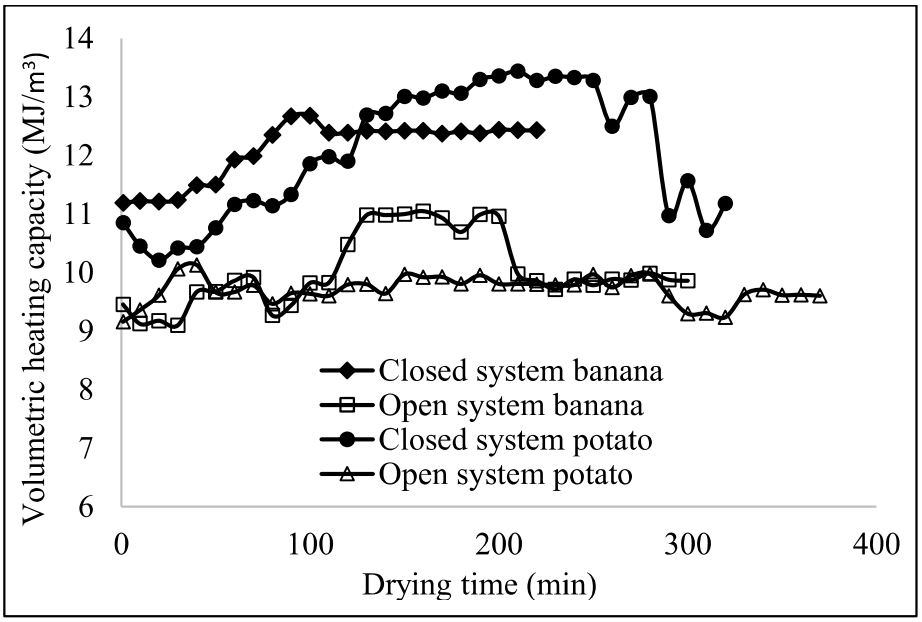

Fig. 3.8: Variation in volumetric heating capacity with time

Volumetric heating capacity in the HPD indicates the heat given by refrigerant in the condenser per unit volume of the refrigerant flow. Fig. 3.8 shows the variation of the volumetric heating capacity according to the drying time. The value of volumetric heating capacity is higher in the case of closed system drying for banana and potato chips as compared to the open system due to the higher saturation condenser pressure and lower

saturation evaporator pressure in a closed system. Higher condenser saturation pressure gives a higher density which leads to higher volumetric heating capacity.

Fig. 3.9 indicates the variation of the COP of the HPD system with drying time. The nature of the variation was fluctuating for the coefficient of the performance according to time. The COP of the open, as well as closed system drying, is fluctuating with time due to the change in the humidity and the temperature inlet to the evaporator. In a closed system, the dryer outlet air is directly recirculated to the evaporator, and the humidity and the temperature of the dryer outlet air continuously changes with time. Thus the COP is also varying with time. In the open system also, the humidity and temperature of the air inlet to the evaporator change, which causes the change in COP of the heat pump system.

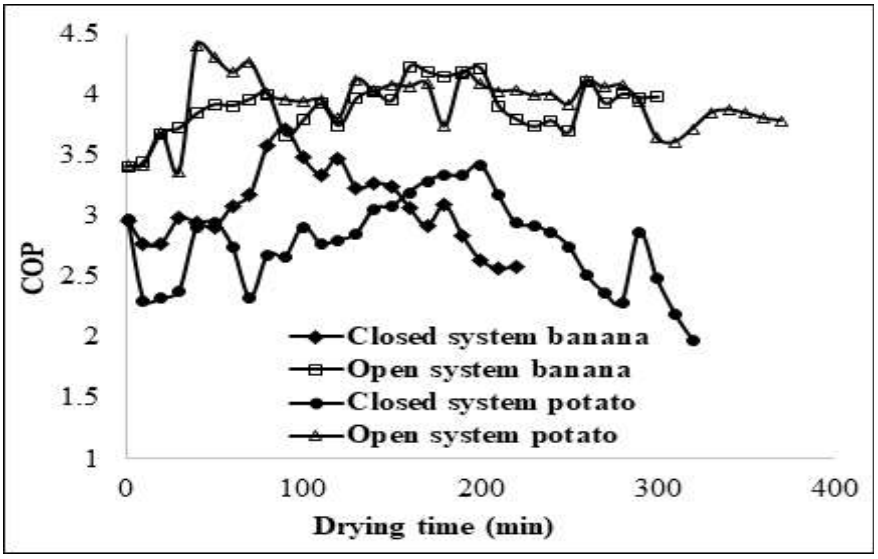

Fig. 3.9: Variation in COP with drying time

The average COP is lower for the closed system as compared to the open drying due to the high humidity ratio and temperature of the air at the evaporator inlet because the degree of superheat at the compressor inlet increases with humidity and temperature, which finally increases the condenser temperature and the energy input to the compressor. Thus the COP of the heat pump system decreases with an increase in the

moisture and temperature of the inlet air to the evaporator. So the COP is better in the case of open system drying for both banana and potato chips and lowest for the closed system drying for banana and potato.

The performance of the HPD depends on that how fast the drying air can carry out the moisture from the drying product, and it varies with the moisture content of the product, diffusivity, mass transfer coefficient, air temperature, and the air velocity. The moisture extraction rate of the HPD first increases with time to the maximum value, but after some time, it decreases because of the decrease in the moisture content of the material as shown in Fig. 3.10.

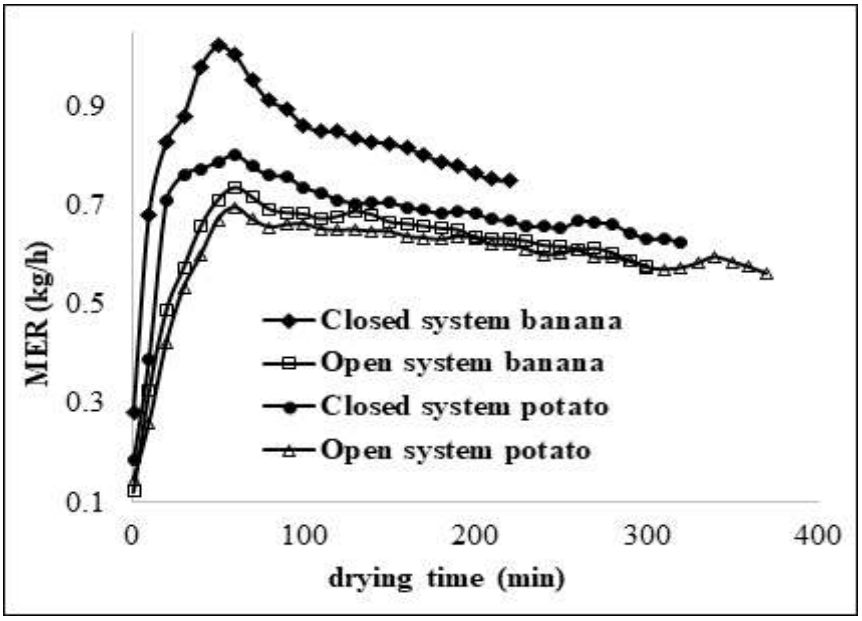

Fig. 3.10: Variation in moisture extraction rate with drying time

The MER is higher for the closed system heat pump drying of banana chips as compared to the other system drying in the present study because of higher drying temperature and the high value of effective diffusivity and hence higher moisture removal potential (in humid ambient conditions). However, the system can give the opposite performance behavior in dry conditions. The average value of MER for banana chips in an open and closed system is 0.62, 0.8127kg/h, and for potato chips drying are

0.6, 0.6745kg/h respectively. For an open system, the MER is lowest due to getting the lower drying temperature because of the loss of energy at the dryer outlet.

Fig. 3.11 indicates the change of the specific moisture extraction rate with the drying time for the banana and potato chips. The SMER is the total amount of moisture removed per unit of energy consumed. The SMER is also dependent on the total moisture content of the drying material, drying air velocity, and temperature. The SMER first increases with time due to the establishment of the heat and mass transfer between the drying product air, but after some time, it decreases due to the decrease in the moisture content of the material.

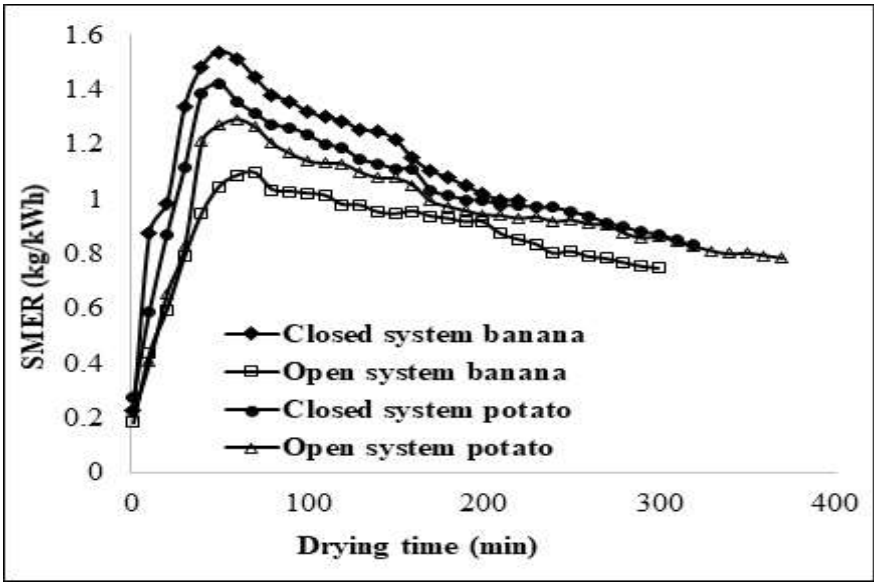

Fig. 3.11: Specific moisture extraction rate with drying time

The average SMER is higher for the closed system heat pump drying of the banana chips compare to the open system drying due to the high drying temperature and the higher value of the effective diffusivity with an average value of 1.248kg/kWh and the minimum is for the open system drying of banana chips with an average value of 0.924kg/kWh. The SMER is lowest in the case of an open system for the banana because of more power consumption as compared to the open system for potato. For the open system, the SMER is low due to the loss of energy at the outlet to the dryer, so the drying temperature is low

for the same mass flow rate of the air. The average values of SMER for potato chip drying in open and closed systems are 0.981 and 1.0498kg/kWh, respectively.

Drying efficiency gives the indication the how efficiently the drying air is removing the moisture from the product in the drying chamber without the loss of heat and bypassing through the drying chamber. The drying efficiency depends on the drying chamber inlet temperature and humidity, outlet temperature, and humidity, and the saturation temperature at a wet-bulb temperature in the drying chamber. Fig. 3.12 shows the variation in drying efficiency with time. The drying efficiency first increases with time due to the decreases in dryer outlet temperature, but after some time it starts to decrease due to the increases in the dryer outlet temperature. The drying efficiency is higher for the closed system drying as compared to the open system because of the higher drying temperature in the closed system. The drying efficiency decreases at a faster rate for the banana chips drying due to a higher heat transfer rate between product and air and a high value of effective diffusivity.

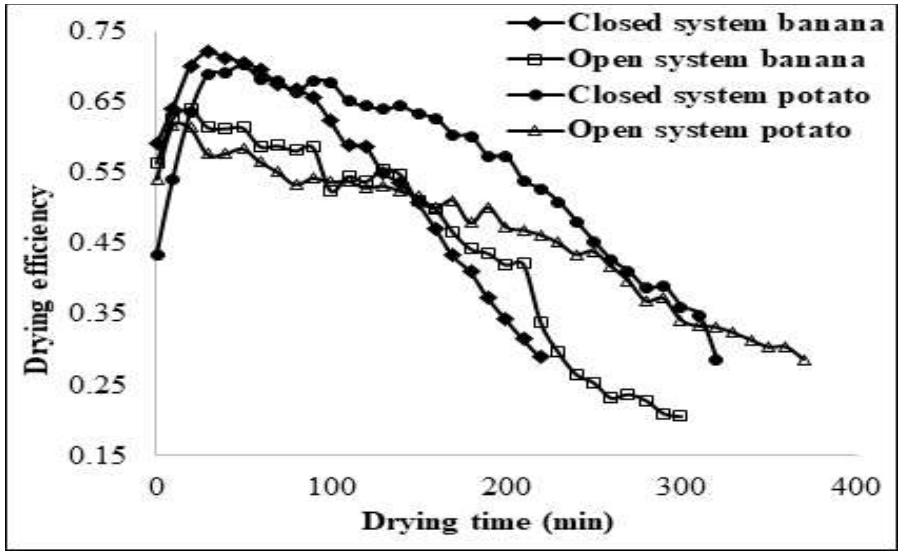

Fig. 3.12: Variation of drying efficiency with drying time

Energy efficiency gives information about the utilization of the total energy input in the moisture removal from the products. Fig. 3.13 shows the variation in the energy

efficiency of the drying system for the banana and potato chips in an open and closed system according to time. The energy efficiency of the system depends upon the vaporization of the moisture from the products and the energy input to the HPD system, and it is the ratio of the energy of the vaporization of moisture to the total energy input to the system.

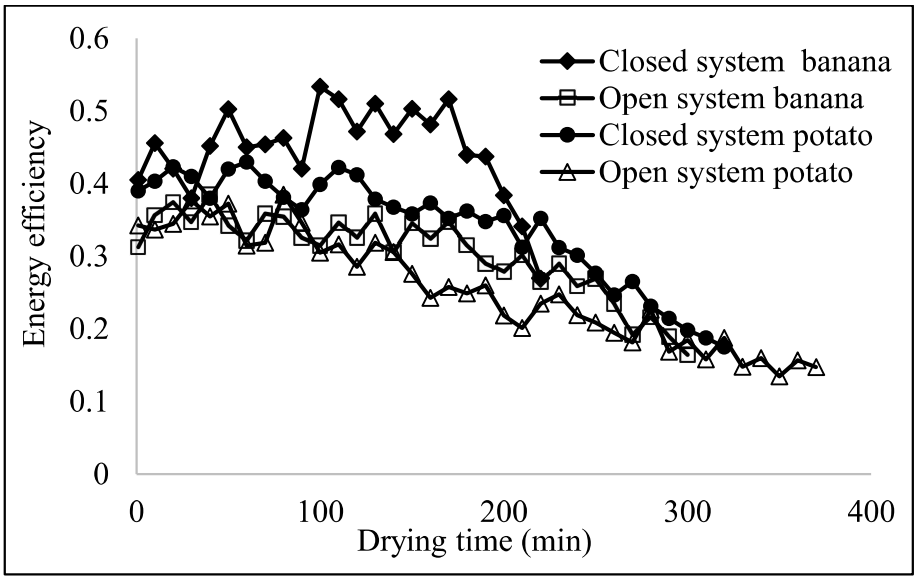

Fig. 3.13: Variation in energy efficiency with drying time

The energy efficiency first increases with time and reaches the peak value and starts to decrease after some time because in starting, the moisture removal from the product initially increases, but after some time moisture removal from the product decreases because of the decrease in the moisture content of the material. The energy efficiency is maximum for the banana chips drying in a closed system and minimum for the banana chips drying in an open system. The energy efficiency is maximum for closed system drying because in a closed system the drying temperature is higher than in an open system which gives the more moisture removal rate from the product. The average values of the energy efficiency for the banana in closed and open system drying are 44.67% and 30.35%, respectively, and for potato chips in closed and open systems, the values are 33.9% and 25.5%, respectively. The obtained values of the energy efficiency for the open

and closed system drying of the banana and potato chips were compared with the literature and the values are in the acceptable range (Aktas et al., 2015).

Table 3.4 shows the energetic performances of different components in the HPD. The exergy destruction is higher in the compressor due to the reciprocating part of the system, and due to the higher degree of superheat. In the evaporator, the exergy losses are higher due to the condensation of the water vapor. The maximum exergy loss takes place in the first stage of the drying, and after that, it decreases slowly. The total exergy losses in a closed system for banana and potato chips drying were 0.5918kW, 0.563kW and for an open system drying are 0.5371kW, 0.5189kW, respectively, and the values are compared with the previous work in the literature and for heat pump dryer are in the acceptable range (Aktas et al., 2015).

Table: 3.4. Exergetic performances of components for banana and potato chips drying

Component	Closed system				Open system			
	Banana chips		Potato chips		Banana chips		Potato chips	
	E_{xdest}	η_{ex}	E_{xdest}	η_{ex}	E_{xdest}	η_{ex}	E_{xdest}	η_{ex}
Compressor	0.233	0.699	0.238	0.661	0.1802	0.771	0.1674	0.761
Condenser	0.0993	0.82	0.0941	0.807	0.153	0.715	0.141	0.736
Capillary	0.0498	0.865	0.0456	0.857	0.0456	0.901	0.0377	0.906
Evaporator	0.1645	0.526	0.142	0.511	0.142	0.598	0.157	0.571
Dryer	0.0452	0.335	0.0433	0.306	0.0163	0.2601	0.0158	0.231

Fig. 3.14 shows the destruction of the total exergy in the HPD drying system with drying time. The exergy destruction is maximum for the closed system as compared to the open system drying because at higher temperature destruction is also higher (exergy

destruction in the condenser is very high due to higher temperature difference between refrigerant and air in the condenser, as discussed earlier). The exergy destruction is minimum in the open system drying due to the lower drying temperature and lower value of superheat.

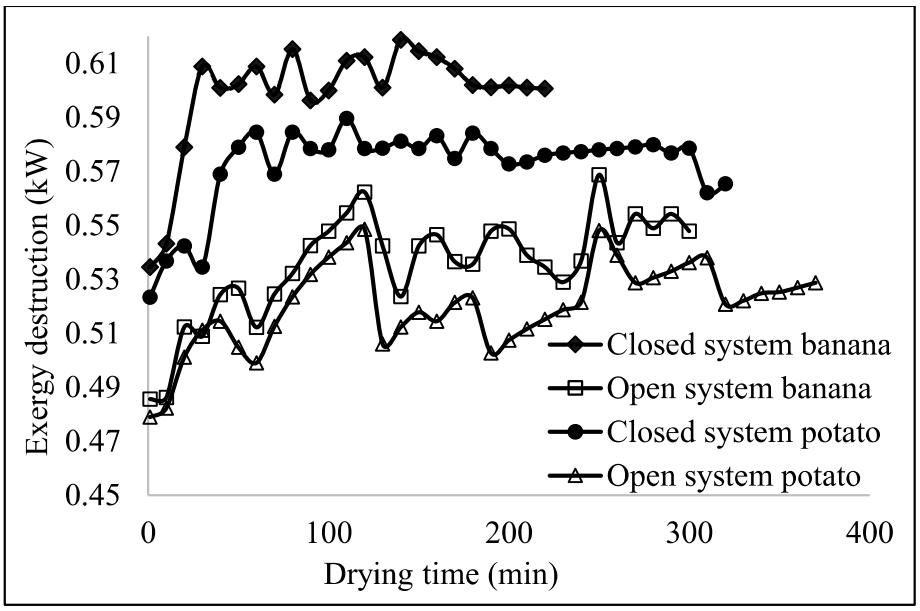

Fig. 3.14: Variation in the total exergy destruction with drying time

3.4 Highlights

A comparative study of open and closed systems heat pump dryers has been carried out experimentally for the drying of the 2 mm thin banana and potato chips at a constant volume flow rate of the air. The drying kinetics of the banana and potato chips is also considered to study the effective moisture diffusivity and the mass transfer coefficient in the drying. The following important points are made for the studied case:

- Total energy consumption is lowest for the closed system heat pump drying of banana and potato chips. The total energy consumptions for banana chips in the open and closed systems were 3.3, and 2.41kWh, and for potato chips are 3.564, and 3.51kWh, respectively.

- COP_{hp} of the open system is better. The average COP_{hp} of open and closed systems for banana chips drying was 3.89, and 3.09, and for potato chips are 3.93, and 2.85, respectively.
- The energy efficiency is higher for the banana chips drying in a closed system and lower for the banana chips drying in an open system.
- The mass transfer coefficient and moisture diffusivity are better for the closed system. Average values of effective moisture diffusivity for banana chips vary between $1.02E^{-10}$ to $2.37E^{-10}$ m^2/s and the mass transfer coefficient varies between $7.78E^{-7}$ to $9.89E^{-7}$ m/s.
- MER is highest for a closed system. The average values of moisture extraction rate for banana chips in the open and closed systems were 0.62, and 0.8127kg/h, and for potato chips in open and closed systems are 0.6 and 0.6745kg/h, respectively.
- SMER is better for the closed system. The average values of SMER for banana chips in open and closed systems are 0.924, 1.248kg/kWh, and for potato chips in open and closed systems were 0.981, 1.0498kg/kWh, respectively.
- Specific energy consumption is lowest for a closed system. SEC for banana chips in open and closed systems are 1.0822, 0.80128 kWh/kg, and for potato chips in open and closed systems are 1.01936, 0.95256 kWh/kg, respectively.
- Total exergy destruction is highest for the closed system and minimum for the open system heat pump drying for both banana and potato chips drying.
- Based on the performance parameters such as MER, SMER, and drying efficiency, the closed system drying is better than the open system drying in the given humid and hot atmosphere for the fruits and the vegetable drying.

This page is intentionally left blank

CHAPTER 4

THEORETICAL ANALYSIS OF HEAT PUMP DRYER

In this chapter, the details of the mathematical modeling and the simulation of the heat pump dryer represented the different low global warming potential (GWP) refrigerants (future refrigerants). The properties of the different refrigerants are provided in Table 4.1. The mathematical model of the heat pump dryer is divided into different sub-model such as the condenser model, compressor model, evaporator model, expansion device model, and the dryer model for an easy understanding of the simulation model. In each sub-model, the detailed calculation steps for the heat and the mass transfer are given. Various refrigerants are compared based on energetic and exergetic performance.

Table: 4.1. Properties of considered refrigerants

Refrigerant	Boiling point (°C)	Critical point (°C)	ODP	GWP	Flammability
R134a	-26.07	101.06	0	1300	No
R290	-42.1	96.7	0	20	Higher
R600	-0.7	152.01	0	4	Higher
R600a	-11.6	134.6	0	20	Higher
R152a	-24.1	113.3	0	140	Lower
R32	-51.7	78.1	0	650	Mild
R1234yf	-29.5	99.7	0	4	Mild
R1234ze(E)	-18.95	109.4	0	6	Mild

4.1. Modeling and simulation

The layout of the simulated batch type open cycle HPD consisting of the air-side working loop and the refrigerant-side working loop is shown in Fig. 4.1. T-s of the refrigerant loop and the psychrometric diagram for the air loop is shown in Figs. 4.2 and 4.3, respectively. The heat pump cycle works between the fixed evaporator temperature of 5°C and a condenser temperature of 40°C. Refrigerant enters the compressor in a superheated state at point 1 and leaves the compressor at point 2 in a superheated state. The superheated refrigerant coming from the compressor enters the condenser at state 2 and leaves the condenser at point 3 in the subcooled or two-phase region depending upon the air velocity and the inlet condition to the evaporator by dissipating heat to drying air. Refrigerant follows the isenthalpic expansion in the capillary tube (3-4) from the condenser pressure to the evaporator pressure. Then, the refrigerant enters the evaporator and leaves the evaporator at point 1 by absorbing heat from the air.

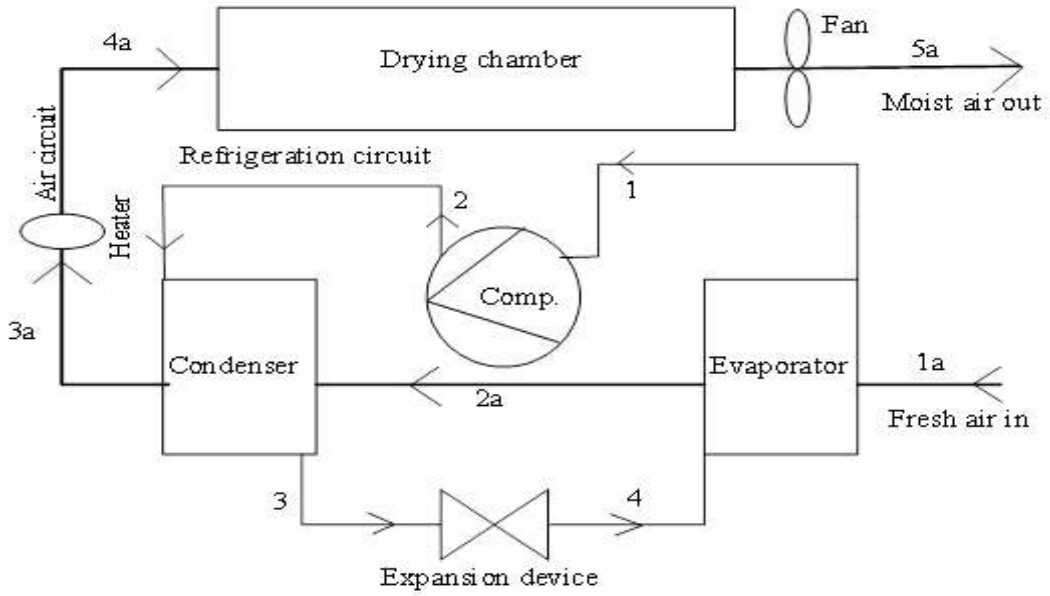

Fig. 4.1. Schematic diagram of open type HPD

The atmospheric air entering the evaporator at point 1a is dehumidified and cooled to a temperature below the dew point temperature and exits the evaporator at point

2a. Then the air enters the condenser at point 2a and sensible heating of air takes place and leaves the condenser at point 3a. A supplementary electric heater is used to heat the air to the desired temperature (process: 3a-4a). Hot and dry air enters the drying chamber at point 4a and extracts the moisture from the drying material while passing through the chamber and the air gets humidified and cooled and leaves the drying chamber at state 5a. In the drying chamber, it is considered that the air coming from the condenser is contacted with the drying material and there is no bypass of the air through the drying chamber.

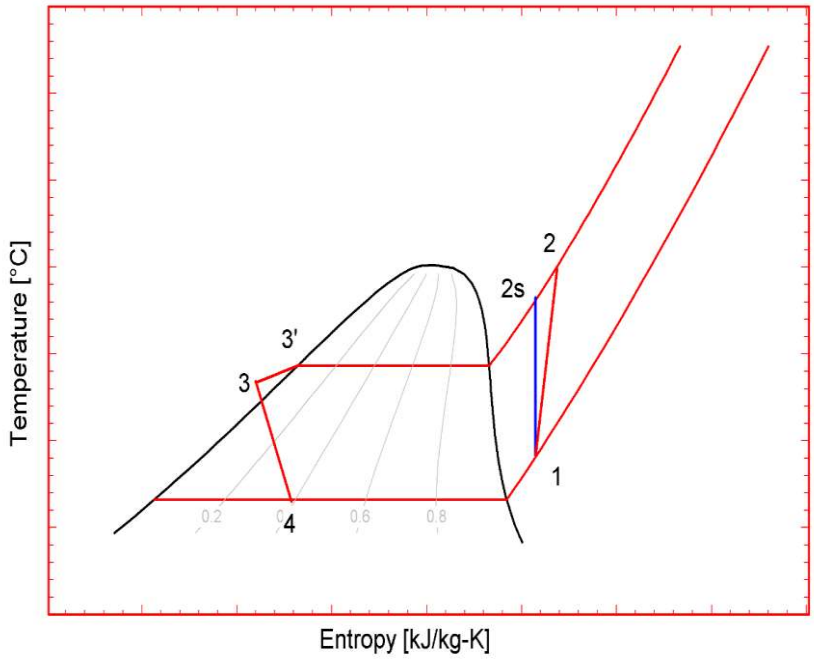

Fig. 4.2. Heat pump cycle on T-s diagram

The mathematical model of the considered HPD has been developed based on the energy and exergy balances of each component (compressor, evaporator, condenser, expansion device, fan, heater, and dryer). The following assumptions have been made for analysis:

- The steady-state operation of HPD is considered.
- The heat transfers of the component with ambient are negligible.

- The ambient conditions and specific heat of the air remain constant.
- The process of refrigerant in the compressor is adiabatic but not isentropic.
- The pressure drop of refrigerant in the different components is negligible.
- Conductive resistance of evaporator and condenser tubes is neglected.
- Air in the dryer follows the constant wet-bulb temperature line on the psychrometric chart.

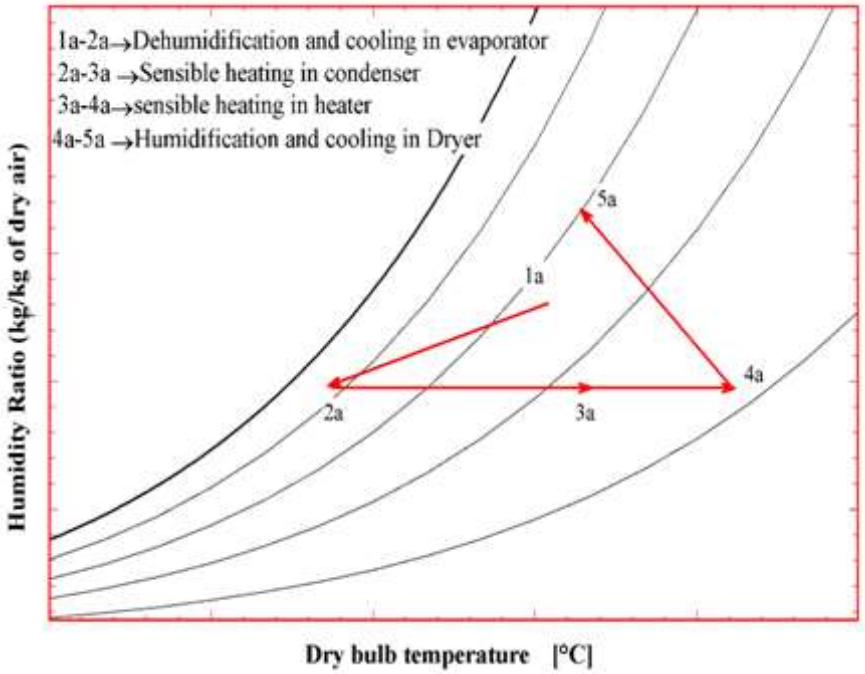

Fig. 4.3. Various processes on a psychrometric chart

4.1.1. Compressor model

Using the given specifications of the compressor, the mass flow rate of the refrigerant through the compressor has been calculated by,

$$\dot{m}_r = \rho_1 \eta_v V_s \left(N/60\right) \tag{4.1}$$

Then the enthalpy at the outlet of the compressor has been evaluated by,

$$h_2 = \frac{\left(h_{2s} - h_1\right)}{\eta_{isen}} + h_1 \tag{4.2}$$

Where volumetric and isentropic efficiencies of the compressor are given by (Bengtsson et al., 2014),

$$\eta_v = 1.04\left(1+0.1\frac{T_{evap}-18}{100}\right)\exp\left(-0.066\frac{p_{cond}}{p_{evap}}\right) \tag{4.3}$$

$$\eta_{isen} = \eta_v \Big/ \exp\left[-2.28\frac{T_{cond}+273}{T_{evap}+273}+2.67\right] \tag{4.4}$$

Then, the work done by the compressor has been calculated by,

$$\mathrm{W}_{comp} = \dot{m}_r\left(h_2 - h_1\right) \tag{4.5}$$

4.1.2. Condenser model

In the condenser, only heat is transferred from the refrigerant to air passing through the fin surface as there is no moisture transfer. The condenser used in this study is a wavy fin and tube cross-flow heat exchanger, which contains several rows and passes. It is considered that the mass flow rate of the air is equally divided in each pass. Total flow length has been divided into three zones for heat transfer calculation: sub-cooled, two-phase, and superheated refrigerant zones. Log mean temperature difference (LMTD) method has been used in each zone for the heat transfer modeling.

For given mass flow rate, an important parameter, air mass velocity has been evaluated by,

$$G_a = \frac{\dot{m}_a}{A_{fr}} \tag{4.6}$$

The heat transfer coefficient of the air over the condenser has been calculated by,

$$h_a = \frac{j_a G_a c_{p,a}}{\mathrm{Pr}_a^{2/3}} \tag{4.7}$$

The Colburn factor correlation for the wavy fin is given by (Jungi et al., 2007),

$$j_a = 0.836\ (R_{ea})^{-0.2309} \left(\frac{F_p}{F_h}\right)^{0.1284} \left(\frac{F_p}{2A}\right)^{-0.153} \left(\frac{L_d}{L_f}\right)^{-0.236} \tag{4.8}$$

The overall efficiency of the fin has been determined by,

$$\eta_o = 1 - \frac{A_f}{A_o}\left(1 - \eta_f\right) \tag{4.9}$$

The fin efficiency of a wavy fin has been predicted by using the approximation method as described (Schmidt, 1949). Nusselt number of refrigerants in both sub-cooled and superheated zones has been evaluated by,

$$Nu_r = 0.023\left(\mathrm{Re}_r\right)^{0.8}\left(\mathrm{Pr}_r\right)^n \tag{4.10}$$

Where n=0.4 for heating and n=0.3 for cooling.

Nusselt number of the refrigerant in the two-phase region has been obtained by (Wang et al., 2002),

$$Nu_r = 0.027\,\mathrm{Pr}_l(\mathrm{Re}_l)^{0.6792} x^{0.02208}\left[\frac{1.376 + 8\left(X_{tt}\right)^{0.5}}{\left(X_{tt}\right)^2}\right] \tag{4.11}$$

Where, $X_{tt} = \left(\mu_l / \mu_v\right)^{0.1}\left((1-x)/x\right)^{0.9}\left(v_l / v_v\right)^{0.5}$

For each zone, the overall heat transfer coefficient based on the air-side area has been calculated by,

$$\frac{1}{(UA)_o} = \frac{1}{\eta_o h_a A_o} + \frac{1}{h_{ri} A_i} \tag{4.12}$$

Then, the heat transfer in each zone has been obtained by,

$$\mathrm{Q}_{cond} = (UA)_o (LMTD) \tag{4.13}$$

Total heat transfer in the cross-flow wavy fin condenser from the refrigerant to air has been calculated by adding the heat transfer in superheated, two-phase, and sub-cooled zones.

4.1.3. Evaporator model

The evaporator model is slightly complicated due to both heat and mass transfers. Here, the evaporator is considered a wavy fin and tube cross-flow type heat exchanger. As shown in Fig. 4, the flow length is divided into three zones: (i) Zone-1: sensible cooling of air and superheating of refrigerant, (ii) Zone-2: sensible cooling of air and evaporation of the refrigerant, and (iii) Zone-3: cooling and dehumidification of air and evaporation of refrigerant. Calculation of heat transfer coefficient of air for all zones and that for superheated refrigerant are the same as in the condenser model.

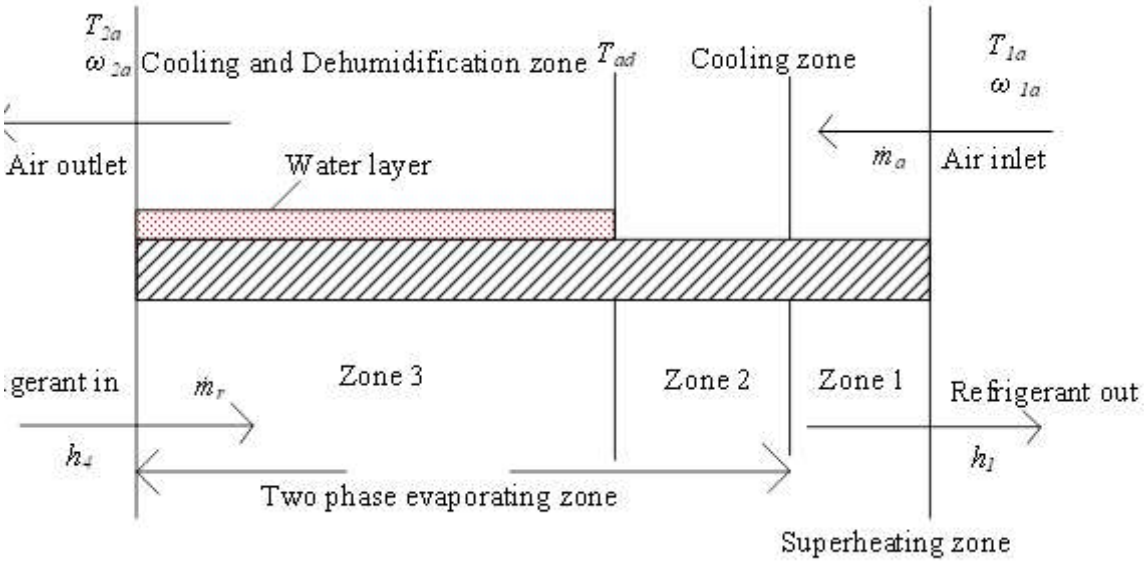

Fig. 4.4. Various heat transfer zone in the evaporator

The heat transfer coefficient for the evaporating zone has been calculated by (Kenning and Cooper, 1989),

$$h_r = \left(1 + 1.8 X_{tt}^{-0.87}\right) h_l \tag{4.14}$$

Where, $h_l = 0.023\left(\mathrm{Re}_l\right)^{0.8}\left(\mathrm{Pr}_l\right)^{0.4}\left(k_l / D\right)$

Eqs. 4.12-4.13 are applicable for the heat transfer calculation for zones 1 and 2. But in zone 3, there will be an extra resistance due to the layer of water over the tubes and extra heat transfer due to condensation of water vapor. At the water layer, the inner

side overall heat transfer coefficient of air with refrigerant evaporating (zone 3) is given by,

$$\frac{1}{(UA)_i} = \frac{1}{h_{ri} A_i} + \frac{w}{k_w A_o} \tag{4.15}$$

Where w = thickness of the water layer on the wet zone.

The outer side overall heat transfer coefficient is presented by,

$$(UA)_o = \eta_o h_a A_o \tag{4.16}$$

And the total heat transfer that takes place in the wet region is calculated by,

$$Q_{evap} = (UA)_o (LMTD) + \dot{m}_a h_{fg} (\omega_{1a} - \omega_{2a}) \tag{4.17}$$

The total heat transfer in the evaporator is calculated by adding the heat transfer in superheated (zone 1), two-phase zone with cooling (zone 2), and two-phase zone with cooling and dehumidification (zone 3).

From the mass balance equation, using the Lewis correlation and replacing the mass transfer coefficient, the humidity ratio of the air at the exit to the evaporator is given by,

$$\dot{m}_a (\omega_{1a} - \omega_{2a}) = \eta_o h_m A_o (\omega_{1a} - \omega_{as}) \tag{4.18}$$

$$\omega_{2a} = \omega_{1a} - \frac{2}{1 + 2\dot{m}_a c_{pam} / (UA)_o} (\omega_{1a} - \omega_{as}) \tag{4.19}$$

Where, h_m is the mass transfer coefficient, evaluated by using Lewis correlation, and [[

ω_{as} is the saturated humidity ratio of air corresponding to the mean water surface (evaporator tube) temperature (T_w), which is given by,

$$T_{w,evap} = \frac{Q_{evap}}{(UA)_i} + T_r \tag{4.20}$$

4.1.4. Capillary tube model

The expansion process in the capillary tube has been assumed to be isenthalpic. The pressure drop takes place inside the capillary tube due to the friction inside the tube as well as due to an increase in the velocity of the refrigerant flow from higher condenser pressure to the lower evaporator pressure.

$$h_3 = h_4 \tag{4.21}$$

4.1.5. Fan model

In the HPD system, the fan is used to develop a pressure difference sufficient to maintain the required airflow rate in the system. Neglecting the air pressure drop in the connecting ducts, the total air pressure drop in the HPD has been calculated by,

$$\Delta p_a = \Delta p_{evap} + \Delta p_{cond} + \Delta p_{dryer} \tag{4.22}$$

Where, $\Delta p = G_a^{\,2} f_a \left(A_o / A_c\right) / \left(2\rho_a\right)$

Where, f_a is a friction factor for dry air and calculated by (Turaga et al., 1988),

$$f_a = 0.589\left(A_o / A_p\right)^{-0.28}\left(R_{ea}\right)^{-0.27} \tag{4.23}$$

$$R_{ea} = G_a\left(4A_cL / A_o\right) / \mu_a$$

The friction factor for pressure drop in the wet region has been calculated by (Turaga et al., 1988),

$$f_w = 0.318 f_a^{-0.04}\left(s_f / T_f\right)^{0.4} R_{ea}^{-0.42} \tag{4.24}$$

Then the fan power has been calculated by,

$$\mathrm{W_{fan}} = \dot{m}_a \Delta p_a / \left(\eta_{fan}\rho_a\right) \tag{4.25}$$

4.1.6. Dryer model

The heat and the mass transfer phenomena in the batch type dryer depend on air inlet condition, flow rate, flow direction, and nature of drying material. The drying kinetics of the material is strongly dependent on the properties of the products being

dried. So it is difficult to predict the behavior of the heat and mass transfer in the dryer due to the many restrictions. The air inside the drying chamber in the flow direction is assumed to follow the constant wet-bulb temperature in the psychrometric chart. In this study, the dryer is treated as fully insulated, and no heat transfer between the dryer and the surroundings. In this theoretical study, the carrot is considered as the drying material and the drying kinetics of the carrot are used for the calculation of moisture removal rate, moisture content and specific moisture extraction rate (SMER), and the moisture ratio (MR) given by Midilli thin-layer drying model (Sonmete et al., 2017). Hence, the moisture content of exit air is given by,

$$\mathrm{MR}=\frac{(M_o - M_e)}{(M_i - M_e)} = a * \exp\left(-K_p t_d^{\,n}\right) + b\, t_d \tag{4.26}$$

Where M_e is the equilibrium moisture content of the material in the drying which depends on the material, drying air temperature, and the relative humidity. The equilibrium moisture content of the modified Henderson model (Khakhanmalee et al., 2008) is given by the following,

$$\mathrm{M_e}=\left[\frac{-\ln(1-\mathrm{RH_{3a}})}{0.00013*(T_{3a}+74.481)}\right]^{\left(\frac{1}{1.3339}\right)} \tag{4.27}$$

Where drying constants for carrot have been evaluated by (Sonmete et al., 2017),

$$a = 1.02 - 0.026\ln(V_a)$$

$$K_p = -4.949 + 1.433\ln(T_{3a})$$

$$n = 0.853\exp(0.856 / T_{3a})$$

$$b = 0.004\exp(0.379 / V_a)$$

Using mass balance between the drying air flowing through the dryer and the drying material, the specific humidity of air at the dryer outlet has been obtained by,

$$\omega_{5a} = \frac{m_p \left(Mi - Mo\right)}{t_d \dot{m}_a} + \omega_{4a} \tag{4.28}$$

Air temperature exit to the drying chamber has been calculated by,

$$T_{5a} = \frac{T_{4a}\left(c_{pa} + \omega_{4a} c_{pv}\right) + h_{fg}\left(\omega_{4a} - \omega_{5a}\right)}{\left(c_{pa} + \omega_{5a} c_{pv}\right)} \tag{4.29}$$

The drying efficiency of the heat pump dryer is a very important performance parameter, which indicates, how efficient the dryer is working and has been evaluated by,

$$\mathrm{DE} = \frac{\left(\omega_{5a} - \omega_{4a}\right)}{\left(\omega_{sat} - \omega_{4a}\right)} = \frac{\left(T_{4a} - T_{5a}\right)}{\left(T_{4a} - T_{sat}\right)} \tag{4.30}$$

The energetic performance parameters are calculated based on the equations as discussed in Chapter 3. The exergy in both refrigerant and air has been obtained by neglecting the kinetic and potential energies of the fluid as well as neglecting the changes in the chemical composition, which is expressed as discussed in Chapter 3.

4.1.7. Simulation and validation

A simulation code has been developed in Engineering Equation Solver (EES) platform based on the above mathematical model. The inputs are as follows: initial moisture content of carrot slices, air volume flow rate, inlet air temperature, and specific humidity, component specifications, evaporator, and condenser saturation temperatures. The calculation steps are as follows: with the guess value of refrigerant superheat (T_1) and the evaporator pressure (P_1), all the states points are calculated using compressor, evaporator, and condenser models, and the exact value of T_1 has been calculated by Newton-Raphson iteration method based on Eq.4.21 (Capillary tube model). The flow chart for the entire simulation is given in Fig. 4.5. Then, the humidity ratio and the temperature of the air at the inlet and exit to the drying chamber have been calculated

based on heater and dryer models. Finally, the different performance parameters of the heat pump dryer have been calculated.

For the validation of the simulation results, open type experimental setup of a heat pump dryer was designed and developed. The developed experimental setup is shown in Fig. 3.2, and the different component of the system is indicated in the HPD system. The specification of the different components of the heat pump dryer is considered for the validation of the simulation result is provided in Table 3.1. For the validation of the simulation model, the same air input conditions, mass flow to the evaporator rate, and the drying material (carrot) in the dryer have been considered. The drying air temperature was measured at the inlet and outlet of the drying chamber, evaporator, and condenser. The total energy consumption for the compressor and the fan was measured by the energy meter. The temperature and the pressure on the refrigerant side are measured by the thermocouple and the pressure gauge at a different positions in the cycle. Hygrometers and thermocouples were used for measuring the evaporator and dryer inlet and outlet air's relative humidity and temperature. The performance parameters considered for the validation are moisture extraction rate (MER), specific moisture extraction rate (SMER) and coefficient of performance(COP), and specific energy consumption (SEC), which are given in Table 4.2. The deviations of the simulation result with experimental for MER, SMER and COP are 5.87%, 19.5%, and 11.3% respectively, which are justifiable.

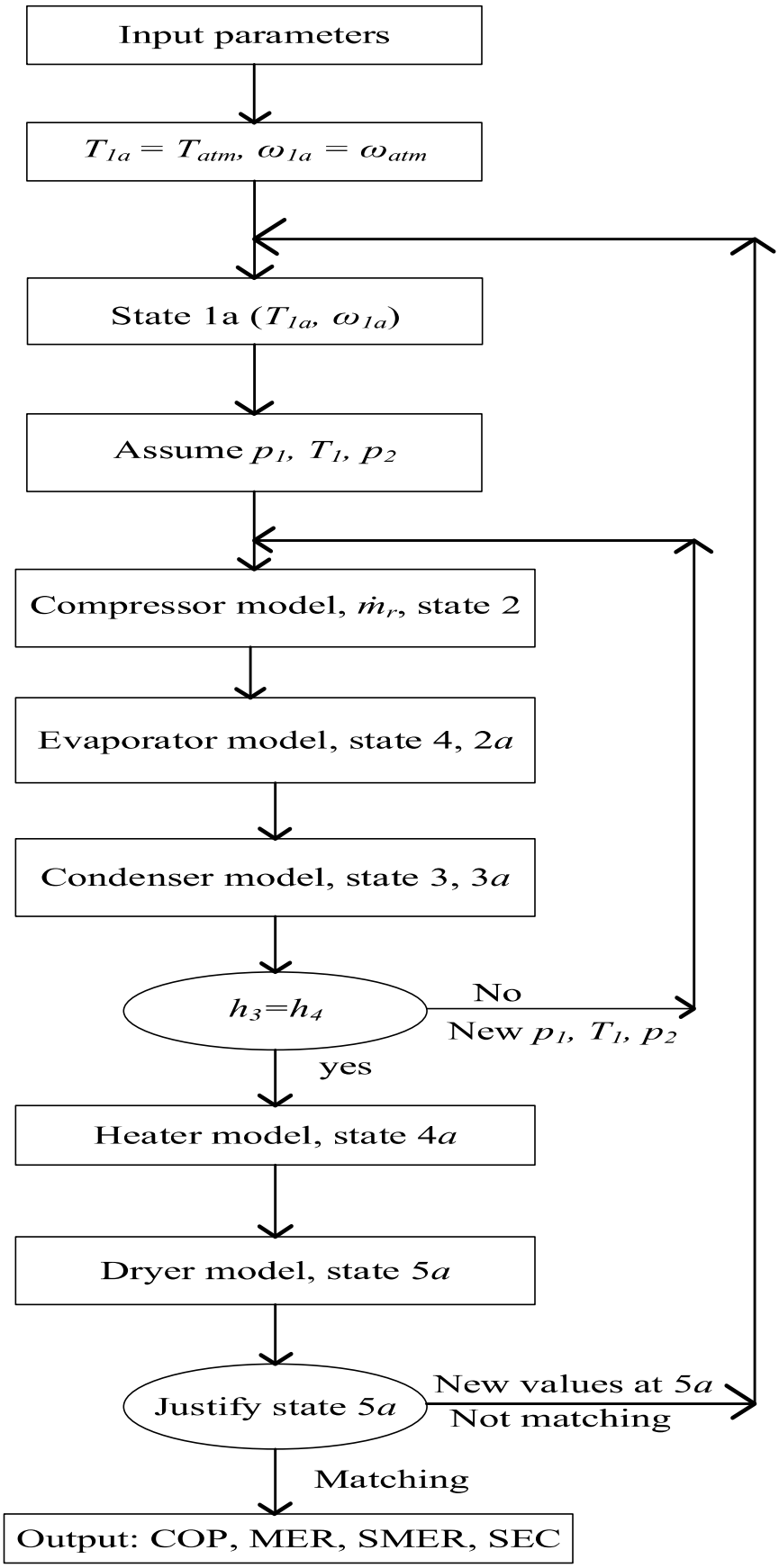

Fig. 4.5. Flow chart of the overall simulation

Table: 4.2. Validation of the simulation result with experimental data

Performance parameter	Simulation result	Experimental result
Air velocity (m/s)	1.0	1.0
Atmospheric air temperature °C)	30	30
Atmospheric air relative humidity (%)	70.6	70.6
MER (kg/h)	0.3931	0.37
SMER (kg/kWh)	1.069	0.86046
COP	4.318	3.83
SEC (kWh/kg)	0.7878	1.1621

4.2 Results and discussion

The performance of the HPD is mainly affected by the drying time and the energy consumption because the increase in drying time causes an increase in power input and a decrease in moisture removal rate from the products. Hence, the variation of various performance parameters such as MER, SMER, drying efficiency, moisture content, and dryer outlet temperature with drying time are studied for the inlet condition of drying air as T_{1a}=28°C and RH_{1a}=76%. The material considered in this analysis is 7 kg of carrot with an initial moisture content of 86% (wet basis). The temperature, humidity ratio, and the velocity of the air at the inlet are 28°C, 0.019 g/g, and 2 m/s, respectively. The specifications of the different components of the heat pump drying system used in the simulation are given in Table 3.1. A comparison of various performance parameters for the heat pump-based dryers is shown in Table 4.3 with the same amount of total power input (2 kW) to the system. Results are shown for the final moisture content of carrot of 12% (wet basis). As shown, heat pump-based drying is superior to hot air drying in terms of all performance parameters.

Table: 4.3. Performance comparison HPD for different refrigerants

Performance parameters	R134a HPD	R290 HPD	R152a HPD	R1234yf HPD	R600a HPD	R32 HPD	R1234ze(E) HPD	R600 HPD
Evaporator outlet temperature (°C)	23.54	23.56	23.65	23.58	23.57	23.4	23.86	23.5
Evaporator outlet humidity ratio	.01848	.0185	.01859	.01853	.01851	.018	.01889	.018
Dryer inlet temperature (°C)	37.32	37.63	37	37.45	38.74	38.9	36.71	37.3
Volumetric heating capacity (MJ/m^3)	8.39	7.358	7.474	8.3031	7.326	8.59	7.135	7.62
COP_{hp}	6.212	4.833	6.386	6.189	4.65	3.18	6.827	4.81
COP_{ws}	1.677	1.666	1.639	1.662	1.689	1.73	1.566	1.68
MER (kg/h)	1.022	1.054	1.061	1.011	1.096	1.11	0.9426	1.02
SMER (kg/kWh)	0.511	0.507	0.557	0.5057	0.5296	0.53	0.4712	0.51

Drying time (h)	5.068	5.11	4.66	5.121	4.977	4.88	5.469	5.06
SEC (kWh/kg)	1.957	1.93	1.799	1.977	1.882	1.88	2.122	1.95
DE	0.2644	0.264	0.2974	0.2665	0.2707	0.26	0.2593	0.26

Fig. 4.6 illustrates the variation of the dryer outlet air temperature with the drying time. As shown, initially the dryer outlet temperature decreases sharply with time due to the more heat transfer between the product and the drying air but after some time as the temperature of the product increases, the heat transfers rate decreases and the dryer outlet temperature starts to increase slowly. The maximum air outlet temperature of the dryer is R32 and the minimum for R1234ze(E) due to the highest and lowest dryer inlet temperature. The air outlet temperature of the dryer for R134a, R290, R152a, R600a, R1234yf, and R600 are in between the R1234ze(E) and R32. Variation of dryer outlet relative humidity (depends on the dryer outlet temperature and the specific humidity of the air) with drying time is shown in Fig. 4.7. As the dryer outlet temperature first decreases with time and hence the relative humidity increases but after some time, the temperature starts to increase. Also, the relative humidity of air starts to decrease with time because there is very less increase in specific humidity of air due decrease in moisture removal rate from the drying material. As shown in the figure, the dryer outlet air relative humidity is maximum for R1234ze (E) due to the lower moisture removal rate from the drying product. Whereas, dryer outlet air relative humidity is minimum for the R32 due to the higher removal rate from the product.

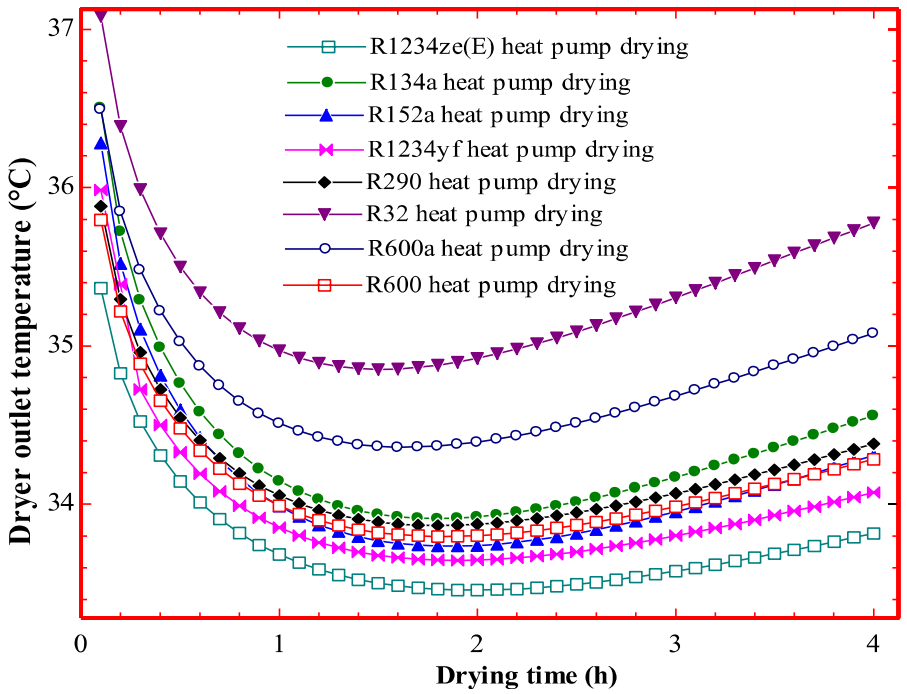

Fig. 4.6. Variation of dryer outlet temperature with drying time

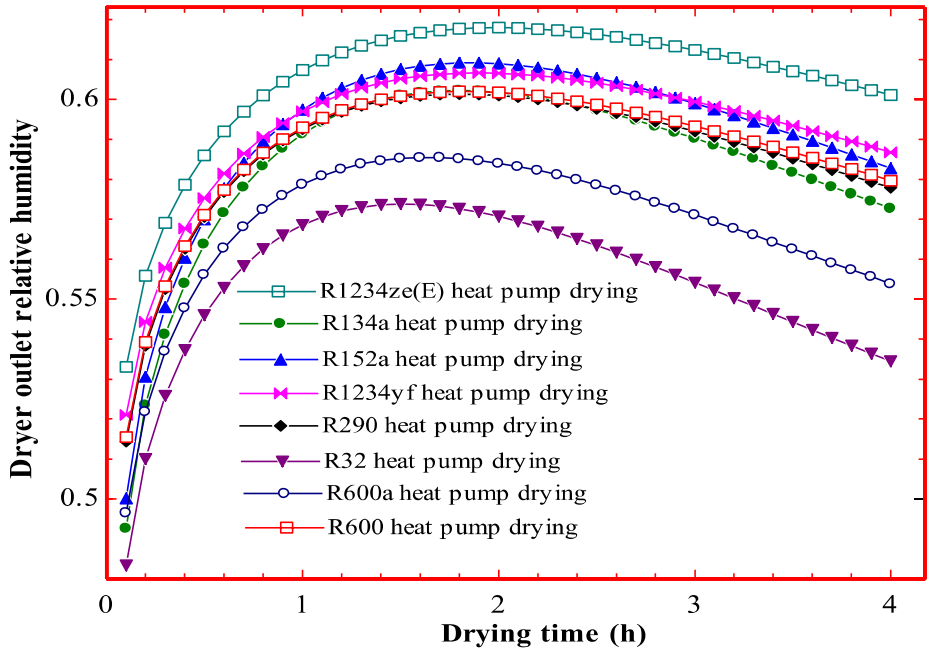

Fig. 4.7. Variation of dryer outlet relative humidity with drying time

Fig. 4.8 shows the variation in the moisture ratio with the drying time for HPD for different refrigerants. As shown, the moisture ratio decreases from the initial value of 0.99 to the final value of 0.12 with drying time due to the moisture removal from the product by air passing through the drying chamber. The moisture content and the

moisture ratio decrease exponentially from the initial to the final value. For heat pump dryer using R32, it decreases more sharply than using other refrigerants due to getting higher condenser outlet temperature of air for the same energy consumption and removing moisture at a faster rate. Values of moisture ratio change are nearly close for the HPD using R135a. R600a, R290, R152a, R1234ze(E), and R600 due to nearly the same condenser outlet temperature.

As shown in Fig. 4.9, the moisture extraction rate first increases with drying time but after some time it starts decreasing due to the decrease in the amount of moisture content of the product in the drying chamber. When the moisture content of the product is high, the moisture removal rate is also high but as the moisture content of the product decreases, the amount of moisture removed from the product decreases and so MER decreases. The maximum moisture extraction rate is 1.111 (kg/h) for the R32 heat pump drying due to higher drying temperature for the same amount of total power input (heater + fan + compressor) and minimum for the R1234ze(E). The average moisture extraction rate for R134a HPD, R290, R152a, R600a, R1234yf, R32, R1234ze(E) and R600 HPD are 1.022, 1.054, 1.061, 1.011, 1.096, 1.111, 09426 and 1.023kg/h, respectively.

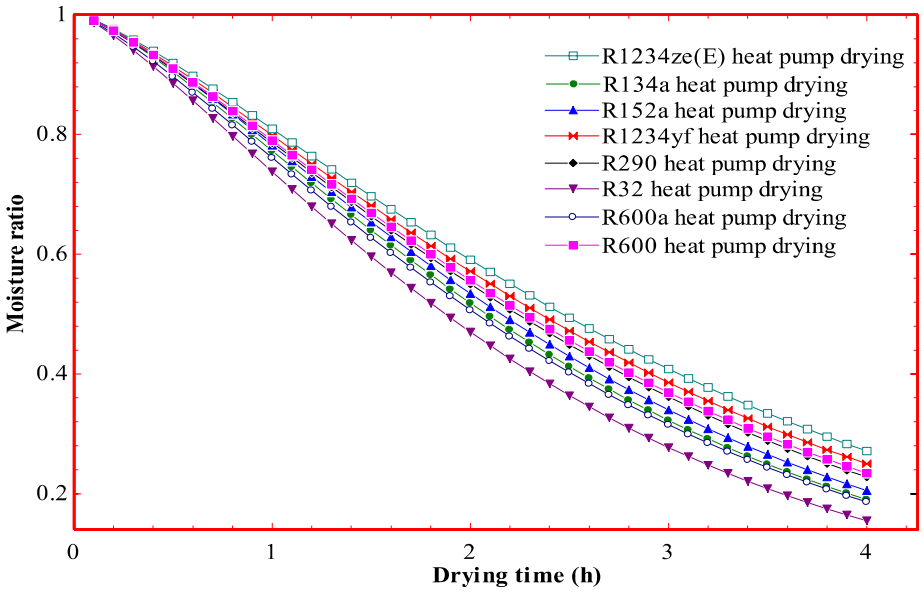

Fig. 4.8. Variation of moisture ratio with drying time

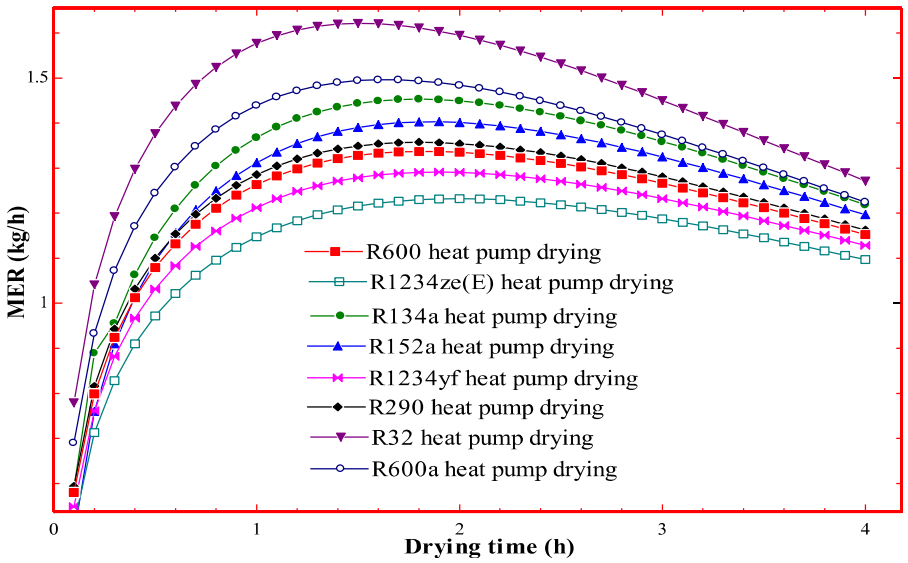

Fig. 4.9. Comparison of change in MER with drying time

Variation of specific moisture extraction rate (SMER) with drying time is shown in Fig. 4.10, which follows the same trend as moisture extraction rate for the HPD because the MER and SMER both depend on the amount of moisture removes from the product. It can be concluded that the SMER has the highest value for R152a and the lowest value for the R1234ze(E) heat pump drying. The specific moisture extraction rate is maximum for R152a because of less drying time required. The average values of SMER for R134a, R290, R152a, R600a, R1234yf, R32, R1234ze(E) and R600 are 0.511, 0.507, 0.557, 0.506, 0.530, 0.530, 0.4712 and 0.5117kg/kWh, respectively.

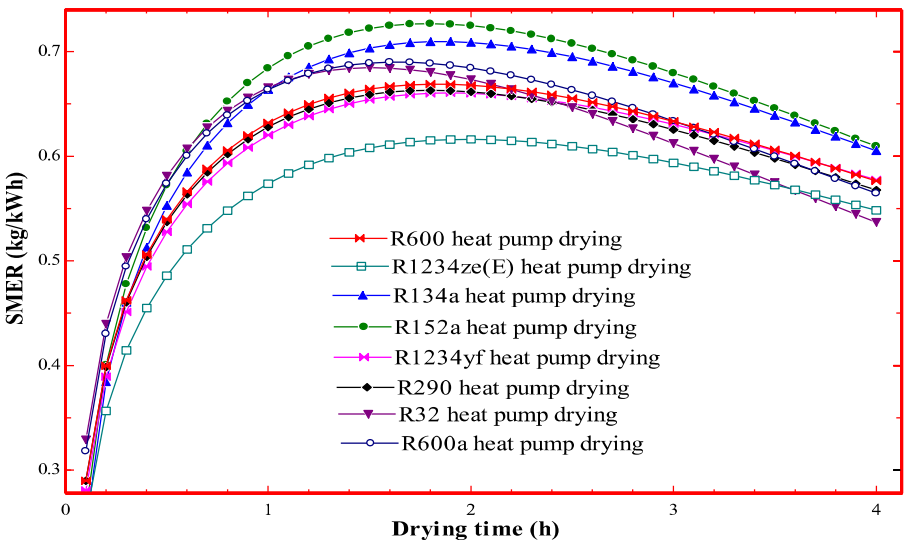

Fig. 4.10. Variation of SMER with drying time

The variation in moisture extraction rate with the moisture content of the drying material is shown in Fig. 4.11. As shown, the moisture extraction rate first increases with moisture content, but after a certain range of moisture content, it starts to decrease. Initially, the air removes less amount of moisture from the product when the moisture content is high due to the start of the establishment of heat and mass transfer between drying air and material, so the moisture extraction rate is low.

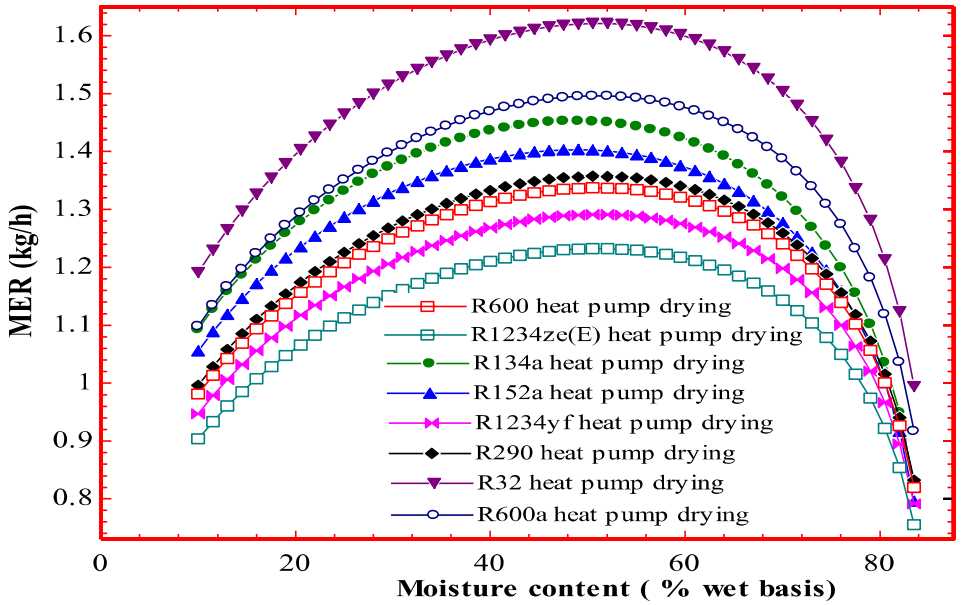

Fig. 4.11. Variation of moisture extraction rate with material moisture content

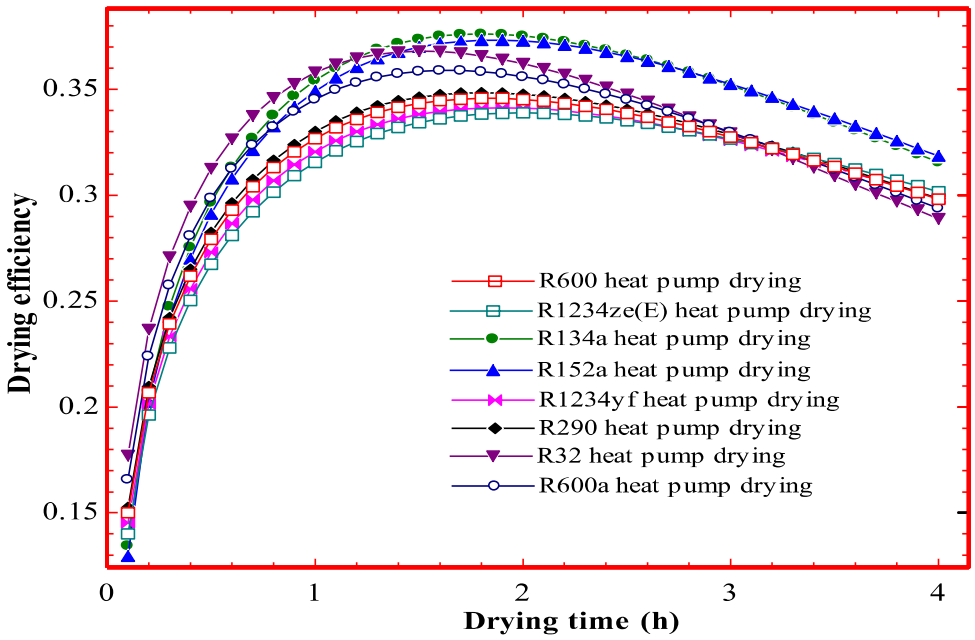

Fig. 4.12. Variation of drying efficiency of HPD with drying time

But at lower moisture content, the MER is low due to a decrease in diffusivity of moisture from the material. The MER is maximum for the R32 followed by R600a and minimum for R1234ze(E).

The variation of drying efficiency with the drying time is shown in Fig. 4.12 for considered refrigerants. The dryer efficiency depends on the dryer outlet temperature and the saturation temperature of the drying air inlet to the dryer. Hence, as shown in the figure, the dryer efficiency first increases as the dryer outlet air temperature decreases but after some time the dryer efficiency starts to decrease due to increases in dryer outlet temperature. The drying efficiency of the heat pump dryer is maximum for R152a.

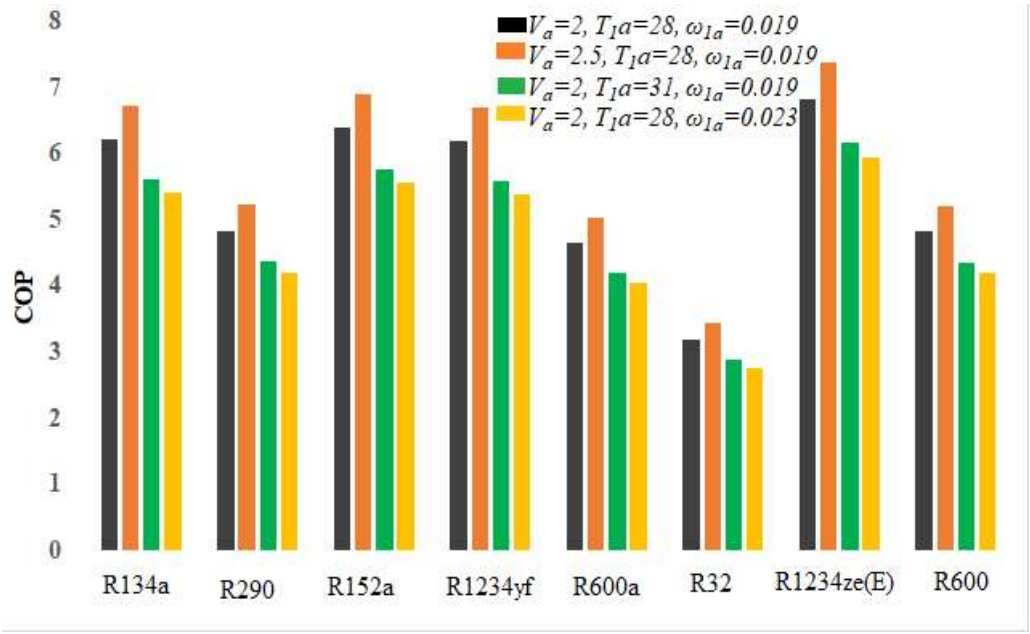

Fig. 4.13. COP of different refrigerants at different atmospheric conditions

Figs. 4.13 and 4.14 show the bar diagram of the COP and the SMER, respectively, for various refrigerants at different atmospheric conditions (inlet to the evaporator). From the figure, it can be seen that the COP of the heat pump drying system increases with an increase in the air velocity but it decreases with an increase in both air inlet temperature and the inlet humidity ratio to the evaporator. The COP decreases with air inlet temperature and humidity ratio due to the increase in the superheat of the refrigerant at

the evaporator outlet and a decrease in the sub-cool of the refrigerant at the condenser outlet. The SMER of the drying system decreases with an increase in the air velocity due decrease in the condenser outlet temperature at a higher velocity and the SMER increases with the increase in the air inlet temperature and the humidity ratio because of an increase in the drying temperature. The drying temperature increases with humidity ratio due increase in the dew point temperature at a higher humidity ratio and evaporator outlet temperature increases finally.

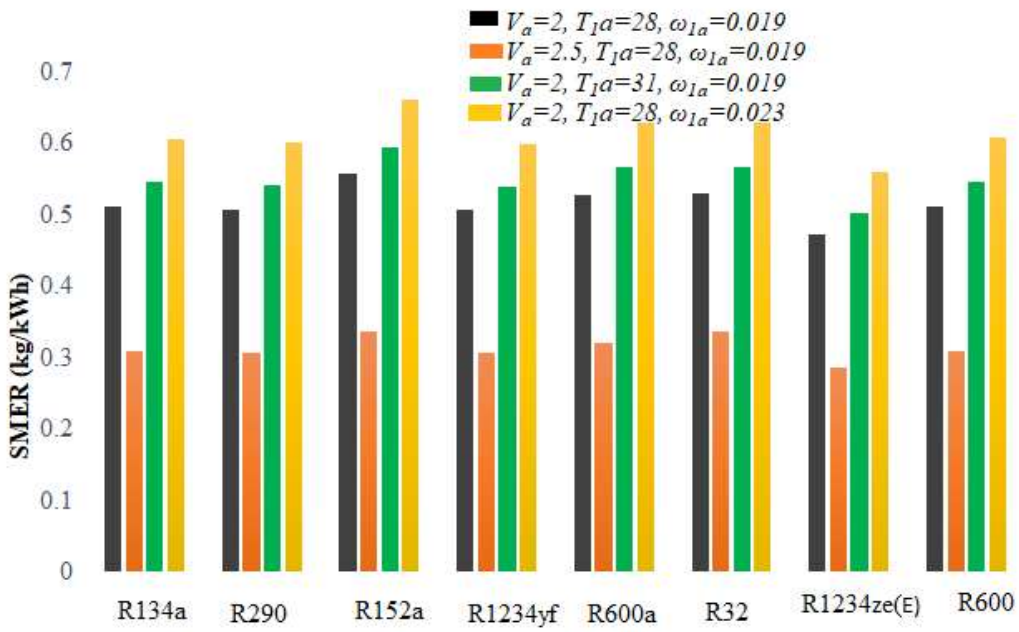

Fig. 4.14. SMER of different refrigerants at different atmospheric conditions

Table 4.4 shows the irreversibility and exergy efficiency of each component in a heat pump drying system using different refrigerants. The irreversibility is maximum in the heat pump dryer using the refrigerant R32 because of the higher temperature at the condenser, higher energy consumption in the compressor, and higher condensation of moisture in the evaporator. The exergy destruction is nearly the same for the refrigerant R134a and R1234yf. The evaporator contributes to maximum exergy destruction due to the condensation of the moisture. Fig. 4.15 shows the total exergy destruction in the

components of HPD using different refrigerants. As shown, total exergy destruction is maximum for R32 (0.7133 kW) and minimum for R1234ze(E) (0.2444 kW). This is due to the higher exergy destruction in the evaporator for R32 than others. R134a and R1234yf are having nearly the same total exergy destruction in the drying system.

Table: 4.4. Irreversibility (W) and exergy efficiency of HPD components

Refrigerant	compressor		condenser		Evaporator		Capillary tube		Dryer		Heater	
	Ex_{dest}	η_{ex}	Ex_{dest}	η_{ex}	Ex_{dest}	η_{ex}	Ex_{dest}	η_{ex}	Ex_{dest}	η_{ex}	Ex_{dest}	η_{ex}
R134a	52.8	0.89	80.6	0.82	95.7	0.71	26.1	0.93	19.1	0.55	38.2	0.022
R290	65.8	0.93	86.0	0.90	91.8	0.85	29.7	0.86	18.8	0.55	36.8	0.0223
R600	67.86	0.92	95.48	0.87	95.9	0.83	19.6	0.86	19.1	0.55	37.16	0.0257
R600a	86.3	0.92	147.2	0.91	96.7	0.90	27.2	0.83	20.1	0.54	33.61	0.0245
R152a	47.8	0.89	78.9	0.80	91.5	0.68	16.1	0.95	18.2	0.55	37.3	0.0211
R32	120.7	0.94	157.1	0.91	99.8	0.93	28.1	0.83	20.3	0.55	33.29	0.0254
R1234yf	52.2	0.90	75.1	0.84	92.3	0.75	32.3	0.92	18.7	0.55	23.79	0.0216
R1234ze(E)	41.3	0.87	61.41	0.79	79.3	0.63	10.6	0.95	16.6	0.56	35.34	0.0207

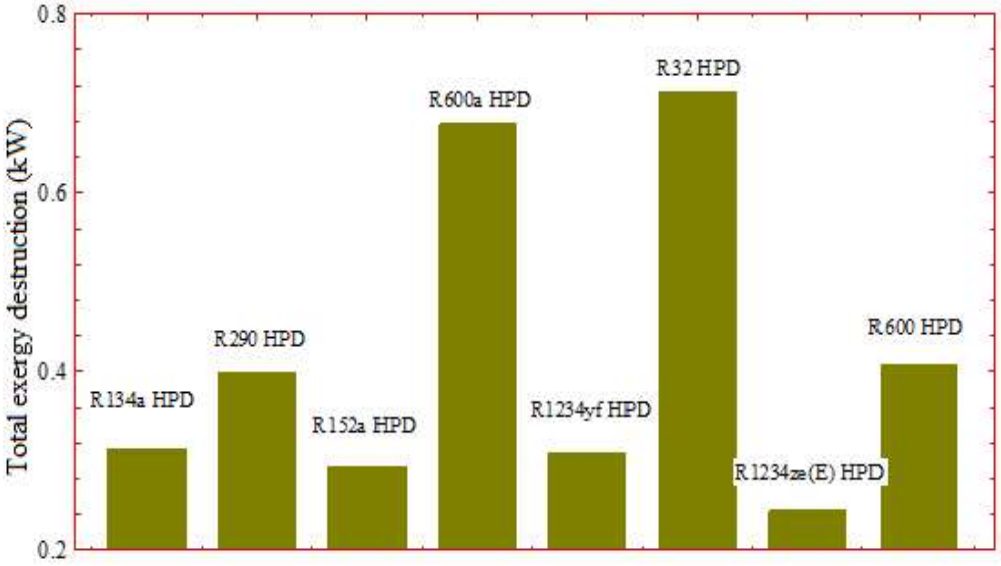

Fig. 4.15. Comparison of total exergy destruction with different refrigerants

4.3 Highlights

The simulation of the batch-type open cycle heat pump dryer has been carried out to predict the energy and exergy performances of the system and compare it with an electric heater-based conventional hot air dryer. Various low-GWP refrigerants have been proposed and compared based on different performance parameters of HPD for carrot drying. The highlights of the study are given below.

- The coefficient of performance of the heat pump (COP_{hp}) and coefficient of performance of the whole system (COP_{ws}) is maximum for R1234zez(E) and R32 respectively, and the (COP_{hp}) minimum for R32.
- The drying efficiency is better for the R152a HPD for the same power input and the average value is 29.74%.
- The moisture extraction rate (MER) is maximum for the R32 (average MER for R32 is about 8.7% more than that for R134a).
- The specific moisture extraction rate (SMER) is maximum for refrigerant R152a (average SMER for R152a is about 9% more than that for R134a).

- The specific energy consumption (SEC) and total drying time are minimum for the R152a HPD and values are 1.79kWh/kg and 4.66h, respectively.
- Total exergy destruction of the heat pump dryer is minimum for R1234ze(E) (0.2444kW) and maximum for R32 (0.713kW) for the same total power input.
- The COP of the system is higher for the higher mass flow rate and lower atmospheric inlet temperature and humidity to the system.
- Within studied refrigerants, R152a and R32 yield better performance; however, R152a may be more favorable for HPD due to lower GWP.

This page is intentionally left blank

CHAPTER 5

EXPERIMENTATION ON SOLAR-INFRARED ASSISTED HEAT PUMP DRYER

This chapter contains the details about the design, fabrication, and experimental performance analysis of the solar-infrared assisted heat pump dryer for the drying of the banana chips in a closed system model. A study on solar-infrared assisted heat pump dryers is carried out because it utilizes the renewable source of energy with an infrared heater to get a faster drying rate as compared to the simple HPD system. An evacuated tube-type solar water heater is used as the solar energy source for the heat pump dryer. In this, the air before entering the drying chamber is heated by hot water coming from a solar water heater. The basic heat pump cycle is used in this system as discussed in Chapter 3. A rectangular convective drying chamber with several trays of the improved design was used in the system. The analysis of solar-infrared assisted HPD was done for both open and closed cycle modes. The coefficient of performance (COP), moisture content, SMER, specific energy consumption, energy efficiency, energy utilization, irreversibility, and second law efficiency were compared for simple HPD, infrared-assisted HPD, solar-assisted HPD, and solar-infrared-assisted HPD.

5.1. Experimental setup and procedure

In this study, the design and development of a batch-type convective compact indirect expansion solar-infrared-assisted heat pump dryer (SIAHPD) were done, and the experiment was performed for the drying of food chips in a closed air cycle mode. Fig. 5.1 represents the schematic diagram of the SIAHPD. The SIAHPD system mainly comprises several subsystems such as a solar heater system, refrigeration cycle (heat

pump system), infrared heater system, drying medium cycle (air cycle), and dryer system. The heat pump system consists of a semi-hermetic R134a compressor, wavy fin condenser, evaporator, and capillary tube expansion device. Four thermocouples (PT100) were used to indicate the refrigerant temperature at the evaporator inlet, compressor inlet, compressor outlet, and condenser outlet. The pressure gauges were used in the heat pump cycle to measure the condenser saturation pressure and the evaporator saturation pressure. Energy meters, as shown in Fig. 5.2, were used to measure the electric energy consumption of the fan, water pump, and compressor. Coriolis mass flowmeter was installed in the experimental setup at the outlet of the compressor to measure the refrigerant mass flow rate in the HP cycle. The HP system was designed so that the refrigerant inlet to the compressor would be in the superheated state and it would be in a sub-cooled state at the condenser outlet. The details of the specification of the different components of the heat pump system and the drying cabin are provided in Table 3.1.

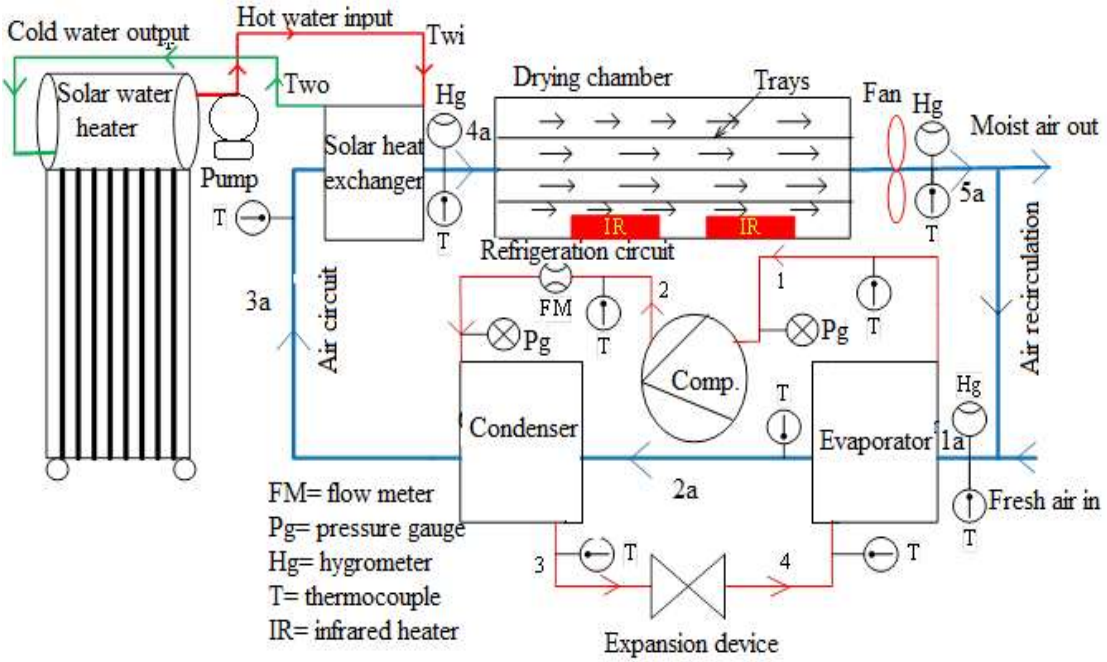

Fig. 5.1: Graphical representation of the heat pump drying system

Fig. 5.2: Photograph of the developed experimental setup of SIAHPD and drying chamber interior

The solar heating system consists of a solar water heater, water pump, and a wavy fin cross-flow heat exchanger. The solar water heater contains an insulated water tank with a capacity of 200 liters and 10 vacuum glass tubes of 54 mm diameter and transmittance of 82%. The total area of solar water heating tubes was $2m^2$. The water from the solar tank was circulated in the heat exchanger (Wavy fin, Cross-sectional dimension = 30.48 cm×33.02 cm, length of tube = 15.85m, diameter = 9.7mm) with the help of a water pump (rated power = 1/12hp, 220V, 50Hz, RPM = 6500). The solar heat exchanger was located just before the inlet of the drying chamber because the drying air coming from the condenser at a lower temperature is heated in the solar heat exchanger. The main advantage of using a solar water heater over the solar air heater or direct expansion solar heater is that in this, the air coming from the evaporator (dehumidified) was heated in a solar heat exchanger, which gives the more SMER rate as compared to the direct expansion solar heater or solar air heater, and it can store the hot water in the insulated water tank and can be used in the day time as well as night time also.

Two ceramic infrared heaters (rated power = 250W, dimension = 122mm×122mm, and rated voltage = 230V at 50Hz) were fitted at centers of two-half

inside the drying cabin (Fig. 5.2) to remove the moisture from inside the product to the product surface and direct vaporization of moisture by infrared radiation. The infrared heater was connected with a load control unit (variac dimmer stat) to regulate the power input to the infrared radiation to get the optimum moisture extraction rate in the infrared radiation range of the 3-4 μm (wavelength) and maintain the material temperature below the 80°C. The infrared radiation source contains the maximum energy in the radiation bandwidth; that's why it was used with solar radiation and HPD to get faster moisture removal with maximum energy utilization. The main advantage of using the infrared radiation source heater is that it deeply penetrates the products and removes the moisture from the inside product at a faster rate (Aktas et al., 2017).

The solar-infrared-assisted heat pump drying system was operated for the drying of the banana chips in four different operational modes: simple-HPD, IAHPD, SAHPD, and SIAHPD. In the SAHPD, only solar energy was used to remove the moisture from the product by heating the drying air, but in the SIAHPD, the solar energy was used to heat the drying air and infrared radiation was used in the drying chamber to in-depth heat the product directly for higher moisture removal from the product. The fresh green color banana bought from the market was washed and sliced into 2 mm size chips. The initial and the final MC of the banana chips were obtained by using the oven method at 102±3°C. A sample of 4.5kg of banana chips was dried separately in the various drying modes. The banana chips were spread out on the tray in the drying chamber, and for the homogeneous drying, the banana chips were mixed from time to time. The velocity of the air and the temperature were adjusted to the desired values for the banana chips drying. After that, the HP system was switched on and waited until the steady-state condition was achieved to get the desired drying temperature. The air volume flow rate was kept the same for the drying of banana chips with different modes. Then the banana

chips were weighted in digital balance and spread over the trays. Then, the trays were loaded inside the drying cabin and the fan was switched on to get the desired air mass flow rate, and infrared heater power was switched on to extract the moisture from the material by direct infrared radiation. The relative humidity and temperature at different positions were recorded periodically after every 15 minutes until the experiment ended. The weight loss from the drying material should be equal to the change in the humidity ratio of the drying air from dryer inlet to outlet and also equal to the moisture condensing in the evaporator. The energy meters were used to obtain the energy required for the pump, compressor, fan, and infrared heater. The average drying air temperature at the dryer inlet was between 62-67°C. Moisture reduction, MER, SMER, total energy input, COP, exergy loss, exergy efficiency, SEC, and drying efficiency were investigated.

5.2. Data analysis

The performance parameters of the solar-infrared-assisted heat pump drying system have been evaluated based on various measured parameters such as temperature, pressure, the flow rate of air as well as refrigerant, power input, etc.

Energy efficiency is the ratio of the energy utilized to remove the water from the drying product to the total energy consumed in the system as given by (Aktas et al., 2017),

$$\eta_{en} = \frac{h_{fg} m_w}{\mathrm{t}_d (W_{comp} + W_{fan} + W_{IR} + W_{pump})} \tag{5.1}$$

SMER is the ratio of the total amount of moisture removed from the material to the energy required in the whole drying process and is given as (Sevik et al.,2019),

$$\mathrm{SMER} = \frac{m_w}{\mathrm{t}_d (W_{comp} + W_{fan} + W_{IR} + W_{pump})} \tag{5.2}$$

SEC of the heat pump drying system is given by the ratio of the amount of energy required to remove the unit mass of the moisture from the product and is given by (Sevik et al., 2019),

$$\mathrm{SEC} = \frac{\mathrm{t}_d (W_{comp} + W_{fan} + W_{IR} + W_{pump})}{\mathrm{m}_w} \tag{5.3}$$

The exergy destruction (or irreversibility) can be estimated by applying the general exergy balance equation as discussed in Chapter 3.

The exergy destruction and the efficiency of the solar water heat exchanger is calculated by,

$$Ex_{\mathrm{dest,SHE}} = \dot{m}_{hw}\left(e_{xw,in} - e_{xw,out}\right) + \dot{m}_a\left(e_{x3a} - e_{x4a}\right) + W_{pump} \tag{5.4}$$

$$\eta_{\mathrm{ex,SHE}} = \frac{\dot{m}_a\left(e_{x3a} - e_{x4a}\right)}{\dot{m}_{hw}\left(e_{xw,in} - e_{xw,out}\right) + W_{pump}} \tag{5.5}$$

The exergy destruction in the drying chamber is mainly due to the heat and the mass exchange between the product and air, and is estimated by the following (Atalay, 2019),

$$Ex_{\mathrm{dest},dryer} = \dot{m}_a\left(e_{x4a} - e_{x5a}\right) + W_{fan} \tag{5.6}$$

$$\eta_{\mathrm{ex},dryer} = \frac{\dot{m}_a\left(e_{x4a} - e_{x5a}\right)}{W_{fan}} \tag{5.7}$$

The exergy efficiency of the drying chamber for the infrared-assisted drying system can be estimated by (Atalay, 2019),

$$\eta_{\mathrm{ex},dryer} = \frac{\dot{m}_a\left(e_{x4a} - e_{x5a}\right)}{W_{fan} + \dot{E}_{abs}} \tag{5.8}$$

Based on the above definition, the absorbed exergy by the material can be given as the product of the energy absorbed by an energy quality factor which is given (Aghbashlo, 2016),

$$\dot{E}_{abs} = \beta \times \dot{Q}_{abs} \tag{5.9}$$

According to the various similar type of studies for obtaining the value of energy absorbed by the material, the quality factor is the ratio of the total exergy to the total energy value. This quality factor is a correlation to estimate the most feasible results. The quality factor is given as follows (Aghbashlo, 2016),

$$\beta = 1 + \frac{1}{3}\left(\frac{T_o}{T_{IR}}\right)^4 (\varepsilon_{IR})^{-1} - \frac{4}{3}(\varepsilon_{IR})^{-0.25}\left(\frac{T_o}{T_{IR}}\right) \tag{5.10}$$

Where T_{IR} is the infrared heater surface temperature,

The absorbed energy by the drying material can be obtained by applying the energy balance between the product and the infrared radiation because some part of infrared radiation is absorbed and the remaining radiations are transmitted, reflected by the surrounding, or emitted by the product. The absorbed energy is given as (Aghbashlo, 2016),

$$\dot{Q}_{abs} = IR_{radation} - IR_{reflected} - IR_{transmitted} - IR_{emitted} \tag{5.11}$$

The energy absorbed by drying material is a portion of energy that is directly exposed to the infrared heater. The radiation network method was used to estimate the actual amount of absorbed energy by the product (Aghbashlo, 2016). In the radiation network method, the drying chamber is considered as a three-surface closed volume with surfaces as a drying chamber wall, infrared heater, and drying product. By balancing the heat flow between the three surfaces, the absorbed energy can be written as (Aghbashlo, 2016),

$$\dot{Q}_{abs} = \frac{\sigma\left(T_{IR}^4 - T_M^4\right)}{\frac{1-\varepsilon_{IR}}{A_{IR}\varepsilon_{IR}} + \frac{1}{1/\left(1/A_{IR}F_{IR-M}\right)+1/\left(1/A_{IR}F_{IR-DC}\right)+1/\left(1/A_M F_{M-DC}\right)} + \frac{1-\varepsilon_M}{A_M\varepsilon_M}} \tag{5.12}$$

For the design and development of SIAHPD, with thermal analysis, the economic analysis must be considered. Economic analysis of SIAHPD depends on initial capital

investment cost and running cost. The capital cost of SIAHPD includes the cost of compressor, heat exchangers (condenser, evaporator, and solar water heat exchanger), refrigerant, expansion device, fan, water heating system (evacuated tube type), water pump, air duct, basic structure, system installation cost, and labor cost. The total running cost of the dried product can be given by the following (Yahya et al., 2018),

$$C_{RU} = C_{RM} + C_P + C_L + C_m \quad (5.13)$$

Where, C_{RM}, C_p, $C_{L,}$ and C_m are raw material cost, energy consumption cost, labor cost, and maintenance cost. Where maintenance cost (C_m) is considered as 2 % of the total capital cost (Yahya et al., 2018),

Hence, the total cost of the drying is given as,

$$C_{Total} = C_{IC} + C_{RU} \quad (5.14)$$

The total profit (C_F) by using a simple HP dryer or a Hybrid-source HP drying system for intermittent drying of banana chips is the difference between the total sale cost of the dried product and the total cost of the solar-assisted-HP dryer system and is given as the following,

$$C_F = C_{Total,\text{sale}} - C_{RU} \quad (5.15)$$

The payback period (P_P) of the solar-assisted-HP dryer for intermittent drying is given as (Yahya et al., 2018),

$$P_P = C_{IC} / C_F \quad (5.16)$$

5.3 Results and discussion

The banana chips (agricultural product) were dried in the solar-infrared assisted HPD with recirculation of the drying air and the performances were estimated for HPD, SAHPD, IAHPD, and SIAHPD modes. For solar-assisted modes, performance is dependent on solar radiation and ambient condition at the location of the experiment.

The hourly solar radiation intensity first increases with becomes highest and then decreases. The average solar intensity is 539.77W/m^2. Hence, to get similar ambient conditions and solar radiation, all the experiments were conducted at similar times on different days. In the literature, people have done the experiment for the air velocity range of 0.5-2.5m/s [Aktas et al.,2017, Sevik et al.,2019] and hence the same velocity range has been considered and 1m/s has been taken as design velocity of drying air. However, due to the limitations of the fan speed installed in the experimental setup and other unaccounted resistances, the actual air velocity was measured as 0.8 m/s. The drying air velocity was 0. 8m/s for all types of drying experiments. Fig. 5.3 shows the photographs of the banana chips before drying and after drying in the solar-infrared-assisted heat pump dryer in the closed-loop system. The desirable product color has been observed.

Fig. 5.3: Photograph of the banana chips before drying (a) and after drying (b)

The experimental results of different modes are listed in Table 5.1. The energy requirement is highest for the infrared-assisted heat pump system drying due to the highest consumption of energy by the infrared heater (two heaters each of 250W). The energy consumption is lowest for the SAHPD due to the very low power consumption by the water pump (50W) and getting higher drying air temperature, which also decreases the drying time and finally energy consumption for the compressor, fan, and pump. In SIAHPD, a higher rate of drying was obtained because of the dual effect of increasing

moisture removal potential of dying air due to temperature increase by solar heating and direct moisture removal by infrared radiation. However, the SMER is less than that of SAHPD due to extra energy consumption by the infrared heaters. The average drying air temperature is between 47-51°C for the simple HPD and IAHPD, and it is between 62-67°C for the SAHPD and SIAHPD. The optimum drying temperature for the banana chips to get the best color and quality of the dried product is in the range of 60-70°C (Liete et al., 2005). It implies that the solar-assisted dying modes yield the best color and quality product.

Table 5.1: Comparison of various parameters

Performance parameter	Types of the drying system			
	HPD	IAHPD	SAHPD	SIAHPD
Moisture content (% w.b), initial-final	83.8-11.5	83.8-11.5	83.8-11.5	83.8-11.5
Total drying time (min)	345	255	225	180
Average drying temperature (°C)	50.25	50.54	65.1	65.7
Total energy consumption (kWh)	2.75	2.98	2.024	2.52
Average MER (kg/h)	0.4747	0.7068	0.8224	1.1618
Average SMER (kg/kWh)	0.975	0.968	1.45	1.351
Average SEC (kWh/kg)	1.0256	1.033	0.6896	0.7402
Average Drying efficiency (%)	31.38	40.39	50.49	61.92
Energy efficiency (%)	54.1	39.44	58.5	47.73

The drying temperature is lowest for the simple-HPD and IAHPD systems for banana chips drying due to using the only heat pump system for air heating before the entrance of the drying cabinet. The dryer inlet temperature depends on the condenser

saturation temperature and the amount of heat delivered by the refrigerant to the air in the condenser and the heat given by the water to the air in the solar heat exchanger. The performance of the drying system depends on the drying air temperature, humidity, air mass flow rate, and the effective diffusivity of the material. The drying process is carried out until the difference between the humidity at the drying chamber outlet and inlet has become negligible. From the result, it can be concluded that the time for drying chips is lowest for the solar-infrared-assisted HPD and highest for the simple HPD. The drying time depends on the mass transfer coefficient, diffusivity, drying air humidity, velocity, and temperature. So the drying time was lowest for the SIAHPD due to the effect of the high-temperature drying and the direct effect of the infrared radiation on the moisture removal from the product. Total drying time for banana chips in a closed system drying with simple HPD, IAHPD, SAHPD, and SIAHPD are 345, 255, 225, and 180min, respectively.

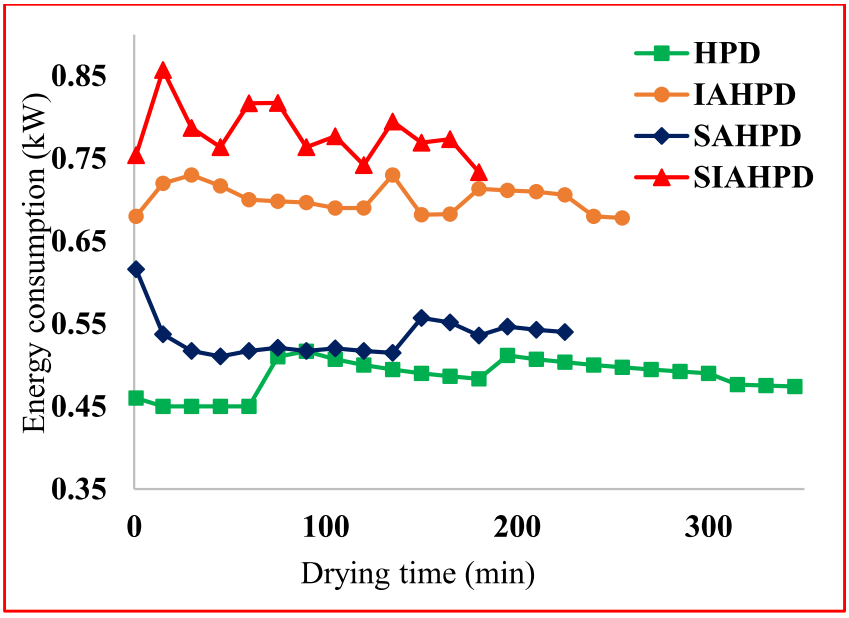

Fig. 5.4: Variation in energy requirement with drying time

Fig. 5.4 shows the energy required for the drying system due to the compressor, fan, infrared heater, and pump for all types of the drying system. As discussed earlier, due to free thermal energy received from the collector for the solar-assisted systems and

extra energy consumed by infrared heaters for the infrared-assisted systems, the energy consumptions are much higher for the infrared-assisted drying system. The average energy consumption for the drying of banana chips in simple-HPD, IAHPD, SAHPD, and SIAHPD are found to be 2.75kW, 2.98kW, 2.024kW, and 2.52kW respectively.

The SEC is highest for the simple HPD system because of getting the low temperature for the same air mass flow rate and lower moisture removal rate and higher energy consumption. SEC is the lowest for the SAHPD drying system due to the high-temperature drying and lower energy consumption by the water pump and compressor. The average values of the SEC for banana chips in simple HPD, infrared-assisted HPD, SAHPD, and solar-infrared-assisted HPD systems are 1.0256, 1.033, 0.6896, and 0.7402kWh/kg, respectively and the SEC is nearly 55.22% more in simple HPD system as compared to the SAHPD drying system. And the specific energy consumption for SAHPD is almost in the range of a solar dryer integrated with a solar air heater (1.07 kWh/kg and 0.56 kWh/kg, respectively, Ekka et al., 2020).

In terms of COP, the simple heat pump drying for banana chips is best because in a simple HPD system the values of humidity and inlet temperature to the evaporator are low (the COP of the heat pump increases with a decrease in humidity and temperature at evaporator inlet). The COP is better for the simple HPD system for given environmental conditions as compared to the other drying systems, and the average values of COP for the simple HPD, IAHPD, SAHPD, and SIAHPD are 2.61, 2.303, 2.01, and 1.94, respectively (Ganjehsarabi et al., 2014). Fig. 5.5 shows the variation of the COP of the various drying system with drying time. The nature of the variation is fluctuating for the coefficient of the performance according to time. The COP of all types of systems is fluctuating with time due to the change in the humidity and the temperature inlet to the evaporator. In a closed system, the dryer outlet air is directly re-circulated to

the evaporator, and the humidity and the temperature of dryer outlet air continuously changes with time, and thus the COP was also varying with time. The average COP is lowest for the SIAHPD system due to the high moisture content and temperature of the air at the evaporator inlet because the degree of superheat at the compressor inlet increases with humidity and temperature which finally increases the energy consumed by the compressor and decreases the heating capacity of drying air in the condenser.

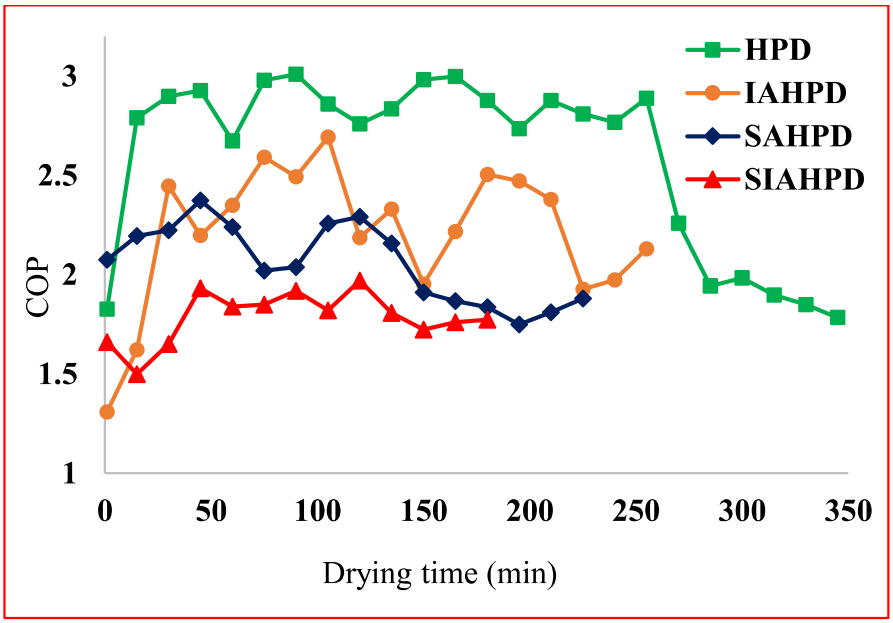

Fig. 5.5: Variation in COP with drying time

Fig. 5.6 represents the variation of the energy efficiency of the drying unit for the simple HPD, IAHPD, SAHPD, and SIAHPD systems according to drying time. The energy efficiency depends upon the vaporization of the moisture from the product and the energy consumption in the HPD system, and it is the ratio of the energy of the vaporization of water from material to the total energy input to the system. The energy efficiency first increases with time and reaches the peak value and then decreases after some time because starting the moisture removal from the product first increases its value with time but after some time moisture removal from the product decreases due to the loss in the moisture content of the material and hence decrease in moisture removal potential (difference in specific humidity of product surface and air). The energy

efficiency is highest for the SAHPD drying due to the higher drying temperature and lowest energy consumption, and lowest for the IAHPD drying system due to the high energy consumption of the infrared heater (Aktas et al., 2017). The average value of the energy efficiency for the simple HPD, IAHPD, SAHPD, and SIAHPD system are 54.1 %, 39.44 % and 58.5%, 47.73%, respectively.

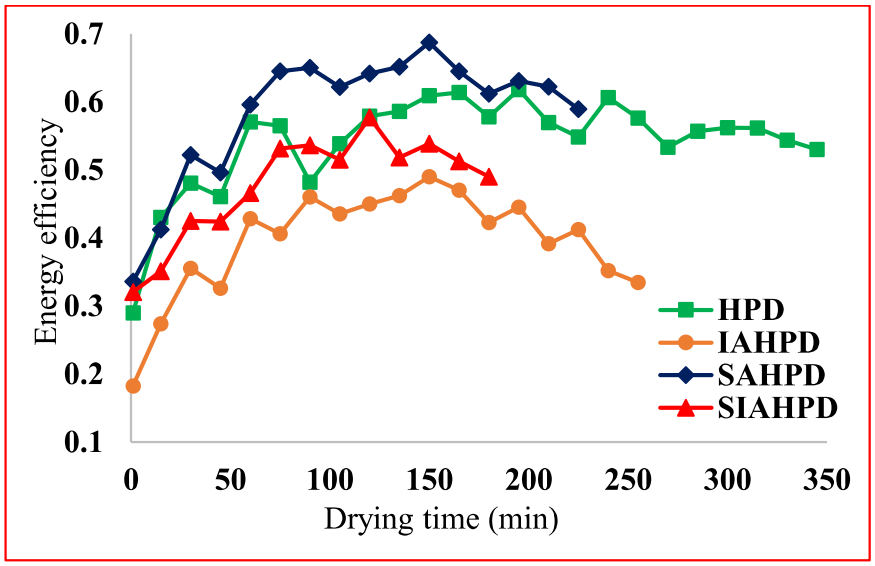

Fig. 5.6: Variation in energy efficiency with drying time

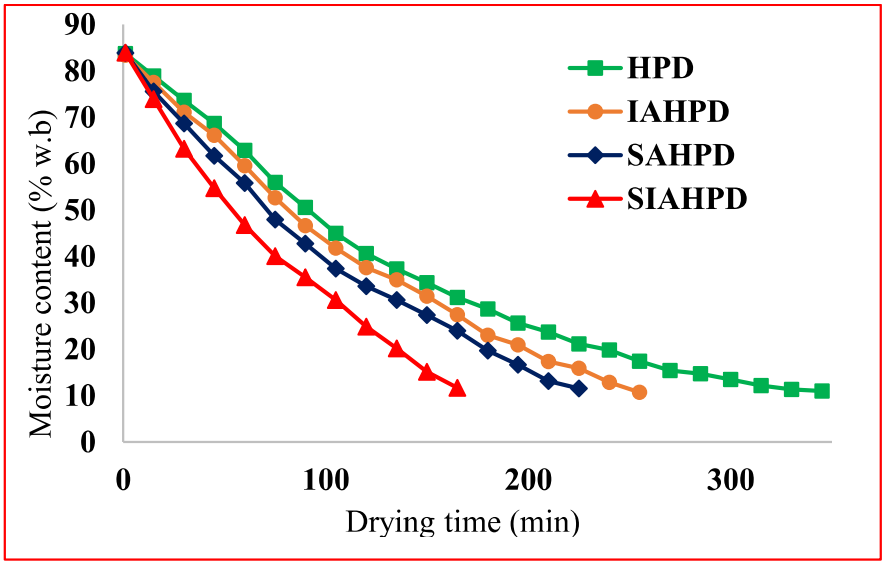

Fig. 5.7: Change in moisture content with drying time

As shown in Fig. 5.7, the moisture content decreases with the drying time because of the removal of the moisture from the material by drying air and the direct effect of

infrared radiation. The MC decreases at a faster rate for the SIAHPD due to the higher drying temperature and direct effect of infrared radiation, which removes the moisture from the product at a higher rate. Initially, the MC decreases at a faster rate, but after some time, as the diffusion of moisture from the inside product to the outer side decreases, it decreases at a slower rate. The change in the MC is slowest for the simple HPD due to low drying temperature.

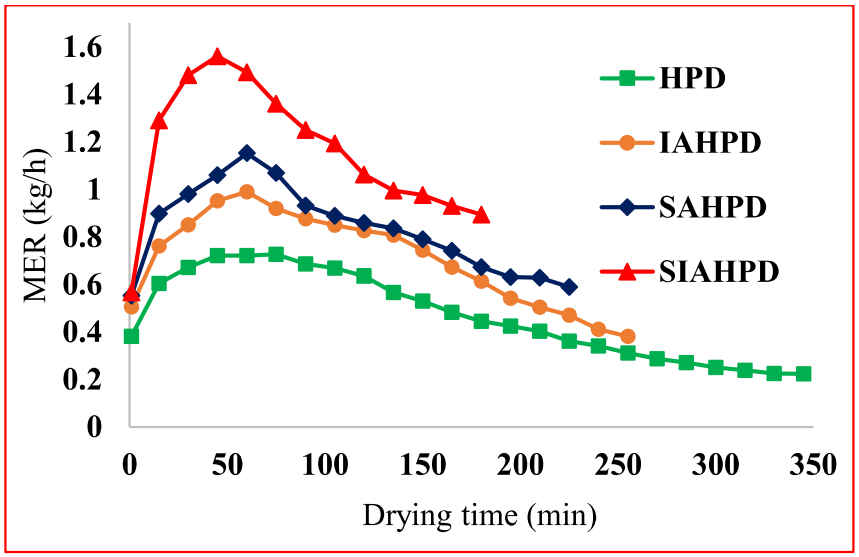

Fig. 5.8: Variation in moisture extraction rate with drying time

The performance of the HPD depends on product MC, diffusivity, mass transfer coefficient, drying air velocity, air temperature, and direct effect of infrared radiation. The MER first increases with time till the maximum value, but later some time, it starts to decrease due to the loss in material MC (decrease in drying air humidity potential) as shown in Fig. 5.8. The MER is highest for the SIAHPD because of the higher drying temperature and faster moisture removal from the product due to the direct effect of the infrared radiation on the product. The infrared radiation directly penetrated the product and removed the moisture from inside to the surface of the product, which is carried away by the high-temperature drying air. The MER rate is lowest for the simple HPD due to the low temperature. The average value of MER for banana chips drying in simple HPD,

IAHPD, SAHPD, and SIAHPD are 0.4747, 0.7068, 0.8224, and 1.1618kg/h, respectively.

Fig. 5.9 shows the change of the SMER with the drying time for the four different types of drying. SMER depends on the MC of drying material, drying air velocity, and temperature. The SMER first increases with time because of the initiation of the mass and heat exchange between the drying air and product, but after some time, it started to decrease due to the loss in the MC from the material. The average SMER is highest for SAHPD due to the high drying temperature (high moisture removal potential) and lower value of the energy input as compared to the SIAHPD with a mean value of 1.45kg/kWh and the lowest is for IAHPD with a mean value of 0.968 kg/kWh, which was nearly similar to the simple HPD. The result of SMER for the simple HPD (0.975kg/kWh) is similar to the result given in the literature (Hadi et al., 2014). The MER is better for IAHPD, but the SMER is minimum because of more power consumption (due to the infrared heater) as compared to the simple HPD. For the SIAHPD system, the SMER is low due to the high-grade energy consumption by the infrared heater as compared to the SAHPD system.

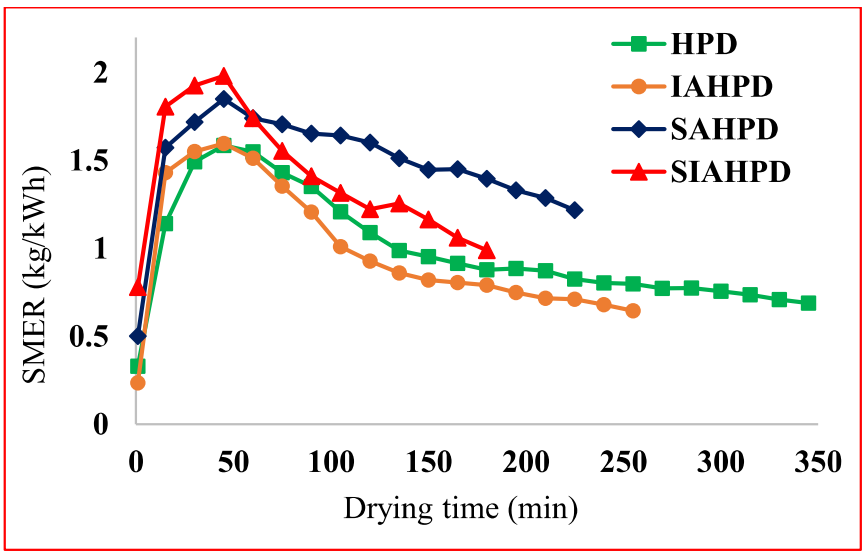

Fig. 5.9: Variation of specific moisture extraction rate with drying time

The drying efficiency depends on the drying chamber outlet humidity and temperature, inlet humidity and temperature, and the saturation temperature and humidity at dryer inlet wet-bulb temperature (Aktas et al., 2016). Fig. 5.10 shows the variation of drying efficiency with time. Its average value was better for the SIAHPD due to the getting of higher drying temperature and higher moisture extraction from the product due to the infrared radiation. The drying efficiency first increases with time due to the decreases in dryer outlet temperature and increase in humidity, but it starts to decrease after some time due to the increase in the temperature of the dryer and decrease in air humidity at the dryer outlet. The drying efficiency is higher for the SIAHPD as compared to other drying systems due to higher temperature drying and humidity extraction. The average drying efficiency of simple HPD, IAHPD, SAHPD, and SIAHPD are 31.8, 39.44, 50.49, and 60.92%, respectively. The drying efficiency of SAHPD (50.49%) was found better than the conventional solar dryer (33.5%) presented in the literature (Lakshmi et al., 2019)

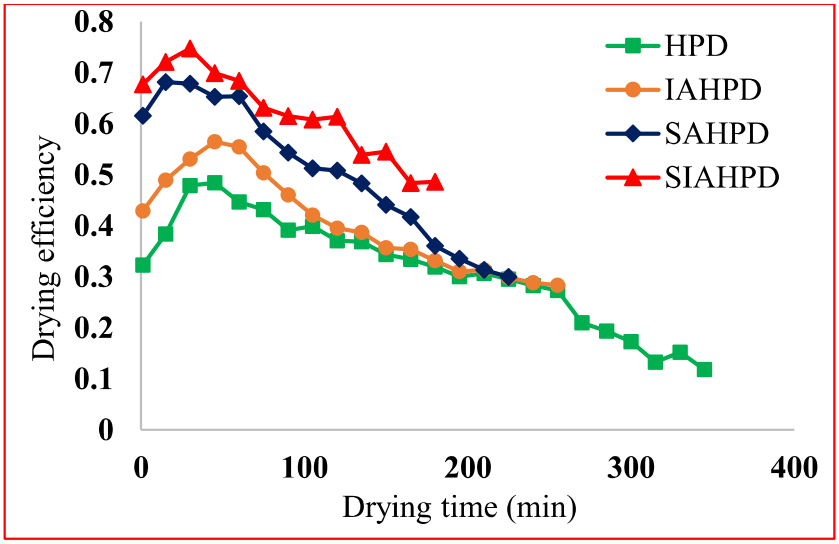

Fig. 5.10: Variation of drying efficiency with drying time

Fig. 5.11 shows the MER variation with the MC of the product. The MER was lower when the MC of the product is low, but the MER increased with an increase in the MC of the material. The MER rate was maximum in between the MC of 40-70%, and

after that, its value was low because at that time, the experiment was in the initial stage. Initially, the MC of the product is high, but the MER is low due to the establishment of the mass transfer and heat exchange between the product and the air.

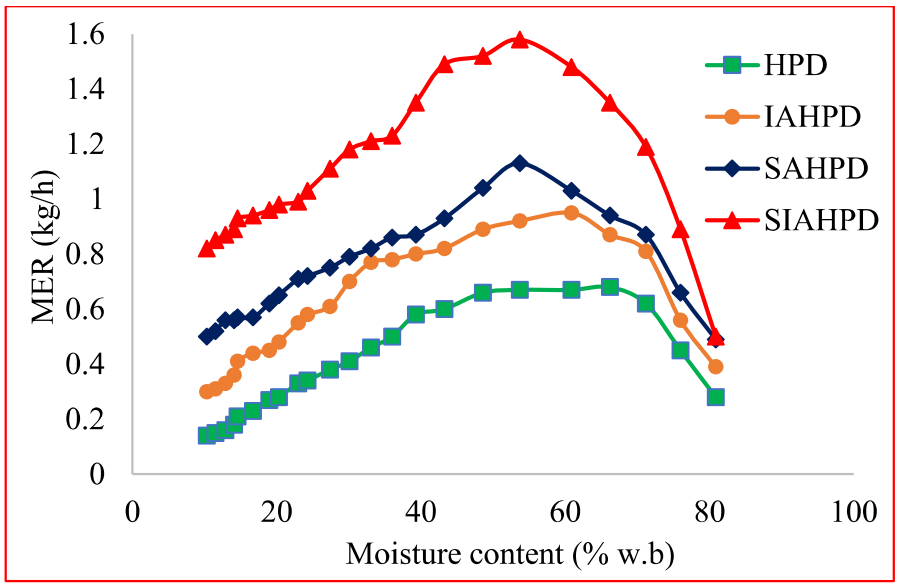

Fig. 5.11: Variation in MER with the moisture content of the product

The component-wise exergy efficiency and exergy destruction are given in Table 5.2. It gives the irreversibility in the components of the drying system due to the energy transfer between air and the refrigerant, between product and hot air, and water and the drying air. The exergy destruction was also highest in the compressor due to the moving part (dissipating more energy due to friction) and a higher degree of superheat. In the evaporator, the exergy destruction was due to the moisture condensation. The infrared heater is also a significant contributor to exergy destruction due to its higher temperature difference.

Table: 5.2. Irreversibility (kW) and exergy efficiency of different components

Type of system/ component	HPD		IAHPD		SAHPD		SIAHPD	
	Ex_{dest}	η_{ex}	Ex_{dest}	η_{ex}	Ex_{dest}	η_{ex}	Ex_{dest}	η_{ex}
Compressor	0.1559	0.659	0.164	0.58	0.2221	0.602	0.296	0.52
Condenser	0.0508	0.868	0.0457	0.907	0.0518	0.925	0.0308	0.912
Expansion device	0.047	0.751	0.0448	0.757	0.0358	0.741	0.0343	0.744
Evaporator	0.1311	0.57	0.112	0.631	0.122	0.71	0.0616	0.743
Drying chamber	0.0196	0.153	0.0213	0.134	0.017	0.24	0.025	0.203
Solar heat exchanger	…….	…….	……	……..	0.071	0.681	0.069	0.711
Infrared heater	…….	…….	0.0766	0.861	……	……	0.0813	0.848
Total Exergy destruction (kW)	0.4044		0.4644		0.5197		0.598	

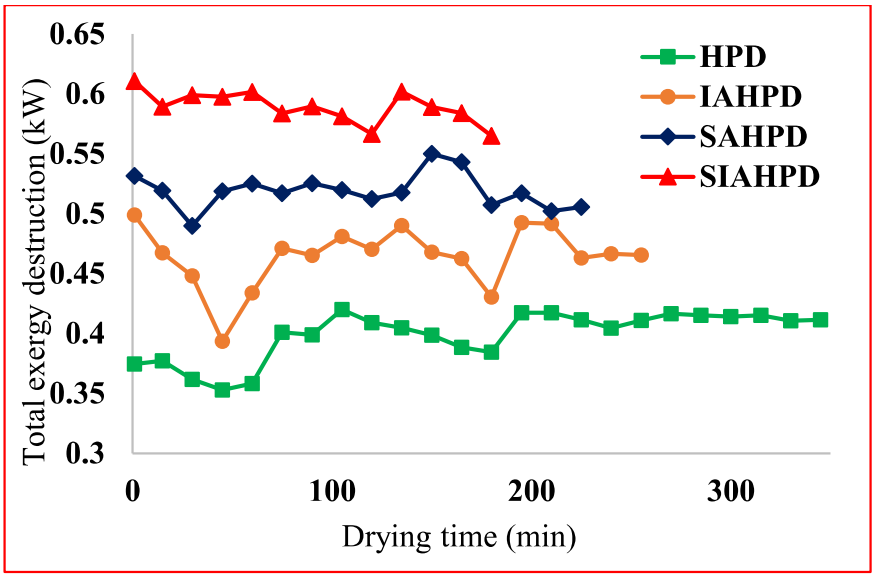

Fig. 5.12: Variation in the total exergy destruction with drying time

Fig. 5.12 shows the destruction of the exergy in the HPD system with drying time. The exergy destruction is highest for the SIAHPD because, at a higher temperature, destruction was also higher and also due to high-temperature water and the infrared heater. The exergy destruction is lowest in the simple HPD system due to the lower drying temperature. The highest exergy destruction was taking place in the first stage of the drying, and after that, it decreases slowly due to the decrease in drying temperature. Total exergy destruction in HPD, IAHPD, SAHPD and SIAHPD for banana chips drying are 0.4001kW, 0.4644kW, 0.5188kW and 0.598kW, respectively.

In the present study, an evacuated tube solar water heater was used to utilize solar energy for the drying of the banana chips. The heating capacity of the solar water heater depends on the available solar radiation, as the radiation incidence on the tubes changes with the daytime, the output temperature of the water may change. Hence, the solar-assisted system may suffer from more fluctuation. The size of the drying system is similar to the simple HPD and IAHPD and smaller as compared to the SAHPD and SIAHPD because the size of the solar water heater with heat exchanger is much larger compared to the infrared heater. Hence, the initial investment cost of the simple HPD is minimum

and maximum for the SIAHPD due to the additional cost of solar heating systems and infrared heaters. The investment cost details of the drying system are given in Table 5.3. The running cost was minimum for SAHPD and maximum for IAHPD. The total initial cost of simple HPD, IAHPD, SAHPD, and SIAHPD are 521.31$, 567.9$, 892.94$, and 939.54$, respectively. The running cost of IAHPD is highest due to the high energy consumption by the infrared heater as compared to the water pump in SAHPD. The drying cost per kg of material for the banana chips in simple HPD, IAHPD, SAHPD and SIAHPD are 0.488$/kg, 0.497$/kg, 0.469$/kg and 0.484$/kg, respectively. The payback period of the all studied system was calculated based on the profit gained by selling the dried material and the total cost of the drying (running cost + initial cost). The payback period for the simple HPD, IAHPD, SAHPD, and SIAHPD is calculated as 0.392 years, 0.436 years, 0.633 years, and 0.969 years, respectively.

Table: 5.3. Economic parameters of components of drying system

Parameter	Cost of the parameter ($)			
	HPD	SAHPD	IAHPD	SIAHPD
The cost of the compressor	136.03	136.03	136.03	136.03
The cost of the condensers	89.75	89.75	89.75	89.75
The cost of the evaporator	72.92	72.92	72.92	72.92
The cost of the expansion device	3.51	3.51	3.51	3.51
The cost of the drying chamber	46.61	46.61	46.61	46.61
The cost of the refrigerant (R134a)	24.68	24.68	24.68	24.68
The purchase cost of the fans	16.83	16.83	16.83	16.83
The cost of the water pump	……..	25.24	……..	25.25

The cost of the solar water heater (evacuated tube)	……	266.45	……	266.45
The cost of the solar heat exchanger	……..	44.88	……..	44.88
Infrared heater	……	……..	46.59	46.59
The setup cost of the dryer	130.98	166.04	130.98	166.04
The total initial cost of the drying system	521.31	892.94	567.9	939.54
Raw material cost ($/day), 13.5 kg/day	5.44	5.44	5.44	5.44
Raw material cost (annual, 300 days)	1632	1632	1632	1632
Labour cost ($/day)	4.03	4.03	4.03	4.03
Labour cost (annual, 300 days)	1209	1209	1209	1209
Maintenance cost (2 % of initial cost), annual	10.43	17.86	11.36	18.79
Energy consumption cost ($/day),	1.13	0.84	1.23	1.04
Energy consumption cost (annual)	339	252	369	312
Total running cost of the dryer ($/day)	10.63	10.37	10.74	10.57
Total running cost of the dryer (annual, 300 days)	3190.43	3110.86	3221.36	3171.79
Total cost ($)	3711. 74	4003.8	3789.26	4111.33

Drying cost per kg material ($/kg)	0.488	0.469	0.497	0.484
Total sale of product ($/day)	15.07	15.07	15.07	15.07
Total sale of product (annual, 300 days)	4521	4521	4521	4521
Total profit (annual, 300 days)	1330.57	1410.14	1299.64	1349.21
Payback period (year)	0.392	0.633	0.436	0.696

5.4 Highlights

The solar-infrared-assisted HPD has been developed and experimentally investigated. A comparative study of four different operational modes of the system (simple HPD, IAHPD, SAHPD, and SIAHPD) has been carried out for the drying of the 2 mm thin banana chips at an air mass flow rate of 0.0966 kg/s. The following highlights can be made from the results and discussion:

- For the decrease in the moisture content of banana chips from 83.8% to 11.5% on a wet basis, the drying time is lowest for SIAHPD (180min) followed by SAHPD (225min), IAHPD (255min), and simple HPD (345min).
- The total energy consumption is lowest for SAHPD and highest for IAHPD. The total energy consumption for simple HPD, IAHPD, SAHPD and SIAHPD are 2.75, 2.98, 2.04 and 2.52kW, respectively.
- COP of simple HPD is better as compared to others. Average COP of simple HPD, IAHPD, SAHPD, and SIAHPD are 2.618, 2.303, 2.04 and 1.94, respectively.
- MER is highest for SIAHPD. Average MER values for simple HPD, IAHPD, SAHPD and SIAHPD are 0.4747, 0.7068, 0. 8224 and 1.1618kg/h respectively.

- SMER was best for SAHPD. Average SMER values for chips in simple HPD, IAHPD, SAHPD and SIAHPD are 0.975, 0.968, 1.45, 1.351kg/kWh, respectively.
- Specific energy consumption is maximum for simple HPD system drying and minimum for SAHPD. Average SEC for simple HPD, IAHPD, SAHPD, and SIAHPD are 1.0256, 1.033, 0.6896 and 0.7402kWh/kg, respectively.
- SAHPD is better based on SMER and SIAHPD was better than others based on MER in the given humid and hot atmosphere for drying of banana chips.
- Exergy destruction is highest for the SIAHPD system and minimum for simple HPD and moderate for the SAHPD and IAHPD system drying of banana chips.
- The drying cost of the material per kg is minimum for the solar-assisted heat pump dryer and it was highest for the infrared-assisted heat pump dryer. The drying cost per kg of material for the banana chips in simple HPD, IAHPD, SAHPD and SIAHPD are 0.488$/kg, 0.497$/kg, 0.469$/kg and 0.484$/kg, respectively.
- The payback period for the simple HPD, IAHPD, SAHPD, and SIAHPD is calculated as 0.392 years, 0.633 years, 0.436 years, and 0.696 years, respectively.
- Compact size batch-type SIAHPD can be recommended for food chip drying, where a faster rate of drying is needed.

CHAPTER 6

EXPERIMENTATION ON WASTE HEAT RECOVERY ASSISTED HEAT PUMP DRYER

This chapter describes the design, development, performance, economic and exergoeconomic analysis of the heat pump dryer assisted with the waste heat recovery from the IC engine exhaust. Waste heat recovery from the various power generating system is an interesting area of research these days so in the current study, an open and closed-loop HPD-assisted with WHR from diesel engine exhaust was developed, and thermal (energy and exergy), economic and exergoeconomic performances are experimentally investigated. The main components of the drying system are the heat pump system, dryer system, and the waste heat recovery unit system with the 4-cylinder diesel engine. The coefficient of performance, moisture content, specific moisture extraction rate, specific energy consumption, energy efficiency, energy-saving potential, irreversibility, second law efficiency, and economic and exergoeconomic parameters are compared for simple HPD and WHR assisted HPD. The effects of drying time and engine load are studied as well.

6.1. Experimental setup and procedure

A convective compact engine WHR-assisted HPD has been designed and developed to study the performance of different agricultural products and fruit drying. Fig. 6.1 is the symbolic diagram of the HPD-assisted with WHR. The HPD assisted with heat recovery is mainly a combination of several subsystems such as the heat pump system, dryer system, diesel engine system, and WHR system. The photograph of the developed experimental facility for the WHR-assisted HPD system is shown in Fig. 6.2.

Detailed descriptions of the heat pump and dryer system have been provided in Table 3.1.

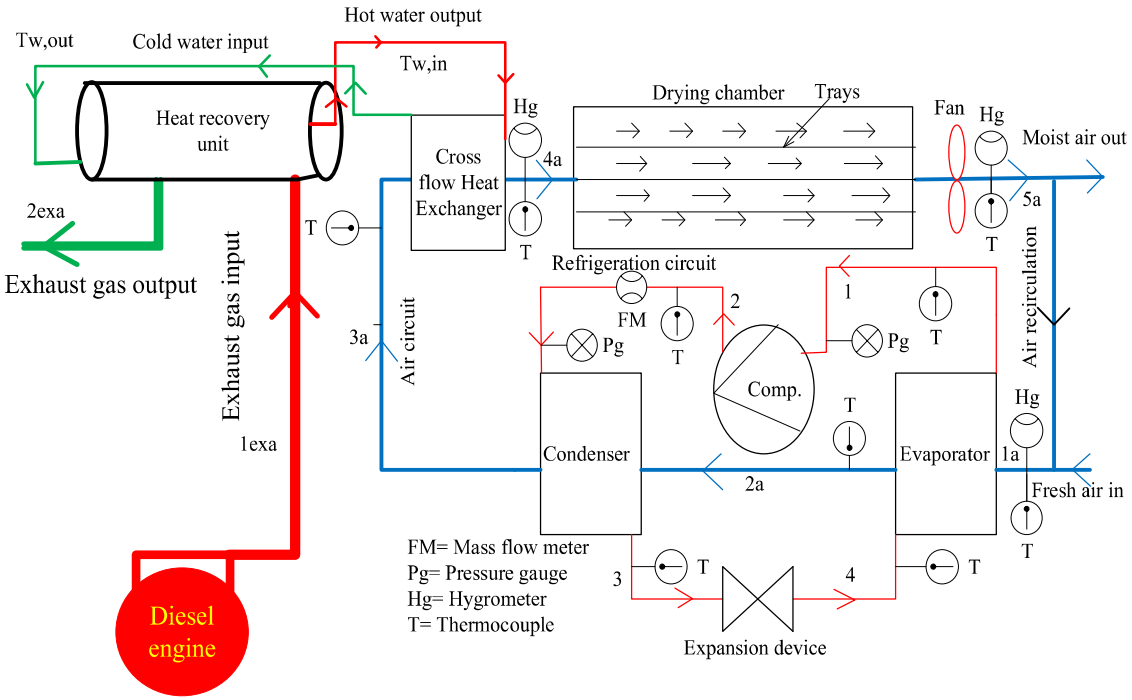

Fig. 6.1: Graphical representation of diesel engine exhaust heat recovery assisted HPD

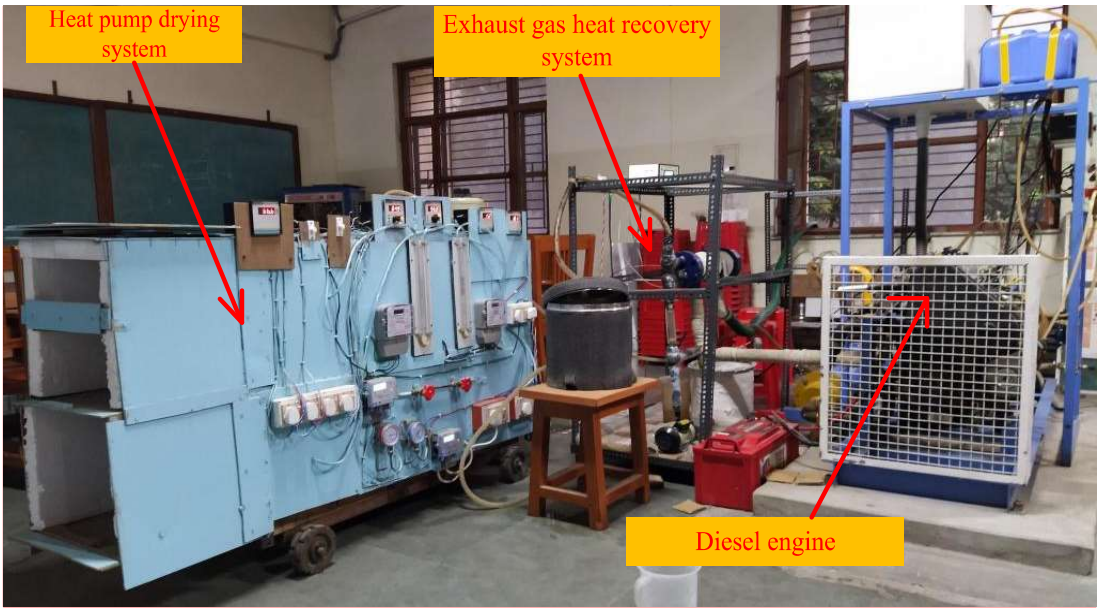

Fig. 6.2: Laboratory prototype of WHR assisted HPD

The heat pump system consists of a condenser, compressor, expansion device, and evaporator. The batch-type drying chamber has an inside dimension of 0.35 m×0.4 m×0.7

m, consisting of several trays inside it. The fan is used to maintain the flow of air in the HPD system.

In experimental setup, 4-stroke 4-cylinder diesel engine (cylinder volume = 1396cc, water-cooled, number of cylinders = 4, bore × stroke = 75mm×79mm, compression ratio = 21) is used. The heat recovery from the diesel engine exhaust system consists of a shell and tube liquid to the air heat exchanger, water pump, and a wavy fin cross-flow heat exchanger (HE). The shell and tube air to liquid HE contains the total no. of tubes = 12, length of tube = 400mm, size of shell = 100 mm×400 mm, no. of baffles = 2, and no. of pass (water side) = 2. The effectiveness of the shell and tube heat exchanger is 70 %. The hot water from the shell and tube HE is circulated in the HE (Wavy fin, Cross-sectional dimension = 30.48cm×33.02cm, length of tube = 15.85m, diameter = 9.7mm) with the help of a water pump (rated power=1/12hp, 220V, 50Hz, RPM=6500). The cross-flow heat exchanger is located just before the inlet of the drying cabin because the air coming from the condenser at a lower temperature is heated in the cross-flow HE.

The heat pump drying system with waste heat recovery from diesel engine exhaust was operated for the drying of the radish chips at the Indian Institute of Technology (BHU), Varanasi. The fresh white color radish was bought from the market and washed with clean water and the chips of 2mm size were prepared. The chips were made by a chip cutting instrument that can cut all chips of the same size. In this instrument, the size of the chips can be also adjusted from 1mm to 10mm size. The initial and the final MC of the radish chips were obtained by using the oven method at 105°C±3 A sample of 5.0 kg of radish chips was dried in the simple-HPD and the HPD-assisted with WHR. The capacity of the dryer is 5 kg and the experiment was performed at the full capacity of the drying system. The radish chips were spread with a similar pattern for all the experiments

on trays for homogeneous drying. Three hygrometers and five thermocouples (PT100) were installed at different locations in the HPD system to estimate the heat exchange in the evaporator, condenser, and the cross-flow HE and also to control the drying temperature of the air. The thermocouples and the pressure gauge were installed to obtain the temperature and the pressure of the refrigerant in the heat pump cycle.

The experiment was carried out to investigate the thermal performance of the HPD-assisted with waste heat recovery (WHR). The diesel engine was started, and the exhaust gas was connected with the inlet to the shell and tube HE. The velocity of air was 1.0 m/s and the temperature was adjusted to the desired values. In many works of literature, many people have conducted experiments between the velocity range of 0.5 to 2.5m/s. So it was decided to experiment with this range of velocity but due to the limits of the fan speed installed in the setup, the maximum velocity of 1.2m/s were measured in the system that's why the experiments were performed at the velocity of 1.0m/s. The drying temperature was adjusted by controlling the flow rate of the air in the system. After that, the heat pump system is switched on and waited until the steady-state condition is achieved at the desired air temperature. The air volume flow rate was kept the same for the drying with HPD and assisted with the WHR. Then the radish chips were loaded inside the drying cabin after weighing in a digital balance and the desired air mass flow rate was obtained by controlling the speed of the fan, and the water pump was switched on to circulate the heated water in the cross-flow heat exchanger (HE) which was installed just before the drying cabin. The humidity and temperature of the air at the inlet and outlet to the evaporator, drying cabin, condenser outlet, and inlet, and the cross-flow heat exchanger were periodically recorded at the interval of 15minutes until the end of the experiment.

The energy meters were used to measure the supplied energy for the pump, compressor, and fan. The average air temperature at the drying cabin inlet was between 65-70°C for the closed system drying with HPD-assisted waste heat recovery (WHR). The experiment was conducted for the HPD-assisted with WHR and moisture reduction, moisture extraction rate (MER), specific moisture extraction rate (SMER), total energy input, coefficient of performance (COP), exergy loss, exergy efficiency, specific energy consumption (SEC), drying efficiency, payback period, exergoeconomic factor, cost of drying and the cost related to the exergy destruction were investigated.

6.2 Data analysis

The performance parameters of the simple HPD and WHR-assisted HPD have been evaluated. It is assumed that there is no pressure drop of refrigerant and heat loss in the heat pump drying system (Gungor et al., 2011).

The performance parameters such as COP, MER, SMER, drying efficiency, energy efficiency, and the SEC are calculated using the equations as discussed in Chapter 3. The Overall heating coefficient of performance (OHCOP), the ratio of the total heat gained in the condenser and cross-flow HE to the total energy input to the system, is given as,

$$\mathrm{OHCOP} = \frac{Q_{Cond} + Q_{HE}}{W_{comp} + W_{fan} + W_{pump}} \tag{6.1}$$

Where, $\dot{Q}_{HE} = \dot{m}_{air} c_{pam} (T_{4a} - T_{3a}) = \dot{m}_{hw} c_{pw} (\mathrm{T}_{w,in} - T_{w,out})$ (6.2)

The exergy destruction (or irreversibility) can be estimated by,

$$Ex_{dest} = Ex_{in} - Ex_{out} \tag{6.3}$$

Exergy destruction and exergy efficiency of different components of simple HPD and WHR assisted HPD is given as,

$$Ex_{\text{dest},comp} = W_{comp} + \dot{m}_r\left(e_{x1} - e_{x2}\right) \qquad \eta_{ex,comp} = \frac{\dot{m}_r\left(e_{x2} - e_{x1}\right)}{\dot{W}_{comp}} \tag{6.4}$$

$$Ex_{\text{dest},cond} = \dot{m}_r\left(e_{x2} - e_{x3}\right) + \dot{m}_a\left(e_{x3a} - e_{x2a}\right) \quad \eta_{ex,cond} = \frac{\dot{m}_a\left(e_{x3a} - e_{x2a}\right)}{\dot{m}_r\left(e_{x2} - e_{x3}\right)} \tag{6.5}$$

$$Ex_{\text{dest},evap} = \dot{m}_r\left(e_{x4} - e_{x1}\right) + \dot{m}_a\left(e_{x1a} - e_{x2a}\right) \quad \eta_{ex,evap} = \frac{\dot{m}_a\left(e_{x2a} - e_{x1a}\right)}{\dot{m}_r\left(e_{x4} - e_{x1}\right)} \tag{6.6}$$

$$Ex_{\text{dest,exp}} = \dot{m}_r\left(e_{x3} - e_{x4}\right) \qquad \eta_{ex,\text{exp}} = \frac{e_{x4}}{e_{x3}} \tag{6.3}$$

$$Ex_{\text{dest,HE}} = \dot{m}_{hw}\left(e_{xw,in} - e_{xw,out}\right) + \dot{m}_a\left(e_{x3a} - e_{x4a}\right) + W_{pump} \quad \eta_{\text{ex,HE}} = \frac{\dot{m}_a\left(e_{x3a} - e_{x4a}\right)}{\dot{m}_{hw}\left(e_{xw,in} - e_{xw,out}\right) + W_{pump}} \tag{6.7}$$

$$Ex_{\text{dest,WHR}} = \dot{m}_{hw}\left(e_{xw,in} - e_{xw,out}\right) + \dot{m}_{exa}\left(e_{x,1exa} - e_{x,2exa}\right) \quad \eta_{\text{ex,WHR}} = \frac{\dot{m}_{exa}\left(e_{x,1exa} - e_{x,2exa}\right)}{\dot{m}_{hw}\left(e_{xw,in} - e_{xw,out}\right)} \tag{6.8}$$

Economic investigation depends on initial investment cost and running cost. The total running cost of dried products can be presented as (Yahya et al., 2018),

$$C_{RU} = C_{RM} + C_P + C_L + C_m \tag{6.9}$$

Where, C_{RM}, C_p, $C_{L,}$ and C_m are raw material cost, energy consumption cost, labor cost, and maintenance cost. Where maintenance cost (C_m) is considered as 2 % of the total capital cost (Yahya et al., 2018),

In the present economic analysis, the Simple HPD system is compared with the HPD with waste heat recovery in a closed system. The raw material cost and the labor cost is the same for both the system and cancel out, thus the economic analysis can be carried out based on energy consumption cost and the maintenance cost, and the equation can be written as,

$$C_{RU} = C_P + + C_m \tag{6.10}$$

The total cost of drying is given as

$$C_{Total} = C_{IC} + C_{RU} \tag{6.11}$$

Total profit from using WHR assisted HPD over simple HPD is the difference between the cost of WHR assisted HPD and simple HPD and given as,

$$C_F = C_{Total,HPD,HR} - C_{Total,HPD} \tag{6.12}$$

The payback period (which indicates the period to recover the capital investment, which is the initial investment cost per average profit) is given as (Atalay, 2019),

$$P_P = \frac{C_{IC}}{C_F} \tag{6.13}$$

Exergoeconomic analysis aims to estimate the cost related to the exergy destruction and component inefficiencies. Exergy cost balance for the different components of the system is given (Ganjehsarabi et al., 2014),

$$\sum_{out} C_{x,out,k} + C_{x,w,k} = C_{x,\mathrm{q},k} + \sum_{in} C_{x,\mathrm{in},k} + C_k \tag{6.14}$$

The overall cost of the WHR-assisted HPD can be determined by equation (17). The cost rate of exergy flow through the system at the exergy inlet, exergy outlet, and the exergy destruction can be estimated by the followings (Ganjehsarabi et al., 2014)

$$C_{x,input} = c_{input} E_{x,input} \tag{6.15}$$

$$C_{x,\mathrm{output}} = c_{output} E_{x,\mathrm{output}} \tag{6.16}$$

$$C_{x,\mathrm{dest}} = c_{dest} E_{x,\mathrm{dest}} \tag{6.17}$$

The following equation can give the total exergy cost rate,

$$C_{x,\mathrm{T}otal} = C_{x,\mathrm{dest}} + C_{Total} \tag{6.18}$$

The system recovery factor can be estimated by applying the initial investment cost, annual running and maintenance cost of the system which depends on the annual interest rate and the repayment period in years and given as (Abuska and Sevik, 2017),

$$CRF = \frac{i(i+1)^n}{(i+1)^n - 1} \tag{6.19}$$

The initial investment cost can be calculated by,

$$C_{IC} = \frac{CRF}{t_{op}} PEC \tag{6.20}$$

Where PEC is the cost of the purchased equipment that is the cost of the components of the drying system as given in Table 6.3.

And the running cost is given by the following,

$$C_{RU} = C_{IC}\phi \tag{6.21}$$

In the present study, n, i, $t_{op,}$ and φ values are taken as 2, 0.12, 3150 (HPD) and 2025 (WHR assisted HPD), and 0.8. Exergoeconomic factor is used to estimate the effect of non-exergy cost on the total cost of a system component and is given (Erbay and Hepbasli, 2017) by,

$$f_{ex} = \frac{C_{Total}}{C_{x,Total}} \tag{6.22}$$

The ratio of the exergy destruction cost to the equipment purchased cost is also an important parameter given by (Ganjehsarabi et al. 2014),

$$R_{ex} = \frac{E_{x,\text{dest}}}{PEC} \tag{6.23}$$

The cost ratio of any component of closed-loop simple-HPD and WHR assisted HPD can be estimated by,

$$(CR)_k = \frac{(PEC)_k}{(PEC)_{Total}} \tag{6.24}$$

6.3. Results and discussion

The radish chips were dried in the simple-HPD and HPD-assisted with the WHR from the engine exhaust, and the performance of the system is estimated with and without recirculation of air. The results obtained from the experiment for the simple-HPD and HPD-assisted with WHR are listed in Table 6.1. The energy requirement is highest for the simple-HPD drying in the open-loop and lowest for the WHR-assisted HPD in the closed-loop system. The drying period is found dependent on mass transfer coefficient, diffusivity, drying air humidity, velocity, and temperature. In many works of literature, authors have concluded that the temperature affects the more on chemical and physical parameters (Silva et al., 2017). In the present study, the drying temperature is the parameter that changes highly in all four types of drying systems because velocity and material were fixed for all four types of systems. Total drying time is highest for the simple-HPD in the open system and lowest for the HPD-assisted with WHR in closed system drying.

Table: 6.1. Comparison of various performance parameters of HPD with WHR

Performance parameter	Types of the drying system			
	Closed-HPD	Open-HPD	Closed-HPD with WHR	Open-HPD with WHR
Moisture content (% w.b), initial-final	93.5-10.5	93.5-10.5	93.5-10.5	93.5-10.5
Total drying time (min)	210	300	135	180

Average dryer inlet temperature (°C)	40.82	54.6	59.3	69.4
Energy consumption (kWh)	2.775	2.95	1.728	2.52
Average COP_{hp}	4.25	5.34	3.48	5.18
Average OHCOP	3.269	4.204	5.58	6.72
Average MER (kg/h)	1.524	0.82	2.322	1.58
$SMER_{average}$ (kg/kWh)	1.6436	1.39	2.4	2.158
$SEC_{average}$ (kWh/kg)	0.6084	0.719	0.4166	0.4634
Average Drying efficiency (%)	32.42	24.5	49.18	42.79
Energy efficiency (%)	43.49	33.25	56.26	48.56
Total Exergy destruction (kW)	0.7249	0.5513	0.9044	0.7957

The total energy consumption is highest for the simple-HPD due to the consumption of energy by the compressor and fan in long drying time due to low drying temperature, and the energy consumption is lowest for the HPD-assisted with WHR in closed-loop loop system due to the very low power consumption by the water pump (50 W) and getting drying air at high temperature. In closed-loop WHR-assisted HPD, the high rate of drying is obtained by just heating the drying air from the high-temperature water coming from the engine exhaust WHR system (with a very less amount of the energy input to the pump).

Fig. 6.3 shows the dependency of the exhaust gas temperature and the water temperature on the engine load, and these parameters increase with applied load because as the load increases, the amount of fuel burning in the engine increases, and exhaust gas temperature increases. The exhaust gas temperature in the heat recovery system

decreases from the value 297°C to 162°C and the heating water average temperature increases from the 55°C to 76°C (Shah et al., 2016).

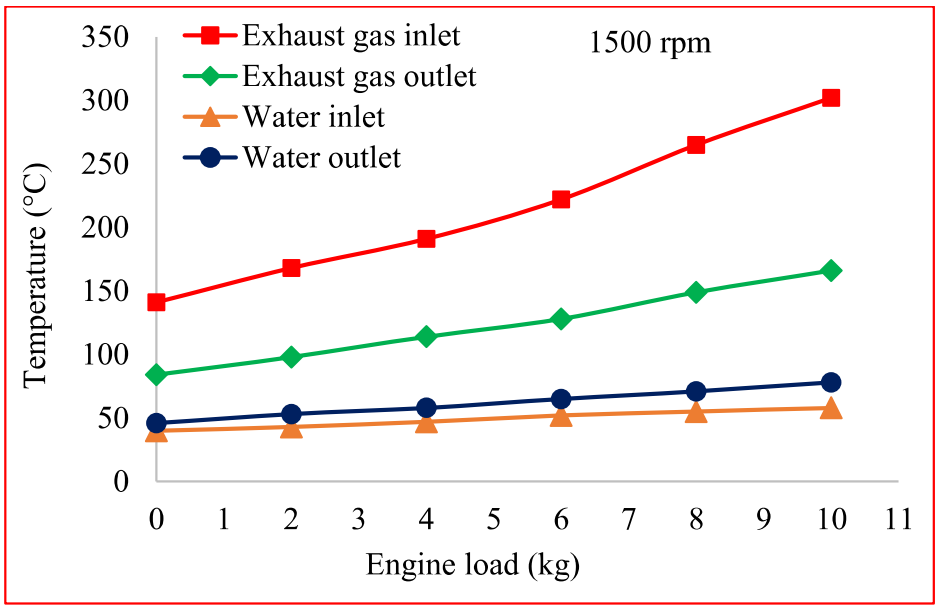

Fig. 6.3: Variation of exhaust gas and water temperature in the WHR system

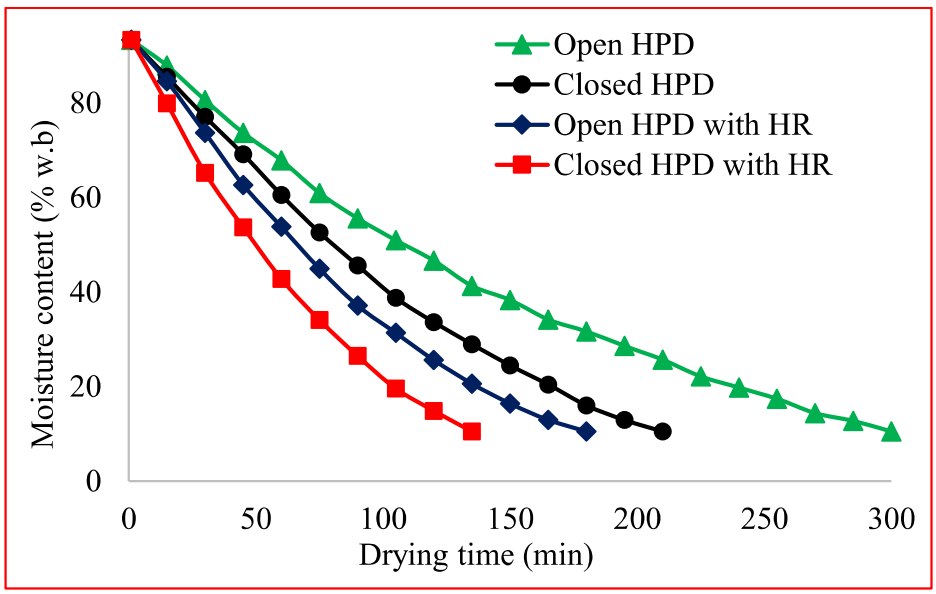

Fig. 6.4: Moisture content with drying time

The performance of the HPD system depends on the humidity, airflow rate, temperature, and effective diffusivity of the material. In literature, people have dried the product up to the 10% (Coogan and Wills, 2008). The drying process was carried out until the final MC of the material reached 10.5% from an initial value of 93.5% on a wet

basis. As shown in Fig. 6.4, the MC of the material reduces with the drying time because of the removal of the moisture from the material by drying air. The MC reduces quickly for HPD-assisted with WHR in closed-loop drying as the greater drying temperature enhances the moisture extraction. For the time being, the diffusion of moisture from the inside of the product to the outer surface decreases, which decreases the moisture extraction rate from the surface of the product.

The SEC is highest for the simple open-loop HPD because of getting the low air temperature for the same air mass flow rate and lower moisture removal rate with high-energy input. SEC is lowest for the HPD-assisted with WHR in the closed-loop system due to the high-temperature drying and lower energy consumption. The result of SEC is listed in Table 6.2, and the SEC is nearly 72.6% more in simple-HPD in the open-loop system as compared to the HPD-assisted with WHR in the closed-loop drying system.

But in terms of COP, the simple-HPD in the open-loop loop is best (Aktaş et al., 2017). The COP of the heat pump decreases with an increase in moisture ratio and the temperature of the air inlet to the evaporator. So in simple-HPD with an open system, the moisture and temperature are minimum as compared to the closed system because in the open system the fresh air inlet, and closed system the drying air is recirculated which has high temperature and moisture. The average values of the COP for the simple-HPD with open loop, simple-HPD with closed-loop, HPD-assisted with WHR in open and HPD-assisted with WHR in closed systems are 5.34, 4.25, 5.18, and 3.48 respectively (Ismaeel and Yumrutas, 2020).

Fig. 6.5 shows the variation of OHCOP with drying time. The OHCOP is found highest for the HPD-assisted with WHR in a closed open system and lowest for the simple-HPD in the closed-loop system because in HPD-assisted with WHR, the energy input to the system is very low to get heat gain in the cross-flow HE due to the lower

power consumption to pump. The average values of the OHCOP for the simple-HPD with open loop, simple-HPD with closed-loop, HPD-assisted with WHR in open, and HPD-assisted with WHR in closed systems are 4.204, 3.269, 6.27, and 5.58, respectively.

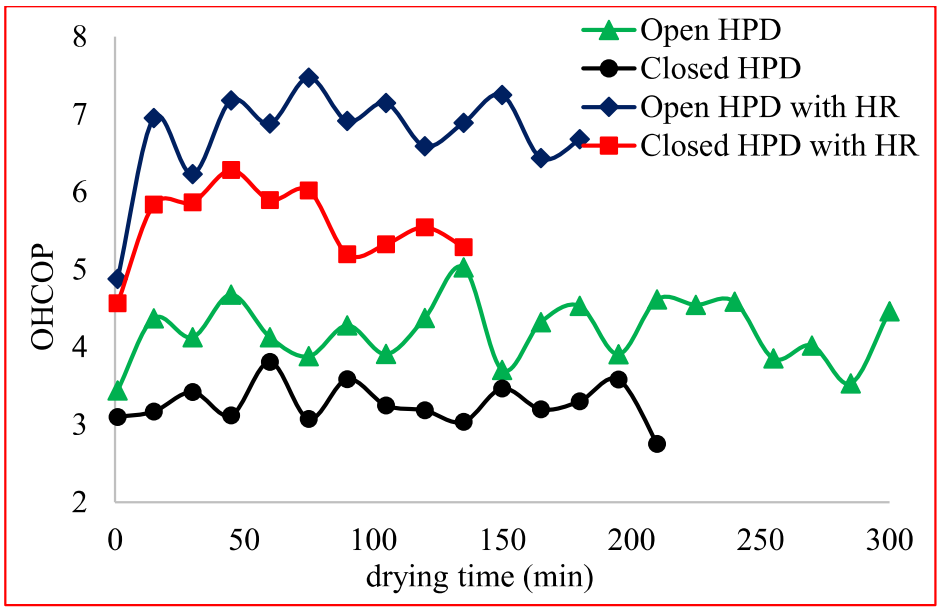

Fig. 6.5: OHCOP variation according to drying time

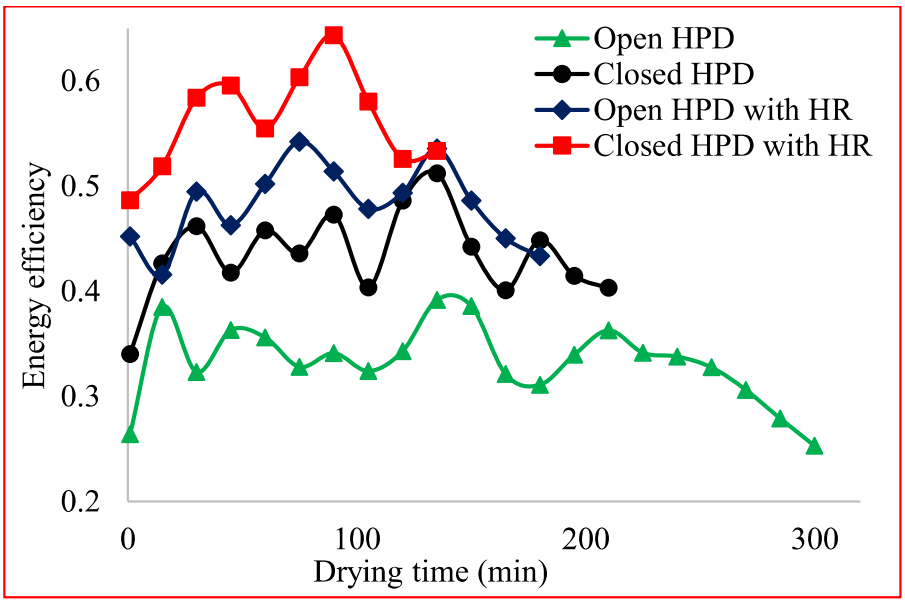

Fig. 6.6: Variation in energy efficiency with drying time

The parameter which gives the information about the utilization of the energy input to the drying system for the moisture extraction from the product is known as energy efficiency. Fig. 6.6 predicts energy efficiency for simple-HPD and HPD-assisted

with the WHR according to drying time. The energy efficiency initially enhances and then decreases due to decreases in the MC of the material. The energy efficiency is highest for the HPD-assisted with WHR drying in a closed cycle because of the lowest energy consumption. The average values of the energy efficiency with simple-HPD in the open and closed cycles are 33.25% and 43.49%, and for the HPD-assisted with the waste heat recovery in the open and closed-loop are 48.56% and 56.26% respectively.

The MER of the HPD first increases, but later some time, it starts to decrease due to the loss in the MC of the material, as shown in Fig. 6.7. The MER was highest for the HPD-assisted with WHR in closed-loop drying of radish chips due to greater drying air temperature. The MER from the drying product depends on the drying temperature, the humidity of the air, diffusivity of the material, and the airflow rate. The MER is found to be the lowest for the simple-HPD in the open-loop system due to the low drying temperature and was highest for the HPD-assisted with WHR. The average MER for simple-HPD in the open and closed-loop system is 0.82kg/h and 1.524kg/h, and for HPD-assisted with WHR in the open and closed-loop system are found to be 1.58kg/h and 2.322kg/h respectively.

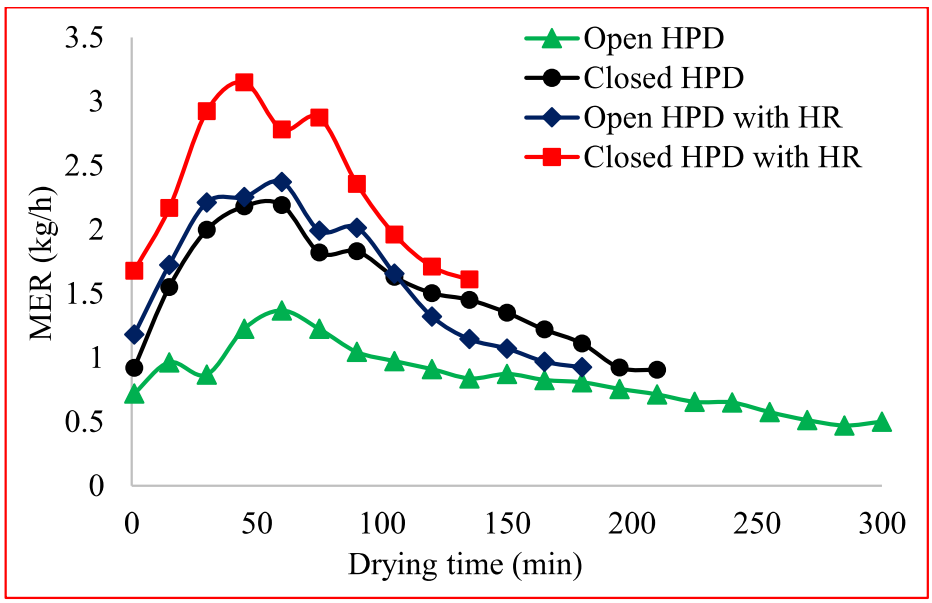

Fig. 6.7: Variation in MER with drying time

Fig. 6.8 shows the variation of the SMER with the drying time for the four different types of drying systems. The SMER initially increases with time because of the initiation of the mass and heat exchange between the drying air and product and the high MC of the product, but after some time, it started to decrease due to the loss in the MC of the product. The SMER is highest for HPD-assisted with WHR in a closed-loop as compared to the simple-HPD with a mean value of 2.4kg/kWh and the lowest is for the simple-HPD in the open-loop system with a mean value of 1.39kg/kWh (Lee and Kim, 2009).

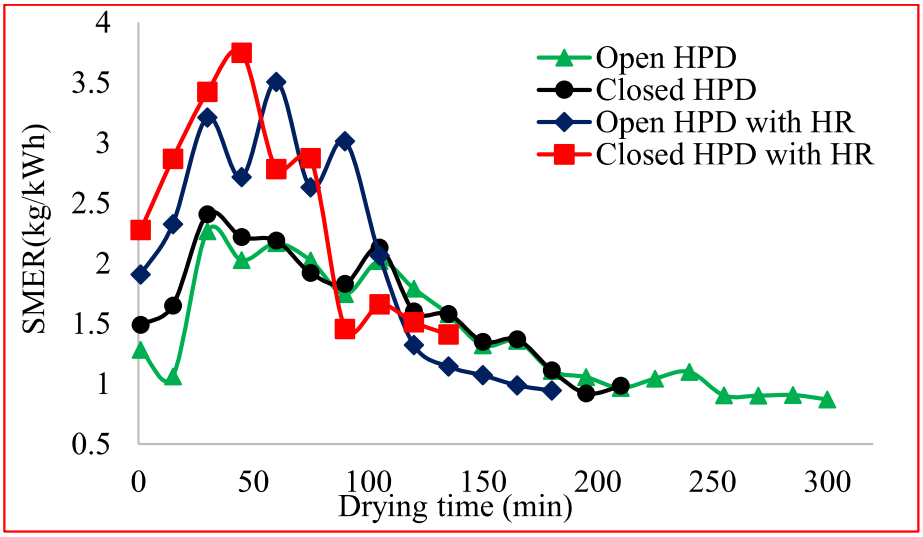

Fig. 6.8: Variation of SMER with drying time

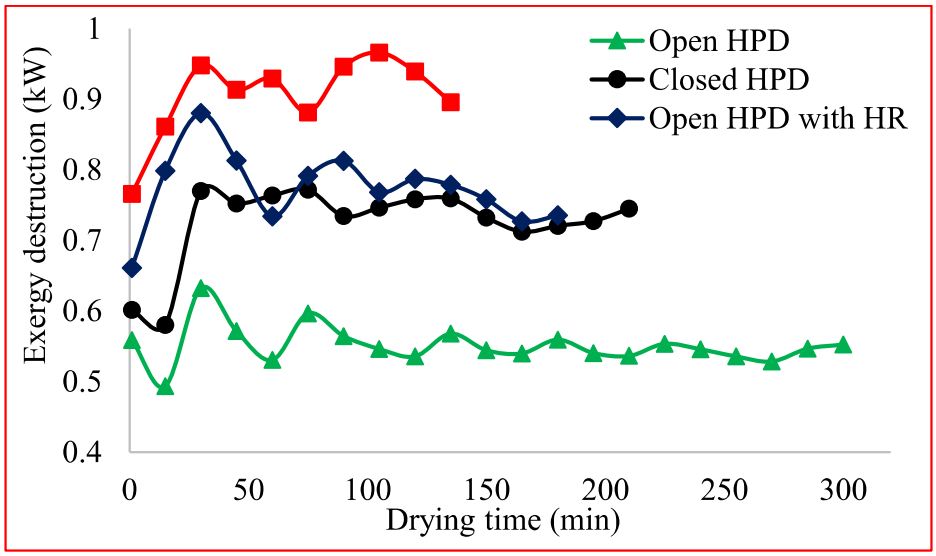

Fig. 6.9: Variation in exergy destruction with drying time

Exergy analysis is an important method to investigate the performance and utilization of energy in any system. It gives the irreversibility in the components of the HPD system. Fig. 6.9 predicts the exergy destruction and is found highest for the HPD-assisted with WHR due to high-temperature water and the very high-temperature exhaust gas. The exergy destruction in the evaporator is due to moisture condensation. Exergy analysis is an important method to investigate the performance and utilization of energy in any system and component-wise is given in Table 6.2. It gives the irreversibility in the components of the HPD system

Table. 6.2: Irreversibility (kW) and exergy efficiency of different components

Type of system / component	Open-HPD		Closed-HPD		Open-HPD with HR		Closed-HPD with HR	
	Ex_{dest}	η_{ex}	Ex_{dest}	η_{ex}	Ex_{dest}	η_{ex}	Ex_{dest}	η_{ex}
Compressor	0.1659	0.679	0.194	0.63	0.1921	0.612	0.236	0.52
Condenser	0.1208	0.858	0.1657	0.897	0.1318	0.905	0.1408	0.912
Expansion device	0.062	0.771	0.0848	0.747	0.0818	0.761	0.0843	0.744
Evaporator	0.1411	0.61	0.155	0.621	0.132	0.731	0.1416	0.743
Drying chamber	0.0616	0.1574	0.1243	0.234	0.093	0.306	0.105	0.359
Cross-flow heat exchanger	…….	…….	……	……..	0.071	0.691	0.089	0.711
Exhaust gas heat recovery system	……..	……..	……	……..	0.094	0.783	0.112	0.766

The economic analysis of the simple-HPD and the HPD-assisted with WHR in a closed-loop drying system was conducted (because the closed system has better performance as compared to the open system) for the net annual profit of using the HPD-assisted with WHR over the simple-HPD system, return period of investment and payback period. The primary investment cost, annual maintenance, running cost, and the cost of the drying system are listed in Table 6.3. The first stage of the economic analysis of the simple-HPD and the HPD-assisted with WHR is done to determine the total primary investment of the drying system. The daily and annual running costs of the system were presented for the simple-HPD and HPD-assisted with WHR in the closed-loop system. The running cost of both types of the system includes energy consumption, raw material, and labor cost. The energy consumption cost is the most important cost among the running costs for the simple-HPD and the HPD-assisted with WHR. The daily average of 15kg of the radish chips are dried in the simple-HPD and HPD-assisted with WHR, and the daily total cost of the raw material in the Varanasi was specified as $6.3. The total installation cost of the simple-HPD and HPD-assisted with WHR are estimated at $130.98 and $166.04, respectively. The yearly average running cost of the simple-HPD and the HPD-assisted with waste heat recovery in the closed-loop system are given as $358.41 and $233.81. The total yearly profit gained by using the HPD-assisted with waste heat recovery instead of the simple-HPD in the closed-loop system is determined as $124.53, and the total difference in the initial investment between the simple-HPD and the HPD-assisted with WHR is $343.15. The average payback period of drying the radish chips in the HPD-assisted with WHR over the simple-HPD in the closed-loop system is estimated at 33 months, which is a better result for the radish drying as compared to the other researchers (Qui et al., 2016). It is a better result for the experiment because after

33 months the HPD assisted with WHR will be more economical as compared to simple HPD in the closed-loop. The life guaranteed life of the compressor used in the present HPD system is much more than the payback period. The overall cost of any drying system can be defined by the two types of cost, one is the system's basic cost, and the second is the energy requirement cost of the system. The overall cost of both simple-HPD and the HPD-assisted with WHR in the closed-loop can be obtained by applying the economic investigation.

Table: 6.3. Economic parameters of different components of HPD with WHR

Parameter	Cost of the parameter ($)	
	HPD	HPD with WHR
The cost of the compressor	136.03	136.03
The cost of the condensers	89.75	89.75
The cost of the evaporator	72.92	72.92
The cost of the expansion device	3.51	3.51
The cost of the drying chamber	46.61	46.61
The cost of the refrigerant (R134a)	24.68	24.68
The purchase cost of the fans	16.83	16.83
The cost of the water pump	……..	25.24
The cost of the heat recovery system (shell and tube)	……	237.97
The cost of the cross-flow heat-exchanger	……..	44.88
The setup cost of the dryer	130.98	166.04
Total initial cost of the drying system	521.31	864.46

Total Energy consumption (kWh/day)	8.265	5.184
Total Energy consumption cost (per day)	1.16	0.74
Total running cost of the dryer (daily)	1.1947	0.7796
Maintenance cost (2 % of the initial cost), annual	10.424	17.289
Total running cost of the dryer (annual, 300 days)	358.41	233.88

The exergy-energy-based cost of both drying methods can be obtained by applying the exergoeconomic investigation of the drying system. When the evaluation of the drying system is estimated based on the exergoeconomic investigation, the parameters that can be analyzed for the simple-HPD and the HPD-assisted with WHR system are the basic purchasing cost of each component, the exergy destruction cost, system recovery factor, the overall cost of the drying system, the ratio of exergy destruction to the total purchase cost of the components, and the exergoeconomic factor. The result obtained from the exergoeconomic analysis of the simple-HPD and HPD-assisted with WHR in a closed system is listed in Table 6.4. The exergy destruction cost is highest for the compressor for both simple-HPD (0.02716$/h) and HPD-assisted with WHR (0.03304 4/h), and lowest for the expansion device for both HPD (0.01187$/h) and the HPD-assisted with WHR (0.0118$/h). The total exergy cost is highest for the compressor for simple-HPD (0.07314$/h) and waste heat recovery unit for the HPD-assisted with WHR (0.05017$/h) and is lowest for the expansion device for the simple-HPD (0.001067$/h) and HPD-assisted with WHR (0.1408 $/h) system. It is estimated that the R_{ex} value was highest for the expansion device for the simple HPD (24.16W/$) and the HPD-assisted with waste heat recovery (24.02W/$) due to the very low purchasing cost of the expansion device, and R_{ex} values were lowest for the compressor for the simple-HPD (1.426W/$) and the waste heat recovery unit for the HPD-assisted

with WHR (0.4706W/$) system. It is estimated that the compressor is having the highest value of the exergoeconomic factor for the simple-HPD (0.6286), and the waste heat recovery unit having the highest exergoeconomic factor value for HPD-assisted with WHR (0.888) system followed by the condenser (0.566) for simple-HPD and 0.705 for HPD-assisted with WHR. The exergoeconomic factor values are lowest for the evaporator (0.0918) for simple-HPD and 0.1348 for the HPD-assisted with WHR. The cost ratio (CR) values were highest for the compressor with 0.348 for simple-HPD and the heat recovery unit with 0.3407 for the HPD-assisted with WHR.

Table: 6.4. Exergoeconomic parameters of HPD with WHR

Drying system		Components						
		Compressor	Condenser	Expansion device	Evaporator	Drying chamber	Cross flow HE	Heat recovery Unit
HPD	R_{ex} (W/$)	1.426	1.846	24.16	2.1256	2.666	…….	…… ….
	C_{Total} ($/h)	0.04598	0.0303	0.0012	0.02465	0.01575	…….	…… …..
	$C_{x,dest}$ ($/h)	0.02716	0.0232	0.01187	0.0217	0.0174	……..	…… …..
	$C_{x,total}$ ($/h)	0.07314	0.0535	0.01307	0.04635	0.03315	……..	…… ….
	f_{ex}	0.6286	0.566	0.0918	0.5318	0.475	……..	…… ….
	CR	0.348	0.229	0.00899	0.1868	0.1194	……..	…… …..

HPD with heat recovery	R_{ex} (kW/$)	1.7348	1.568	24.02	1.942	2.2527	1.986	0.4706
	C_{Total} ($/h)	0.07153	0.0472	0.00184	0.03834	0.0245	0.0236	0.12513
	$C_{x,dest}$ ($/h)	0.03304	0.0197	0.0118	0.0198	0.0147	0.01246	0.01568
	$C_{x,\text{total}}$ ($/h)	0.10457	0.0669	0.01364	0.05814	0.0392	0.03606	0.1408
	f_{ex}	0.668	0.705	0.1348	0.659	0.625	0.654	0.888
	CR	0.195	0.1285	0.00502	0.1044	0.0667	0.0642	0.3407

6.4 Highlights

The WHR-assisted HPD has been developed and experimentally investigated in open and closed loops. A comparative study of two different operational modes of the system (with and without WHR) has been carried out for 2mm thin radish chips drying at a constant airflow rate. The following highlights are made from the results:

- For the decrease in the moisture content of radish chips from 93.5% to 10.5% on a wet basis, the drying time is lowest for HPD-assisted with WHR in closed-loop (135 min) and highest for the simple-HPD (300min).
- COP of simple-HPD is better as compared to WHR-assisted HPD. The average COP of simple-HPD in an open loop, simple-HPD in a closed-loop, HPD-assisted with WHR in the open, and HPD-assisted with WHR in a closed loop are 5.34, 4.25, 5.18, and 3.48, respectively.

- OHCOP values are higher for WHR-assisted HPD as compared to simple-HPD. The average values of OHCOP for simple-HPD in open loop, simple-HPD in closed-loop, HPD assisted with WHR in open and HPD-assisted with WHR in closed loops are found to be 4.204, 3.269, 6.72, and 5.58, respectively.
- MER is highest for the HPD-assisted with WHR in the open and closed-loop system. The MER of simple-HPD in open loop, simple-HPD in closed-loop, HPD-assisted with WHR in open loop, and HPD-assisted with WHR in closed-loop are 0.82kg/h, 1.52kg/h, 1.58kg/h and 2.322kg/h, respectively.
- SMER is much higher for WHR-assisted HPD as compared to the simple-HPD. The average values of SMER of simple-HPD in open loop, simple-HPD in closed-loop, WHR assisted HPD in open loop and HPD-assisted with WHR in closed-loop are 1.39kg/kWh, 1.6436kg/kWh, 2.158kg/kWh and 2.4kg/kWh, respectively.
- The payback period of using HPD-assisted with WHR over the simple-HPD in the closed-loop is found to the 33 months.
- The lowest exergoeconomic factor for simple-HPD and HPD-assisted with WHR are 0.0918 and 0.1348, respectively. Thus based on exergoeconomic factors, the HPD-assisted with WHR is better as compared to the simple-HPD in a closed loop.
- The cost of exergy destruction for the simple-HPD and HPD-assisted with WHR in a closed-loop is 0.10148$/h and 0.1266$/h, respectively.
- A compact size batch-type HPD-assisted with WHR from the diesel engine exhaust can be recommended for the food chips drying, where a faster rate of drying is needed with low energy consumption.

CHAPTER 7

EXPERIMENTATION ON INTERMITTENT DRYING WITH SOLAR-ASSISTED HEAT PUMP DRYER

This chapter describes the design, development, thermal performance, and economic analysis of the intermittent drying of radish chips with a solar-assisted heat pump dryer. The application of renewable energy sources in the area of heat pump drying is very interesting due to the high drying rate with energy savings and very less environmental effect. In this direction, a solar-assisted heat pump dryer (SAHPD) utilizes renewable sources of energy (free of cost) (Khanlari et al., 2020). Hence it enhances the SMER with reduced energy requirement (electricity). On the other hand, the drying performance should be high at a higher drying temperature but the product temperature may be increased continuously by continuous drying and the drying material (both product surface and quality) can be deteriorated due to high temperature due to continuous heat input and hence the drying should be carried out at optimum temperature. To avoid the deterioration of the food products, intermittent drying may be applied because in intermittent, the energy supply is in different steps and the drying temperature may be maintained at an optimum level. Hence, people are taking great interest in the field of intermittent drying, especially heat-sensitive materials. It also increases the SMER and product quality. When the rate of diffusion from inside to the surface of the product is lower than that from the product surface to the dying air, the energy input to the system is stopped, and the moisture diffusion from the inside of the product to the surface is extracted naturally due to vapor pressure difference (this period is known as tempering period), which decreases the energy consumption (Herritsch et al., 2010).

Hence, SAHPD with intermittent drying may be an energy-efficient method. So in the present study, solar energy is utilized to increase the drying temperature using a solar water heater and air to a water heat exchanger with a heat pump system for intermittent drying. The main components of the drying system are the heat pump system, dryer system, and the evacuated tube type solar water heating system. In this study, the new generation future refrigerant R1234yf is used in the heat pump cycle and the COP of the overall system, energy efficiency, MER, specific SMER, exergy destruction, drying efficiency, payback period, and drying cost per unit material is investigated and compared for the different intermittent ratio for the drying of radish.

7.1. Material and methods

The present study focused on the design and fabrication of a convective solar-assisted-HP dryer for the intermittent drying of the food products using the solar water heater as a renewable source of energy and a future refrigerant R1234yf in the HP cycle, and the experiment was carried out for radish drying to analyze the system and dryer performance. Fig. 7.1 reveals the schematic diagram of the Solar assisted-HPD. The solar-assisted-HPD can be expressed by several sub-systems, evacuated tube solar water heater, hot water circulation system, heat pump (refrigerant) system, and drying system. The basic components of the heat pump system are a new future refrigerant (R1234yf), semi-hermetic compressor, wavy fin cross flows heat exchanger (condenser, evaporator), and expansion device (capillary tube), details are provided in Table 3.1. The fabricated experimental facility is shown in Fig. 7.2 with the HP drying and solar water heating system. To compute the refrigerant temperature in the HP cycle at the location of compressor input, compressor output, condenser output, and evaporator input, four resistant thermometers (PT100) are installed. The low temperature (evaporator) side pressure and the high temperature (condenser) side pressure is estimated by using the

pressure gauges as shown in Fig. 7.2. Three energy meters are installed to measure the electric energy requirement by the compressor, pump, and fan.

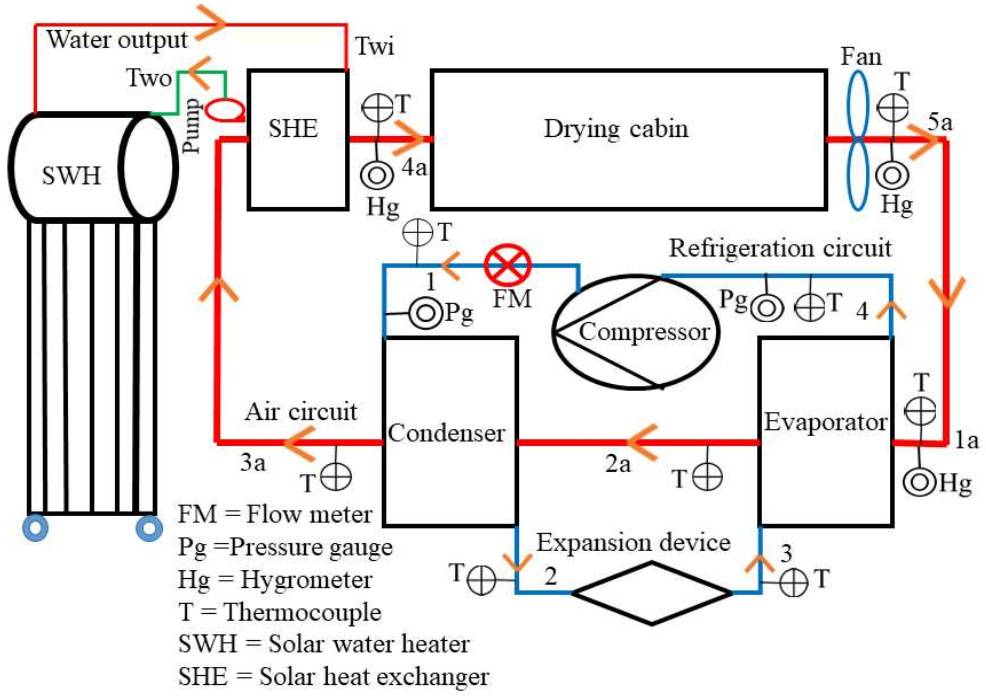

Fig. 7.1: Schematic of the presentation of the solar-assisted-HP dryer for intermittent drying

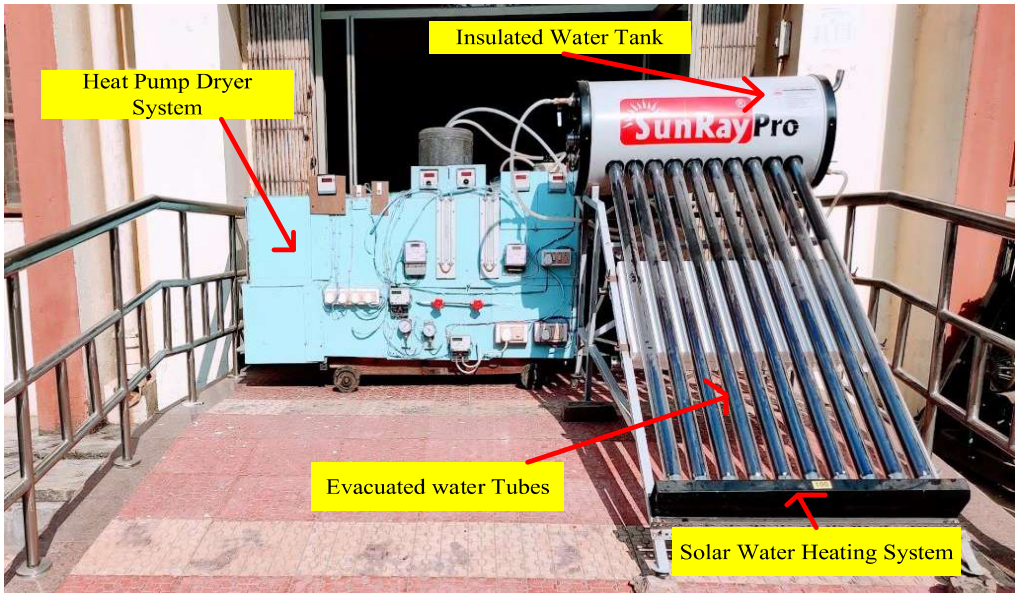

Fig. 7.2: Experimental facility of SAHPD for intermittent drying

The SWH system is the integration of the different sub-systems as evacuated tube type SWH, centrifugal pump, and heat exchange. Two resistant thermometers (Pt100)

and a rotameter is installed to measure the hot water inlet and outlet temperature to the SWHE and to measure the flow rate of the water through the SWHE. The details and the specification of the solar water heating system are provided in the previous literature (details are provided in Chapter 5). The most advantage of the SWH system instead of the solar-air-heating system is that the SWH system can be used at night time also because, in this system, the heated water is stored in an insulated tank. In the SWH system, the dehumidified air coming out from the evaporator is heated in the SWHE after the condenser of the HP cycle, which enhances the SMER and energy efficiency as compared to the solar air heating system due to getting high drying air temperature. The convective drying cabin of the inside dimension of 0.35m × 0.4m × 0.7m and the drying chamber consisted of several trays inside it. The drying air flows in the HP drying system with help of a fan (220/230V, speed= 1350rpm, 50 Hz, power =70W, sweep = 300mm). The resistant thermometers and pressure transducer were used in the system to estimate the drop in pressure and temperature of the air in the drying cabin and the whole system.

The solar-assisted HP dryer system was designed and fabricated for the intermittent drying of the radish. The radishes were washed and sliced into 2 mm size. The moisture content (final and initial) of the radish chips was estimated by applying the oven method at 105°C. 4.5kg of radish chips was taken for the experiment in the solar assisted-HP dryer for different intermittency ratios. The radish chips on the trays loaded inside the drying cabin. Three hygrometers (at the inlet to the evaporator, drying cabin output, and input) and the resistant thermometers (Pt100) were used in the HP drying system to measure the evaporator inlet and outlet, condenser outlet, SWHE outlet, and drying cabin outlet temperature which was also used to optimize the drying air temperature by controlling the airflow rate through the system.

The intermittent drying experiment was carried out to evaluate the exergy, economic, and energy performance of the solar-assisted-HPD at different intermittency ratio for the radish chips. The solar water heating system was filled with water and kept in the sun until the temperature of water in the insulated tank reached the value (of 68-69°C). The fan and the pump connected to the SWH were switched on and the drying air velocity (1.0m/s) was fixed to the desired value. After that, the R1234yf HP system made switched on to reach the steady-state condition and required drying temperature at the drying cabin inlet. The airflow rate and the hot water recirculated through the system was kept the same for all intermittency ratio with solar assisted-HPD. Then the initial readings of the resistant thermometers, hygrometers, and the energy meters were recorded, and during the experiment (intermittent), the humidity at the evaporator inlet, drying cabin inlet and outlet, and drying air temperature at outlet and inlet to the SWHE, the evaporator, the condenser and drying cabin was recorded after every 10 minutes until the end experiment. The experiment was performed for the intermittency ratio of α = 1, 0.2, 0.33, 0.5, and 0.66 with a solar-assisted-HP dryer, and the experiment was considered ended and the system is switched off when the drying cabin inlet and outlet humidity become same (no increase in humidity at dryer out). The decrease of MC from the product should be equal to the increase of drying air humidity in the drying cabin and also equal to the amount of moisture condensed over the evaporator for the closed system. The energy measuring device is connected to measure the energy required for the fan, pump, and compressor.

7.2. Data extraction

The intermittency ratio depends on the on/off mode of the drying process for which the system will remain in on condition for some time and in off condition for some other time. The intermittency ratio used in this study is based on/off period. Some people

have used the intermittency ratio of the system as the ratio of on-time to the off time of the system and investigated the energy savings by this intermittency ratio (Chin and Law, 2010). Some people have used the intermittency as the ratio of on-time to the total time (on + off), and in this study, to get the advantages of intermittent drying, the intermittency ratio used is given by (Ong et al., 2012),

$$\alpha = \frac{t_{on}}{t_{on} + t_{off}} \Rightarrow \alpha = \frac{t_{on}}{t_d} \tag{7.1}$$

Where t_{on} is the period for which the drying system is on mode and t_{off} is the period for which the drying system is kept in off mode and off period is also known as the tempering period.

So, a higher intermittency ratio means a higher active drying period. If the intermittency ratio increases then the energy efficiency will decrease, but the drying time will also decrease and needed a shorter drying time (Zhu et al., 2016). But the energy efficiency will increase as the intermittency ratio will decrease due to an increase in the tempering (off time) period which needed a longer drying time. For intermittent drying of food chips, a solar assisted-HP dryer consists of a drying medium cycle (air cycle), a refrigerant circuit, an SWH, and a solar water heat exchanger cycle. In the HP drying system, the airflow rate, the air temperature, and the air humidity are the most common parameters to figure out the performance and economic analysis of solar assisted-HP dryer for intermittent drying. By applying the energy-exergy analysis to the solar assisted-HP dryer intermittent drying system for radish chips were accomplished to find out the total energy transfer in the condenser, evaporator, and SWHE, energy efficiency, and the behavior of drying air temperature and the total cost of the drying per kg of material.

The heat exchange rate between the refrigerant and drying air in the HP condenser is given by,

$$Q_{cond} = \dot{m}_{air} c_{pam} (T_{3a} - T_{2a}) = \dot{m}_r (h_2 - h_3) \quad (7.2)$$

Where $\dot{m}_{air}$ is the mass flow rate and c_{pam} is the isobaric specific heat of moist air.

The heat gained by drying air from SWH through the SWHE is estimated by,

$$Q_{SWHE} = \dot{m}_{air} c_{pam} (T_{4a} - T_{3a}) = \dot{m}_{hw} c_{pw} (T_{wi} - T_{wo}) \quad (7.3)$$

Where $\dot{m}_w$ is the mass flow rate and c_{pw} is the isobaric specific heat of the water.

The heat pump cycle coefficient of performance (COP) is calculated by,

$$\text{COP} = \frac{Q_{cond}}{W_{comp.}} = \frac{h_2 - h_3}{h_2 - h_1} \quad (7.4)$$

The overall heating COP (OHCOP) is used to evaluate the combined performance of heat pump + solar heating systems, and it is estimated as the ratio of the amount of heat recovered in the HP condenser and SWHE to the total fan, compressor and pump energy input. The OHCOP is given as follows,

$$\text{OHCOP} = \frac{Q_{cond} + Q_{SWHE}}{W_{comp.} + W_{fan} + W_{pump}} \quad (7.5)$$

The moisture extracted from the product is calculated by,

$$m_w = (m_{pi} - m_{pt}) = \dot{m}_{air} (\omega_{5a} - \omega_{4a}) t_{on} \quad (7.6)$$

Where t_d is the on-period drying time step in an hour (10 min is taken for calculation) and m_w is moisture removed from the product during the time step.

The total moisture removal rate from the drying material is given as follows,

$$\text{MER} = \frac{m_w}{t_{on}} \quad (7.7)$$

Total moisture extracted from the product per unit energy input to the whole drying system is called specific moisture extraction rate (SMER) and is given as,

$$\text{SMER} = \frac{m_w}{\text{t}_{on}(W_{comp.} + W_{fan} + W_{pump})} \tag{7.8}$$

The energy efficiency of the drying system is an important parameter that indicates how efficiently the energy is consumed to remove the moisture from the product. Energy efficiency is the ratio of the energy utilized for the removal of moisture from the drying product to the total energy consumed in the system. The energy efficiency of the solar-assisted-HP dryer system is given by

$$\eta_{en} = \frac{h_{fg} m_w}{\text{t}_{on}(W_{comp.} + W_{fan} + W_{pump})} \tag{7.9}$$

Where h_{fg} is the water latent heat of vaporization.

The economic analysis of intermittent drying with a solar-assisted HP dryer depends on the initial cost and operating cost of the drying system. The capital cost of the drying system includes the costs of heat exchangers (condenser, SWHE, evaporator), compressor, capillary tube, fan, refrigerant, SWH, pump, duct, base structure, system fabrication, and labor. The thermal performance and the economic parameters are calculated by using the Eq. as discussed in previous Chapters 3 and 5.

7.3. Results and discussion

The chips (radish) were dried in the SAHPD for different intermittency ratio with a closed-loop system, and the economic, energetic, and exergetic performance of the drying system was investigated for different intermittency ratio of α=0.66, α=0.33, α=0.2 and compared with the continuous (α=1) drying. The experimental results observed for intermittent drying of radish with the SAHPD system are presented in Table 7.1. From the experimental result, it can be observed that the energy required for the system

increases with the value of the intermittency ratio because as the intermittency ratio the on-time period of the system increases, and the energy requirement is higher for the continuous drying and lower for the intermittency ratio of α=0.2 respectively. The energy input is highest for continuous drying due to the continuous supply of energy for the drying system. But in intermittent drying, the energy is supplied for the on period and then stopped for the tempering period (in the tempering period, the moisture from inside material to the surface is extracted due to the vapor pressure difference) which increases the energy efficiency and decreases the energy requirement. The total energy consumption for the continuous, α=0.66, α=0.33, and α=0.2 are 3.035kWh, 2.288kWh, 2.018kWh, and 1.89kWh respectively.

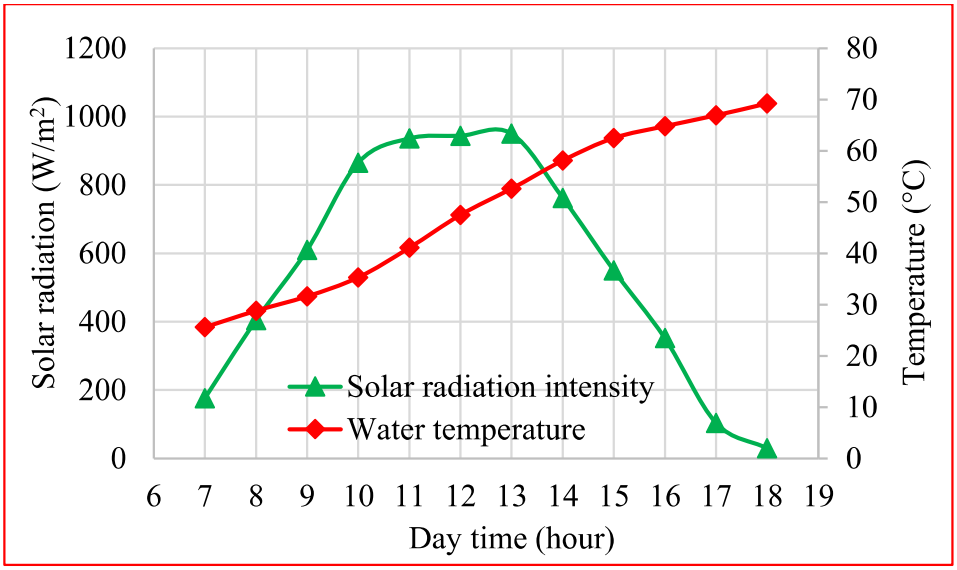

Fig. 7.3: Solar radiation and water temperature variation with day hour

For the solar-assisted HP dryer, the solar radiation intensity coming solar water heater, the atmospheric temperature, and humidity are important parameters at a specific location for the intermittent drying. In this intermittent drying with SAHPD, the solar radiation was utilized to heat the water in the SWHS and finally, this hot water heats the drying air coming out from the HP condenser. The hourly radiation data for March and the water temperature inside the insulated tank are shown in Fig. 7.3. The sun radiation

(intensity) increases with day hours reaching the maximum value and then starts to decrease. The temperature of water in the insulated tank increases with the day hour as the water is heated with solar radiation continuously. The average solar intensity and the maximum water temperature were 604.91W/m^2 and 68.7°C respectively.

The thermal performance of the intermittent drying with a solar-assisted HP dryer depends on the intermittency ratio, air temperature and humidity, air velocity, and diffusivity of the drying product. The drying of the radish was carried out to get the final MC of 11.9% from the initial value of 92.4% (wet basis) for the different intermittency ratio (α= 1, α= 0.66, α= 0.33, α= 0.2). From the experimental result, it can be observed that the total drying time is lower for the continuous drying and higher for the intermittency ratio of 0.2, but the actual drying time (on period) is lower for the intermittency ratio of 0.2 and higher for the continuous drying. The total drying time for the intermittency ratio of α= 1, α= 0.66, α= 0.33 and α= 0.2 are 220min, 230min, 390min and 480minutes respectively. But the actual drying time for which the system is in on condition for intermittency ratio of α= 1, α= 0.66, α= 0.33, and α= 0.2 are 220min, 170min, 150min, and 120minutes respectively. The average drying temperature for the intermittent drying with the SAHPD system is 52.32°C. The experimental results obtained from the intermittent drying of radish chips with SAHPD for different intermittency ratio is provided in Table 7.1.

Table: 7.1. Performance comparison of experimental results for intermittent drying

Performance parameter	Intermittency ratio (α)			
	Continuous (α=1)	α=0.66	α=0.33	α=0.2
Average drying temperature (°C)	52.1	52.3	52.3	52.6
Total drying time (min)	220	230	390	480

Total actual drying time (min)	220	170	150	120
Total energy consumption (kWh)	3.035	2.288	2.018	1.89
Avg. COP_{hp}	4.7	4.62	4.48	4.32
Avg. OHCOP	5.82	5.75	5.61	5.53
Avg. SMER (kg/kWh)	1.334	1.77	2.007	2.143
Avg. MER (kg/h)	1.1045	1.43	1.736	2.025
Avg. energy efficiency (%)	31.43	38.3	43.15	49.16
Avg. drying efficiency (%)	26.93	35.63	39.62	44.25

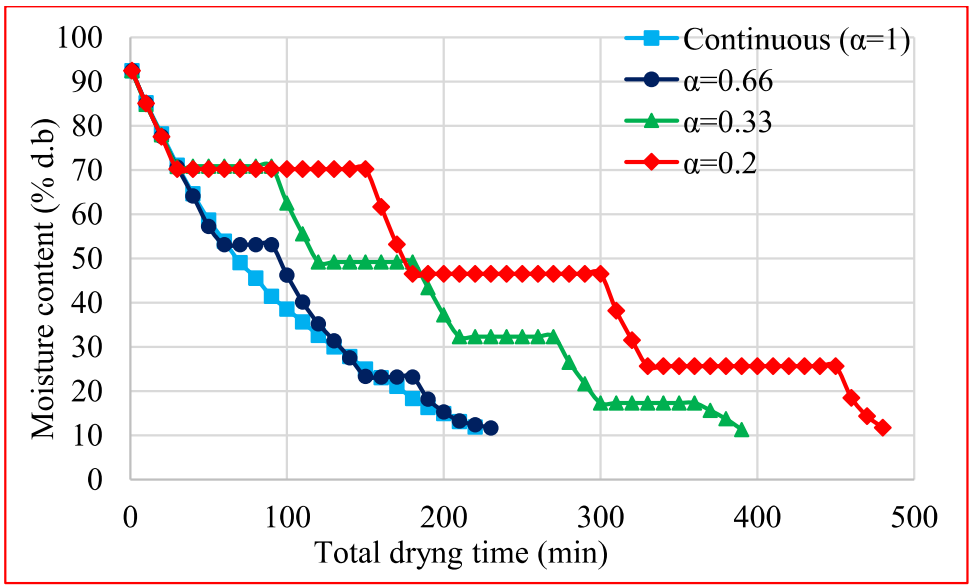

Fig. 7.4: Moisture content variation of product with total drying time

The velocity of air (1.0m/s) and water flow rate of 1.5LPM for all experiments were kept constant with the SAHPD system. Fig. 7.4 depicts the variation of the MC of the material for the different intermittency ratio with the total drying time. The MC decreases at a faster rate for the intermittency ratio of 0.2 in the active drying time because of the higher tempering (off time) period which causes the natural extraction of moisture from the inner product to the surface due to vapor pressure difference and increases the moisture extraction rate as compare to the continuous drying.

The COP of the HP system was a little bit higher for the higher value of the intermittency ratio (α=1) due to the lower values of temperature and humidity input to the evaporator (the value of COP of HP decreases with an increase in evaporator inlet air temperature and humidity) as compared to the higher intermittency ratio. The COP of the SAHPD system for intermittency ratio of α= 1, α= 0.66, α= 0.33 and α= 0.2 are 4.7, 4.62, 4.48 and 4.32 respectively. The OHCOP is the function of heat exchange in the condenser, SWHE, and the energy input to the compressor, pump, and fan in the drying system. The OHCOP of the overall SAHPD system was a little bit higher for the higher value of the intermittency ratio. Fig. 7.5 shows OHCOP variation with total drying for the continuous and the intermittent drying and the for the tempering period, the values of OHCOP are zero as shown in the figure. The average values of OHCOP for the intermittency ratio of α= 1, α= 0.66, α= 0.33 and α= 0.2 are 5.82, 5.75, 5.61 and 5.53 respectively.

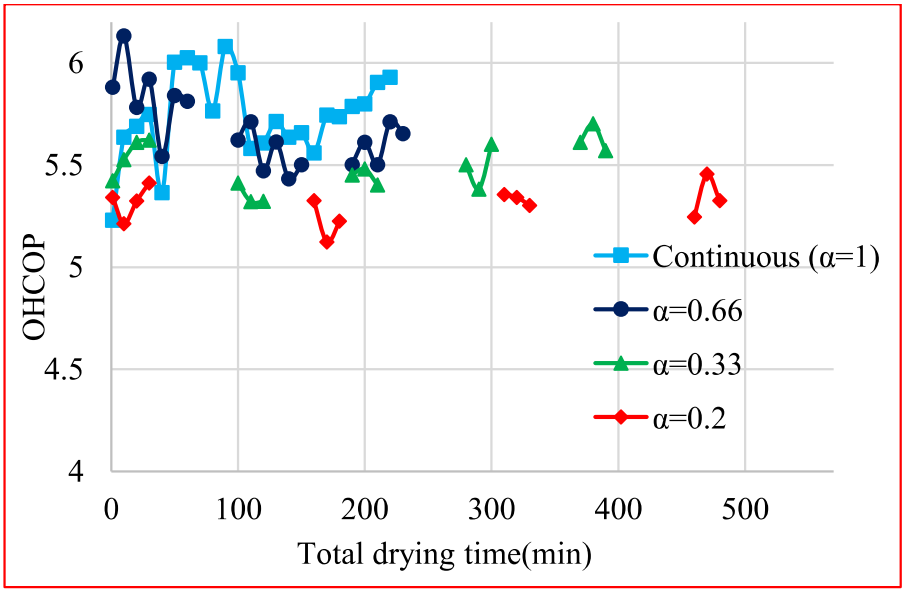

Fig. 7.5: OHCOP variation with total drying time

Fig. 7.6 represents the variation of the MER with the total drying time with a solar-assisted-HP dryer for different intermittency ratio. For the intermittent drying during one period, initially, the MER increases with time due to the higher MC of the

product but after some time it decreases due to the decrease in the MC of the product, and for the intermittent drying it repeated the same trend for every cycle of drying again and again. The average MER is higher for the intermittency ratio of 0.2 (due to a higher tempering period in which, the moisture from the product is extracted to the surface due to the natural vapor pressure difference without any external means) and lower for the continuous drying (drying air extract the moisture first inside to the surface of the product and then carried out the moisture from the surface which decrease the rate of moisture extraction). The average values of MER with SAHPD drying for the intermittency ratio of continuous (α =1), α = 0.66, α = 0.33 and α = 0.2 are 1.1045kg/h, 1.43kg/h, 1.736kg/h and 2.025kg/h respectively.

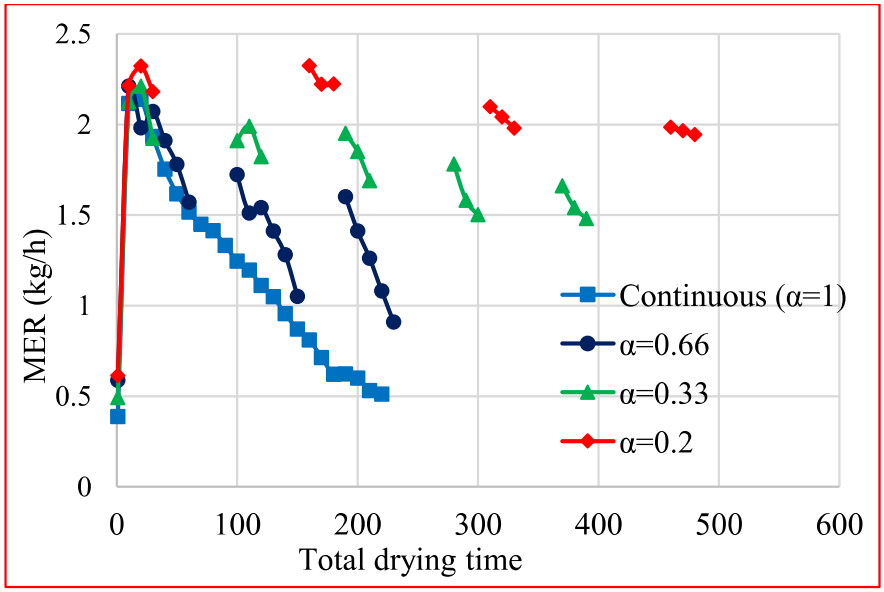

Fig. 7.6: MER variation with total drying time

Fig. 7.7 shows the SMER variation with the total drying time for the intermittent and continuous drying. For the continuous and the intermittent drying during on period, the SMER increases with time due to having a higher MC of product, but after some time it decreases due to the decrease in the MC of the product, and for the intermittent drying it is repeated the same trend for every cycle of drying. The average SMER is higher for the intermittency ratio of 0.2 and lower for the continuous drying. The average value of

SMER increases with the decrease in intermittency ratio because a lower intermittency ratio means a higher the tempering period and higher the moisture extraction from products with the same energy input. The average values of SMER with SAHPD drying for the intermittency ratio of continuous (α = 1), α = 0.66, α = 0.33 and α = 0.2 are 1.334kg/kWh, 1.77kg/kWh, 2.007kg/kWh and 2.143kg/kWh respectively.

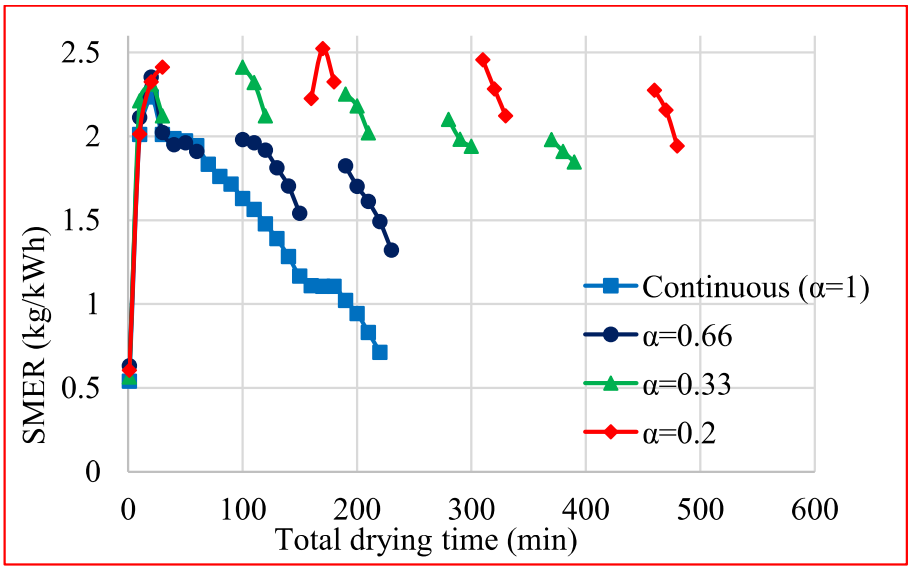

Fig. 7.7: SMER variation with total drying time

Drying efficiency tells the information about how efficiently the air extracts the moisture from material in the drying cabin. Fig. 7.8 represents the variation of the drying efficiency with the total drying time (on period + off period) with the SAHPD system for intermittent and continuous drying. For continuous drying, the drying efficiency decreases with time due to a decrease in the MC of the product and finally moisture extraction from the product because drying efficiency depends on the inlet and outlet temperature and the saturation temperature of the air in the drying cabin. For the intermittent drying, the drying efficiency is higher as compared to the continuous drying due to the higher moisture removal in the drying cabin (because of the tempering period), and the value of drying efficiency increases with a decrease in the intermittency ratio.

The average values of drying efficiency for the intermittency ratio of continuous (α=1), α = 0.66, α = 0.33 and α = 0.2 are 26.93 %, 35.63 %, 39.62 % and 44.25 % respectively.

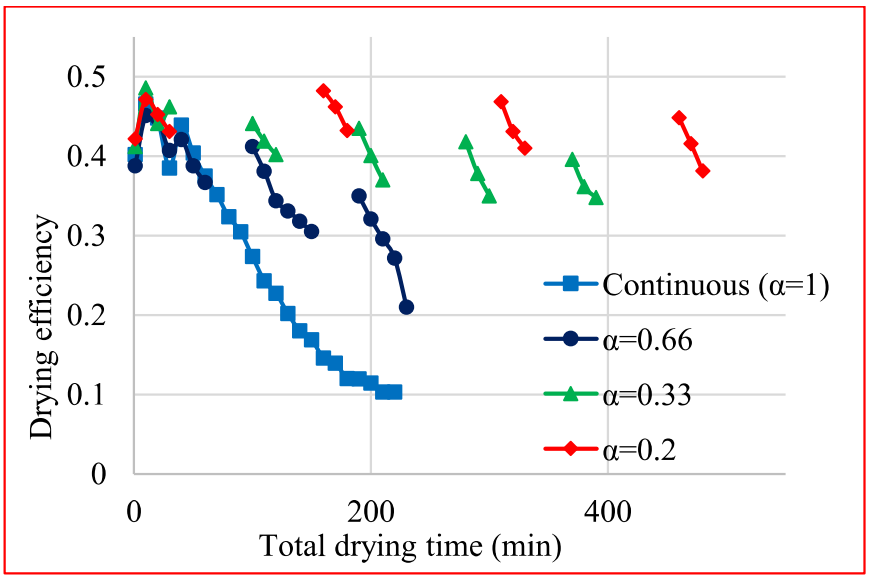

Fig. 7.8: Drying efficiency variation with total drying time

The energy efficiency of the solar-assisted HP dryer indicates the efficient utilization of the input energy for the evaporation of moisture from the product. Fig. 7.9 shows the energy efficiency variation of intermittent drying for radish with the SAHPD system with total drying time. The energy efficiency is highest for the lower value of the intermittency ratio, and lower for the higher value of the intermittency ratio (continuous). The value of the intermittency ratio increases with the increase in the tempering period (off time) which finally increases the average value of energy efficiency (due to the natural extraction of moisture from the inner surface of product to outer surface in tempering period without external energy input). The average energy efficiency value for the intermittency ratio of continuous (α =1), α = 0.66, α = 0.33 and α = 0.2 are 31.43%, 38.3%, 43.15% and 49.16% respectively.

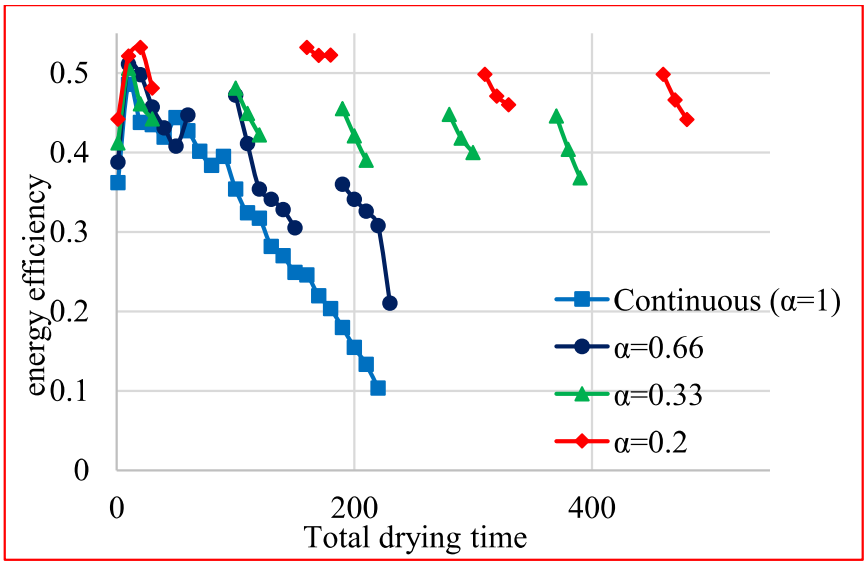

Fig. 7.9: Energy efficiency fluctuations with total drying time

Exergetic investigation is the most relevant methodology to evaluate the thermal performance and efficient energy utilized in any solar-assisted HP dryer. The exergy destruction and efficiency of components are provided in Table 7.2. The destruction of exergy was higher for the compressor and the solar water heat exchanger. The exergy destruction through the evaporator was due to the cooling and the condensation of air and moisture over the cold finned surface. The exergy destruction was lower for the expansion device for both continuous and intermittent drying due to the negligible heat exchange in the expansion device. The exergy destruction was a little bit higher for the lower value of intermittency ratio due to the high MC of air in the system. The total values of exergy destruction with SAHPD system for the intermittency ratio of continuous ($\alpha = 1$), $\alpha = 0.66$, $\alpha = 0.33$ and $\alpha = 0.2$ are 0.953, 0.972, 0.986 and 1.023kW respectively.

Table: 7.2. Component wise exergy destruction (kW) and efficiency for intermittent drying

Component	Intermittency ratio (α)							
	Continuous (α = 1)		A =0.66		A =0.33		A =0.2	
	$E_{x,dest}$	η_{ex}	$E_{x,dest}$	η_{ex}	$E_{x,dest}$	η_{ex}	$E_{x,dest}$	η_{ex}
Condenser	0.221	0.882	0.212	0.854	0.214	0.853	0.226	0.836
Compressor	0.248	0.683	0.255	0.672	0.262	0.668	0.278	0.654
Expansion device	0.106	0.851	0.108	0.826	0.109	0.819	0.112	0.792
Evaporator	0.143	0.582	0.151	0.576	0.157	0.568	0.167	0.552
Dryer cabin	0.0182	0.243	0.0181	0.233	0.0186	0.227	0.0195	0.221
Solar water heat exchanger (SWHE)	0.221	0.697	0.232	0.676	0.227	0.658	0.234	0.648

The economic investigation of the SAHPD for different intermittency ratio was considered for the total profit (annual) by selling the dried product, initial capital investment, total annual running cost, and payback period for continuous and intermittent drying. The annual maintenance, initial investment cost, effective running cost, total selling cost, net profit, the cost of the dryer, and the payback period are listed in Table 7.3. The annual (300 days) and daily running costs of the solar-assisted-HP dryer were calculated for the radish chips with the SAHPD system for different intermittency ratio (α = 1, α = 0.66, α = 0.33, and α = 0.2). The running cost for all intermittency ratio includes the energy requirement cost, product cost, and labor cost. The energy

requirement cost is the most important cost among the running costs for the SAHPD system for intermittent drying. The payback period for different intermittency ratio is predicted based on the running cost (annual) and the annual selling cost of dried product. The total initial cost of the solar-assisted HP dryer system is calculated as $892.94. The annual (300 days) total running cost for the intermittency ratio of the continuous (α = 1), α = 0.66, α = 0.33 and α = 0.2 are calculated as $2333.86, $2243.86, $2210.86 and $2192.86 respectively. The annual (300 days) total selling cost of the dried product for all the intermittency ratio is $2754. The annual total profit gain for radish drying with the SAHPD system for the intermittency ratio of the continuous (α =1), α = 0.66, α = 0.33, and α = 0.2 are calculated as $420.14, $510.14, $543.14 and $561.14 respectively. The payback period of the solar-assisted-HP dryer for the intermittency ratio of the continuous (α=1), α= 0.66, α= 0.33, and α= 0.2 are estimated as 2.17 years, 1.75 years, 1.644 years, and 1.591 years respectively. The per kg drying cost of the radish chips with SAHPD is lower for the intermittency ratio of 0.2 and higher for the continuous drying and the value of per kg drying cost for the intermittency ratio of α =1, α = 0.66, α = 0.33, and α = 0.2 are calculated as 0.576$/kg, 0.554$/kg, 0.545$/kg, and 0.541$/kg respectively.

Table: 7.3. Economic analysis for intermittent solar-assisted-HP dryer

Parameter	Cost of the parameter ($) / intermittency ratio			
	Continuous (α =1)	α =0.66	α =0.33	α =0.2
Compressor	136.03	136.03	136.03	136.03
Condensers	89.75	89.75	89.75	89.75
Evaporator	72.92	72.92	72.92	72.92

Expansion device	3.51	3.51	3.51	3.51
Drying cabin	46.61	46.61	46.61	46.61
Refrigerant (R134a)	24.68	24.68	24.68	24.68
Fan	16.83	16.83	16.83	16.83
Water pump	25.24	25.24	25.24	25.24
Solar water heater	266.45	266.45	266.45	266.45
Solar heat exchanger	44.88	44.88	44.88	44.88
The fabrication cost of the system	166.04	166.04	166.04	166.04
The total initial investment in the system	892.94	892.94	892.94	892.94
Total energy consumption (kWh/day)	9.105	6.864	6.054	5.67
Cost of the raw product (radish, 13.5 kg/day)	2.45	2.45	2.45	2.45
Raw material cost (annual, 300 days)	735	735	735	735
Labour cost ($/day)	4.03	4.03	4.03	4.03
Labour cost (annual, 300 days)	1209	1209	1209	1209
Maintenance cost (2 % of initial cost), annual	17.86	17.86	17.86	17.86
Running cost of the system($/day)	1.24	0.94	0.83	0.77
Running cost of the system(annual, 300 days)	372	282	249	231
Total running cost of system (annual, 300 days)	2333.86	2243.86	2210.86	2192.86
Total selling cost of dried material ($/day)	9.18	9.18	9.18	9.18

Total selling cost of dried material ($/year)	2754	2754	2754	2754
Total profit ($/year)	420.14	510.14	543.14	561.14
Payback period (year)	2.125	1.75	1.644	1.591
Total drying cost per kg drying material ($/kg)	0.576	0.554	0.545	0.541

7.4. Highlights

The SAHPD system has been designed and fabricated in the laboratory and the thermal performance of the system was experimentally investigated for the different intermittency ratio (α =1, α = 0.66, α = 0.33, and α = 0.2). A comparative study of different operating modes of the system (with different intermittency ratio) has been carried out for drying radish at a constant flow rate of air (v = 1.0 m/s). Effects of total drying time (on period + off period) on energy, exergy, and economic parameters for intermittency ratio of α =1, α = 0.66, α = 0.33, and α = 0.2 have been investigated. The following conclusions can be made from the discussion section:

- The total drying time for the intermittency ratio of α=1, α=0.66, α=0.33, and α=0.2 is 220 min, 230 min, 390 min, and 480 minutes respectively. But the actual drying time for which the system was in on condition is 220min, 170min, 150min, and 120minutes respectively for the same intermittency ratio.
- The total energy consumption for the continuous, α =0.66, α=0.33, and α=0.2 are 3.035kWh, 2.288kWh, 2.018kWh, and 1.89kWh respectively.
- The COP of the SAHPD system for intermittency ratio of α =1, α = 0.66, α = 0.33, and α =0.2 are 4.7, 4.62, 4.48, and 4.32 respectively.

- The average value of OHCOP is higher for the intermittency ratio of 0.2 and the average values of OHCOP for the intermittency ratio of α =1, α =0.66, α =0.33, and α =0.2 are 5.82, 5.75, 5.61 and 5.53 respectively.
- The average values of MER with SAHPD drying for the intermittency ratio of continuous (α=1), α= 0.66, α= 0.33 and α= 0.2 are 1.1045kg/h, 1.43kg/h, 1.736kg/h and 2.025kg/h respectively.
- The SMER is higher for the intermittency ratio of 0.2 and lower for the continuous drying. The average values of SMER with SAHPD drying for the intermittency ratio of continuous (α =1), α = 0.66, α = 0.33 and α = 0.2 are 1.334kg/kWh, 1.77kg/kWh, 2.007kg/kWh and 2.143kg/kWh respectively.
- The total values of exergy destruction with SAHPD system for the intermittency ratio of continuous (α =1), α = 0.66, α = 0.33 and α = 0.2 are 0.953kW, 0.972kW, 0.986kW and 1.023kW respectively.
- The per kg drying cost of the radish chips with SAHPD is lower for the intermittency ratio of 0.2 and higher for the continuous drying and the value of per kg drying cost for the intermittency ratio of α=1, α = 0.66, α = 0.33, and α = 0.2 are calculated as 0.576$/kg, 0.554$/kg, 0.545$/kg, and 0.541$/kg respectively.
- The annual total profit gain for radish drying with the SAHPD system for the intermittency ratio of the continuous (α =1), α = 0.66, α = 0.33, and α= 0.2 are calculated as $420.14, $510.14, $543.14 and $561.14 respectively.
- The payback period of the solar-assisted-HP dryer for the intermittency ratio of the continuous (α =1), α = 0.66, α = 0.33, and α = 0.2 are estimated as 2.17 years, 1.75 years, 1.644 years, and 1.591 years respectively.

This page is intentionally left blank

CHAPTER 8

EXPERIMENTATION ON HEAT PUMP DRYER INTEGRATED WITH AIR CONDITIONING

In this chapter, the thermal performance of the heat pump convective drying system with air conditioning is carried out for hot and dry atmospheric conditions. For the hot atmospheric condition, people use the air conditioner for living comfort, which utilizes a large amount of electrical energy and contributes to environmental pollution. Furthermore, the dehumidification of air is not necessary for open-loop drying due to having low humidity for dry ambient conditions. Hence, it is possible to reduce energy consumption and environmental pollution by combining the heat pump drying and the air conditioning in one system for the hot and dry atmospheric conditions. The main advantage of the combined heat pump drying and air conditioning system is that it utilizes the waste heat of the condenser from the air conditioner for drying as the heat pump dryer has a better overall system performance coefficient because it combines the performance coefficient of the heat pump and the air conditioner. Thus in this study, the experimental investigation of the heat pump system for combined air conditioning and food product drying has been carried out. The new generation future refrigerant R1234yf is used in the HP cycle. The effects of drying time, airflow rate, and air inlet temperature in both evaporator and condenser on the COP of the heat pump system, COP of the air conditioning system, COP of the overall system, evaporator outlet air temperature, condenser outlet air temperature, SMER, and exergy destruction are investigated for the drying of radish in hot and dry atmospheric conditions. The economic comparison of the integrated heat pump system with the individual systems is presented as well.

8.1. Material and methods

The current investigation focuses on the design and fabrication of a convective HP dryer for the drying of the food products with air conditioning using a future refrigerant R1234yf in the HP cycle, and the experiment was carried out for radish drying to analyze the air conditioning system and dryer performance in hot and dry atmospheric conditions. Fig. 8.1 reveals the schematic presentation of the HP dryer with air-conditioning system. The basic components of the heat pump system are a new future refrigerant (R1234yf), semi-hermetic compressor, wavy fin cross-flow heat exchangers (condenser, evaporator), expansion device (capillary tube), two fans (one for condenser and one for evaporator) [details are provided in Chapter 3]. The fabricated experimental facility is shown in Fig. 8.2 for the combined HP drying and air conditioning system. To measure the refrigerant temperature in the HP cycle at the location of compressor input, compressor output, condenser output, and evaporator input, four resistant thermometers (PT100) are installed. The low temperature (evaporator) side pressure and the high temperature (condenser) side pressure is estimated by using the pressure gauges as shown in Fig. 8.2. Three energy meters are installed to estimate the electric energy requirement by two fans (one for evaporator and another for both condenser and dryer) and the compressor.

In the heat pump system with air conditioning, two separate fans are installed to control the airflow through the condenser and the evaporator to get the desired drying and cooling properties of air. The main advantage of this type of system is that it can be used for both purposes as a heat pump dryer and air conditioner with a very low global warming effect because it utilizes the waste heat of the condenser for drying. This system is having two fresh air inlets, one for the heat pump dryer (through the condenser) and the second for the air conditioner (through the evaporator). The convective drying cabin

of the inside dimension of 0.35m ×0.4m ×0.7m and the drying chamber consisted of several trays inside it. The drying air flows in the HP drying system with the help of a fan (220/230V, speed = 1350rpm, 50Hz, power = 70W, sweep = 300mm). The resistant thermometers and pressure transducer were used in the system to estimate the drop in pressure and temperature of the air in the drying cabin and the whole system.

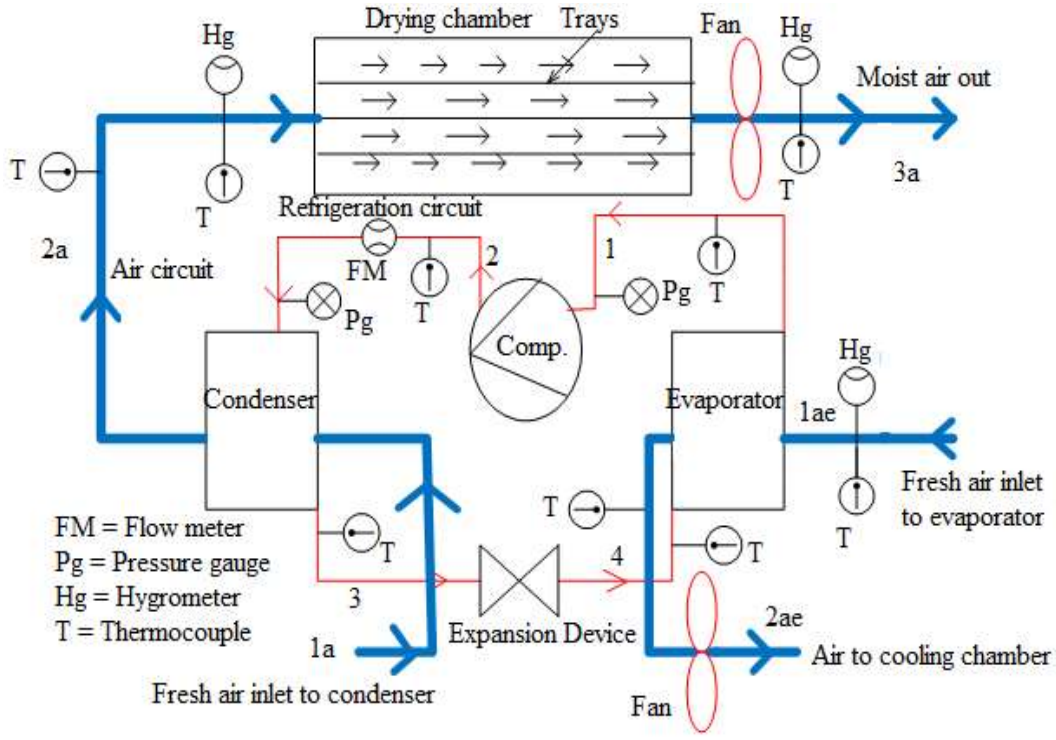

Fig. 8.1: Schematic of the presentation of HP dryer with cooling of air

The integrated heat pump system for both drying and air conditioning is designed and fabricated to investigate the performance of the air conditioner and HP dryer for the drying of the radish. The radishes are washed and sliced into 2 mm size. The moisture content (final and initial) of the radish chips is estimated by applying the oven method at 105 °C. 4.5kg of radish chips was taken for the experiment in the new system. The radish chips on the trays loaded inside the drying cabin. Four hygrometers (at inlet and outlet to drying cabin and evaporator) and the resistant thermometers (PT100) are used in the HP drying with an air conditioning system to measure the evaporator inlet and outlet,

condenser outlet, and drying cabin outlet temperature which is also used to optimize the drying air temperature by controlling the airflow rate through the system.

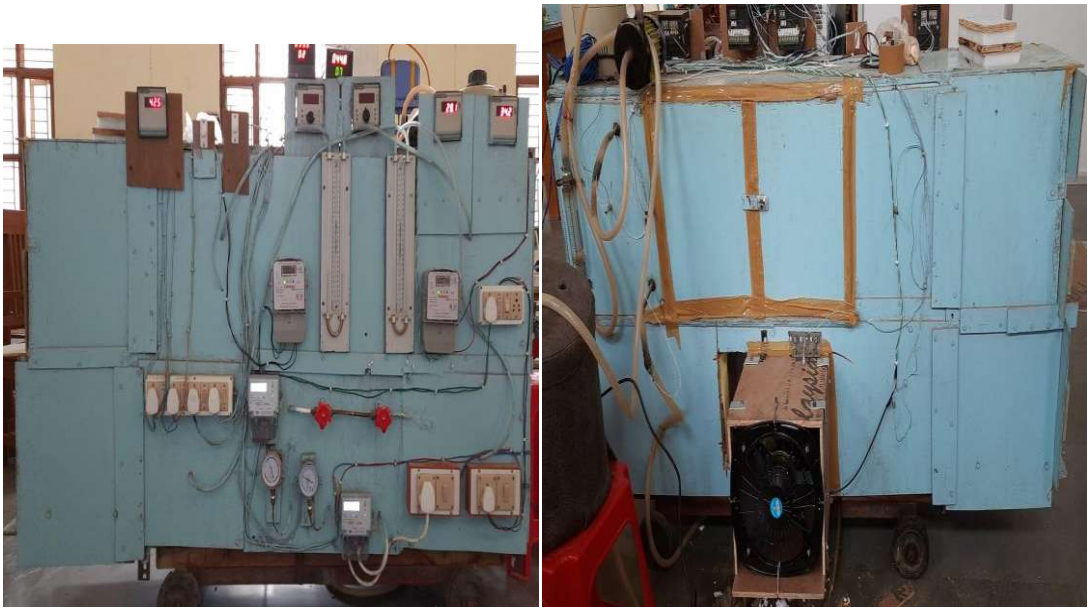

Fig. 8.2: Developed experimental facility of HP dryer with cooling of air

The experiment is carried out to evaluate the exergy, economic, and energy performance of the HP system at different airflow rates through the condenser and evaporator and at different atmospheric conditions (inlet to evaporator and condenser) for the radish chips drying in the system. The fans connected to the evaporator and condenser were switched on and fixed to the desired value of the airflow rate. After that, the R1234yf HP-system made switched on to reach the steady-state condition for the first fixed condition of inlet temperature and flow rate. Then the initial readings of the resistant thermometers, energy, and hygrometers meters were recorded, and during the experiment, the humidity at evaporator inlet and outlet, drying cabin inlet and outlet, and drying air temperature at outlet and inlet to the drying chamber, evaporator, and condenser was recorded after every 10minutes until the end experiment. The experiment is performed for the different velocities of air 1.0m/s, 1.5m/s, 2.0m/s, and 2.5m/s through the evaporator and condenser and at different inlet temperatures oar air to the HP drying

and air conditioning system. For the current study, the system is operated in open mode (separate inlet for condenser and evaporator) without mixing of air. The decrease of moisture content from the product should be equal to the increase of drying air humidity in the drying cabin and also equal to the amount of moisture condensed over the evaporator for the closed system. The energy measuring devices are connected to measure the energy required for the fan (condenser and evaporator) and compressor.

8.2. Data extraction

The heat exchange in the HP condenser between refrigerant and air is given by,

$$Q_{cond} = \dot{m}_{a,cond} c_{pam} (T_{2a} - T_{1a}) = \dot{m}_r (h_2 - h_3) \tag{8.1}$$

The heat exchange in the HP evaporator is given by,

$$Q_{evap} = \dot{m}_{a,evap} (h_{1ae} - h_{2ae}) = \dot{m}_r (h_1 - h_3) \tag{8.2}$$

The performance of the heat pump is generally evaluated as heating COP. But, here, the new term overall heating coefficient of the performance is used for the performance evaluation of the heat pump and it is given as (Byrne and Ghoubali, 2019),

$$\text{OHCOP} = \frac{Q_{cond}}{W_{comp} + W_{fan,evap} + W_{fan,cond}} \tag{8.3}$$

The performance of the air conditioner (cooling effect) is evaluated in terms of cooling COP. But here, the new term overall cooling coefficient of the performance is used for the performance evaluation of air conditioners and it is given as,

$$\text{OCCOP} = \frac{Q_{evap}}{W_{comp} + W_{fan,evap} + W_{fan,cond}} \tag{8.4}$$

The overall system coefficient of performance (OSCOP) is used to evaluate the combined performance of the system (heat pump dryer + air conditioner), and it is estimated as the ratio of the amount of heat transfer in the HP-condenser and evaporator to the total fan

and compressor energy inputs. The OSCOP is given as follows (Byrne and Ghoubali, 2019),

$$\text{OSCOP} = \frac{Q_{cond} + Q_{evap}}{W_{comp} + W_{fan,evap} + W_{fan,\text{cond}}} \tag{8.5}$$

The overall energy efficiency of the heat pump drying with the air conditioning system indicates the utilization of the amount of total energy supplied to the system. In this system, the drying and the air conditioning if performed simultaneously, then the energy efficiency of the overall heat pump drying with air conditioning system can be given by,

$$\eta_{en} = \frac{(m_w / t_d)\, h_{fg} + Q_{evap}}{W_{comp} + W_{fan,cond} + W_{fan,evap}} \tag{8.6}$$

In the exergy analysis of drying and air conditioning with HP, the exergy output, input, and destruction of exergy in the HP system for various components are figured out. Based on the exergy flow of refrigerant and humid air various components of the system, the component exergy destruction and exergy efficiency have been evaluated. The exergy analysis is carried out based on Eq. discussed in previous Chapters.

The economic analysis of the drying with an air conditioning system is related to the investment cost and operating cost of the drying system. The capital cost of the drying system includes the costs of heat exchangers (condenser, evaporator), compressor, capillary tube, fan, refrigerant, duct, base structure, system fabrication, and labor. The amount running cost of the drying system is estimated by (Yahya et al.,2018),

$$C_{RU} = C_{RM} + C_P + C_L + C_m \tag{8.7}$$

Where C_{RU} is the running cost (\$), C_{RM} is the cost of material (\$), C_p is the cost of energy requirement (\$), C_L is the labor cost (\$), C_m is the maintenance cost (\$). Where maintenance cost (C_m) is considered as 2 % of the total capital cost (Yahya et al., 2018),

In the present economic analysis, the HPD or air-conditioning system is compared with the combined (heat pump dryer and air-conditioning) system. The raw material cost and the labor cost is the same for both the system and canceled out in comparison, thus the economic analysis can be carried out based on energy consumption cost and the maintenance cost only, and the equation can be written as,

$$C_{RU} = C_P + C_m \tag{8.8}$$

The total cost (C_{Total}) of the HP drying with an air conditioning system is given as,

$$C_{Total} = C_{IC} + C_{RU} \tag{8.9}$$

Where C_{IC} is the initial investment cost ($)

The annual profit by using the proposed integrated HP system for drying radish chips and air conditioning is the difference between the total cost to run the HP system separately for drying and air conditioning and the total cost to run the HP system for combined drying and air conditioning. Hence, annual profit is given as the following,

$$C_F = C_{RU,dryer} + C_{RU,airconditioning} - C_{RU,dryer+airconditoning} \tag{8.10}$$

Where C_F is the total profit ($)

8.3. Experimental results and discussion

The chips (radish) were dried in the HP dryer with an air conditioner for different atmospheric temperatures in hot and dry conditions, and the energetic and exergetic performances of the drying with the air conditioning system were considered for analysis. Performance of the cooling system, drying system, and the overall system was investigated for different airflow rates and atmospheric conditions. The performance of the HP and air-conditioning system depends on the atmospheric conditions and the airflow rate in the system. The human comfort zone and the various process of air on the psychrometric chart are shown in Fig. 8.3. Fig. 8.4 represents the variation of the

evaporator outlet temperature (cooling temperature) with different evaporator inlet temperatures and airflow rate for fixed condenser inlet conditions and airflow rate. The cooling temperature is higher for the higher mass flow rate of the air through the evaporator for the same inlet temperature, and also, the cooling temperature increases with inlet atmospheric temperature at a fixed flow rate. The evaporator output temperature is lower for the lower mass flow rate of air and found to be in the comfort zone (temperature varies between 22 to 27°C, relative humidity between 40-60%) of cooling for the higher outside atmospheric temperature of 45°C in the current HP drying and air conditioning system.

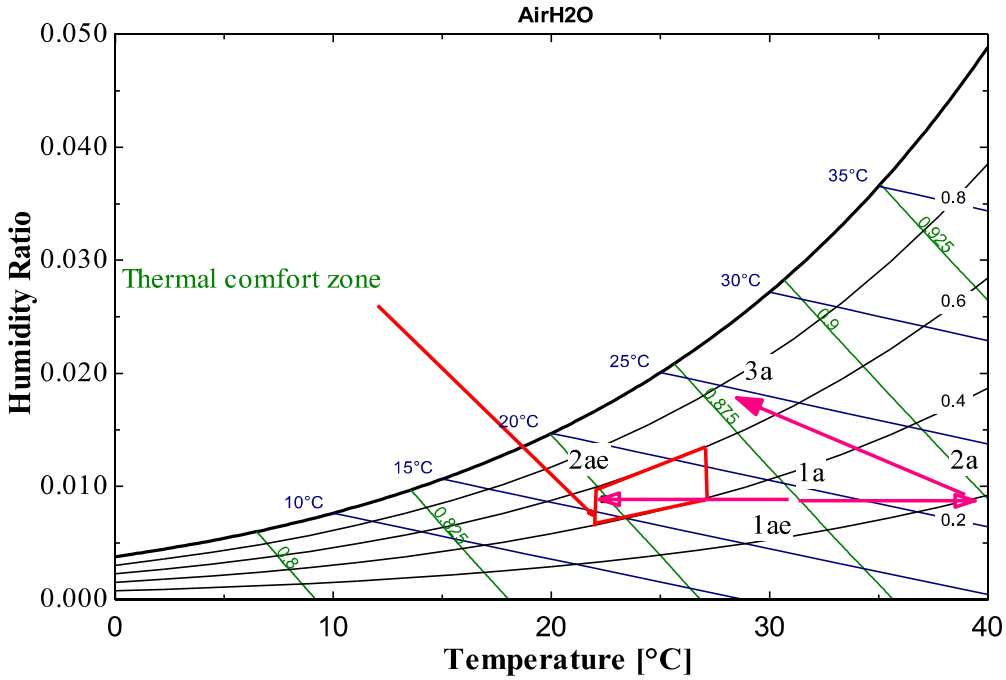

Fig. 8.3: Human thermal comfort zone and various air processes on a psychrometric chart

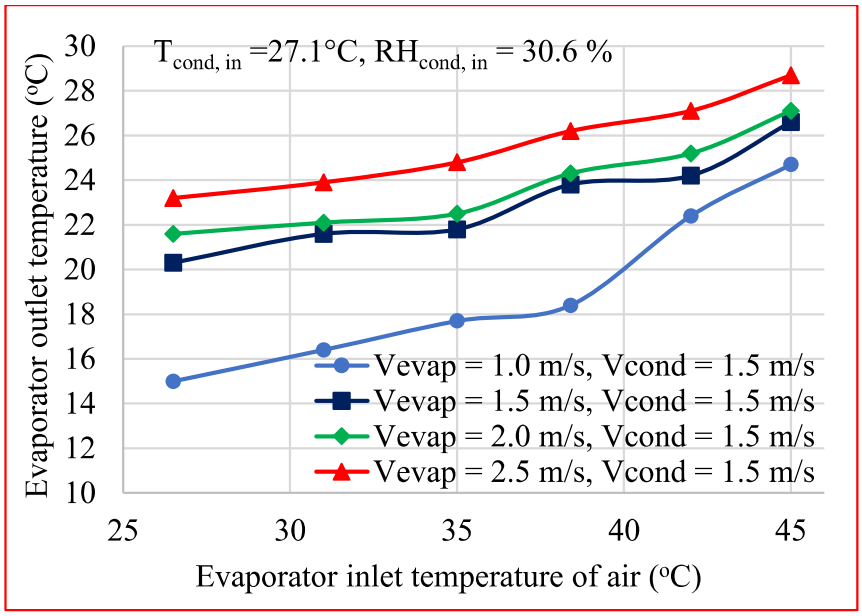

Fig. 8.4: Variation of evaporator outlet temperature according to atmospheric temperature

Fig. 8.5 indicates the effect of the different evaporator inlet (air) temperatures on the condenser outlet temperature that is drying temperature for the fixed airflow through the condenser and inlet temperature. The drying temperature is higher for the higher mass flow rate and inlet temperature of air through the evaporator. A higher drying temperature of 54.6°C is found for the evaporator inlet temperature of 45°C and air velocity of 2.5m/s through the evaporator. Fig. 8.6 represents the evaporator outlet relative humidity of the air for the different inlet conditions of the atmospheric for the fixed inlet condition of the condenser for the combined system. The evaporator outlet relative humidity (50.2%) of air is found in the comfort zone for the air velocity of 1.0m/s for both condenser and evaporator for the atmospheric temperature of 42°C. Thus the result from the experiment shows that the developed HP dying system can be used for the air conditioning and also for the atmospheric temperature of between 42-45°C in the hot and dry zone.

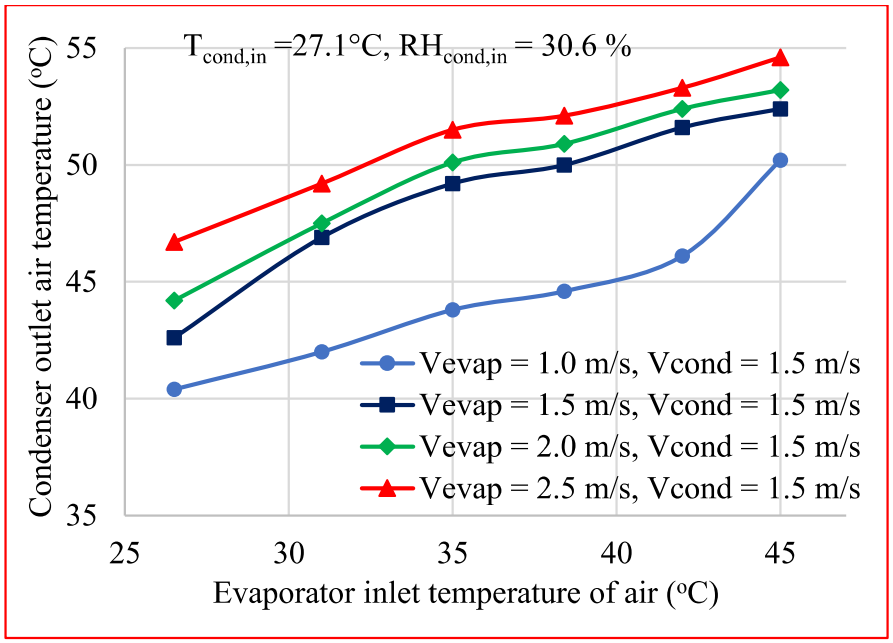

Fig. 8.5: Condenser outlet temperature variation with atmospheric temperature

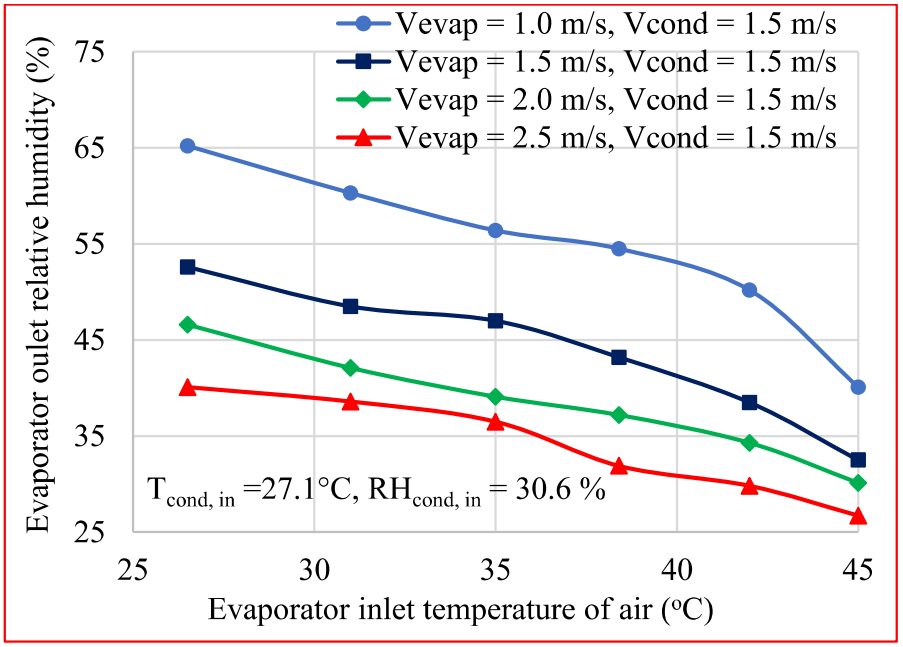

Fig. 8.6: Evaporator outlet relative humidity with atmospheric temperature

The COP of the HP system and air conditioning system was a little bit higher for the lower values of temperature and humidity input to the evaporator (the value of COP of HP and air conditioner decreases with an increase in evaporator inlet air temperature and humidity) as compared to the higher value of input air temperature and humidity. In the current study of the HP system and the air conditioning system, three types of

performance coefficients were defined. The overall cooling coefficient of the performance (OCCOP) for the air condition system, the overall heating coefficient of the performance (OHCOP) for the HP system, and the overall system coefficient (OSCOP) for the combined system of the air conditioning and the heat pump. Fig. 8.7 indicates the effect of the evaporator inlet temperature on the OCCOP for the fixed inlet condition of the condenser at different air velocities through the evaporator. From the figure, it can be concluded that the OCCOP decreases with an increase in the evaporator inlet temperature as well as with air flow rate due to considering fresh atmospheric air inlet to the evaporator (Bellos and Tzivanidis, 2019). But the OCCOP of the system increases with the increase in the inside temperature of the cooling chamber (evaporator outlet temperature). The average OCCOP is found to be 3.227 for the velocity of 2.5m/s in the inlet temperature range of 27-45°C.

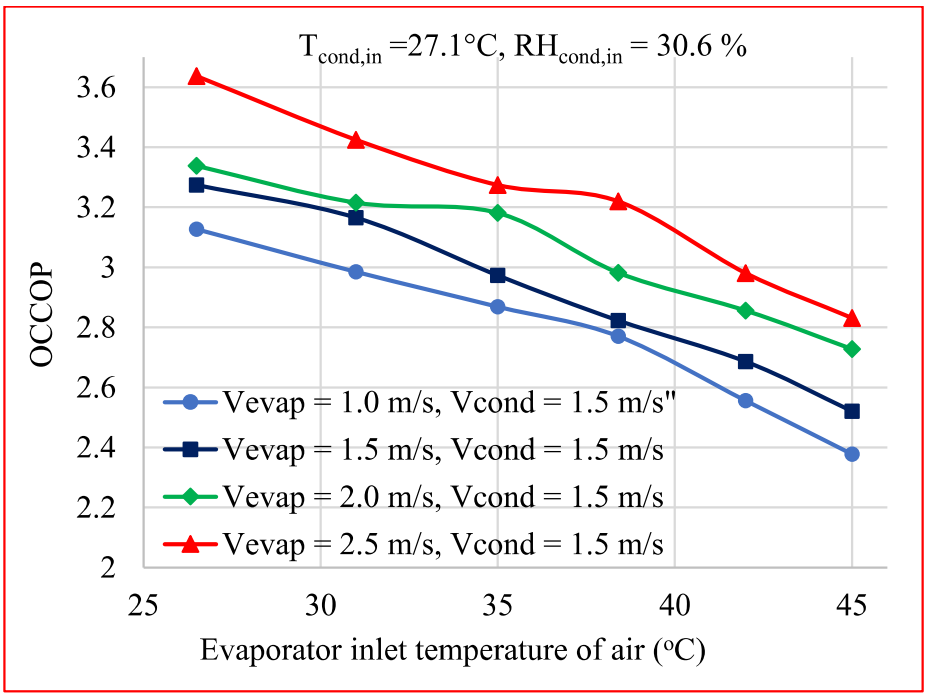

Fig. 8.7: OCCOP variation with evaporator inlet temperature

The most important performance parameter of the combined heat pump and the air conditioning system is the overall system coefficient of performance because it

represents the combined effect of the cooling and heating on the system. OSCOP gives the combined efficiency of the system for the same energy consumed by the system. Fig. 8.8 shows the variation of OSCOP with evaporator input temperature, and the value of the OSCOP is found to be higher for the higher air velocity through the evaporator for the fixed input condition of the condenser and its value decreases with an increase in input temperature to the evaporator (Bellos and Tzivanidis, 2019). The average value OSCOP for the velocity of 2.5m/s in the temperature range of 26-45°C is 7.456.

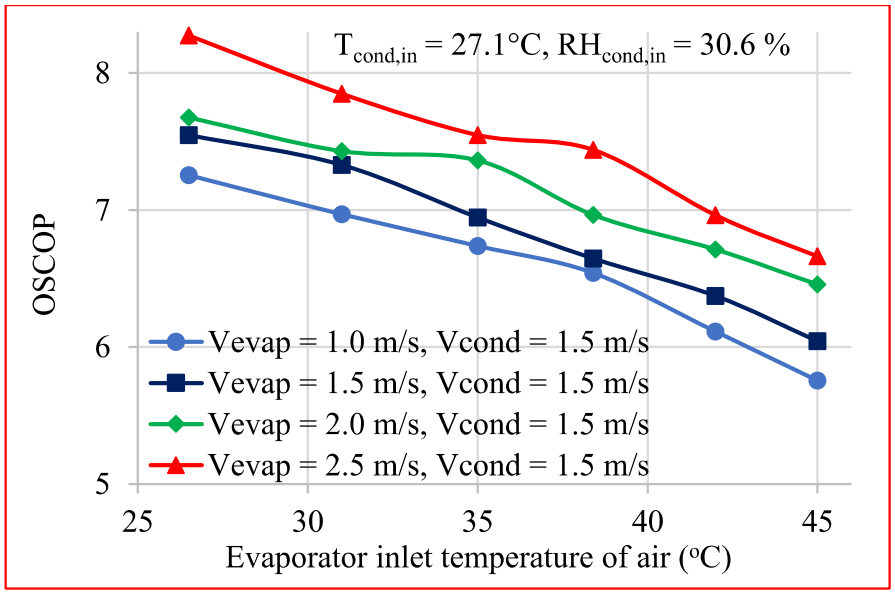

Fig. 8.8: OSCOP variation with evaporator inlet temperature

Fig. 8.9 depicts the outlet air temperature variation of both evaporator (for cooling) and condenser (for drying) with the atmospheric temperature at a fixed mass flow rate (V_{cond} = 1.0 m/s, V_{evap} = 1.0 m/s) through both condenser and evaporator. The cooling and the drying temperature of the air at the atmospheric temperature of between 42-45°C are found to be 22.6-24.7°C and 62.1-63.9°C, respectively. The cooling temperature and the humidity of the evaporator outlet were found to be in the comfort zone for the current studied combined system if a higher atmospheric temperature of between 42-45°C in hot and dry conditions.

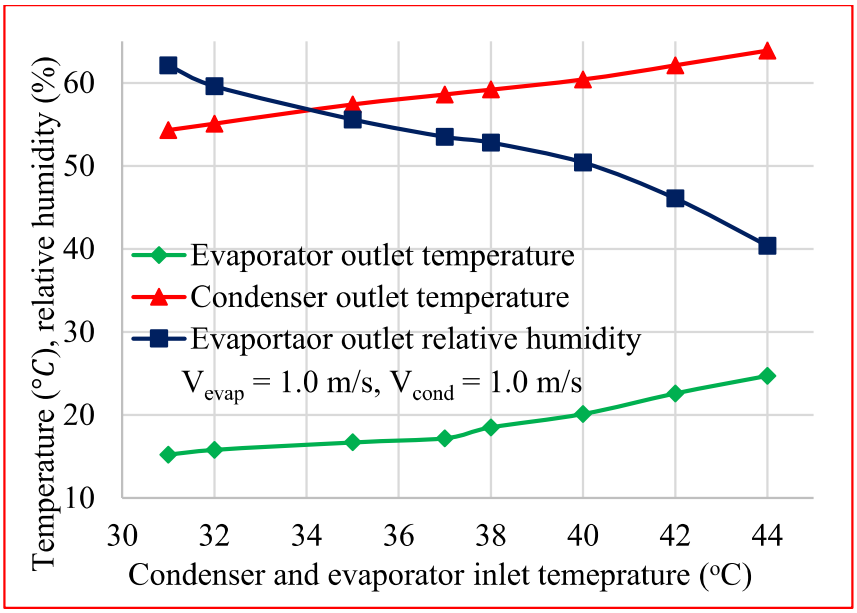

Fig. 8.9: Temperature and relative humidity variation with atmospheric temperature

The effect of the condenser inlet air condition on the cooling and the heating temperature for the fixed evaporator inlet condition and mass flow rate is presented in Fig. 8.10. For the figure, it can be concluded that there is no effect of the condenser inlet air temperature on the air outlet condition of the evaporator as refrigerant state points are the same if the other parameters are constant. The condenser outlet temperature only increases with an increase in condenser inlet temperature due to the same reason.

Fig. 8.11 indicates the variation of the SMER for the drying of the product at the mean inlet temperature of 38.4°C to the condenser and evaporator. In this system, there are two inlets, one for the condenser and one for the evaporator. The SMER first increases with drying time because initially product having higher moisture content, so moisture removal is also higher. But after some time, it decreases due to the loss of water content from the product. The average SMER is found to be 2.098kg/kWh.

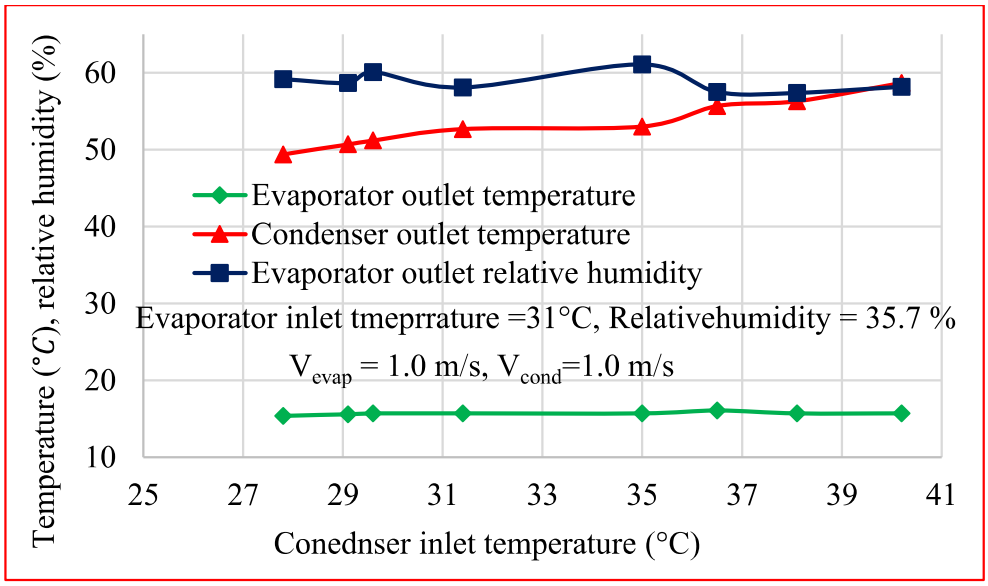

Fig. 8.10: Temperature and relative humidity variation with condenser inlet temperature

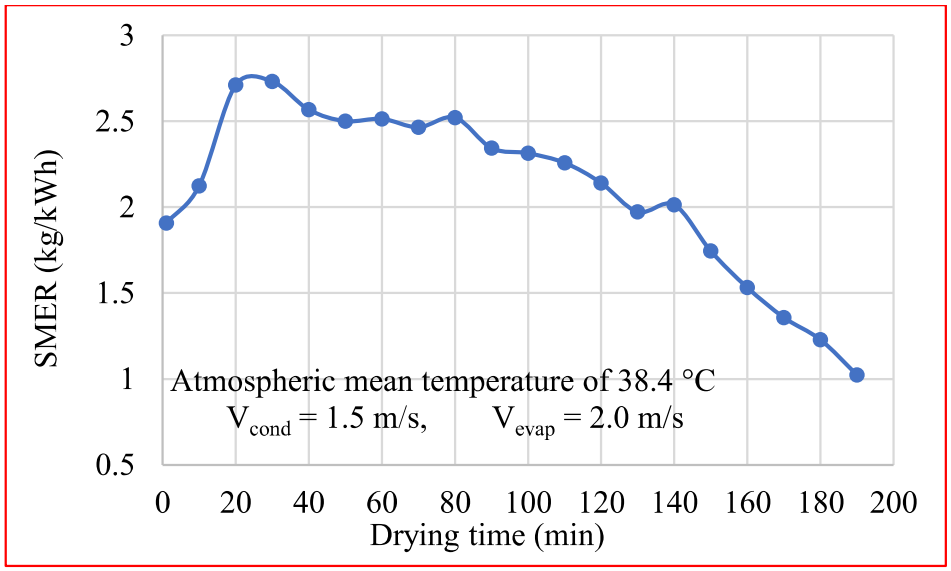

Fig. 8.11: SMER for drying at a mean atmospheric temperature of 38.4°C

Exergetic investigation is the most relevant methodology to evaluate the thermal performance and efficient energy utilization in any HP system. The irreversibility occurs in the evaporator due to the sensible cooling and the condensation of air and moisture over the cold finned surface. The value of exergy destruction and the exergy efficiencies are given in Table 8.1 for the mean inlet temperature of 38.4°C to the condenser and evaporator. The exergy destruction was lower for the expansion device due to the

negligible heat exchange in the expansion device. The exergy (destruction) was higher for the higher inlet temperature of the condenser and evaporator in the HP and air conditioning system. The total values of exergy destruction for the different atmospheric conditions are presented in Fig. 8.12.

Table: 8.1. Component-wise irreversibility and exergy efficiency

System component	Irreversibility (kW)	Exergy efficiency
Compressor	0.203	0.631
Condenser	0.1705	0.912
Expansion device	0.0866	0.753
Evaporator	0.162	0.728
Drying chamber	0.1268	0.315

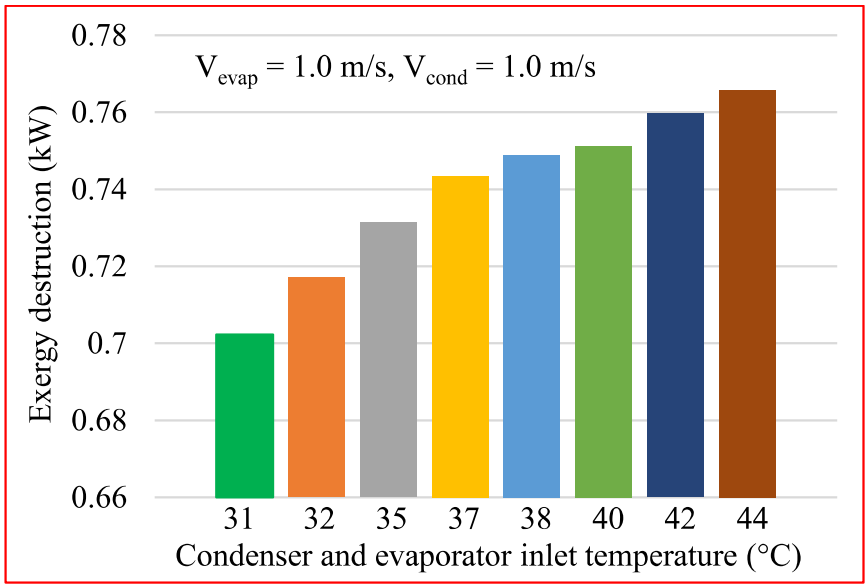

Fig. 8.12: Exergy destruction of the system at different atmospheric temperatures

The component-wise exergy destruction is shown in Fig. 8.13 for a mean atmospheric (evaporator and condenser inlet condition) temperature of 38.4°C. From the figure, it can be observed that the maximum exergy destruction occurs in the compressor and is minimum in the expansion device. In the compressor, the exergy destruction is

higher due to the mechanical and electrical losses, and in the expansion device, exergy destruction is lower due to negligible heat exchange (isenthalpic expansion).

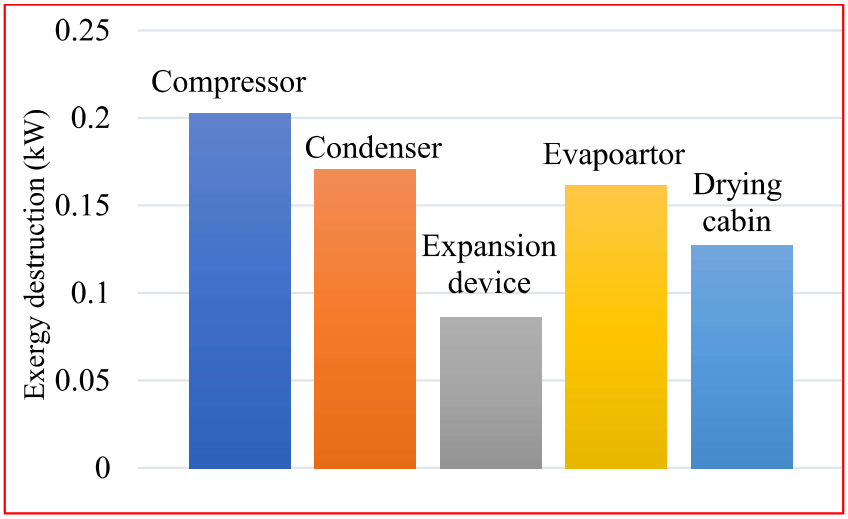

Fig. 8.13: Component wise exergy destruction at an atmospheric temperature of 38.4°C

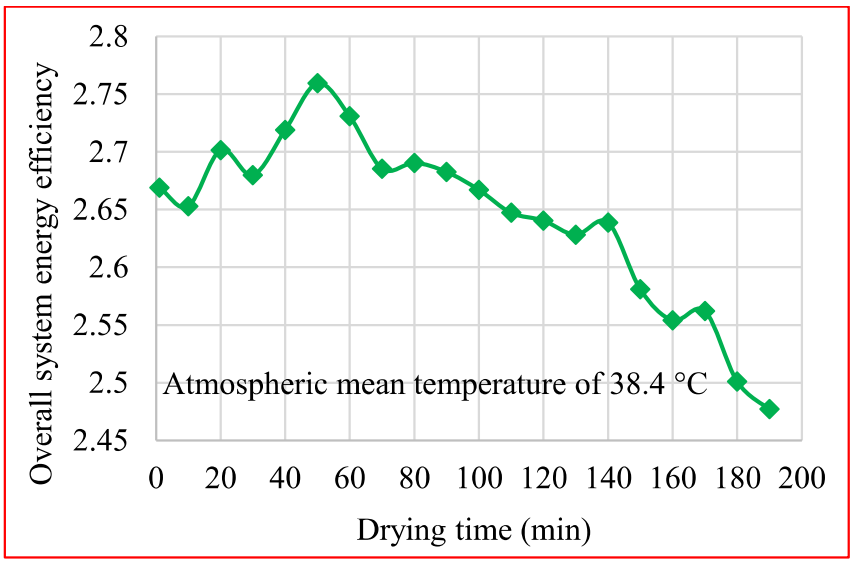

Fig. 8.14: Overall system energy efficiency at mean atmospheric temperature of 38.4°C

The overall energy efficiency represents the utilization of the input energy in the drying with an air conditioning system. in the present system, the drying and the cooling of the air were carried out simultaneously, so the energy utilization occurred in both cooling and drying (moisture removal from the product). Fig. 8.14 shows the variation of the overall system energy efficiency with drying time at atmospheric (condenser and evaporator inlet temperature) of 38.4°C for condenser and evaporator air velocity of

1.5m/s and 2.0m/s, respectively. The overall energy efficiency first increases with time due to an increase in moisture removal from the product, but after some drying time, its value reduces due to the reduction in moisture content of the product.

The economic investigation of the HP dryer with air conditioning for different input conditions to the system was considered for the total profit (annual) by saving the energy to dry product with air conditioning simultaneously, initial capital investment, total annual running cost, and payback period for HP drying with air conditioning at the atmospheric condition of 38.4°C. The annual maintenance, initial investment cost, effective running cost, total selling cost, net profit, the cost of the dryer, and the payback period are listed in Table 8.2. The annual (300 days) and daily running costs of the HP dryer and air conditioning (as a single system) and HP dryer with air conditioning (combined system) were calculated. The running cost includes the energy requirement, and product and labor costs. The energy requirement cost is the most significant parameter within the running costs for the air conditioning and heat pump drying systems. The initial cost of the HP dryer system and the HP drying with air conditioning are calculated as $573.2 and $577.3, respectively. The total (daily) running cost of both single system HP dryer and air conditioning is $ 2.05/day and the running cost (daily) of the combined HP drying and the air condition system was $1.02/day. The total annual running cost of both single system HP dryer and air conditioning is $615/day and the running cost (daily) of the combined HP drying and the air condition system is $306/day. The total annual profit gain by using the combined system (HP dryer + air conditioning) instead of the separate systems of HP dryer and air conditioning is $309.

Table: 8.2. Economic analysis for heat pump drying with air conditioning

Component cost ($)	Separate running	Combine running
Compressor ($)	136.03	136.03

Condenser ($)	89.75	89.75
Evaporator ($)	72.92	72.92
Expansion device ($)	3.51	3.51
Drying cabin ($)	46.61	46.61
Refrigerant (R1234yf) ($)	24.68	24.68
Fan (Two) ($)	33.66	33.66
System fabrication cost ($)	170.14	170.14
Initial investment ($)	577.3	577.3
Energy consumption (kWh/day)	15.24	7.62
System running cost ($/day)	2.05	1.02
Maintenance cost (2 % of the initial cost), annual	11.546	11.546
System running cost ($/year)	626.546	317.546
Total profit ($/year)	.....	309

8.4. Highlights

The HP drying system with air conditioning has been designed and fabricated in the laboratory and the thermal performance of the system was experimentally investigated for the different atmospheric temperatures and airflow through the system. A comparative investigation of different input temperatures to the system has been carried out (for drying of radish) at a different flow rate of air. The effect of the different input conditions on the combined system has been investigated. The conclusions are as follows:

- The COP of the HP system and air conditioning system decreases with increases in the input temperature to the evaporator (atmospheric air inlet) and its value is higher for the higher mass flow rate of air through the system.
- The overall system coefficient of performance (OSCOP) is found to be much higher than the COP of the single system (heat pump or air conditioner) with an average value of 7.456 in the input temperature range of 26-45°C because it gives the advantage of both systems with the single energy input source.
- The evaporator outlet air temperature and the humidity were between 22.6-24.7°C and 40.4-50.2 %, with a drying temperature of 62.1°C for the atmospheric temperature of 42°C. Thus this system can be used for both purposes as an HP dryer and air conditioner for the maximum atmospheric temperature of 45°C.
- Overall system performance mostly depends on the inlet condition and mass flow rate of air through the evaporator.
- Condenser inlet conditions is having a negligible effect on the system performance if the evaporator inlet conditions are fixed.
- The total exergy destruction is highest for compressor and lowest for expansion device.
- The total annual profit gain by using the combined system instead of the separate systems of HP drying or air conditioning is $309.
- Thus this system can be recommended for the application where both drying and air conditioning are required (such as hotels where both laundry and air conditioning are required) because it gives the advantage of both systems in single-unit energy saving (only single energy input for both systems).
- The energy savings can be achieved by using the combined heat pump dryer and air conditioning system instead of the individual system.

This page is intentionally left blank

CHAPTER 9

CONCLUDING REMARKS AND FUTURE SCOPE

9.1. Conclusions

Experimental as well as numerical studies on the multipurpose heat pump dryer are conducted for the simple heat pump dryer and the hybrid source heat pump dryer. Various low-GWP refrigerants are compared for the heat pump dryer. Experimental energy, exergy, and economic analysis are carried out for different hybrid heat pump dryers and also for the heat pump dryer integrated with air conditioning. Various performance parameters such as moisture extraction rate, specific moisture extraction rate, energy efficiency, drying efficiency, payback period, and exergoeconomic factor are considered.

From present investigations, the main inferences can be summarized as:

- Total energy consumption was lowest for the closed system heat pump drying of banana and potato chips. The total energy consumptions for banana chips in the open and closed system are 3.3, 2.41kWh and for potato chips are 3.564, and 3.51kWh, respectively.
- Based on the performance parameters such as MER, SMER, and drying efficiency, the closed system drying is better than the open system drying with simple HPD in the given humid and hot atmosphere for the fruits and the vegetable drying.
- Within studied refrigerants, R152a and R32 yield better performance; however, R152a may be more favorable for HPD due to lower GWP.
- SAHPD system is better based on SMER, and SIAHPD is better than others based on MER in the given humid and hot atmosphere for drying banana chips.

- The drying cost of the material per kg and the total energy consumption to the system are minimum for the solar-assisted heat pump dryer and it is highest for the infrared-assisted heat pump dryer.
- The MER, SMER, and energy efficiency are much higher for waste heat recovery assisted HPD as compared to the simple-HPD in the closed-loop system drying.
- The payback period of using waste heat recovery assisted HPD over the simple-HPD in the closed-loop is found to the 33 months.
- The performance parameters such as MER, SMER, energy efficiency, energy consumption, and drying efficiency are better for the intermittent drying of food chips with solar-assisted HPD as compared to continuous drying.
- The per kg drying cost of the radish chips with SAHPD is lower for the intermittency ratio of 0.2 (higher off time) and higher for the continuous drying.
- The intermittent drying can be recommended as compared to continuous drying for the better quality of product at higher drying temperature with better performance and lower energy consumption.
- The overall system coefficient of performance (OSCOP) is found to be much higher than the COP of the single system (heat pump or air conditioner) with an average value of 7.456 in the input temperature range of 26-45°C because it gives the advantage of both systems with the single energy input source.
- The total annual profit gain by using the combined system (HP drying + air conditioning) instead of the separate systems of HP drying or air conditioning is $309, thus the energy savings can be achieved by using the combined heat pump dryer and air conditioning system instead of the individual system.

9.2. Future scope

- Development and experimental analysis of the solar-assisted heat pump dryer with air conditioning for hot and humid environments.
- Numerical and experimental analysis of the solar-assisted chemical heat pump dryer for food and vegetable drying.
- Numerical and experimental analysis of the solar-assisted radio-frequency heat pump dryer.
- Experimental analysis of intermittent drying of food and biomaterials with heat pump dryer assisted with waste heat recovery from thermal power plants.
- Experimental analysis of intermittent drying of food and biomaterials with ground source assisted heat pump dryer.

This page is intentionally left blank

REFERENCES

Alves-Filho O, Thorbergsen E, Strommen I. A component model for simulation of multiple fluidized bed heat pump dryers. InDrying 98-Proceedings of the 11th International Drying Symposium (IDS 98), Halkidiki, Greece, 1998, pp. 19-22.

Ahmed N, Singh J, Chauhan H, Anjum PG, Kour H. Different drying methods: their applications and recent advances. International Journal of food nutrition and safety. 2013, v.4, pp.34-42.

Amellal H, Benamara S. Vacuum drying of common date pulp cubes. Drying Technology. 2008, v.26, pp.378-82.

Alves-Filho, O., Eikevik, T.M. and Goncharova-Alves, S.V. Single-and multistage heat pump drying of protein. Drying Technology, 2008, v.26, pp.470-475.

Achariyaviriya S, Soponronnarit S, Terdyothin A. Mathematical model development and simulation of heat pump fruit dryer. Drying Technology. 2000, v.18, pp.479-91.

Adapa PK, Schoenau GJ, Sokhansanj S. Performance study of a heat pump dryer system for specialty crops—part 1: development of a simulation model. International Journal of Energy Research. 2002, v.26, pp.1001-19.

Aktaş, M., Khanlari, A., Aktekeli, B. and Amini, A. Analysis of a new drying chamber for heat pump mint leaves dryer. International Journal of Hydrogen Energy, 2017, v.42, pp.18034-18044.

Ameen, A. and Bari, S. Investigation into the effectiveness of heat pump assisted clothes dryer for humid tropics. Energy Conversion and Management, 2004, v.45, pp.1397-1405.

Aktaş, M., Şevik, S. and Aktekeli, B. Development of heat pump and infrared-convective dryer and performance analysis for stale bread drying. Energy Conversion and Management, 2016, v.113, pp.82-94.

Aboltins, A. Theoretical study of material drying coefficient. Engineering for Rural Development, Jelgava 2013, v.23.

Aghbashlo, M. Exergetic simulation of a combined infrared-convective drying process. Heat Mass Transfer, 2016, v. 52, pp.829–844.

Aktaş, M., Şevik, S., Aktekeli, B. Development of heat pump and infrared-convective dryer and performance analysis for stale bread drying. Energy Conversion Management, 2016, v.113, pp.82-94.

Abuşka, M. and Şevik, S. Energy, exergy, economic and environmental (4E) analyses of flat-plate and V-groove solar air collectors based on aluminium and copper. Solar Energy, 2017, v.158, pp.259-277.

Aktaş, M., Khanlari, A., Amini, A. and Şevik, S. Performance analysis of heat pump and infrared–heat pump drying of grated carrot using energy-exergy methodology. Energy Conversion and Management, 2017, v.132, pp.327-338.

Adapa, P.K. and Schoenau, G.J. Re-circulating heat pump assisted continuous bed drying and energy analysis. International journal of Energy research, 2005, v.29, pp.961-972.

Artnaseaw, A., Theerakulpisut, S. and Benjapiyaporn, C. Development of a vacuum heat pump dryer for drying chilli. Biosystems engineering, 2010. v.105, pp.130-138.

Aktaş, M., Şevik, S., Özdemir, M.B. and Gönen, E. Performance analysis and modeling of a closed-loop heat pump dryer for bay leaves using artificial neural network. Applied Thermal Engineering, 2015, v.87, pp.714-723.

Aktaş, M., Ceylan, İ. and Yilmaz, S. Determination of drying characteristics of apples in a heat pump and solar dryer. Desalination, 2009, v.239, pp.266-275.

Atalay, H. Comparative assessment of solar and heat pump dryers with regards to exergy and exergoeconomic performance. Energy, 2019, v.189, p.116180.

Braun JE, Bansal PK, Groll EA. Energy efficiency analysis of air cycle heat pump dryers. International Journal of refrigeration. 2002, v.25, pp.954-65.

Byrne, P. and Ghoubali, R. Exergy analysis of heat pumps for simultaneous heating and cooling. Applied Thermal Engineering, 2019, v.149, pp. 414-424.

Bellos, E. and Tzivanidis, C. Investigation of the environmentally-friendly refrigerant R152a for air conditioning purposes. Applied Sciences, 2019, v.9, pp.119.

Bengtsson P, Berghel J, Renström R. Performance study of a closed-type heat pump tumble dryer using a simulation model and an experimental set-up. Drying Technology. 2014, v.32, pp.891-901.

Bockholt M, Katter M, Pohl G, Michael J, Alpögger T. A Tool Chain for Model-Based Development of Heat Pump Dryers. Procedia Technology. 2016, v.26, pp.357-64.

Brandt N, Alpoegger T, Tegethoff W, Bockholt M, Moehlenkamp A, Koehler J. Exergetic analysis of different R744 heat pump tumble dryer system topologies. Applied Thermal Engineering. 2019, v.161, pp.114107.

Bellomare, F. and Minetto, S. Experimental analysis of hydrocarbons as drop-in replacement in household heat pump tumble dryers. Energy Procedia, 2015, v.81, pp.1212-1221.

Bansal, P., Mohabir, A. and Miller, W. A novel method to determine air leakage in heat pump clothes dryers. Energy, 2016, v.96, pp.1-7.

Best, R., Cruz, J.M., Gutierrez, J. and Soto, W. Experimental results of a solar assisted heat pump rice drying system. Renewable energy, 1996, v.9, pp.690-694.

Castell-Palou, Á. and Simal, S. Heat pump drying kinetics of a pressed type cheese. LWT-Food Science and Technology, 2011, v.44, pp.489-494.

Chua, K.J. and Chou, S.K. A modular approach to study the performance of a two-stage heat pump system for drying. Applied Thermal Engineering, 2005, v.25, pp.1363-1379.

Colak N, Hepbasli A. A review of heat pump drying: Part 1–Systems, models and studies. Energy conversion and management. 2009, v.50, pp.2180-6.

Claussen IC, Ustad TS, Strommen I, Walde PM. Atmospheric freeze drying—A review. Drying Technology. 2007, v.25, pp.947-57.

Ceylan I, Aktaş M. Modeling of a hazelnut dryer assisted heat pump by using artificial neural networks. Applied Energy. 2008, v.85, pp.841-54.

Catton W, Carrington G, Sun Z. Exergy analysis of an isothermal heat pump dryer. Energy. 2011, v.36, pp.4616-24.

Coşkun, S., Doymaz, I., Tunçkal, C. and Erdoğan, S. Investigation of drying kinetics of tomato slices dried by using a closed loop heat pump dryer. Heat and Mass transfer, 2017, v.53, pp.1863-1871.

Chapchaimoh, K., Poomsa-ad, N., Wiset, L. and Morris, J. Thermal characteristics of heat pump dryer for ginger drying. Applied Thermal Engineering, 2016, v.95, pp.491-498.

Chin, S.K. and Law, C.L. Product quality and drying characteristics of intermittent heat pump drying of Ganoderma tsugae Murrill. Drying Technology, 2010, v.28, pp.1457-1465.

Ceylan, I., Aktaş, M. and Doğan, H. Energy and exergy analysis of timber dryer assisted heat pump. Applied Thermal Engineering, 2007, v.27, pp.216-222.

Çolak, N., Kuzgunkaya, E. and Hepbasli, A. Exergetic assessment of drying of mint leaves in a heat pump dryer. Journal of Food Process Engineering, 2008, v.31, pp.281-298.

Ceylan, İ. and Gürel, A.E. Solar-assisted fluidized bed dryer integrated with a heat pump for mint leaves. Applied Thermal Engineering, 2016, v.106, pp.899-905.

Cengel, Y.A., Ghajar, A.J. Heat and mass transfer fundamentals and applications. 4th ed. McGraw-Hill, New York, 2011.

Coogan, R.C. and Wills, R.B.H. Flavour changes in Asian white radish (Raphanus sativus) produced by different methods of drying and salting. International Journal of Food Properties, 2008, v.11, pp.253-257.

Dincer, I., Hussain, M.M. Development of a new Bi–Di correlation for solids drying. International Journal Heat Mass Transfer, 2002, v.45, pp.3065-9.

Deng, Y., Wu, J., Su, S., Liu, Z., Ren, L. and Zhang, Y. Effect of far-infrared assisted heat pump drying on water status and moisture sorption isotherm of squid (Illex illecebrosus) fillets. Drying Technology, 2011, v.29, pp.1580-1586.

Dikmen, E., Ayaz, M., Kovacı, T. and Şencan Şahin, A. Mathematical modelling of drying characteristics of medical plants in a vacuum heat pump dryer. International Journal of Ambient Energy, 2019, v.40, pp.616-623.

Dai B, Zhao P, Liu S, Su M, Zhong D, Qian J, Hu X, Hao Y. Assessment of heat pump with carbon dioxide/low-global warming potential working fluid mixture for drying process: Energy and emissions saving potential. Energy Conversion and Management. 2020, v.222, pp.113225.

Dincer I. Refrigeration systems and applications. John Wiley & Sons; 2003.

Duan, Q., Wang, D., Li, X., Li, Y. and Zhang, S. Thermal characteristics of a novel enclosed cascade-like heat pump dryer used in a tunnel type drying system. Applied Thermal Engineering, 2019, v.155, pp.206-216.

Erbay, Z. and Hepbasli, A. Exergoeconomic evaluation of a ground-source heat pump food dryer at varying dead state temperatures. Journal of cleaner production, 2017, v.142, pp.1425-1435.

Erdem S, Heperkan H. Numerical investigation of the effect of using CO2 as the refrigerant in a heat pump tumble dryer system. Drying Technology. 2014, v.32, pp.1923-30.

Erbay, Z. and Icier, F. Optimization of drying of olive leaves in a pilot-scale heat pump dryer. Drying Technology, 2009, v.27, pp.416-427.

Erbay, Z. and Hepbasli, A. Advanced exergy analysis of a heat pump drying system used in food drying. Drying Technology, 2013, v.31, pp.802-810.

Erbay, Z. and Hepbasli, A. Application of conventional and advanced exergy analyses to evaluate the performance of a ground-source heat pump (GSHP) dryer used in food drying. Energy Conversion and Management, 2014, v.78, pp.499-507.

Ekka, J.P., Bala, K., Muthukumar, P. and Kanaujiya, D.K. Performance analysis of a forced convection mixed mode horizontal solar cabinet dryer for drying of black ginger (Kaempferia parviflora) using two successive air mass flow rates. *Renewable Energy*, 2020, vol.*152*, pp.55-66.

El Khadraoui, A., Bouadila, S., Kooli, S., Farhat, A. and Guizani, A., 2017. Thermal behavior of indirect solar dryer: Nocturnal usage of solar air collector with PCM. *Journal of cleaner production*, *148*, pp.37-48.

Ekka, J.P. and Palanisamy, M. Determination of heat transfer coefficients and drying kinetics of red chilli dried in a forced convection mixed mode solar dryer. *Thermal Science and Engineering Progress*, 2020, vol.*19*, p.100607.

Fatouh, M., Metwally, M.N., Helali, A.B. and Shedid, M.H. Herbs drying using a heat pump dryer. Energy Conversion and Management, 2006, v.47, pp.2629-2643.

Fadhel, M.I., Sopian, K. and Daud, W.R.W. Performance analysis of solar-assisted chemical heat-pump dryer. Solar Energy, 2010, v.84, pp.1920-1928.

Ganjehsarabi, H., Dincer, I. and Gungor, A. Exergoeconomic analysis of a heat pump tumbler dryer. Drying Technology, 2014, v.32, pp.352-360.

Gan, S.H., Ong, S.P., Chin, N.L. and Law, C.L. A comparative quality study and energy saving on intermittent heat pump drying of Malaysian ediblebird's nest. Drying Technology, 2017, v.35, pp.4-14.

Gungor, A., Erbay, Z. and Hepbasli, A. Exergetic analysis and evaluation of a new application of gas engine heat pumps (GEHPs) for food drying processes. Applied Energy, 2011, v.88, pp.882-891.

Gatarić, P., Širok, B., Hočevar, M. and Novak, L. Modeling of heat pump tumble dryer energy consumption and drying time. Drying Technology, 2019, v.37, pp.1396-1404.

Geeraert B. Air drying by heat pumps with special reference to timber drying. Heat pumps and their contribution to energy conservation. Leydon: Noordhoff. 1976, pp.219-46.

Goh LJ, Othman MY, Mat S, Ruslan H, Sopian K. Review of heat pump systems for drying application. Renewable and Sustainable Energy Reviews. 2011, v.15, pp.4788-96. Food Engineering. 2003, v.59, pp.369-77.

Gungor, A., Erbay, Z. and Hepbasli, A. Exergoeconomic (thermoeconomic) analysis and performance assessment of a gas engine–driven heat pump drying system based on experimental data. Drying Technology, 2012, v.30, pp.52-62.

Gao, R., Yuan, L., Yu, M. and Liu, W. Effects of heat pump drying parameters on the volatile flavor compounds in silver carp. Journal of Aquatic Food Product Technology, 2016. v.25, pp.735-744.

Hepbasli, A., Colak, N., Hancioglu, E., Icier, F. and Erbay, Z. Exergoeconomic analysis of plum drying in a heat pump conveyor dryer. Drying Technology, 2010, v.28, pp.1385-1395.

Holtkötter J, Michael J, Henke C, Trächtler A, Bockholt M, Möhlenkamp A, Katter M. Rapid-Control-Prototyping as part of Model-Based Development of Heat Pump Dryers. Procedia Manufacturing. 2018, v.24, pp.235-42.

Herritsch, A., Dronfield, J. and Nijdam, J.J. Intermittent and continuous drying of red beech timber from the green condition. Drying Technology, 2010, v.28, pp.269-277.

Hii CL, Law CL, Law MC. Simulation of heat and mass transfer of cocoa beans under stepwise drying conditions in a heat pump dryer. Applied Thermal Engineering. 2013, v.54, pp.264-71.

Hawlader, M.N.A., Chou, S.K., Jahangeer, K.A., Rahman, S.M.A. and KW, E.L. Solar-assisted heat-pump dryer and water heater. Applied Energy, 2003, v.74, pp.185-193.

Hossain MA, Gottschalk K, Hassan MS. Mathematical model for a heat pump dryer for aromatic plant. Procedia Engineering. 2013, v.56, pp.510-20.

Holman, J.P., Gajda, W.J., 2001. Experimental methods for engineers. McGraw-Hill, New York.

Hawlader, M.N.A., Perera, C.O. and Tian, M. Properties of modified atmosphere heat pump dried foods. Journal of Food Engineering, 2006, v.74, pp.392-401.

Hawlader, M.N.A., Perera, C.O. and Tian, M. Comparison of the retention of 6-gingerol in drying of ginger under modified atmosphere heat pump drying and other drying methods. Drying Technology, 2006, v.24, pp.51-56.

Hii, C.L., Law, C.L. and Suzannah, S. Drying kinetics of the individual layer of cocoa beans during heat pump drying. Journal of Food Engineering, 2012, v.108, pp.276-282.

Hawlader, M.N.A. and Jahangeer, K.A., 2006. Solar heat pump drying and water heating in the tropics. Solar Energy, 2006, v.80, pp.492-499.

Ismaeel, H.H. and Yumrutaş, R. Thermal performance of a solar-assisted heat pump drying system with thermal energy storage tank and heat recovery unit. International Journal of Energy Research, 2020, v.44, pp.3426-3445.

Jinjiang, Z. and Yaosen, W. Experimental study on drying high moisture paddy by heat pump dryer with heat recovery. International Journal of Food Engineering, 2010, v.6.

Jokiel M, Bantle M, Kopp C, Verpe EH. Modelica-based modelling of heat pump-assisted apple drying for varied drying temperatures and bypass ratios. Thermal Science and Engineering Progress. 2020, v.19, pp.100575.

Jeyaprakash, S., Frank, D.C. and Driscoll, R.H. Influence of heat pump drying on tomato flavor. Drying Technology, 2016, v.34, pp.1709-1718.

Junqi, D., Jiangping, C., Zhijiu, C., Yimin, Z. and Wenfeng, Z. Heat transfer and pressure drop correlations for the wavy fin and flat tube heat exchangers. Applied Thermal Engineering, 2007, v.27, pp.2066-2073.

Kenning, D.B.R. and Cooper, M.G. Saturated flow boiling of water in vertical tubes. International Journal of Heat and Mass Transfer, 1989, v.32, pp.445-458.

Khakhanmalee, B., Wattanaboriboon, S. and Polwiboon, N. The Study of Desorption Isotherm for ginger. Department of Food Technology, Khon Kaen University, 2008.

Kuzgunkaya, E.H. and Hepbasli, A. Exergetic evaluation of drying of laurel leaves in a vertical ground-source heat pump drying cabinet. International Journal of Energy Research, 2007, v.31, pp.245-258.

Khanlari, A., Sözen, A., Şirin, C., Tuncer, A.D. and Gungor, A. Performance enhancement of a greenhouse dryer: Analysis of a cost-effective alternative solar air heater. Journal of Cleaner Production, 2020, v.251, pp.119672.

Kuan, M., Shakir, Y., Mohanraj, M., Belyayev, Y., Jayaraj, S. and Kaltayev, A. Numerical simulation of a heat pump assisted solar dryer for continental climates. Renewable Energy, 2019, v.143, pp.214-225.

Klöcker, K., Schmidt, E.L. and Steimle, F. Carbon dioxide as a working fluid in drying heat pumps. International journal of refrigeration, 2001, v.24, pp.100-107.

Kumar, M.A., Kumaresan, G. and Rajakarunakaran, S. Experimental study of moisture removal rate in Moringa leaves under vacuum pressure in closed-loop heat pump dryer. Materials Today: Proceedings, 2020.

Khanlari, A., Sözen, A., Şirin, C., Tuncer, A.D. and Gungor, A. Performance enhancement of a greenhouse dryer: Analysis of a cost-effective alternative solar air heater. *Journal of Cleaner Production*, 2020, vol.*251*, p.119672.

Kumar, D., Mahanta, P. and Kalita, P. Performance analysis of a solar air heater modified with zig-zag shaped copper tubes using energy-exergy methodology. *Sustainable Energy Technologies and Assessments*, 2021, vol.*46*, p.101222.

Liu, Y., Zhao, K., Jiu, M. and Zhang, Y. Design and drying technology research of heat pump Lentinula edodes drying room. Procedia Engineering, 2017, v.205, pp.983-988.

Li, M., Ye, B., Guan, Z., Ge, Y., Li, J. and Ling, C.M. Impact of ultrasound-assisted osmotic dehydration as a pre-treatment on the quality of heat pump dried tilapia fillets. Energy Procedia, 2017, v.123, pp.243-255.

Liete, J.B., Macini, M.C., Boges, S.V. Effect of drying temperature on the quality of dried banana cv. Food Sci. Technol, 2005, v.40, pp.319–323.

Lee BH, Sian RA, Wang CC. A rationally based model applicable for heat pump tumble dryer. Drying Technology. 2019, v.37, pp.691-706.

Le Lostec B, Galanis N, Baribeault J, Millette J. Wood chip drying with an absorption heat pump. Energy. 2008, v.33, pp.500-12.

Li M, Ma Y, Gong W, Su W. Analysis of CO2 transcritical cycle heat pump dryers. Drying Technology. 2009, v.27, pp.548-54.

Lee KH, Kim OJ. Investigation on drying performance and energy savings of the batch-type heat pump dryer. Drying Technology. 2009, v.27, pp.565-73.

Lee KH, Kim OJ, Kim J. Performance simulation of a two-cycle heat pump dryer for high-temperature drying. Drying Technology. 2010, v.28, pp.683-9.

Li, Y., Li, H.F., Dai, Y.J., Gao, S.F., Wei, L., Li, Z.L., Odinez, I.G. and Wang, R.Z. Experimental investigation on a solar assisted heat pump in-store drying system. Applied Thermal Engineering, 2011, v.31, pp.1718-1724.

Lakshmi, D.V.N., Muthukumar, P., Layek, A. and Nayak, P.K. Performance analyses of mixed mode forced convection solar dryer for drying of stevia leaves. *Solar Energy*, 2019, vol.*188*, pp.507-518.

Mortezapour, H., Ghobadian, B., Minaei, S. and Khoshtaghaza, M.H. Saffron drying with a heat pump–assisted hybrid photovoltaic–thermal solar dryer. Drying Technology, 2012, v.30, pp.560-566.

Mancini, F., Minetto, S. and Fornasieri, E. Thermodynamic analysis and experimental investigation of a CO2 household heat pump dryer. International journal of refrigeration, 2011, v.34, pp.851-858.

Mohanraj, M. Performance of a solar-ambient hybrid source heat pump drier for copra drying under hot-humid weather conditions. Energy for Sustainable Development, 2014, v.23, pp.165-169.

Minea, V. Efficient energy recovery with wood drying heat pumps. Drying Technology, 2012, v.30, pp.1630-1643.

Mujumdar AS. Handbook of industrial drying. CRC press; 2006.

Mujumdar AS, editor. Handbook of industrial drying, revised and expanded. CRC Press; 1995.

Minea V. Improvements of high-temperature drying heat pumps. International Journal of Refrigeration. 2010, v.33, pp.180-95.

Mohammadi, I., Tabatabaekoloor, R. and Motevali, A. Effect of air recirculation and heat pump on mass transfer and energy parameters in drying of kiwifruit slices. Energy, 2019, v.170, pp.149-158.

Ogura, H., Yamamoto, T., Kage, H., Matsuno, Y. and Mujumdar, A.S. Effects of heat exchange condition on hot air production by a chemical heat pump dryer using CaO/H2O/Ca (OH) 2 reaction. Chemical Engineering Journal, 2002, v.86, pp.3-10.

Oktay, Z.. Testing of a heat-pump-assisted mechanical opener dryer. Applied thermal engineering, 2003, v.23, pp.153-162.

Onyeocha, E.I., Nwaigwe, K.N., Ogueke, N.V. and Anyanwu, E.E., 2020. Design and construction of an integrated tetrafluoroethane (R134a) refrigerator-waste heat recovery dryer for fabric drying in tropical regions. Heliyon, 2020, v.6, pp.04838.

Queiroz, R., Gabas, A.L. and Telis, V.R.N. Drying kinetics of tomato by using electric resistance and heat pump dryers. Drying Technology, 2004, v.22, pp.1603-1620.

Qiu, Y., Li, M., Hassanien, R.H.E., Wang, Y., Luo, X. and Yu, Q. Performance and operation mode analysis of a heat recovery and thermal storage solar-assisted heat pump drying system. Solar Energy, 2016, v.137, pp.225-235.

Oktay, Z. and Hepbasli, A. Performance evaluation of a heat pump assisted mechanical opener dryer. Energy Conversion and Management, 2003, v.44, pp.1193-1207.

Ogura H, Mujumdar AS. Proposal for a novel chemical heat pump dryer. Drying Technology. 2000, v.18, pp.1033-53.

Ong, S.P., Law, C.L. and Hii, C.L. Optimization of heat pump–assisted intermittent drying. Drying Technology, 2012, v.30, pp.1676-1687.

Pal US, Khan MK. Calculation steps for the design of different components of heat pump dryers under constant drying rate condition. Drying technology. 2008, v.26, pp.864-72.

Perera CO, Rahman MS. Heat pump dehumidifier drying of food. Trends in Food Science & Technology. 1997, v.8, pp.75-9.

Patel, V.K., Gluesenkamp, K.R., Goodman, D. and Gehl, A. Experimental evaluation and thermodynamic system modeling of thermoelectric heat pump clothes dryer. Applied Energy, 2018, v.217, pp.221-232.

Pal, U.S., Khan, M.K. and Mohanty, S.N. Heat pump drying of green sweet pepper. Drying technology, 2008, v.26, pp.1584-1590.

Phoungchandang, S., Srinukroh, W. and Leenanon, B. Kaffir lime leaf (Citrus hystric DC.) drying using tray and heat pump dehumidified drying. Drying Technology, 2008, v.26, pp.1602-1609.

Phoungchandang, S. and Saentaweesuk, S. Effect of two stage, tray and heat pump assisted-dehumidified drying on drying characteristics and qualities of dried ginger. Food and Bioproducts processing, 2011, v.89, pp.429-437.

Phoungchandang, S., Nongsang, S. and Sanchai, P. The development of ginger drying using tray drying, heat pump–dehumidified drying, and mixed-mode solar drying. Drying Technology, 2009, v.27, pp.1123-1131.

Rezk K, Forsberg J. Geometry development of the internal duct system of a heat pump tumble dryer based on fluid mechanic parameters from a CFD software. Applied Energy. 2011, v.88, pp.1596-605.

Rahman, S.M.A., Saidur, R. and Hawlader, M.N.A. An economic optimization of evaporator and air collector area in a solar assisted heat pump drying system. Energy conversion and management, 2013, v.76, pp.377-384.

Rabha, D.K., Muthukumar, P. and Somayaji, C. Energy and exergy analyses of the solar drying processes of ghost chilli pepper and ginger. *Renewable Energy*, 2017, vol.*105*, pp.764-773.

Şevik, S., Aktaş, M., Doğan, H. and Koçak, S. Mushroom drying with solar assisted heat pump system. Energy Conversion and Management, 2013, v.72, pp.171-178.

Saensabai P, Prasertsan S. Effects of component arrangement and ambient and drying conditions on the performance of heat pump dryers. Drying technology. 2003, v.21, pp.103-27.

Shane Clements XJ, Jolly P. Study of heat pump assisted microwave drying. Drying technology. 1993, v.11, pp.1583-616.

Senadeera, W., Alves-Filho, O. and Eikevik, T. Influence of atmospheric sublimation and evaporation on the heat pump fluid bed drying of bovine intestines. Drying Technology, 2012, v.30, pp.1583-1591.

Sarkar J, Bhattacharyya S, Gopal MR. Transcritical CO2 heat pump dryer: Part 1. Mathematical model and simulation. Drying technology. 2006, v.24, pp.1583-91.

Sarkar J, Bhattacharyya S, Gopal MR. Transcritical CO2 heat pump dryer: Part 2. Validation and simulation results. Drying Technology. 2006, v.24, pp.1593-600.

Şevik, S. Experimental investigation of a new design solar-heat pump dryer under the different climatic conditions and drying behavior of selected products. Solar Energy, 2014, v.105, pp.190-205.

Schmidt EL, Klöcker K, Flacke N, Steimle F. Applying the transcritical CO2 process to a drying heat pump. International journal of refrigeration. 1998, v.21, pp.202-11.

Söylemez MS. Optimum heat pump in drying systems with waste heat recovery. Journal of Food Engineering. 2006, v.74, pp.292-8.

Shi, Q., Zheng, Y. and Zhao, Y. Mathematical modeling on thin-layer heat pump drying of yacon (Smallanthus sonchifolius) slices. Energy Conversion and Management, 2013, v.71, pp.208-216.

Sian RA, Wang CC. Comparative study for CO2 and R-134a heat pump tumble dryer–A rational approach. International Journal of Refrigeration. 2019, v.106, pp.474-91.

Shi, Q.L., Xue, C.H., Zhao, Y., Li, Z.J. and Wang, X.Y. Drying characteristics of horse mackerel (Trachurus japonicus) dried in a heat pump dehumidifier. Journal of Food Engineering, 2008, v.84, pp.12-20.

Silva, B.G., Fileti, A.M.F., Foglio, M.A., Rosa, P.D.T.V. and Taranto, O.P. Effects of different drying conditions on key quality parameters of pink peppercorns (Schinus terebinthifolius Raddi). Journal of Food Quality, 2017.

Shah, N.N., Huang, M.J. and Hewitt, N.J. Performance analysis of diesel engine heat pump incorporated with heat recovery. Applied Thermal Engineering, 2016, v.108, pp.181-191

Slim, R., Zoughaib, A. and Clodic, D. Modeling of a solar and heat pump sludge drying system. International journal of refrigeration, 2008, v.31, pp.1156-1168.

Shen, J., Guo, T., Tian, Y. and Xing, Z. Design and experimental study of an air source heat pump for drying with dual modes of single stage and cascade cycle. Applied Thermal Engineering, 2018, v.129, pp.280-289.

Silva, C.M.D.S., Silva, W.P.D., Farias, V.S.D.O., Gomes, J.P. Effective diffusivity and convective mass transfer coefficient during the drying of bananas. Engenharia Agrícola, 2012, v.32, pp. 342-353.

Şevik, S., Aktaş, M., Dolgun, E.C., Arslan, E., Tuncer, A.D. Performance analysis of solar and solar-infrared dryer of mint and apple slices using energy-exergy methodology. Solar Energy 2019, v.180, pp.537-549.

Schmidt, T.E. Heat transfer calculations for extended surfaces. Refrigerating Engineering, 1949, v.57, pp.351-357.

Sonmete, M.H., Mengeş, H.O., Ertekin, C. and Özcan, M.M. Mathematical modeling of thin layer drying of carrot slices by forced convection. Journal of Food Measurement and Characterization, 2017, v.11, pp.629-638.

Turaga, M., Lin, S. and Fazio, P.P. Correlations for heat transfer and pressure drop factors for direct expansion air cooling and dehumidifying coils. ASHRAE transactions, 1988, v.94, pp.616-630.

Tham, T.C., Ng, M.X., Gan, S.H., Chua, L.S., Aziz, R., Chuah, L.A., Hii, C.L., Ong, S.P., Chin, N.L. and Law, C.L. Effect of ambient conditions on drying of herbs in solar greenhouse dryer with integrated heat pump. Drying Technology, 2017, v.35, pp.1721-1732.

Tunckal, C. and Doymaz, İ., 2020. Performance analysis and mathematical modelling of banana slices in a heat pump drying system. Renewable Energy, 2020, v.150, pp.918-923.

Tajudin, N.H.A., Tasirin, S.M., Ang, W.L., Rosli, M.I. and Lim, L.C. Comparison of drying kinetics and product quality from convective heat pump and solar drying of Roselle calyx. Food and Bioproducts Processing, 2019, v.118, pp.40-49.

Teeboonma U, Tiansuwan J, Soponronnarit S. Optimization of heat pump fruit dryers. Journal of

TeGrotenhuis W, Butterfield A, Caldwell D, Crook A, Winkelman A. Modeling and design of a high efficiency hybrid heat pump clothes dryer. Applied Thermal Engineering. 2017, v.124, pp.170-7.

Taşeri, L., Aktaş, M., Şevik, S., Gülcü, M., Seckin, G.U. and Aktekeli, B. Determination of drying kinetics and quality parameters of grape pomace dried with a heat pump dryer. Food chemistry, 2018, v.260, pp.152-159.

Vieira, M.G., Estrella, L., Rocha, S.C. Energy efficiency and drying kinetics of recycled paper pulp. Drying Technology, 2007, v. 25, 1639-48.

Wang JF, Brown C, Cleland DJ. Heat pump heat recovery options for food industry dryers. International Journal of Refrigeration. 2018, v.86, pp.48-55.

Wang, D.C., Zhang, G., Han, Y.P., Zhang, J.P. and Tian, X.L. Feasibility analysis of heat pump dryer to dry hawthorn cake. Energy conversion and management, 2011, v.52, pp.2919-2924.

Wang, Y., Yue, J., Liu, Z., Zheng, Y., Deng, Y., Zhao, Y., Liu, Z. and Huang, H. Impact of far-infrared radiation assisted heat pump drying on moisture distribution and rehydration kinetics of squid fillets during rehydration. Journal of Aquatic Food Product Technology, 2016, v.25, pp.147-155.

Wang, W.W.W., Radcliff, T.D. and Christensen, R.N. A condensation heat transfer correlation for millimeter-scale tubing with flow regime transition. Experimental Thermal and Fluid Science, 2002, v.26, pp.473-485.

Xie, Y., Song, L. and Liu, C. Analysis of a solar assisted heat pump dryer with a storage tank. In International Solar Energy Conference, 2006, v.47454, pp. 383-387.

Yang, Z., Zhu, Z. and Zhu, E. Experimental research on parallel conversion control of drying temperature in a closed-loop heat pump dryer. Drying Technology, 2013, v.31, pp.1049-1055.

Yang, Z., Zhu, Z. and Zhao, F. Simultaneous control of drying temperature and superheat for a closed-loop heat pump dryer. Applied Thermal Engineering, 2016, v.93, pp.571-579.

Yahya, M., Fudholi, A., Hafizh, H. and Sopian, K. Comparison of solar dryer and solar-assisted heat pump dryer for cassava. Solar Energy, 2016, v.136, pp.606-613.

Yahya, M., Fahmi, H., Fudholi, A. and Sopian, K. Performance and economic analyses on solar-assisted heat pump fluidised bed dryer integrated with biomass furnace for rice drying. Solar Energy, 2018, v.174, pp.1058-1067.

Zhu, Z., Yang, Z. and Wang, F. Experimental research on intermittent heat pump drying with constant and time-variant intermittency ratio. Drying Technology, 2016, v.34, pp.1630-1640.

Zielinska, M., Zapotoczny, P., Alves-Filho, O., Eikevik, T.M. and Blaszczak, W. Microwave vacuum–assisted drying of green peas using heat pump and fluidized bed: A comparative study between atmospheric freeze drying and hot air convective drying. Drying Technology, 2013, v.31, pp.633-642.

Zambrano, M.V., Dutta, B., Mercer, D.G., MacLean, H.L. and Touchie, M. Assessment of moisture content measurement methods of dried food products in small-scale operations in developing countries: A review. Trends in Food Science & Technology, 2019.

LIST OF PUBLICATIONS

Journals:

1. **Singh A,** Sarkar J, Sahoo RR. Comparative analyses on a batch-type heat pump dryer using low GWP refrigerants, *Food and Bioproducts Processing*, 2019; 117: 1-13.
2. **Singh A,** Sarkar J, Sahoo RR. Energetic and exergetic performance simulation of open-type heat pump dryer with next generation refrigerants, *Drying Technology*, 2020; 38(8): 1011-1023.
3. **Singh A,** Sarkar J, Sahoo RR. Experimental energy-exergy performance and kinetics analyses of compact dual-mode heat pump drying of food chips. *Journal of Food Process Engineering*, 2020; 43(6): e13404.
4. **Singh A,** Sarkar J, Sahoo RR. Experimental performance analysis of novel indirect-expansion solar-infrared assisted heat pump dryer for agricultural products, *Solar Energy,* 2020; 206: 907-917.
5. **Singh A,** Sarkar J, Sahoo RR. Experimental energy, exergy, economic and exergoeconomic analyses of batch-type solar-assisted heat pump dryer, *Renewable Energy*, 2020; 156: 1107-1116.
6. **Singh A,** Sarkar J, Sahoo RR. Experiment on waste heat recovery-assisted heat pump drying of food chips: Performance, economic, and exergoeconomic analyses, *Journal of Food Processing and Preservation*, 2020; 44(9): No. 14699.
7. **Singh A,** Sarkar J, Sahoo RR. Experimentation on solar-assisted heat pump dryer: Thermodynamic, economic and exergoeconomic assessments, *Solar Energy*, 2020; 208: 150-159.
8. **Singh A**, Sarkar J, Sahoo RR. Performance analysis of intermittent drying of food products with solar-assisted heat pump dryer, *ASME Journal of Solar Energy Engineering*, 2021; in press.
9. **Singh, A**., Sarkar, J., & Sahoo, R. R. (2022). Experimental investigation on novel heat pump system for combined drying and air conditioning for arid climate. *Drying Technology*, 1-12.

Conferences:

1. **Singh A**, Sarkar J, Sahoo RR. 1-D transient simulation model of batch type convective heat pump dryer for agricultural product drying and experimental validation. 25th National and 3rd International ISHMT-ASTFE, Heat and Mass Transfer Conference (IHMTC-2019), December 28-31, 2019, IIT Roorkee, India.
2. **Singh A**, Sarkar J, Sahoo RR. Heat and Mass Transfer Characteristics of Intermittent Drying, Proceedings of the 26th National and 4th International ISHMT-ASTFE Heat and Mass Transfer Conference December 17-20, 2021, IIT Madras, Chennai-600036, Tamil Nadu, India.